THE SLIDING WEAR OF POLYMERS

UNDER VARIOUS FLUIDS

BY

PHILIP MICHAEL DICKENS B.Sc.

A thesis submitted for the degree of

DOCTOR OF PHILOSOPHY

THE UNIVERSITY OF ASTON IN BIRMINGHAM

APRIL 1984

THE UNIVERSITY OF ASTON IN BIRMINGHAM

THE SLIDING WEAR OF POLYMERS UNDER VARIOUS FLUIDS

By PHILIP MICHAEL DICKENS

A thesis submitted for the degree of

DOCTOR OF PHILOSOPHY

1984

SUMMARY

A study of the friction and wear characteristics of the polymers Polyphenylene Oxide (P.P.O.),Polyetheretherketone (P.E.E.K.) and Polytetrafluoroethylene (P.T.F.E.) has been undertaken under both dry and lubricated conditions using three wear machines with different sliding configurations. The importance of constructing a Stribeck curve to indicate the regime of lubrication has been illustrated, and the dry and lubricated friction values have been shown to be dependent upon the type of sliding geometry employed.

One of the most important observations of this work is that when using unfilled polymers as a bearing material, any trapped debris may form an agglomerate layer and considerably reduce the dry wear rate. This reduction, however, does not occur at high sliding speeds because thermal softening and polymer extrusion overrides any benefit obtained with the trapped debris.

Previous work indicated that polydimethyl-siloxane (silicone fluid) plasticised P.P.O. under sliding conditions and provided long periods of lubrication after excess fluid had been removed from the system. It was supposed, in that study, that the fluid was retained by the bulk of the polymer.

This work has shown that although P.P.O. is plasticised by silicone fluid, no significant penetration of the fluid occurs into the bulk of the polymer. It is the presence of a debris layer on the surface which retains the fluid in a physical mixture. Under lubricated conditions this debris layer only occurs with P.P.O. on one wear machine and is a consequence of its unique design. No evidence of plasticisation of P.E.E.K. or P.T.F.E. arose and debris layers were never observed with these materials under lubricated conditions.

Analysis of the wear pins and debris with a Scanning Electron Microscope clearly showed the surface features produced and the presence of the silicone fluid in the debris layer.

Polymers/Lubrication/Friction/Wear/Plasticisation

ACKNOWLEDGEMENTS

I would like to thank my internal supervisors; Dr.T.F.J.Quinn (1st year) and Mr.J.L.Sullivan (subsequent years) of the Physics Department, University of Aston. They have given me encouragement and good advice which has always been of great help. I am also indebted to my external supervisor Dr.J.K.Lancaster who has shown a keen interest in the work described in this thesis, and has helped the work to remain on a practical and realistic base.

I am grateful to the staff of the Physics Workshop, both past and present, in particular Mr.H.Arrowsmith for his interest in the apparatus used. I would also like to thank Mr.A.Abbot for his technical assistance in the laboratory and Mr.R.G.Howell (Metallurgy Department, University of Aston) for instruction in the use of the Scanning Electron Microscope.

Financial assistance for the project was provided by the Science Research Council and by the Royal Aircraft Establishment, Farnborough.

CONTENTS

TABLES

FIGURES

NOMENCLATURE

b	half contact band width
c	constant
cc	cubic centimetres
cm	centimetres
c.p.m.	cycles per minute
cs	centistokes
d	measured density (grams cm^{-3})
da	amorphous density (grams cm^{-3})
dc	crystalline density (grams cm^{-3})
e	elongation to break
g	acceleration due to gravity
grms	grams
k	constant
kg	kilograms
kJ	kiloJoules ($Jx10^{3}$)
kN	kilo Newtons
kW	kilo Watts
k_2	wear coefficient
m	metres
mm	millimetre ($mx10^{-3}$)
mol	mole
n	viscosity
nf	number of cycles to failure
p	applied pressure
pm	flow pressure
r	radius of sphere
r_{av}	average radius of curvature

r.m.s.	root mean square
r.p.m.	revs per minute
s	seconds
s'	shear strength of adhesive junctions
s_o	constant
t	exponent in the fatigue relationship
Ar	real area of contact
C	Carbon
Cr	Chromium
Cs	specific heat
C.L.A.	centre line average
^oC	degrees Centigrade
D	diameter of sphere
Dp	pin diameter
D.C.	Direct Current
E	modulus of elasticity
E'	storage modulus
E"	loss modulus
Fa	adhesive component of friction
Fd	deformation component of friction
G	materials parameter
H	indentation hardness
J	mechanical equivalent of heat
K	thermal conductivity
Kd	deformation constant
MN	Mega Newtons ($Nx10^6$)
MoS_2	Molybdenum disulphide
MPa	Mega pascal
N	Newtons
N'	sliding speed in revs.per.second
O	Oxygen

P	Pressure
P'	load per unit length
Pb	Lead
Pp	pin penetration
Q	density
R	radius of cylinder
Ra	roughness average
Rc	radial clearance
Rt	thermal resistance constant
S	ultimate breaking strength
So	failure stress
Ss	bulk shear stress
T	total asperity contact temperature (^{o}C)
Ta	mean temperature of bearing interface (^{o}C)
Tf	flash temperature
Tg	glass transition temperature (^{o}C)
Tm	crystalline melting point (^{o}C)
To	ambient temperature
U	speed parameter
V	velocity (ms^{-1})
V.P.N.	Vicker's pyramidal number
W	Watts
W'	applied load (N)
Wr	wear rate ($m^{3}m^{-1}$)
X	load parameter
α	constant
$\alpha\phi$	energy loss in the ploughing process
β	fraction of energy lost in rolling
δ	loss tangent
δ_c	critical surface tension

θ	base angle of an indenting asperity
μ	coefficient of friction
μm	micrometres ($mx10^{-6}$)
ν	poisson's ratio
π	pi
σ	applied stress
σ_o	ultimate failure stress
σ_s	standard deviation of asperity heights
ϕ	elastic work done in sliding
Ω	Ohms
ψ	semi-apical angle of a conical indentor

CHAPTER 1

INTRODUCTION

1. INTRODUCTION

1.1 BACKGROUND

In recent years the industrialised world has become 'energy-conscious' and a great deal of effort has gone into improving the efficiency of machinery, particularly in the automobile(1) and aerospace(2) industries. This consciousness was heightened during the 'Oil Crisis' in the early 1970s, when it was realised that more efficient use of material resources was required. In conjunction with this a change was occurring in consumer's expectations of the useful working life of all types of machinery and equipment. This has manifested itself in the automobile world, where:

> "there has been a tendency for the life expectancy of cars to grow longer, from an average of 10 years in 1970 to about 14 years in 1980." (3)

One small part of the drive to improve efficiency and reliability has been directed at the materials used in dry bearings (i.e. those which do not rely upon lubrication for their operation). This has involved extending the range of materials available and determining their individual characteristics. Obviously the use of bearing materials with a low coefficient of friction will increase energy efficiency, but this low coefficient of friction may be associated with a high wear rate. There is therefore an incentive to find materials which give both low coefficients of friction and low wear rates.

The most common materials used in dry bearings fall into four groups:-

I) Metals

II) Ceramics

III) Carbon and graphites

IV) Polymers and their composites.

Examples of the latter group are the subject of this study and will be discussed in detail.

Polymers and their composites are becoming increasingly important as dry bearing materials in a wide variety of areas. They usually have lower coefficients of friction than metals, for example it has been recognised for a long time that Polytetrafluoroethylene (P.T.F.E) sliding on itself or on a metal can give coefficients of friction as low as 0.05(4,5). In contrast, steel sliding on steel will give a coefficient of friction of about 0.5 or higher(6). Polymers also have a lower specific gravity than most metals and Table 1.1 shows that low alloy steel (E.N.31) has a specific gravity which is 4 to 8 times greater than most polymers. The weight savings possible when using polymer bearings may thus be significant, and this is particularly important in the aerospace industry. One of the main reasons, however, for the prolific use of polymers is the ease with which they can be produced into final components. The majority of polymers can be injection or compression moulded in one simple operation, and this lends itself to automated manufacture. Moulding usually leaves the components with a smooth surface so that the

need for finish machining is eliminated. If necessary fillers may also be incorporated during moulding to provide particular mechanical and thermal characteristics.

Polymers and their composites are used widely in the form of bearing cages, low friction pads, thrust washers and simple sleeves in many industrial machines and consumer-durables. They are particularly important in providing maintenance-free bearings where it may be impossible or costly to provide routine servicing. Civil and military aircraft use polymer-based bearings in vast numbers in both critical and non-critical areas, ranging from flight control mechanisms to simple door hinges.

Polymer bearings are used dry or with lubricants but whereas the more traditional bearing materials, such as metals and graphite, have been the subject of extensive tribological studies, plastics have received less attention and especially so under lubricated conditions. This has led to uncertainty in the expected behaviour of polymer bearings when in practical use. An example of this is the use of polymer based bearings on the wing flaps of aircraft. Although these bearings are designed to run under dry conditions, they are likely to encounter contaminant fluids such as water, aviation fuel, anti-icing fluids, hydraulic fluids and oils. Rubenstein(7) has shown that fluids can penetrate a polymer and alter its mechanical properties, and this may lead to a change in its friction and wear properties. Therefore, a knowledge of the friction and wear behaviour of polymers and composites is necessary for both

dry and lubricated conditions. Evans and Lancaster(8) examined the friction and wear properties of several polymers sliding on stainless steel in the presence of a wide range of fluids. They found that fluids generally reduced the coefficient of friction but the wear rate either increased or decreased depending on the polymer-fluid combination. This work by Evans and Lancaster(8) was followed by a previous project with the Aston Tribology group, where Skelcher(9,10) studied one particular polymer of possible commercial interest (Polyphenylene Oxide - P.P.O) in the presence of a contaminant fluid. He found that when the P.P.O was sliding against hardened steel in the presence of Polydimethyl Siloxane (silicone fluid), surface modification took place. The result of this modification was that when all excess fluid was removed from the sliding system, the coefficient of friction still remained at the lubricated value, instead of rising relatively rapidly to the dry value. It was also noticed that the amount of wear which took place before the friction finally rose to its dry value, was much greater than the apparent depth of surface modification observed by Electron probe microanalysis and Rutherford backscattering of α -particles. It was therefore proposed that the silicone fluid entered cracks in the polymer caused by the wear process. The polymer was then considered to be plasticised by the fluid to a depth of approximately 10 μm. When the excess fluid was removed and the sliding recommenced it was further suggested that the retained fluid continued to penetrate the polymer and hence the system was able to maintain a low coefficient of friction for very long periods.

This work by Skelcher(9,10) was an interesting initial study of one polymer system under lubricated conditions, but resulted in many unanswered questions on the mechanism responsible for friction, wear and fluid modification of polymer surfaces.

The object of the present study (supported by R.A.E, Farnborough, through a C.A.S.E. Studentship) was to look in more detail at the surface modification of P.P.O. seen by Skelcher, to see if similar behaviour was exhibited by other polymers, and to investigate the fundamental mechanisms of friction and wear under both dry and lubricated conditions. More complete details can be found in the Research Program - Section 1.9.

1.2 POLYMER MATERIALS

Polymers are comprised of very large molecules linked into chain or network structures. The atoms in the chain form into basic groups called mers, a simple example being the carbon-fluorine combination shown in Figure 1.1a. A chemical reaction is then used to join these basic groups (repeat units) together. For example the mer in Figure 1.1a is joined to other mers of similar identity to give the polymer-Polytetrafluoroethylene (P.T.F.E) shown in Figure 1.1b. This is a linear polymer but it is also possible to produce non-linear polymers by the use of branching. Linear Polyethylene (P.E) in Figure 1.2a can be compared to branched Polyethylene shown in Figure 1.2b. The Polyethylene molecules may have short side branches about 4 repeat units long every 100 repeat units or so along the main chain, and occasionally form long branches in addition(11).

Polymers fall into three main groups, thermoplastics, thermosets and elastomers.

1.2.1 Thermoplastic Polymers

In thermoplastics the atoms along a polymer chain are joined by primary chemical bonds (covalent bonds) whereas the forces between individual chains are collectively known as van der Waal's forces. The energy of the primary bonds in polymers is around 350 $kJmol^{-1}$ (12) whereas the energy between individual chains is much less and not

a)

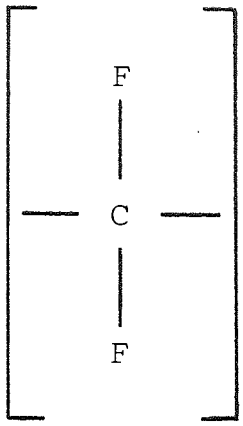

b)

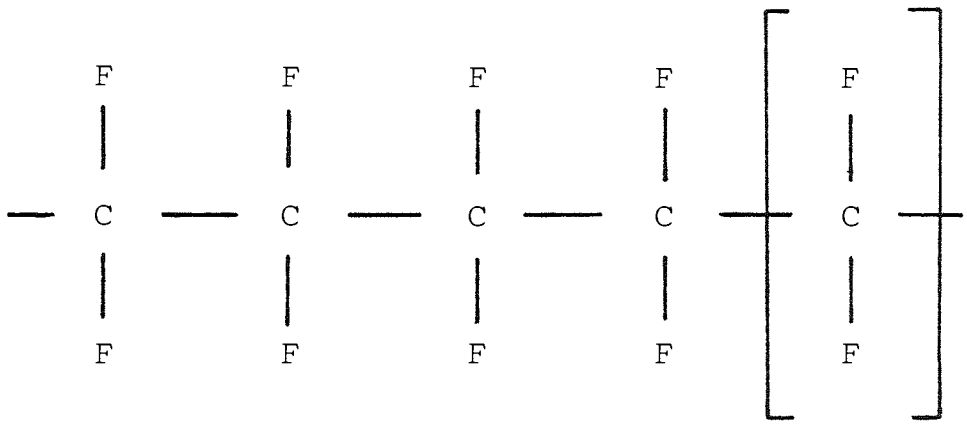

Figure 1.1a Carbon-Fluorine group (mer).

Figure 1.1b The polymer Polytetrafluoroethylene (P.T.F.E.)

a)

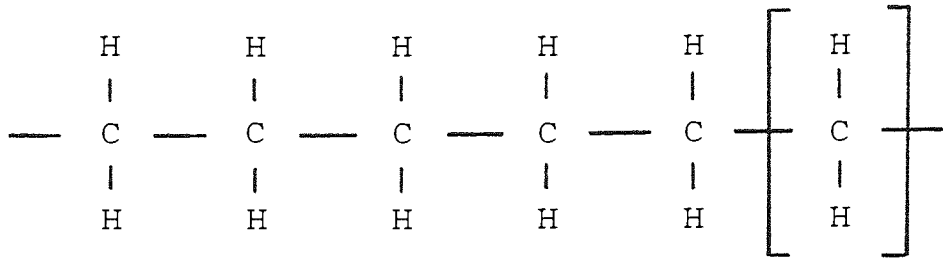

b)

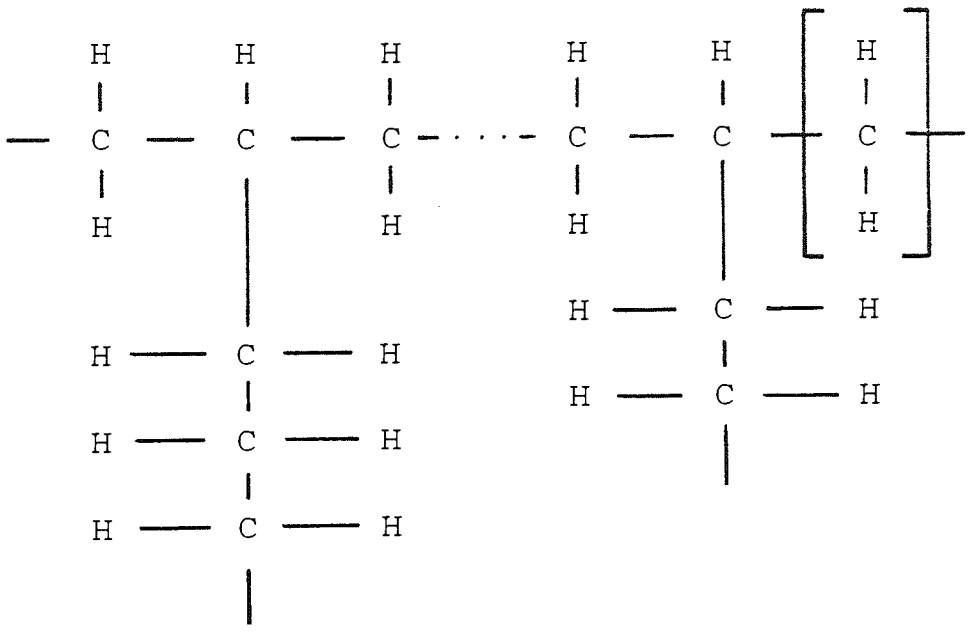

Figure 1.2a Linear Polyethylene

Figure 1.2b Branched Polyethylene

usually greater than 40 $kJmol^{-1}$ (13).

Thermoplastics are characterised by their ability to be repeatedly softened by heating and hardened by cooling. Essentially, thermoplastics in the solid state are either amorphous where the polymer chains have no recognisable structural pattern, or crystalline where the polymer contains regions of ordered material. A simple representation of the amorphous and crystalline structures is shown in Figure 1.3. The degree of crystallinity in a polymer depends upon the polymer in question and its history of processing. Branching reduces the crystallinity because the branch impedes the formation of structured regions in the polymer network (11). Polymers are rarely completely crystalline, and the crystalline regions are usually surrounded by amorphous material. It is,however, possible to obtain a high degree of crystallinity with P.T.F.E. (up to 94%)(13) and high density P.E. (80%)(12). Amorphous polymers tend to be transparent whereas crystalline polymers range from cloudy to opaque, depending upon the amount of crystallinity (14). This is believed to be due to the crystal surfaces in the material scattering the light. The two main single crystal structures discussed in the literature are spherulites and lamellae.

Spherulite crystals can be easily observed when molten P.E. is compressed into a thin film between a microscope slide and a coverslip, and rapidly cooled to solidification. When viewed under a microscope with crossed polarisers, the spherulites can be seen to be up to 1 mm in diameter (11).

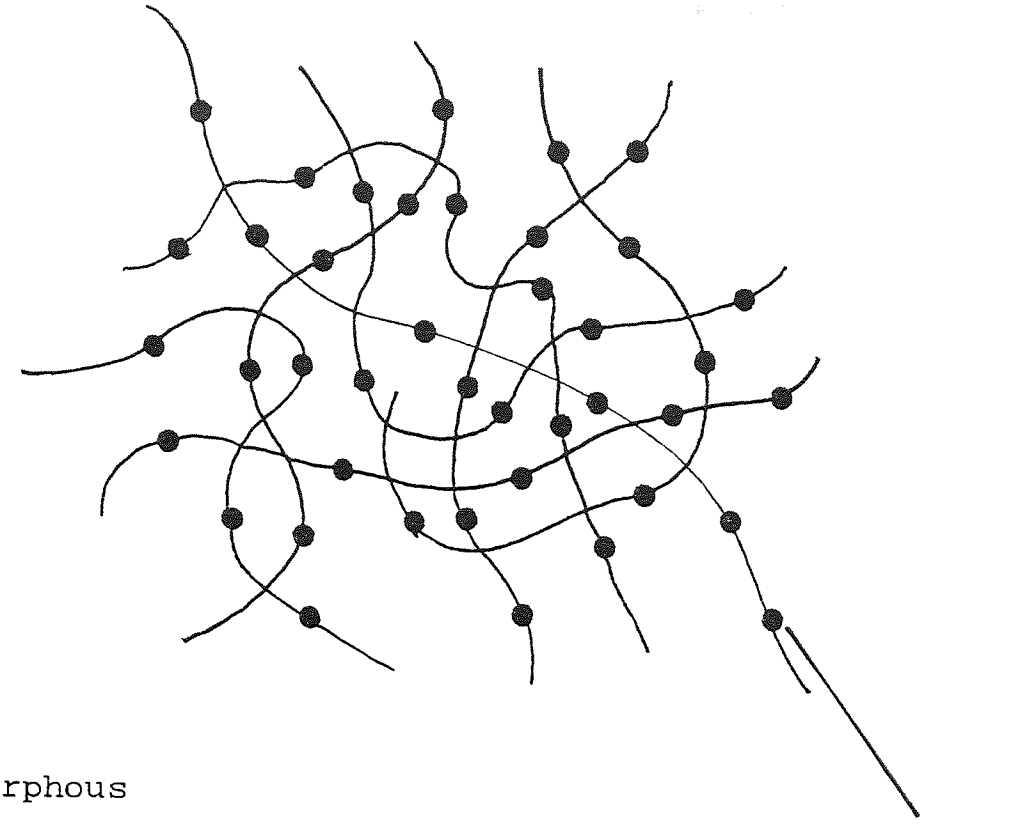

a) Amorphous

b) Crystalline

Figure 1.3 Representation of Thermoplastic Structures:
a) Amorphous b) Crystalline

Rapid cooling from the melt to the solid reduces spherulite growth and leaves the structure with many small spherulites, whereas slow cooling leaves large spherulites (15).

Lamella crystals have been observed by electron microscopy (11,15) and it has been discovered that the polymer chain direction lies transverse to the plane of the lamella. Figure 1.4 shows the proposed structure of the lamella where the polymer chains fold at regular intervals along the chain. It has also been suggested that this lamella structure is the basic structure of spherulites (11).

Bunn et al (16) studied the structure of P.T.F.E. with an electron microscope and found well-marked regions of crystalline material. This work was followed by Speerschneider and Li (17) who proposed that the structure consisted of two phases; crystalline platelets, separated by viscous amorphous material, and Figure 1.5 shows their proposed model of the P.T.F.E. structure. Speerschneider and Li also suggested that deformation of the material resulted in severe distortion of the structure, and that the crystalline platelets slipped past one another or became kinked. The relevance of the structure of P.T.F.E. to its friction and wear behaviour will be discussed more fully in Section 1.7.

The transition from a solid to liquid for a thermoplastic is difficult to define and may occur over a wide temperature range.

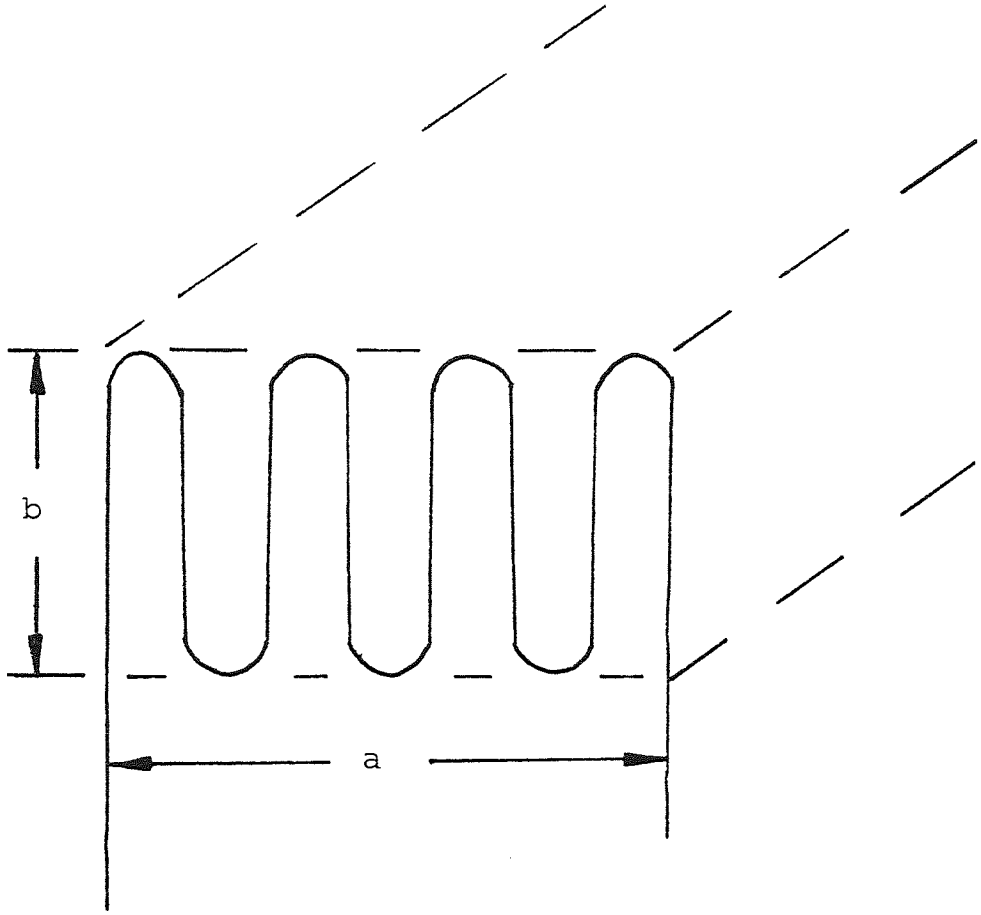

Figure 1.4 Schematic diagram of lamella structure
(A crystal would have a thickness b very much smaller than its distance a)

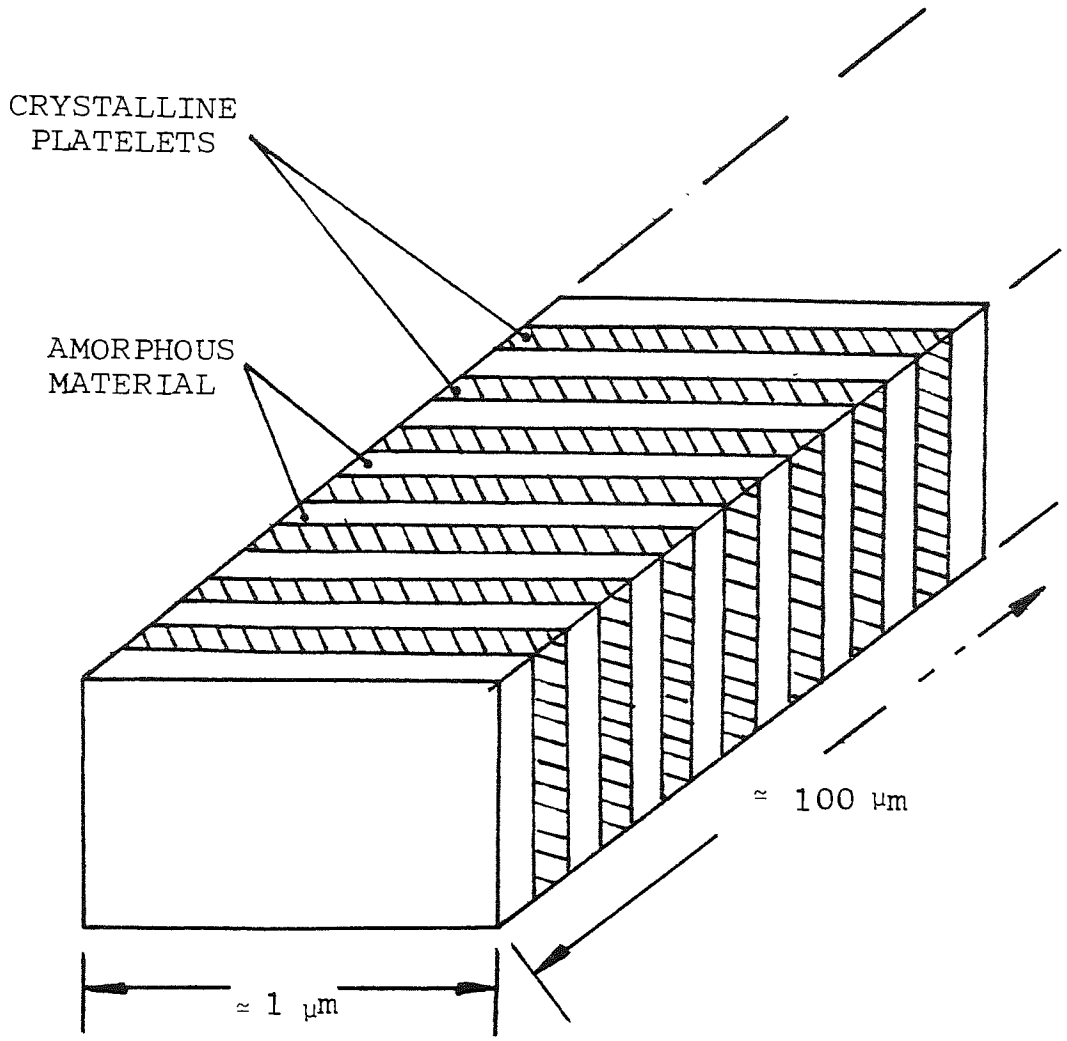

Figure 1.5 Proposed model of P.T.F.E. structure by Speerschneider and Li.

For amorphous thermoplastics there is no sudden transition from the solid to the liquid as the temperature is raised. Instead two transitions may be observed:-

I) a rigid solid to rubber-like material

II) an indefinite rubber-like material to liquid.

At temperatures below the first transition the material is hard, rigid and sometimes transparent. Therefore, as the material is glass-like this state is often referred to as the glassy state and the first transition is referred to as the glass-transition temperature (Tg).

At temperatures above Tg the polymer is less rigid and very high deformations are possible. When the second transition is reached the polymer is able to flow and may be processed by injection moulding (this transition is usually referred to as the melting point of the polymer-Tm).

For crystalline thermoplastics there is an extra transition, the three transitions now include:-

I) a rigid to flexible polymer

II) a flexible polymer to rubber-like material

III) a rubber-like material to liquid.

Below the first transition temperature the polymers are again hard and brittle so this temperature is called the glass transition temperature (Tg). Between the second and third transition the polymer is less brittle but tougher, and the third transition is known as the melting point (Tm).

The glass transition temperature (Tg) is generally considered to be the upper limit for the working temperature range of the polymer, and the lower limit for processing (18). Most polymers have additional transitions below their glass transition temperature (Tg), for example; P.E. has two additional transitions at -100°C and 0°C. The major changes in mechanical properties occur at Tg but properties such as Young's Modulus, damping capacity and toughness can change slightly at the secondary transitions. These changes, however, may influence a polymer's friction and wear behaviour and this will be discussed later.

1.2.2 Thermoset Polymers

Thermoset polymers are also made up of chains of atoms, however, when a chemical reaction is initiated the chains begin to form primary bonds between neighbouring chains. Many thermoset polymers are cross-linked by these primary bonds with the application of a catalyst* (14), but the application of heat and x-ray irradiation may also cause cross-linking (11). This cross-linking between the polymer chains forms a three dimensional structure, reducing the plasticity of the material. The rigidity and hardness is proportional to the amount of cross-linking between the chains. Thermosets are usually brittle materials and cannot be significantly softened by further heating. Indeed, exposure to excess heating will cause degradation of the polymer.

* chemical agent

1.2.3 Elastomers

The elastomers (rubbers) like the thermosets are cross-linked. The difference between thermosets and rubbers is caused by the extent of cross-linking. Thermosets are heavily cross-linked whereas rubbers have relatively few cross-links. Thermosets also show little elongation under stress, whereas rubbers are capable of elongations of the order of 1,000% at tensile failure (19). It is, however, possible to obtain hard, rigid rubbers such as ebonite which is a highly cross-linked material. This is produced by cross-linking (vulcanising) natural rubber with sulphur as a catalyst. Whereas ordinary vulcanised rubber as used in tyres normally contains 2-3% sulphur, a typical sulphur content for ebonite is 32% (13).

1.2.4 Mechanical Properties of Polymers

Polymers have lower specific gravities than metals and this gives them a relatively high strength to weight ratio (e.g. Polyetheretherketone-P.E.E.K. has a strength to weight ratio which is twice that of low alloy steel). The thermoplastics and elastomers are generally more ductile than metals, whereas the thermosets tend to be less ductile. The tensile strengths of polymers are generally lower than metals by a factor of 10^1, their modulus of elasticity is lower by a factor between 10^1 and 10^2 and their thermal conductivities are lower by a factor of 10^2. To improve these properties fillers may be used which are mixed into the polymer. Examples of the

common polymers used in bearings and their physical properties compared to E.N.31 steel are shown in Table 1.1. The main fillers used with the polymers are shown in Table 1.2.

TABLE 1.1

COMPARISON OF THE PHYSICAL PROPERTIES BETWEEN POLYMERS AND STEEL

(All polymer details except P.E.E.K. from Ref.20, P.E.E.K from Ref.21, Steel from Ref.22)

U.H.M.W.P.E. is Ultra High Molecular Weight Polyethylene

		THERMOPLASTICS					
PROPERTY	UNITS	P.P.O.	P.E.E.K.	P.T.F.E.	ACETAL (HOMO)	NYLON 6	U.H.M.W.P.E.
Specific Gravity	$kg.m^{-3}x10^{3}$	1.06	1.265-1.320	2.13-2.18	1.42	1.08-1.14	0.94
Tensile Strength	MNm^{-2}	76	100	13.8-34.6	60.8-69.1	51.1-85.7	17-24.2
Elongation	%	50-80	15	75-400	12-75	60-300	300-500
Izod Impact Strength 12.5x12.5mm Bar	Jm^{-2} $x10^{3}$	80-102	-	No Break	59-75	48-214	No Break
Coefficient of Thermal Conductivity	$Wm^{-1}K^{-1}$	0.216	0.251	0.230	0.230	0.247	0.335
Coefficient of Thermal Expansion	K^{-1} $x10^{-5}$	5.2	-	5.5	8.1	4.6-5.8	7.2
Volume Resistivity	Ω cm^{-1}	10^{16}	$>10^{15}$	$>10^{18}$	10^{14}	10^{14}-10^{15}	$>10^{16}$

cont.....

TABLE 1.1 (cont.)

PROPERTY	UNITS	THERMOSETS		ELASTOMERS		E.N. 31
		PHENOLIC	POLYESTER CAST RIGID	POLYISO-PRENE	SILICONE RUBBER	
Specific Gravity	$kg.m^{-3}x10^{3}$	1.236-1.320	1.1-1.46	0.9	1.1-1.6	7.8
Tensile Strength	MNm^{-2}	34.6-62.2	41.5-89.9	17.3-24.2	4.2-8.9	590-1020
Elongation	%	1.5-2.0	<5.0	750-850	100-500	10-28
Izod Impact Strength 12.5x12.5mm Bar	Jm^{-2} $x10^{3}$	13-21	11-21	-	-	-
Coefficient of Thermal Conductivity	$Wm^{-1}K^{-1}$	0.147	0.168	0.142	0.225	50
Coefficient of Thermal Expansion	K^{-1} $x10^{-5}$	6.8	5.5-10.0	37	45	1.1
Volume Resistivity	Ω cm^{-1}	-	10^{10}-10^{13}	10^{15}-10^{17}	10^{11}-10^{17}	0.15

TABLE 1.2

MAIN FILLERS OF INTEREST FOR DRY BEARINGS

Asbestos	
Carbon black	
Carbon fibres	
Ceramic	used to improve
Glass fibres	mechanical properties
Metals & oxides	
Mica	
Textile fibres	
Asbestos	
Bronze	
Copper	used to improve
Graphite	thermal properties
Silver	
Graphite	
Molybdenum disulphide (MoS_2)	used to improve
P.T.F.E.	friction properties

(Fillers listed in Reference 23)

1.3 POLYMER BEARINGS

Thermosets were the first polymers to be used for bearing applications in any quantity, where phenolic or cresylic resins were reinforced with fabrics or non-oriented fibres (24). These materials were able to withstand high pressures and were not affected by water. They were therefore used in water-cooled bearings in rolling mills in the early 1930s.*

In the late 1940s and early 1950s the thermoplastics nylon and P.T.F.E began to be used, followed by the polyacetals in the 1960s and then polypropylene and polyethylene (24).

The range of materials has grown and there are now about a dozen major polymers used in bearings (25). As these polymers have come into existance their friction and wear properties have been examined, in an attempt to discover a polymer with a low coefficient of friction and low dry wear rate. Fillers have been used in varying proportions in an attempt to achieve better friction, wear, mechanical and thermal properties (these effects are discussed in more detail in later sections).

P.T.F.E. is commonly used in dry bearings because of its low coefficient of friction, but unfortunately it has a high specific wear rate at around 8×10^{-3} $mm^3 N^{-1} m^{-1}$. Fillers can reduce this wear rate by 2 or 3 orders of magnitude depending on the combination used (26). Carbons and graphites are useful fillers in P.T.F.E. because they

* a brief history of polymer bearings is given in Ref. 24

exhibit low friction and wear in their own right, reduce expansion coefficients, and increase strength and thermal conductivity. Other filled polymers include Nylon, Polyester, Polyphenylene sulphide (P.P.S.), Polyacetal, Polyimide, P.E.E.K., etc. (25).

Guides for the use of polymer bearings have been produced and indicate the limiting conditions the bearing may operate under. These guides may include a graph of the relationship between the maximum pressure (P) and sliding velocity (V) used for a specific wear rate or wear life. These PV graphs are readily available (e.g.27) and show that to obtain a specific bearing life any increase in bearing pressure (P) will necessitate a reduction in sliding velocity (V). Alternatively, a graph of the limiting pressure P and temperature (T) may be used to indicate the extent of the operating conditions for a particular material (25). The limiting dry sliding speed for a polymer is usually between 1 and 10 ms^{-1} (23) but this depends upon the polymer in question and the thermal conductivity of the wear counterface (reasons for this dependency are discussed in Section 1.6).

Polymer bearings have been used very successfully under dry conditions in the following areas (28).

I) where fluids are ineffective (e.g. at low temperatures or in reactive environments).

II) where fluids cannot be tolerated because of the possibility of contamination of the product or the environment (29).

III) where fluids are undesirable because of lack of opportunity for, or the impossibility of maintenance.

Under dry conditions most polymers, apart from P.T.F.E., require solid lubricant additives, to reduce the friction to an acceptable level so that heat generation is reduced. P.T.F.E. itself is often used as a solid lubricant in other polymers but there is a wide range of other materials available such as graphite, MoS_2, Lead Oxide (PbO) and many others (30).

Polymer bearings are often used with a lubricant to reduce the coefficient of friction and the wear rate. As far as lubrication is concerned polymer bearings fall into three distinct categories:-

a) Dry operation where the bearing is designed to operate without any form of lubricant. However, here the bearing may be contaminated by stray fluids (31).

b) Lubricated operation where oils or greases may be applied to the bearing continually during its service life (32).

c) 'Lubricated for life'. This involves moulding fluids or greases into the bulk of the polymer such as mineral oil (33) and silicone fluid (34-37). Small percentages of silicone fluid have led to lower friction and wear rates, the fluid being released from the bulk as the surrounding polymer is worn away. Alternatively lubricants may be used which diffuse through the bulk of the polymer and collect at the surface to lubricate

the contacting asperities (38). This diffusion, however, is temperature dependent and only suitable for slow sliding speeds, intermittent motion or where the operating temperature is high enough to promote rapid diffusion.

1.4 FRICTION OF POLYMERS

When one material is loaded against another they will be in contact over localised areas. The sum of these areas is known as the real-area of contact and this is usually much less than the apparent area of contact as shown in Figure 1.6, depending upon the combination of materials and the applied load. The applied load will be supported by the real areas of contact, and as the applied load is increased the materials will deform so that the real contact area increases sufficiently to support the new load. The contact area may increase by either an increase in each individual contact area, or by new areas being formed as the materials move close together. A large amount of work has been undertaken to try and determine the real areas of contact and these have included the use of electrical resistance (4,39,40), optical and acoustic methods (41). These methods, however, usually employ indirect techniques and are limited to very simple contacts. It still remains extremely difficult to determine the real area of contact in practical engineering systems, especially when relative motion occurs. Unfortunately, there does not seem to be any imminent breakthrough in this area as yet. Without a detailed knowledge of the real areas of contact further work on the mechanisms of friction, wear and lubrication will be hampered.

When two materials move relative to each other the movement will be opposed by the forces existing over the real areas of contact. The sum of these opposing forces is known as

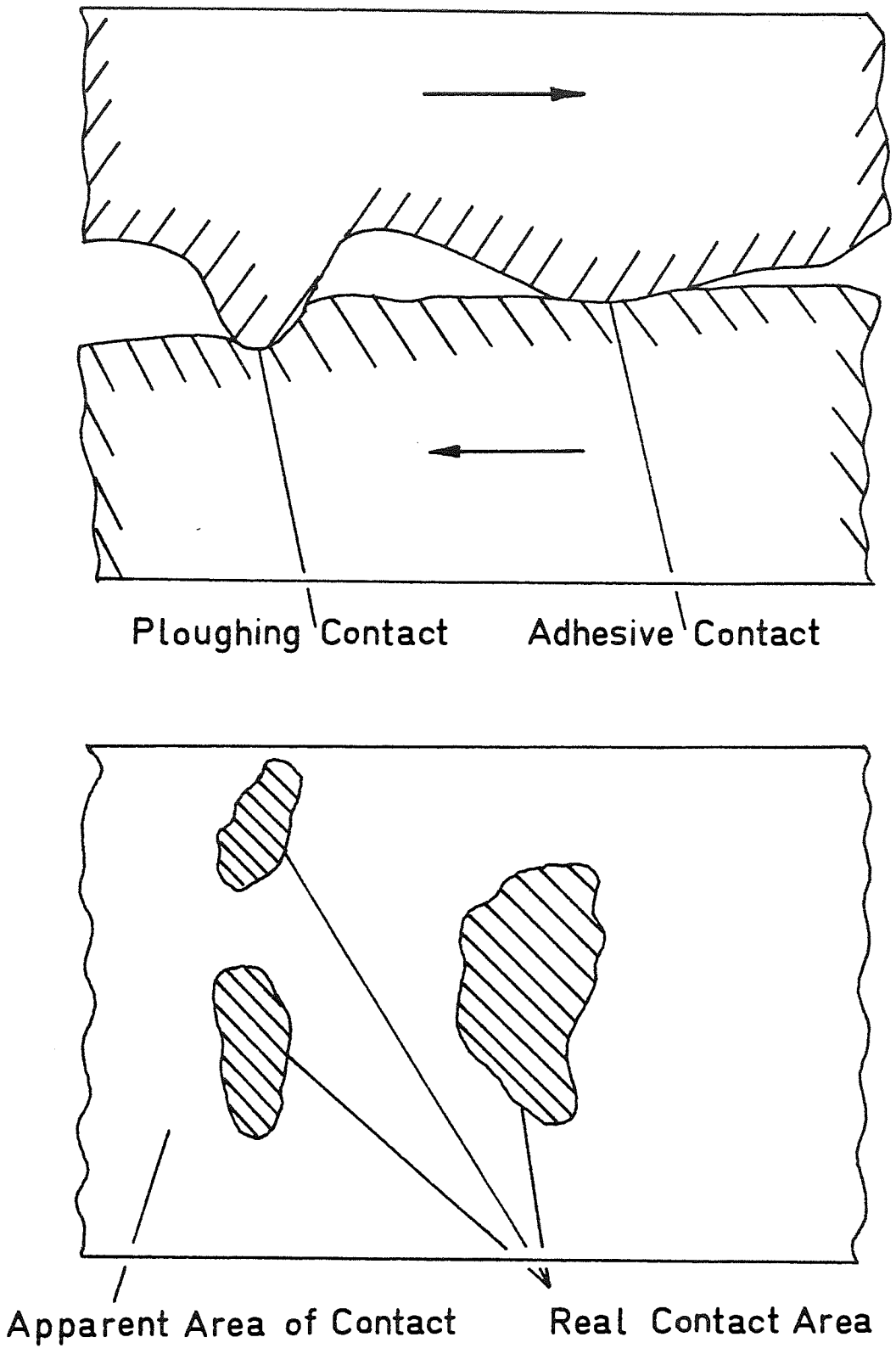

Figure 1.6 Areas of contact in a sliding situation (cross-section and plan views).

the frictional force and is dependent upon a host of variables such as material characteristics, sliding speed, temperature, load, atmospheric conditions, etc. which are in turn dependent on each other.

There is a great deal of debate as to the origin of the frictional force but it is generally accepted that it arises from mechanisms involving adhesion and deformation of the contacting surfaces. These two sources will be discussed in turn and some of the debate surrounding each one will be illustrated with reference to polymer/metal friction.

1.4.1 Adhesion

According to Bowden and Tabor (4)* adhesion is one of the principal components contributing to the frictional force arising at the real area of contact. They suggested that the adhesive component of the frictional force is given by:-

$$Fa = Ar \cdot s'$$

where Ar is the real area of contact and s' is the shear strengths of the adhesive junctions.

It has been suggested that with polymers these junctions are formed by van der Waal's forces and electrostatic forces (42,43). Lee (44) however, has shown that the electrostatic forces in polymers contribute very little to the adhesive force, if indeed, they exist at all. Lee has also

* see also Ref. 120

suggested that the adhesive force is given by:-

$$Fa = Fa^{d} + Fa^{o} + Fa^{i} + Fa^{h} + Fa^{e}$$

where superscripts d, o, i, h, e denote dispersion, orientation, induction, hydrogen bonding and electrostatics. Unfortunately deriving the values of each of the above forces is difficult and therefore the above formula is of little practical use.

Tabor (42) has proposed that the adhesion component is responsible for the major part of the friction force with polymers, and Brainard and Buckley (45) have shown a strong adhesive force between P.T.F.E. and metals in a vacuum, indeed so strong that the P.T.F.E. removed pieces of metal from the bulk when soft metals such as aluminium were used. It is possible to determine the adhesive component of the friction force by observing the overall reduction in the friction force due to surface lubrication. The work of Bartenev and Lavrentev (46), however, is in direct contradiction to Tabor's proposal, because they have shown that the ratio of the adhesion to deformation components in the frictional force can be very low, e.g. P.T.F.E.-0.025; Polyethylene-0.032; Nylon-0.06. This dispute on the relevance of adhesive friction for polymers, is further complicated by Bikerman's claim (47) that the adhesive component does not even exist at all. He has stated that in the first place there is no adhesive attraction between two materials in normal friction experiments (i.e. not in vacuum conditions). The reasoning for this is that when a slider (A) is placed on a support (B) in air, a film of

adsorbed air (plus moisture and numerous impurities) remains between the two solids, and no true contact between atoms of A and atoms of B occurs anywhere along the surface of the apparent contact area. His 'proof' for this argument can be seen by lifting the slider, that is, moving it in the direction normal to the geometrical contact area. The force needed for this motion is equal to the weight of the slider, and no force component attributable to adhesion can be detected. It is, however, possible that an adsorbed film could be disrupted during the sliding process. This could occur because heat generation at the real areas of contact would promote desorption of the film and therefore permit adhesion between the two surfaces.*

Bikerman also suggests that the formula $Fa = Ar \cdot s'$ does not hold for true adhesive junctions (i.e. the junction of two materials A and B when an adhesive material C is used to bond A and B together). By reducing the actual area of contact between an adhesive junction he achieved virtually the same adhesive force. In this case, however, the method of loading the adhesive junction was probably responsible for the unusual results found. It would be interesting to observe the relation between Fa and $Ar \cdot s'$ in other loading situations.

Bowden and Tabor's theory ($Fa = Ar \cdot s'$) has been developed to give the coefficient of friction as

$$\mu = \frac{s'}{pm}$$ where pm is the flow pressure of the material.

* see also Ref. 121 and 122

This formula is derived by assuming that localised plastic deformation occurs and therefore

$$Ar = \frac{W'}{pm} \quad \text{where } W' \text{ is the applied load}$$

$$\text{then if } \mu = \frac{Fa}{W'}, \quad \mu = \frac{Ar \cdot s'}{W'} = \frac{W' \cdot s'}{pm \cdot W'} = \frac{s'}{pm}$$

The above derivation has two main assumptions, the first one being that deformation is entirely plastic and not elastic or a combination of both. Lancaster (26) suggests that deformation of asperity contacts involving polymers is much more likely to be elastic than in the case of metals, because Young's Modulus for polymers is much lower than for metals (See Section 1.5.1). The second and most debatable assumption is that the friction force is entirely adhesive. As shown before this is in direct contradiction to the work of Bartenev and Lavrentev (46).

For polymers with the same modulus it has been shown (44) that μ increases with increasing surface energy and West and Senior (48)* have suggested an empirical relation to account for the effect of surface energy on the friction force.

$$Fa = Ar \cdot s' \left(\frac{\delta c - 15}{11}\right)$$

where δc is the critical surface tension of the polymer. They have claimed that with the above correction they were able to obtain a better correlation between

$$\mu \text{ and } \frac{s'}{pm}$$

* see also Ref. 123

It has been shown (49,50) that the shear strength s' of the interface is approximately equal to the bulk shear strength of the polymer. Briscoe (51)*, however, has shown a linear relationship between the interface shear strength s' and the contact pressure P, with s' increasing with P.

This well known relationship has led to the formula

$$s' = s_o + \alpha P$$

where s_o and α are constants which have been tabulated for various polymers (e.g. 51).

1.4.2 Deformation

Deformation loss is a collective term which includes hysteresis losses, grooving losses and viscous losses. These three losses will be discussed in turn and some of their theories will be illustrated:-

a) Hysteresis losses** occur, for example, in viscoelastic materials, where deformation is not plastic and part of the deformation energy is recovered. This model assumes that energy is introduced into the polymer ahead of the asperity (See Figure 1.7), some of this is restored at the rear of the asperity and urges it forward. The net loss of energy is related to the input energy and the loss properties of the polymer at the particular temperature, contact pressure, and rate of deformation of the process. Originally, Bowden and Tabor (49) derived a formula to calculate the deformation component of the friction force when a hard sphere

* see also Ref. 124

** see Ref. 125

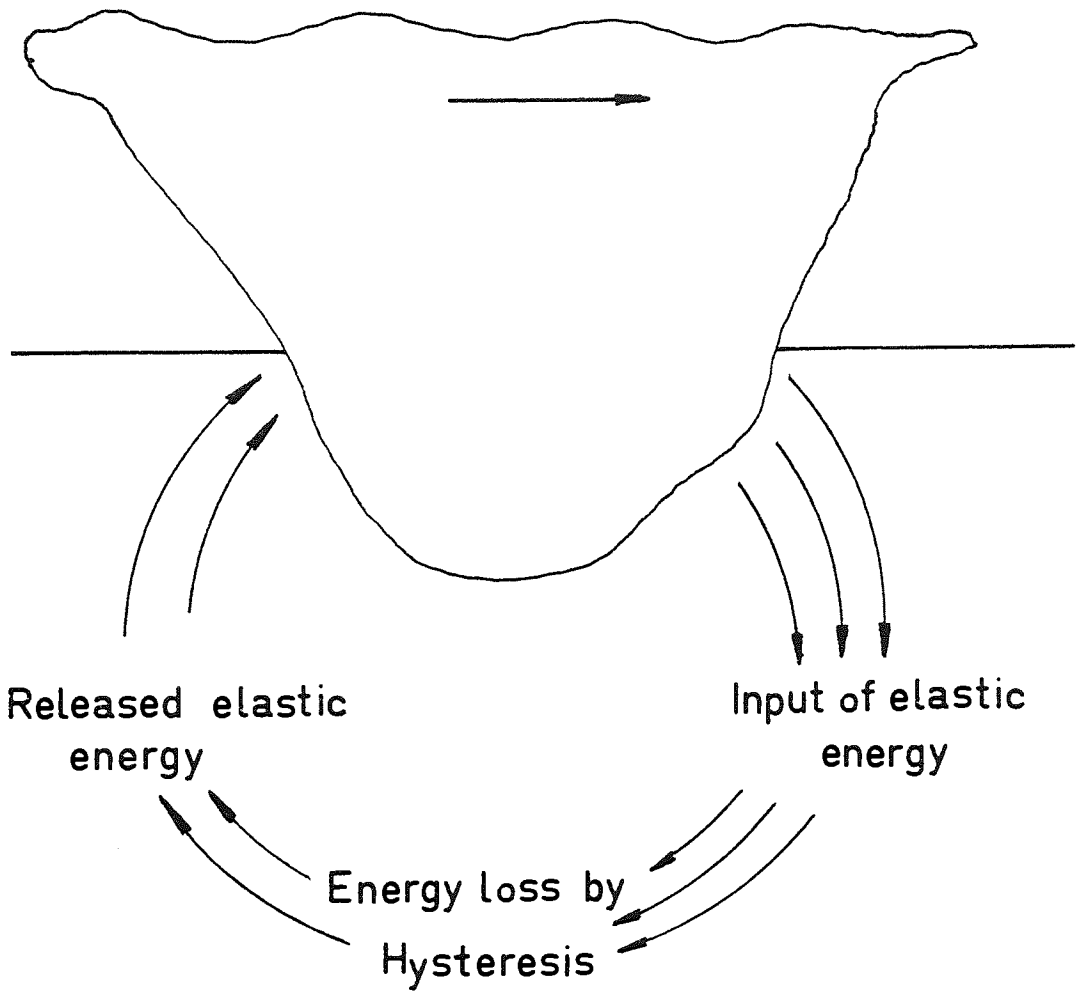

Figure 1.7 The Deformation model of friction

rolls over a perfectly elastic material -

$$Fd = \beta \cdot 0.27\left(\frac{W'^{4/3}}{D^{2/3}}\right)\left(\frac{1-\nu^2}{E}\right)^{1/2}$$

where W' = applied load

ν = poisson's ratio

D = diameter of sphere

E = modulus of elasticity

β = fraction of energy lost in rolling

They found that $\beta = 0.7$ for the first pass and $\beta = 0.55$ for second and subsequent passes on balsam wood.

More recently, Lee (44) has suggested that the deformation component of the friction force is given by -

$$Fd = Kd(W')^{n} \tan\delta$$

where $\tan\delta = \frac{E''}{E'}$

E'' = loss modulus

E' = storage modulus

Kd = deformation constant

W' = load

n = constant

Briscoe (51) has suggested a simpler equation in which the fraction of deformation energy lost in the hysteresis process is approximately $2.5\pi \tan\delta$ where $\tan\delta$ is the loss tangent of the polymer at the deformation frequency. It is possible to find $\tan\delta$ for polymers using standard Dynamic

Mechanical Thermal Analysis (D.M.T.A.) equipment (52), therefore this relationship should be much easier to use in practice. Some work has been undertaken to compare the friction of polymers with their hysteresis properties, for example McLaren and Tabor (53) have shown a similarity between the graphs of friction versus speed for P.T.F.E. on P.T.F.E., and damping losses of P.T.F.E. with frequency. Tabor (42) then went on to compare the friction of a rolling sphere over P.T.F.E. with the hysteresis loss property of P.T.F.E. There was a great similarity between the graphs of rolling friction and loss property against temperature. (See Ref. 53 for polymer frequency, equipment range :- 0.033 to 90Hz)

b) Grooving losses - these may be of two types (51); "Nascent viscoelastic grooving" where no permanent deformation is produced, or "plastic grooving" which is observed with plastic and elastic materials stressed beyond their yield point (this implies permanent deformation).

In the case of grooving with no permanent deformation Briscoe (54) has proposed that the force required to continue sliding while deformation takes place is -

$$Fd = \alpha \phi$$

where ϕ is the elastic work done in deforming the polymer by a slider per unit distance of sliding, and $\alpha \phi$ is the energy loss in the ploughing process. For a sphere of radius r traversing a surface under a load W', Briscoe derived a value for ϕ given by:-

$$\phi = 0.17 W'^{\frac{4}{3}} r^{-\frac{2}{3}} (1-\nu^2)^{\frac{1}{3}} (E)^{-\frac{1}{3}}$$

where E is the real part of Young's Modulus

ν is poisson's ratio

For a conical indentor of semi-opical angle ψ :-

$$\phi = \left(\frac{W'}{\pi}\right) \text{Cot } \psi$$

c) Viscous losses - these do not usually occur in the polymer surface but within the fluid separating the polymer from its opposing surface. Viscous losses, however, may also occur in the polymer surface if local melting occurs.

Although it is difficult to allocate accurate proportions to the adhesion and deformation components of friction it seems reasonable to assume that both mechanisms play a significant role. The proportions will depend upon the sliding geometry, the materials used and the presence of any lubricant. For simple sliding contacts the adhesive component is likely to be larger than the deformation component, whereas in rolling contacts and single point contacts deformation is likely to be much greater. The use of a lubricant should reduce the interfacial shear strength and leave deformation as the main friction component. Where both sliding materials are very hard then less deformation is likely to occur than when one or both materials are soft.

1.5 WEAR OF POLYMERS

There are many different mechanisms which may be involved in the process of wear, but five main ones are thought to be associated with polymer-metal wear.

1.5.1 Abrasive Wear

Two-body abrasive wear occurs when a hard sharp particle cuts material from the polymer. Rabinowicz (55) proposed that the wear rate is proportional to $\tan\theta$, where θ is the base angle of the indenting asperity. This leads to the relationship -

$$Wr = k\left(\frac{W'}{H}\right) \times \tan\theta$$

where Wr = wear rate in m^3m^{-1}

W' = applied load

H = indentation hardness of the polymer (which corresponds to flow pressure pm)

and k expresses the fact that only a proportion of the material undergoing deformation appears as loose wear debris.

This type of wear requires plastic rather than elastic deformation and two criteria have been developed to define this condition -

a) Halliday (56) proposed that if θ satisfies the following condition then plastic flow will occur:

$$\theta = c\left(\frac{H}{E}\right)(1-\nu^2)$$

where E = Young's Modulus

ν = poisson's ratio

c = constant where $c = 0.8$ for the onset of plasticity and $c = 2$ for full plasticity.

For metals, plastic deformation and abrasive/cutting type wear occurs when $\theta \simeq 1^{o}$ or more. However, for this type of wear to occur with polymer $\theta \simeq 5\text{-}10^{o}$, this is because Young's Modulus for polymers are considerably lower than those of metals and therefore the load can be supported elastically more easily. Therefore plastic deformation of polymers only becomes the predominant mode when the indentor is very sharp (57). These larger angles are only likely to be found on very rough surfaces, of the order of 12 μm Ra (58) or greater. Abrasive papers are typical of such surfaces.

b) Greenwood and Williamson (59) proposed that when $(\frac{E}{H})\ (\frac{\sigma s}{r_{av}})^{\frac{1}{2}}$ is used as a 'plasticity index'

where σs is the standard deviation of the asperity heights and r_{av} is their average radius of curvature.

Plasticity and abrasive wear occurs only when the above ratio is greater than or equal to unity.

It has been generally observed that the wear rate for polymers on metals increases with increasing surface roughness (e.g. 23, 25, 57, 58, 60, 61). For very rough surfaces it is believed that abrasive wear predominates and the large asperities on the counterface then plough through the polymer removing material by a cutting process.

As the counterface surface becomes less rough, the smaller asperities remove less of the polymer. For very smooth counterfaces (e.g. up to 0.3 μm Ra) however, for which the asperity radii are too large to induce plasticity and cutting, wear is more likely to be caused by a fatigue process (57, 58, 60, 61). With some polymers (23, 25, 61) it has been found that there is an optimum surface roughness at which the wear rate becomes a minimum. Dowson et al (61) have determined the variation in wear rate for polyethylene with surface roughness and found the minimum to occur at 0.03 μm Ra. They noticed that 'lumpy' transfer of the polymer occurred at values less than 0.03 μm Ra. and suggested that this might cause an increase in abrasion; however, it is more likely that an increase in fatigue wear was occurring.

Ratner et al (62) have derived a simple formula for the abrasive wear of polymers, which relates the volume of wear per unit sliding distance, Wr to the polymer properties -

$$Wr = \frac{\mu W'}{H S e}$$

where μ is the coefficient of friction

W' is the applied load

H is the hardness

S is the ultimate breaking strength

e is the elongation to break.

The most important parameters appear to be S and e, and both Ratner (62) and Lancaster (26) have shown that there is a significant inverse correlation between the wear

rates of a wide range of polymers against rough steel and their values of S.e.

So far only two-body abrasion has been discussed but three-body abrasion may also occur. This can happen when abrasive particles are introduced into a sliding system, either as environmental contaminants or as the products of corrosion or two-body abrasion (57). For a polymer sliding against a metal, abrasive particles may wear both components. Alternatively the particles may be embedded in the polymer and then cause wear of the metal, thus reverting the system to two-body abrasion. Lancaster (26) has shown that when abrasive grains are embedded in a polymer, greater wear on the opposing metal surface occurs with polymers having the highest hardness (or elastic modulus). This is because the softer polymers allow the grains to be almost completely embedded, and therefore less of the abrasive grains protrude from the polymer.

This type of abrasion is likely to be very common in many practical situations where polymer bearings are unsealed.

1.5.2 Erosive Wear

Erosive wear can occur from particle impact at a normal or oblique angle. Damage tends to be greater when erosion occurs at an oblique angle because abrasive, cutting type wear can then occur. The angle for most materials when maximum wear occurs is about 20^{o}. Pipes and conduits are particularly prone to erosive wear when slurries are being

pumped through them.

1.5.3 Fatigue Wear

Fatigue wear occurs as a consequence of repeated contact over small, localised areas and, for polymers, becomes increasingly important with materials of lower elastic modulus and decreasing counterface roughness. Lancaster (26) has proposed a theory of fatigue wear, assuming sliding of a polymer of modulus E over a rigid surface, containing hemispherical asperities of radius r under an applied load W'.

The wear rate -

$$Wr \text{ is proportional to } \frac{r^{-2\left(\frac{t-1}{3}\right)} \cdot W^{\left(\frac{t+2}{3}\right)} \cdot E^{2\left(\frac{t-1}{3}\right)}}{\sigma_o t}$$

where t is the exponent in the fatigue relationship,

$$nf \propto \left(\frac{\sigma o}{\sigma}\right)^t$$

, nf being the number of cycles to failure

σ is the applied stress

σ_o is the ultimate failure stress.

Values of t, derived from conventional fatigue data, range from 1.5 to 3.5 for elastomers and 3-10 for the more rigid thermoplastics and thermosets (26).

Jain and Bahadur (63) have also developed an equation for fatigue wear -

$$Wr = \frac{k_2 W'}{So}$$

where k_2 is a wear coefficient

and So is the failure stress corresponding to the application of a single stress cycle.

They claim that the variation of wear with the parameters involved in the equation is in agreement with experimental studies already reported in the literature. The formula used for deriving the value of k_2, however, is quite complicated and they do not give any proof of its usefulness in practice. Fatigue is claimed to be one mechanism in the wear of tyres (64).

A specific type of fatigue wear is delamination, in which subsurface cracking leads to the removal of large 'sheets' of wear debris. This has been observed by Suh (65) in metals and by Clerico (66) and Clerico and Patierno (67) in polymer composites.

1.5.4. Corrosive Wear

Corrosive wear occurs when stresses are applied in the presence of a chemically active medium. This may occur, for example, when a polymer is plasticised by a lubricant and subsequent removal of the plasticised surface layer occurs. Corrosive wear, however, is only usually found when thermosetting resins slide in very severe conditions, causing oxidation degredation.

1.5.5. Adhesive Wear

Bikerman's suggestion that adhesion does not occur (47)

also implies that adhesive wear cannot occur. Polymer fragments however, are often observed to adhere to metals and glass in the form of a transferred film (e.g. 43, 45, 51, 58, 68. See also Section 1.7 on Polymer Transfer). The generally accepted view of transfer and adhesive wear is that it occurs when the shear strength (s') of the adhesive junctions becomes greater than the bulk shear strength (Ss) of the polymer.

1.6 TEMPERATURE EFFECTS

With thermoplastics wear can increase dramatically when the values of the applied load, speed and temperature reach a certain point. This is associated with thermal softening of the polymer caused by frictional heating over the real areas of contact, leading to extrusion of the polymer.

Unfortunately, there is no direct method for measuring the localised temperatures involved (except in idealised experiments - See later), which are generally referred to as 'flash temperatures'. Theoretical estimates are therefore needed, and these necessarily involve many assumptions.

The total asperity contact temperature is given by:

$$T = Ta + Tf$$

where Ta is the mean temperature rise at the sliding interface

and Tf is the flash temperature.

Ta can be calculated from the formula given in Reference 23.

$$Ta = To + R_t \mu P V$$

where To is ambient temperature

R_t is a thermal resistance constant

μ is the coefficient of friction

P is the bearing pressure

and V is the sliding speed.

Values of R_t are between 0.8 and 1.8×10^{-3} $^{o}C.m.s.N^{-1}$ for typical thrust or journal bearing test rigs (23).

Alternatively, it is relatively easy to measure Ta by embedding thermocouples into the bearing materials. Using this method Spurr (69) found close agreement between measured values of Ta and those calculated by Jaeger's analysis (70).

To determine the value of Tf, a number of analyses have been made. The simplest of these were derived by Archard (71) who obtained four general expressions from Jaeger's (70) original analyses to determine the flash temperatures in sliding conditions. The four cases cover plastic and elastic conditions at high or low sliding speeds -

a) $Tf = \frac{\mu g}{J} \left(\frac{\pi pm}{8K}\right)^{\frac{1}{2}} W'^{\frac{1}{2}} V$ (for low speeds and plastic deformation)

b) $Tf = \frac{\mu g}{J} \frac{1}{3.25} \frac{(\pi pm)^{\frac{3}{4}}}{(KQC_s)^{\frac{1}{2}}} W^{\frac{1}{4}} V^{\frac{1}{2}}$ (for high speeds and plastic deformation)

c) $Tf = \frac{\mu g}{J} \frac{1}{8.8K} \left(\frac{E}{r}\right)^{\frac{1}{3}} W^{\frac{2}{3}} V$ (for low speeds and elastic deformation)

d) $Tf = \frac{\mu g}{J} \frac{1}{3.8} \left(\frac{E}{KQC_s r}\right)^{\frac{1}{2}} W^{\frac{1}{2}} V^{\frac{1}{2}}$ (for high speeds and elastic deformation)

where g = acceleration due to gravity

J = mechanical equivalent of heat

K = thermal conductivity

Q = density

C_s = specific heat

r = radius of asperity

Lancaster (27) has further simplified Jaeger's analysis (70) for polymer/steel combinations with the additional assumptions that :

a) since the thermal conductivity of steel is very much greater than that for polymers (See Table 1.1) all the frictionally-generated heat is conducted away through the steel. This then enables the thermal conductivity of the polymer to be taken as zero.

b) the contact is a single circular area

c) the deformation is plastic.

The two derived formulas are -

a) $Tf = 1x10^{-1}{}_{\mu}.pm^{\frac{1}{2}}.W'^{\frac{1}{2}}.V$ (for low speeds)

b) $Tf = 5.7x10^{-5}{}_{\mu}.pm^{\frac{3}{4}}.W'^{\frac{1}{4}}.V^{\frac{1}{2}}$ (for high speeds)

It is also assumed in the above that the polymer hardness remains independent of temperature but a correction factor can be included to offset this. When the calculated values were compared to experimental results, close agreement was found between the conditions at which rapid wear occurred (presumably due to surface flow and extrusion) and the calculated flash temperatures (which corresponds to the glass transition temperatures of the polymers).

The measurement of the actual flash temperatures is very difficult, but various methods have been suggested such as the use of infra-red cells (4,46); observing the change

in structure of the surface layers (46) and by analysis of the gases emitted from the sliding surfaces (72). Most of these are indirect methods of measurement and are therefore not very accurate and most unsuitable for practical situations.

As already mentioned the wear of a polymer is heavily dependent upon the wear counterface and its associated thermal conductivity (26) because of the low thermal conductivities of polymers. The wear rates for polymers sliding on polymers at low speeds are not very much different from those for polymers sliding on metals. Lancaster (26), however, found the critical speeds at which melting occurred to be greatly reduced (e.g. $0.05\,ms^{-1}$ for acetal on acetal compared to $10\,ms^{-1}$ for acetal on steel). Therefore, polymer-polymer sliding combinations are much more restricted in their maximum sliding speeds and loads than polymer-metal sliding combinations.

1.7 POLYMER TRANSFER

If repeated sliding occurs over the same wear track, the wear rate of polymers on metals generally decrease with time until a limiting value is achieved (60). This reduction in the wear rate is usually caused by modification of the counterface topography, and with a small group of polymers, this may occur by the development of a transferred polymer film which adheres to the metal. The transferred film is caused by adhesive wear when the shear strength of the adhesive junctions becomes greater than the bulk shear strength of the material, leading to cohesive failure within the polymer. This transfer may occur on the wear counterface as a thin film a few molecules thick (43, 45, 73-77) or in the form of lumps up to a few microns thick (43, 75-77). The transfer of ductile polymers such as P.T.F.E and polyethylene, which give smooth films, tends to reduce the wear rate. The transfer of more brittle polymers, however, such as polyester or polystyrene, occurs in the form of irregular lumps, and may increase the wear rate (60). The transfer of P.T.F.E. has been studied with x-ray Photoelectron Spectroscopy by Wheeler (73), whilst Pepper (74) has studied P.T.F.E., Polychlorotrifluoroethylene (P.C.T.F.E.) and Polyvinyl chloride (P.V.C.) using Auger electron spectroscopy. The object of Wheeler's work was to determine whether any chemical bonding took place between the polymer and metal. So far no strong evidence has arisen to support this.

It has been shown (43, 75-77) that the transferred layer

of P.T.F.E. becomes preferentially oriented after several traversals and this reduces the coefficient of friction. This behaviour does not seem to depend on the degree of crystallinity or on the width of the crystalline platelets (78) shown in Figure 1.5.

From the results of the work undertaken so far it seems there are two modes of wear for P.T.F.E. -

1) Initial and high speed wear where it has been suggested that wear occurs due to interlamellar shear (See Section 1.2.1 on crystallinity of thermoplastic polymers). This type of wear is associated with a thick transferred film which is relatively loosely attached.

2) Low speed wear where the polymer molecules are oriented in the direction of sliding. Wear then occurs by thin sheets of molecules being drawn out from the bulk material and being transferred to the counterface. This type of wear is associated with a very thin transferred film which is strongly attached to the counterface.

There is still some debate as to the mode of wear for P.T.F.E. and Kar and Bahadur (79) have suggested that interlamellar shear occurs at both low and high sliding speeds.

Pooley and Tabor (43) have attributed the low friction of P.T.F.E. to its smooth molecular profile. They observed

the static initial friction to be much higher than the kinetic friction (0.2 instead of 0.06 at $1x10^{-3}$ ms^{-1}) and attributed this to molecular orientation of the polymer surface during sliding. During the very early stages of wear the polymer is thought to be undergoing bulk shear, which causes high friction, whereas when orientation of the molecules has taken place, there is relatively easy slip between the individual molecular chains. Briscoe (75) found similar results with both P.T.F.E. and high density polyethylene. When one of these polymers began to wear, the friction was high until the polymer pin had progressed approximately one contact diameter. For this initial wear the transfer was relatively thick (about 1 μm) and then became much thinner as the friction decreased. Other semi-crystalline polymers such as low-density polythene, polypropylene and partially perfluoromethylated P.T.F.E., did not show a reduction to the lower friction accompanied with a change in material transfer. In the latter cases the friction remained high with thick transfer and no signs of orientation of the polymer.

The effects of lubricants on polymer transfer are described in Section 1.8.

1.8 LUBRICATION OF POLYMERS

Lubricants are usually used to achieve two main aims, these being a reduction in the coefficient of friction and the wear rate associated with a particular sliding situation. There are four regimes of lubrication and these will be discussed in turn -

1.8.1 Hydrodynamic

The credit for the early work in this field must go to Osborne Reynolds (24) for his concept of the 'physical wedge'. Reynolds proposed that if one plane surface was inclined to another (as in Figure 1.8) and a relative motion imparted between the two, then any fluid between the surfaces would undergo a pressure increase as it moved from the 'entry' to the 'exit'. The pressure between the two surfaces depends upon the viscosity of the fluid, the relative speed between the two surfaces, the distance between the two surfaces and the applied load. This film of fluid between the two surfaces is known as a hydrodynamic film and is essential for the efficient operation of many journal bearings. In hydrodynamic lubrication there is no contact between the two materials and all of the load is supported by the lubricant. The hydrodynamic wedge may occur in the clearance between a shaft and liner (See Figure 1.9) or between surface asperities (80) as shown in Figure 1.10. Along with the necessity of a geometric wedge, hydrodynamic systems require high speeds, high viscosity fluids and relatively light loads.

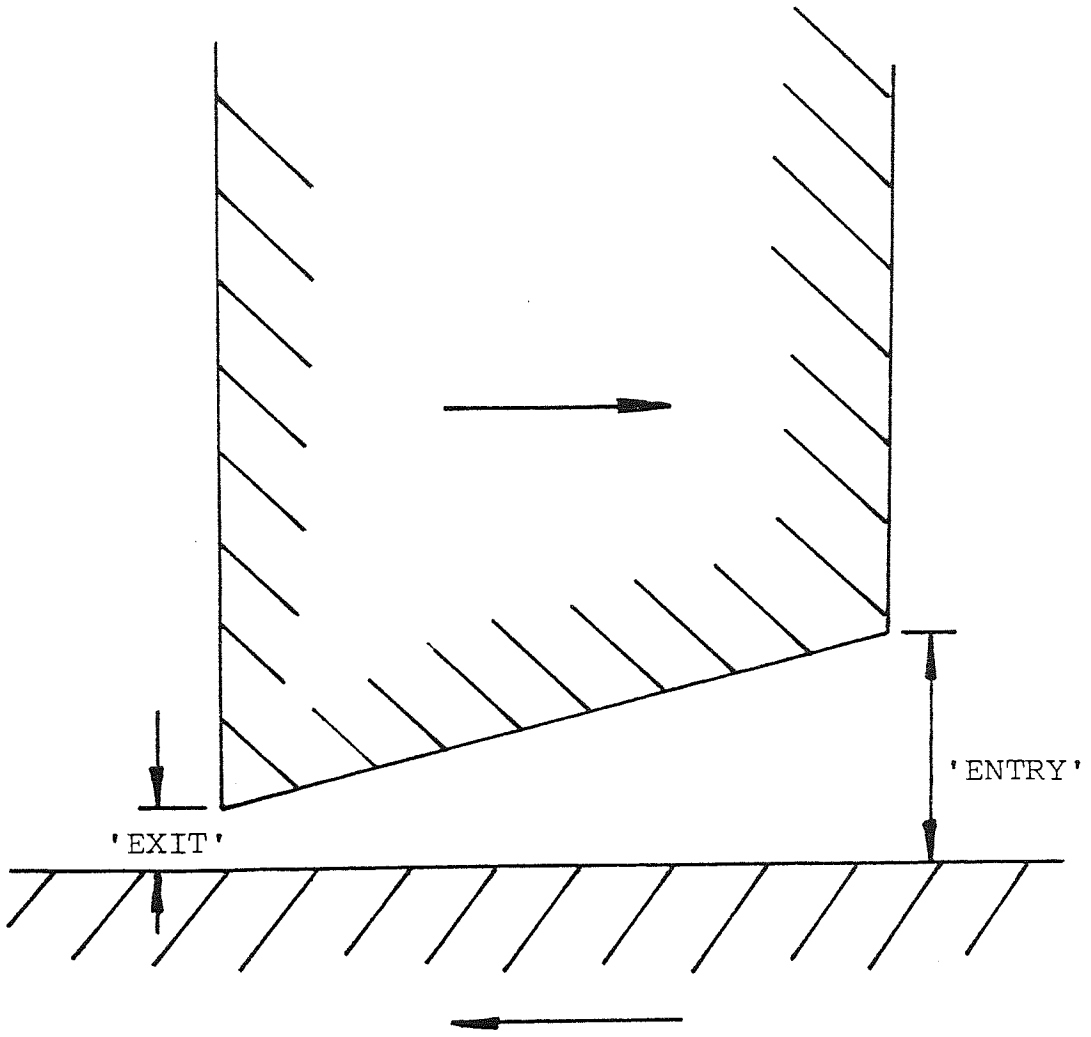

Figure 1.8 General principle of the Hydrodynamic-wedge.

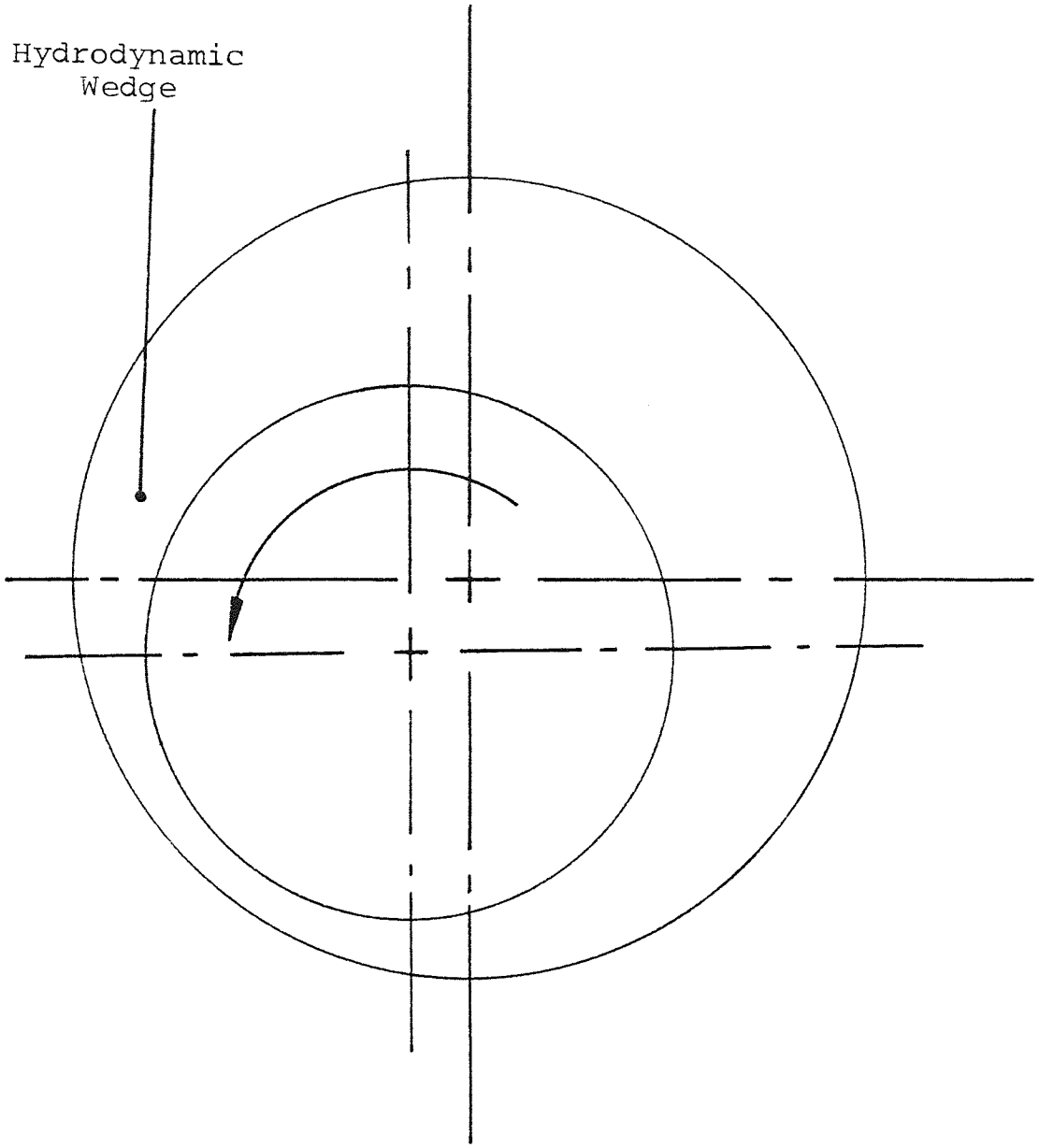

Figure 1.9 The Hydrodynamic Wedge in a journal bearing

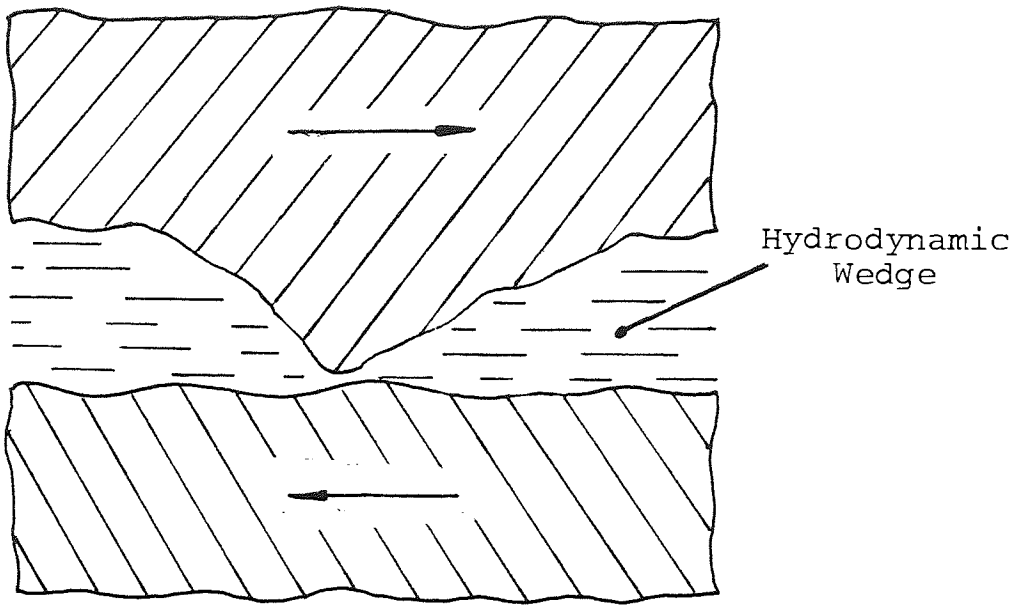

Hydrodynamic

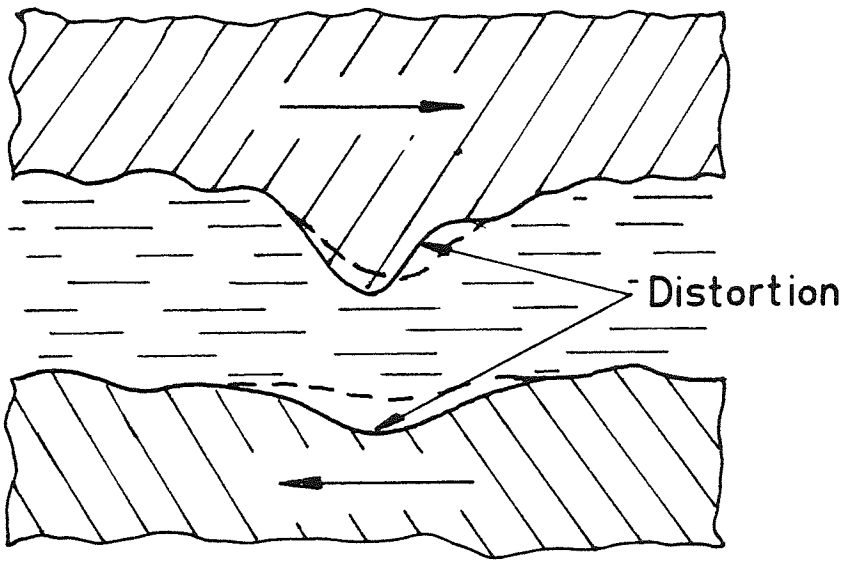

Elastohydrodynamic

Figure 1.10 Representation of Hydrodynamic wedge between asperities

Figure 1.11 Representation of Elastohydrodynamic Lubrication

The amount of fluid film support increases with increasing sliding speed and fluid viscosity and as the opposing surfaces are not in contact then the wear rates are ideally zero (4). The coefficient of friction varies with the sliding speed and the viscosity of the fluid. In general, the higher the viscosity of the fluid then the greater will be the coefficient of friction, as the friction is entirely due to the viscous shearing of the fluid (81). Temperature has an indirect effect on the coefficient of friction because an increase in temperature leads to a decrease in viscosity of the fluid and hence to a decrease in the coefficient of friction. The minimum film thickness for full hydrodynamic lubrication normally exceeds 0.25μm (81).

1.8.2 Elastohydrodynamic

Dowson (81) has defined this regime as -

> "a condition in which the elastic deformation of the bounding solids play a significant role in the hydrodynamic lubrication process."

This regime of lubrication is similar to hydrodynamic lubrication with complete separation of the surfaces by a fluid film. High pressures are transmitted through the fluid film to cause deformation of the opposing surfaces (See Figure 1.11). As the pressure is increased the fluid viscosity increases and greater fluid film support is possible. Elastohydrodynamic lubrication occurs most readily in highly stressed point or line contacts between machine elements such as gears, cams and rolling contact

bearings. For normal engineering contact the film thickness is of the order 0.025μm - 2.5μm (81).

1.8.3. Mixed

Mixed lubrication occurs when the support of the applied load is shared between the fluid film and some contacting asperities (See Figure 1.12). The surfaces are separated by films of molecular proportions and the film thickness ratio can be calculated to give an indication of the lubrication conditions where -

$$\text{film thickness ratio} = \frac{\text{equivalent film thickness (Ft)}}{\text{surface roughness}}$$

where $Ft = 2.65 \dfrac{G^{0.54} U^{0.70}}{X^{0.13}}$ (for a cylinder near a plane surface)

and $Ft = 1.40 \dfrac{(GU)^{0.74}}{(X)^{0.074}}$ (for a sphere near a plane)

where G is a materials parameter
U is a speed parameter
and X is a load parameter

The surface roughness is normally described by a C.L.A. or r.m.s. value (81).

For mixed lubrication conditions the film thickness ratio is normally between 1 and 5, whereas for elastohydrodynamic lubrication this ratio normally exceeds 5 (81).

As there is always some contact between the two surfaces

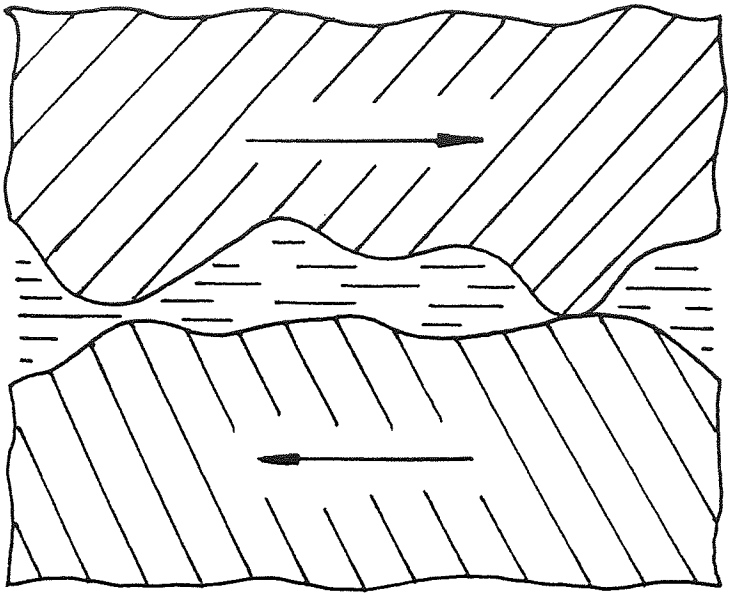

Mixed

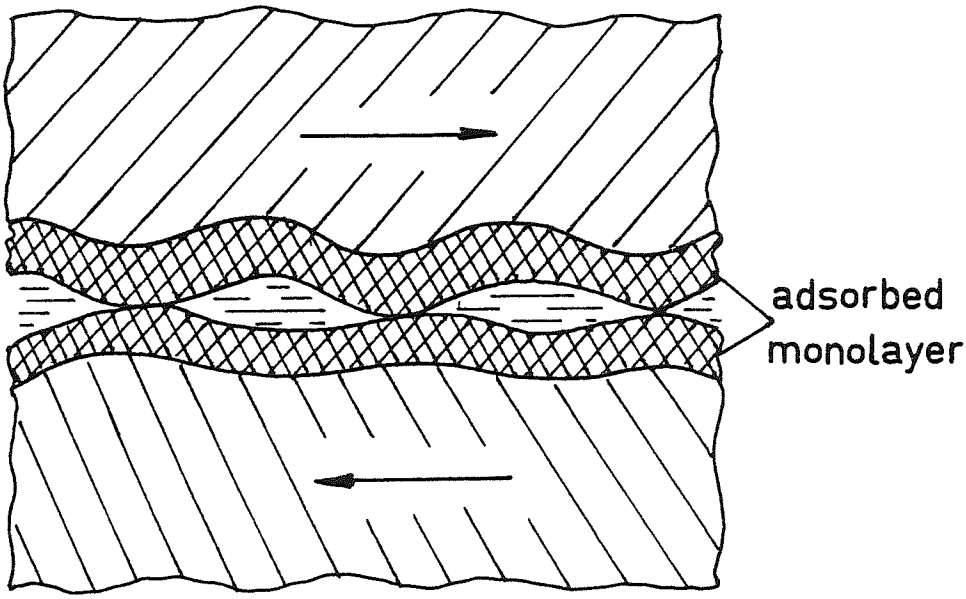

Boundary

Figure 1.12 Representation of Mixed Lubrication

Figure 1.13 Representation of Boundary Lubrication

wear can occur and the coefficient of friction will tend to increase with the amount of such contact.

1.8.4 Boundary

In the boundary lubrication regime hydrodynamic support from the interposing fluid is zero, and in true boundary lubrication the load must be supported by either a chemisorbed or physisorbed layer (See Figure 1.13) covering the contacting asperities (82). Boundary lubrication conditions occur with a combination of low sliding speeds, high loads and low viscosity fluids, and the friction in this regime is virtually independent with changes in these variables (82). One important factor determining the friction is the shear strength of the adhesive junctions. The adsorbed films of organic molecules reduce adhesion and hence friction because shear then occurs within these layers. Polar molecules, such as long-chain fatty acids, are particularly effective on metals because they exhibit both strong adsorption and appreciable lateral cohesion between the chains. In some conditions, there may also be a chemical reaction between fatty acids and metals to form metallic soaps.

By constructing a graph for a particular sliding system, commonly known as a Stribeck curve after the German engineer (83), it is possible to determine the lubrication regime the system is operating in. The curve is a plot of the coefficient of friction against the dimensionless parameter $\frac{nN'}{p}$

where n is the viscosity of the fluid in Nsm^{-2}

N' is the sliding speed in revs per second

and p is the applied pressure in Nm^{-2}

$$= \frac{Ns \times revs \times m^2}{m^2 \quad s \quad N} \qquad \left(\frac{nN'}{p} \text{ has no units by convention} \right)$$

A typical Stribeck curve is shown in Figure 1.14 and the four lubrication regimes are illustrated.

The regime of lubrication in which a sliding system is operating will also be affected by the mechanical characteristics of the opposing surfaces. For example the elastic distortion of the relatively soft articular cartilage which covers the harder bone material has been shown to permit hydrodynamic conditions at much lower values of $\frac{nN'}{p}$ than for rigid surfaces (84). This observation may also be significant in polymer-metal sliding systems where the modulus of elasticity for polymers are much less than for steels. Indeed, one report has already shown that where a metal-metal sliding system would operate in the mixed regime a polymer-metal system operates in the elastohydrodynamic regime under the same conditions (85). This is because the polymer asperities are much more likely to be deformed by the high pressure fluid, and are therefore less likely to come into contact with the opposing metal asperities. The coefficient of friction in the elastohydrodynamic region for polymers will also be less than for metals (86). This is because the limiting pressure will be the flow pressure of the polymer; the fluid viscosity cannot, therefore,

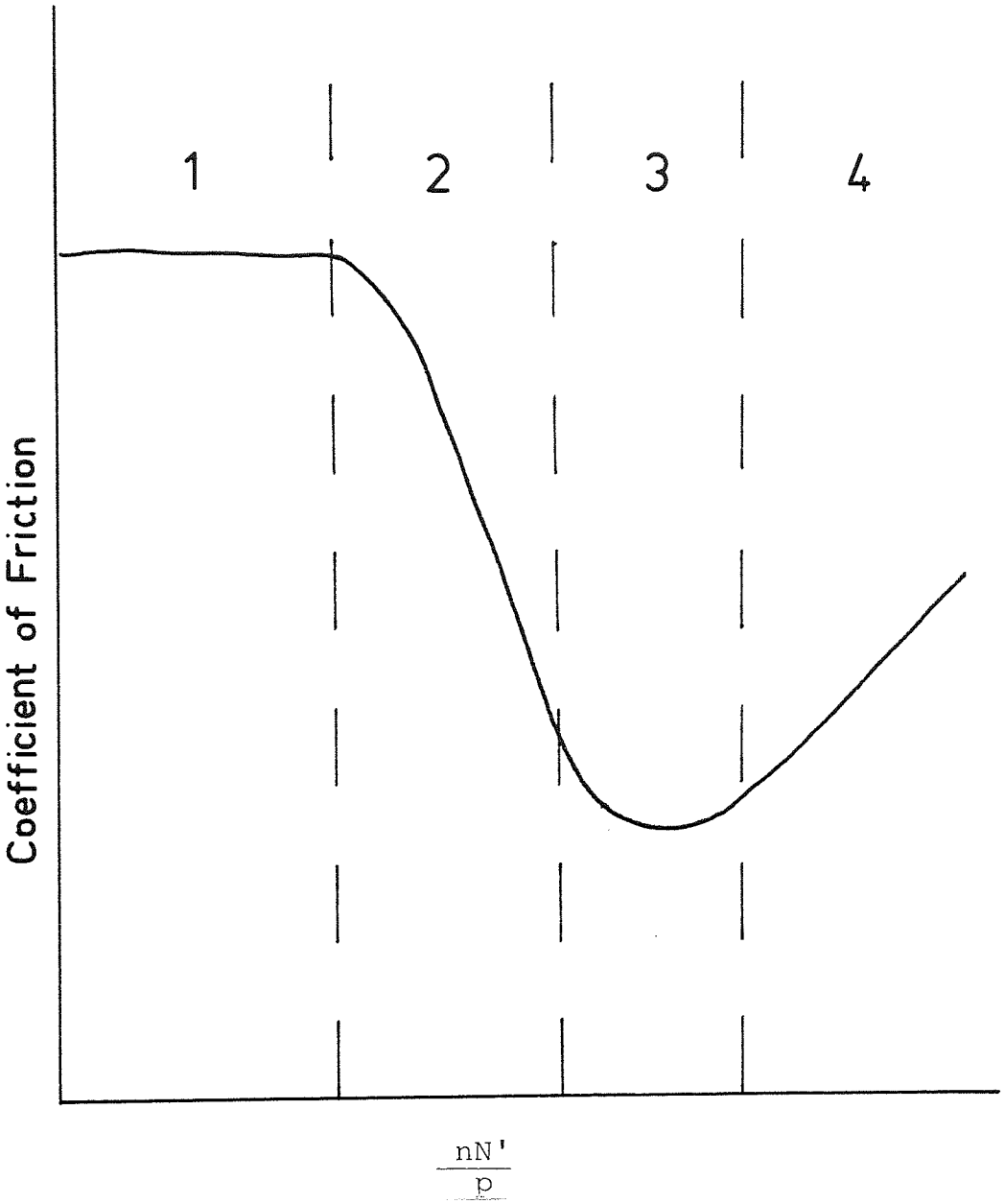

1 Boundary
2 Mixed
3 Elastohydrodynamic
4 Hydrodynamic

Figure 1.14 Typical Stribeck curve showing the different regimes of lubrication

increase sufficiently and so, in turn, the coefficient of friction due to viscous shear remains low.

Although Koutkov (87) has proposed that under sliding conditions, polar active molecules form boundary lubricant films on both polar and non-polar polymer surfaces, the use of a boundary lubricant in a polymer-polymer sliding system does not appear to reduce friction and wear appreciably. This is due to the difficulty in forming a fully condensed adsorbed monolayer on polymers, to prevent asperity contact (88,89). It is also difficult to wet some polymers with lubricants due to their low surface energies. Boundary lubricants, however, do appear to be more useful in polymer-metal systems where the lubricant can interact with the metal (90).

Polymers may contain residual stresses from their processing or stresses may be applied during their service life. This may lead to failure of the polymer by the formation of a crack, this phenomena is known as 'stress-cracking'. In this situation the crack may originate at the polymer surface and migrate into the bulk of the polymer, or may originate beneath (and form perpendicular to) the surface without breaking through the surface. These are known as crazes and can be considered as introducing porosity into the polymer. Some polymers exhibit an increase in stress cracking and crazing in the presence of certain fluids (58,91,92), and this in turn has been shown to give rise to an increase in the wear rate. Other polymers may be plasticised by fluids (93) and this will also affect the

wear rate. In addition polymers which rely on the formation of a transferred-film for low wear may exhibit an increase in wear in the presence of fluids. This is because fluids, and water in particular, impede or completely prevent the formation of transfer films (58). Lubricants, however, generally reduce the wear rates of crystalline polymers (e.g. unfilled P.T.F.E. and polyacetal) and some amorphous polymers (e.g. P.P.O. and Polymethylmethacrylate) (8).

Some polymers absorb fluids (7) (e.g. nylon absorbs water) and this can lead to prolonged periods of lubrication even though excess fluid has been removed. This is because the absorbed fluid is released when necessary to provide the required lubrication. This phenomena has been studied by Booser et al (94) and they found that only very small amounts of lubricant were required to give prolonged periods of lubrication. It is observations such as this that led to the incorporation of fluids into polymers by deliberately mixing-in, discussed in the earlier section (Section 1.3).

1.9 RESEARCH PROGRAM

One of the initial aims of the work described in this dissertation was to examine in more detail the observation of Skelcher (9,10), with respect to fluid retention when P.P.O. is worn against steel in the presence of silicone fluid. Skelcher's work (9,10) has already been mentioned briefly in Section 1.1. Using a wear apparatus specifically designed to operate under conditions of boundary lubrication, he demonstrated that during lubricated wear silicone fluid was absorbed into the P.P.O. and thus was able to provide prolonged periods of lubrication even after all excess fluid had been removed.

With the aid of surface analytical techniques Skelcher (9,10) concluded that the silicone fluid initially penetrated the polymer to a depth of around 10 μm, and continued to penetrate even further during subsequent wear after the excess fluid had been removed. Although, two different mechanisms of fluid penetration were proposed (i.e. direct plasticisation of the polymer surface by the silicone fluid; and cracking of the polymer surface followed by plasticisation). Skelcher considered that the latter mechanism was the most probable.

This observation had possible importance in practical situations where polymer bearings could be pretreated to give low friction in starved lubrication conditions.

The first phase of the present work has used the same

wear-testing machine as used by Skelcher, together with samples of P.P.O. and silicone fluid derived from the same source. This was to ensure consistency in the results. Initial experiments were undertaken to confirm the shape of the Stribeck curve and the relationship between wear rate and sliding speed, and to confirm the existence of penetration of the silicone fluid into the polymer.

As Skelcher (9,10) had proposed that plasticisation was the cause of fluid retention in the polymer, and in the light of experiences of other workers (7,8,93), the second phase of the present work has been to examine other polymers which were unlikely to be plasticised and to see if fluid retention still occurred with these. The two additional polymers chosen were P.T.F.E. and P.E.E.K. both of which are highly resistant to most fluids and unlikely to be plasticised in any conditions.

P.T.F.E. has been an important material in polymer bearings for many years. It has been widely studied and it was therefore possible to compare the results of the present work with those by other workers. Filled P.T.F.E. has indicated some fluid retention in the past (95) when worn against steel in the presence of a petroleum oil. In this case, however, the oil probably penetrated the interface between the filler and the P.T.F.E., rather than penetrating the bulk polymer.

P.E.E.K. is a new engineering polymer and preliminary tests have indicated that it could be used successfully in many

bearing applications because of its high temperature stability and low wear rate.

The complex geometrical design employed by Skelcher (9,10) to maintain conditions of boundary lubrication involved a line contact with high Hertzian stresses. It was suspected that this particular geometrical configuration might have been responsible for the fluid retention observed. In particular, line contact was achieved by rotation of the polymer pin about an axis normal to that of the opposing metal disc (known as the Rotating Line Contact machine) and it has been shown elsewhere that a combination of rotation with sliding can significantly influence wear (75,96,97). The present work has therefore included experiments on a conventional pin on disc machine (known as a Uni-Directional pin on disc machine) with a distributed contact area.

To check on the possible significance of a line contact, as opposed to a distributed contact area, a further line contact apparatus (known as a Reciprocating Line Contact machine) was also used, based on the reciprocation of a metal strip over a rotating ring.

It was decided to construct graphs of friction and wear rate versus speed for both dry and lubricated conditions for each polymer on the Rotating Line Contact and Uni-Directional pin on disc machine. The amount of work involved restricted the friction and wear rate graphs to P.T.F.E. only on the Reciprocating Line Contact machine.

Before Stribeck curves could be constructed for the two line-contact machines it was necessary to know how contact pressure varied with changes in the applied load for each polymer. The contact band-width (2b) can be calculated using a theory by Hertz (98) which can be simplified to:

$$b = \sqrt{4 P' d R}$$

for the case of a hard cylinder loaded against a soft flat surface (as with the two line contact machines).

where P' = load per unit length ($kg\,cm^{-1}$)

$$d = \frac{1 - \nu^2}{\pi E}$$

ν = Poissons ratio for the polymer

E = Young's Modulus for the polymer ($kg\,cm^{-2}$)

R = radius of cylinder (cm)

Unfortunately, there are problems in using the Hertz theory in calculating the contact conditions, these are:

i) There are large differences in the published values for Young's Modulus in polymers. (e.g. P.T.F.E. is quoted at $24.8 \times 10^4\ kNm^{-2}$ and $56 \times 10^4\ kNm^{-2}$) (99).

ii) Young's Modulus of Elasticity for polymers varies with temperature, crystallinity and rate of strain (19).

iii) The Hertz theory is suitable for rectangular contact areas between two cylinders and is therefore only suitable on the Rotating Line Contact machine when small loads give a narrow contact band width. As the

load is increased to a maximum the contact area will tend towards a circular cross-section and this will introduce errors into the calculations.

Therefore, it was thought necessary to measure the contact band widths directly.

It was decided to undertake autoclave experiments to determine any possibility of silicone fluid plasticising or diffusing into the polymers.

It was hoped that the use of physical and chemical analytical techniques would finally elucidate the mechanism of friction and wear for each polymer, and the mechanism of fluid retention; if any. Details of these techniques are provided later.

CHAPTER 2

EXPERIMENTAL DETAILS

2. EXPERIMENTAL DETAILS

2.1 GENERAL DETAILS

The three different wear machines used in the friction and wear experiments are diagrammatically shown in Figure 2.1. The stress situations on the Rotating Line Contact and Reciprocating Line Contact machines are much more complex than on the single pin on disc machine (Uni-Directional pin on disc machine). It has been shown before (e.g.100) that indentation by a hard sphere may produce a circular crack in the surface of brittle materials. This is because the stresses under the centre of the sphere are compressive, whilst the stresses at the circumference of the contact are tensile (See Figure 2.2a). This situation is similar to the stress distribution on the two line contact machines, however, a cylinder instead of a sphere is loaded against a plane surface and the stress distribution is slightly modified as in Figure 2.2b.

As the stresses are higher on the two line contact machines than on the Uni-Directional pin on disc machine for the same load, cracks may occur more readily in the surface, and this was one of the main reasons for using the Uni-Directional pin on disc machine to compare results for the two different types of configurations. It has been shown that by applying a tangential force to a sphere the cracks produced are hemispherical (91) and the critical load for cracking is reduced as the coefficient of friction is increased (101). It was therefore hoped that studies of the

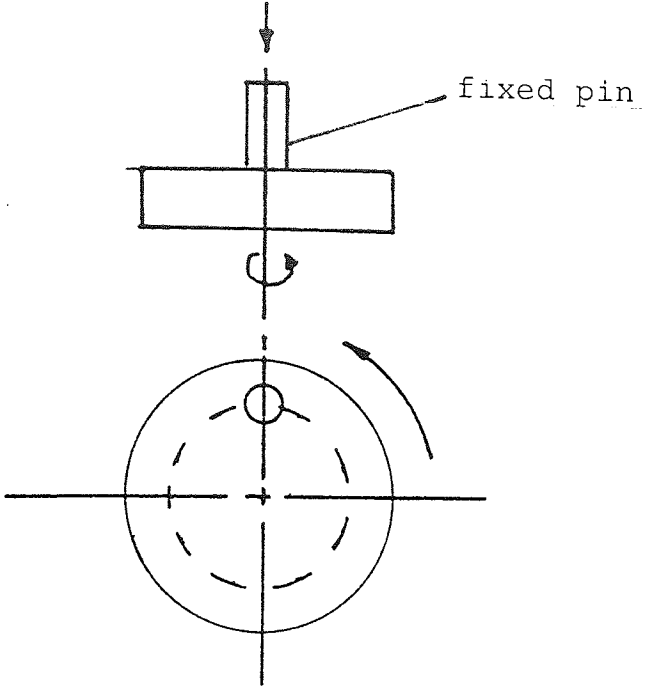

a) Uni-Directional Pin on Disc Machine

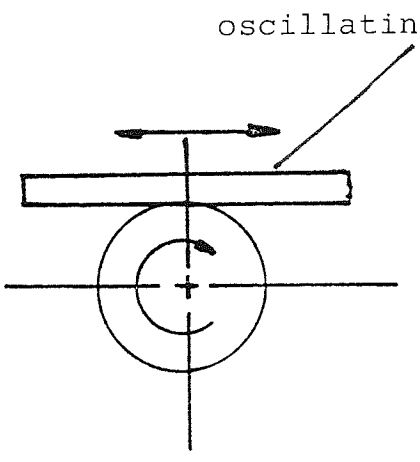

b) Reciprocating Line Contact Machine

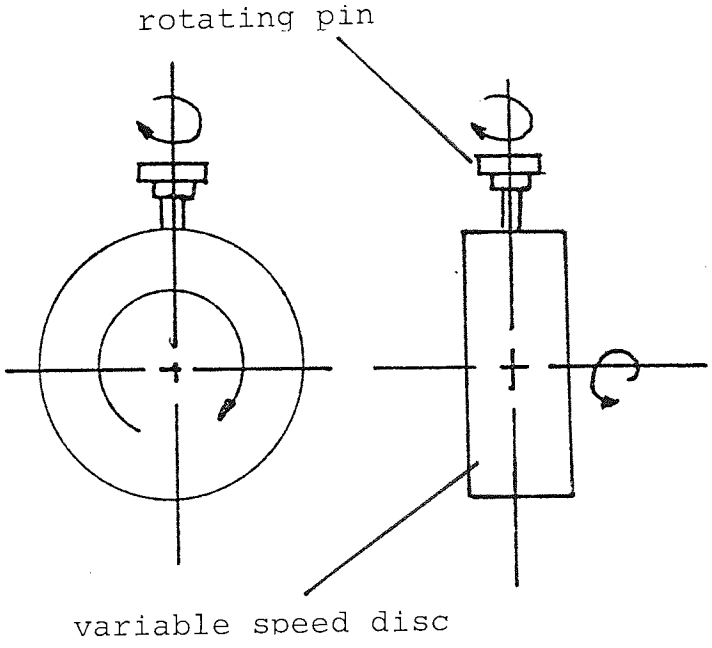

c) Rotating Line Contact Machine

FIGURE 2.1 The Three Wear Configurations

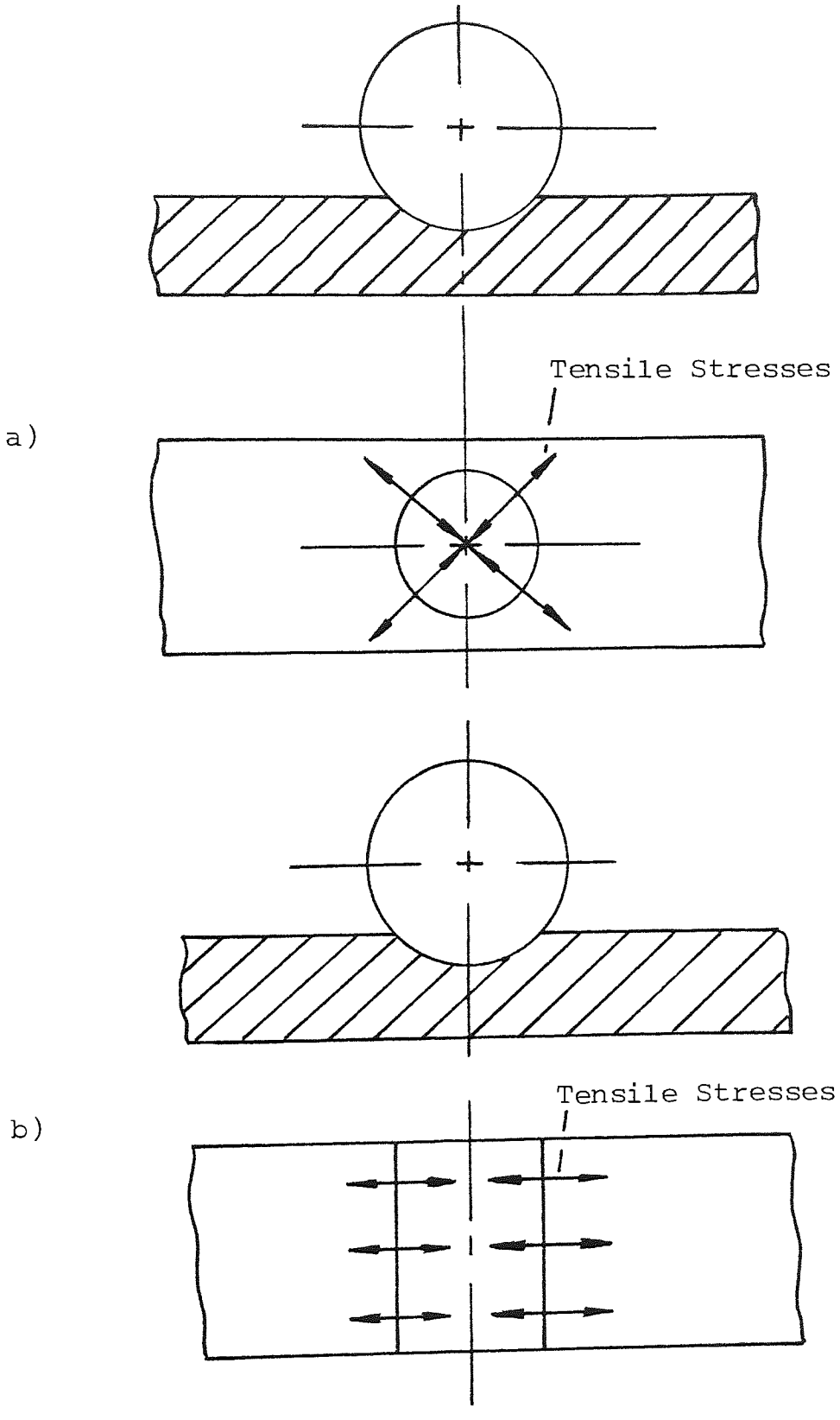

Figure 2.2 Stress situations for:

(a) a sphere and

(b) a cylinder on a plane surface

polymer wear surface from the two line contact machines would indicate whether surface cracking was occurring during sliding.

The analyses of worn specimens and wear debris were undertaken on the Scanning Electron Microscope, described in Section 2.9.1.

2.2 ROTATING LINE CONTACT MACHINE

2.2.1 General Features

This machine is shown in Figure 2.3a and maintains nominal Hertzian line-contact conditions throughout the experiment, irrespective of wear. This feature minimises the possibility of hydrodynamic lubrication and maximises the possibility of boundary lubrication over a wide speed range.

Essentially a cylindrical polymer pin is loaded against a rotating metal ring which is in turn mounted on a special holder fitted to a commercially available lathe.

Continuous lubrication is possible except at speeds greater than 1 ms^{-1}, whereupon, the lubrication begins to break down as fluid is flung off the disc.

Friction and wear may be continuously monitored and recorded using a variable speed chart recorder.

2.2.2 Wear Counterface

The outer races of commercially available bearings made from EN31 (containing $\simeq$ 1% C, $\simeq$ 1.5% Cr) and hardened to $\simeq$ 700 V.P.N. were used for all friction and wear experiments.

A surface roughness of 0.1μm C.L.A. (Centre Line Average) was obtained on the counterface surfaces by randomly abrading first with 180 grade silicon carbide paper (mean

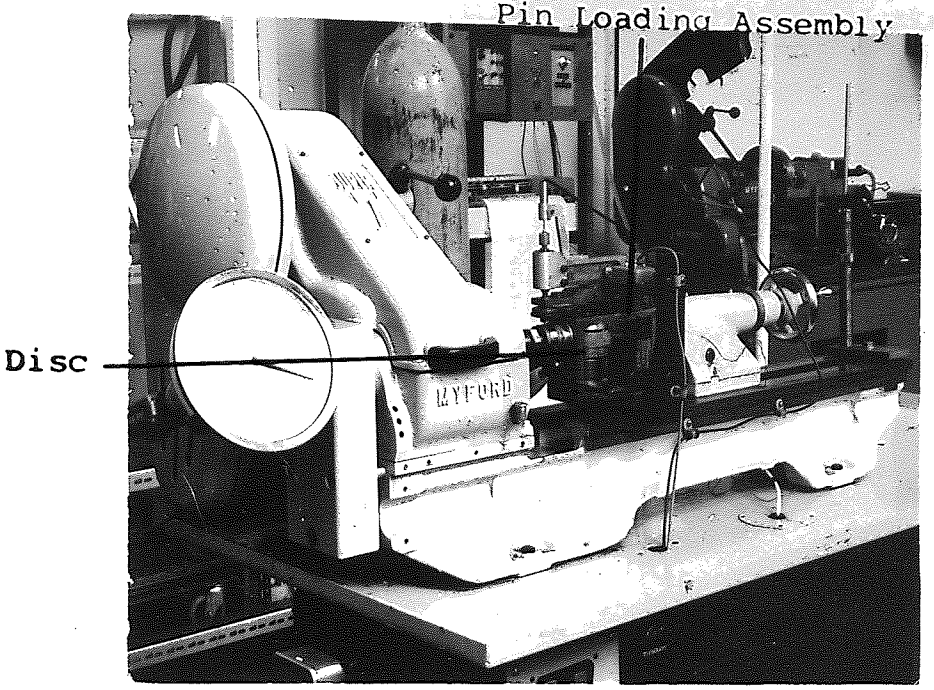

(a)

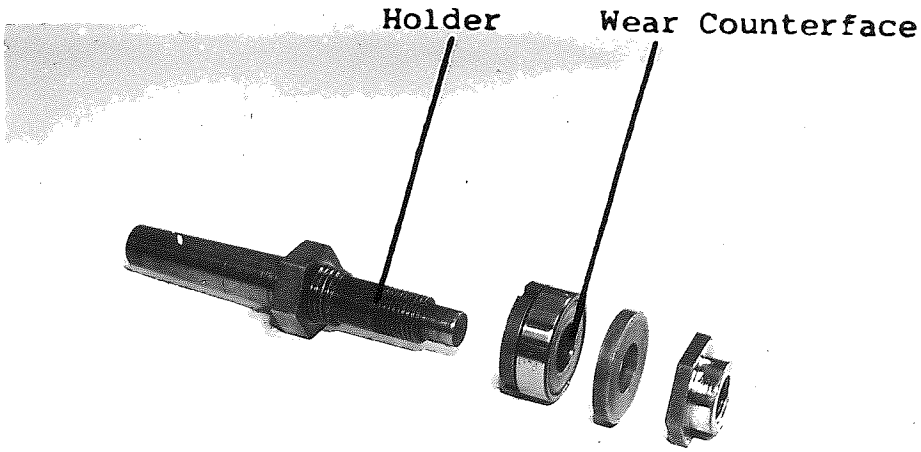

(b)

FIGURE 2.3a General view of the Rotating Line Contact machine

FIGURE 2.3b Wear counterface and holder for the Rotating Line Contact machine

particle size 74μm) and then 240 grade silicon carbide paper (particle size 53μm). The bearing races were then ultrasonically cleaned in a solvent to remove any surface debris from the polishing process. Acetone was originally used for washing but as impurities* were occasionally left behind the solvent was changed to Iso-propyl alcohol. The wear counterface was an interference fit onto a notched holder, which in turn was mounted onto a Morse taper using a washer and cap nut (See Figure 2.3b). One end of the taper was then located in the headstock, whilst the other end was fitted into the front bearing in the main frame of the pin loading assembly. A splash washer was used between the bearing race holder and the front bearing of the main frame, to prevent any contamination of the wear counterface. An extractor was used to remove the bearing race from the holder (See Figure 2.4a).

2.2.3 Wear Pins and Holder

The pins were machined on a lathe into a 3-tier shape so that the largest tier had a diameter of 6 mm. This tier was used to locate and fix the pin to the pin holder. The smallest tier had a diameter of 2 mm and its plane surface was worn against the wear counterface. The middle tier was simply for strengthening purposes.

The pin holder comprised two major parts:-

i) The final drive gear and pin clamp; and

ii) The supporting shaft

* impurities from the original acetone

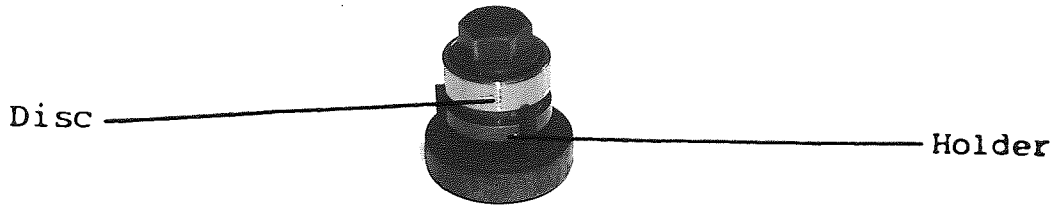

(a)

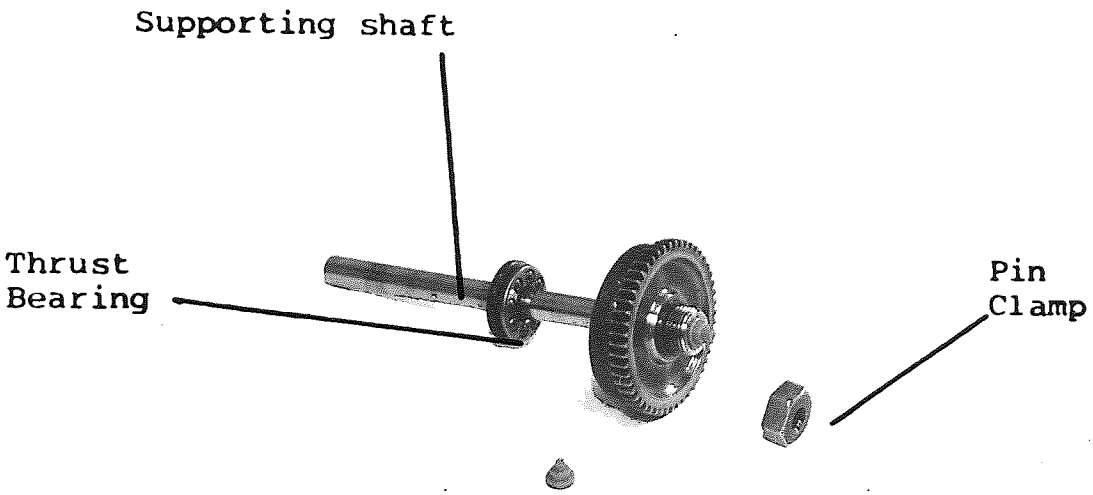

(b)

FIGURE 2.4a Wear counterface and Extractor

FIGURE 2.4b Wear pin and holder

The final drive gear was made of brass and contained a thrust bearing housing on one side and the pin clamp on the other (See Figure 2.4b).

The supporting shaft was made from hardened and ground silver steel which fitted into the final drive gear with an interference fit.

2.2.4 Measurement of Wear

The supporting shaft on the pin holder was connected to a liner voltage-displacement transducer, which continuously monitored any vertical movement of the pin and hence any wear. The transducer response was linear over 1 mm of movement with a rated error of 0.3% and had a zero shift of less than $0.008\%\ ^{o}C^{-1}$. The armature of the transducer was 'free-moving' enabling it to rotate and move linearly simultaneously. The transducer was connected to an oscillator demodulator unit with adjustable span and zero controls. The output signal from this unit was fed into one input of a double channel chart recorder.

Since a nonconforming geometry was used the pin surface remained flat, and it was a simple matter to calculate volume removal from the linear displacement of the pin during wear.

Wear rates were usually calculated after a number of counterface revolutions ($\simeq$ 1000) when steady state wear was occurring.

2.2.5 Measurement of Friction

The complete pin-loading assembly was pivoted about the axis of rotation of the counterface and finely balanced in the vertical position. Therefore any movement of the pin loading assembly was caused solely by the frictional force between the wear pin and the counterface (See Figure 2.5a). This frictional force was measured by a commercially available Tensile/Compressive Load Transducer, and was designed to measure steady and rapidly fluctuating tensile or compressive forces. The transducer was mounted in a horizontal position, using an upright support connected to the lathe bed, and was positioned a distance of three times the radius of the wear counterface above the axis of rotation. Therefore, the recorded friction had to be multiplied by a factor of three to obtain the actual value.

The output signal from the transducer was fed into an amplifier and then to the second input of the chart recorder previously mentioned in 2.2.4. Therefore, like the wear measurements a continuous record of the friction values was obtained. The transducer range was $\pm$450 grams with a maximum excursion of the sensing armature at 40μm.

A slight amount of friction was produced in the front and rear bearings of the pin-loading assembly (0.4 to 4% of contact friction over the complete speed range). This bearing friction was measured by rotating the counterface with the pin in the no-load position and then used as a 'zero'.

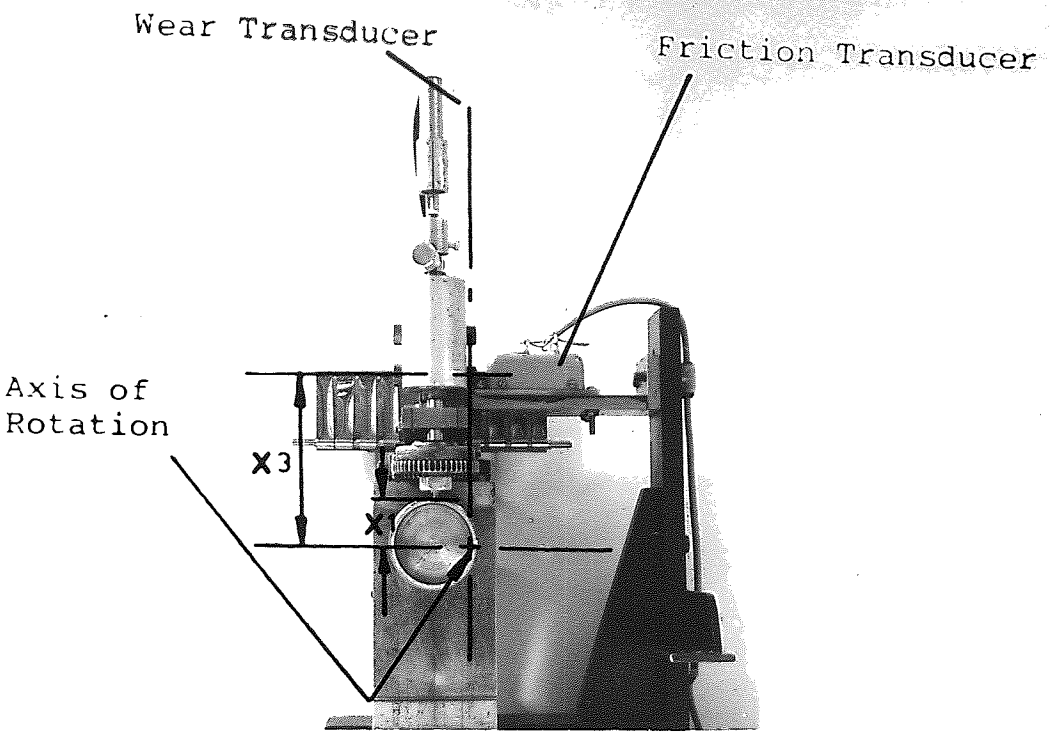

(a)

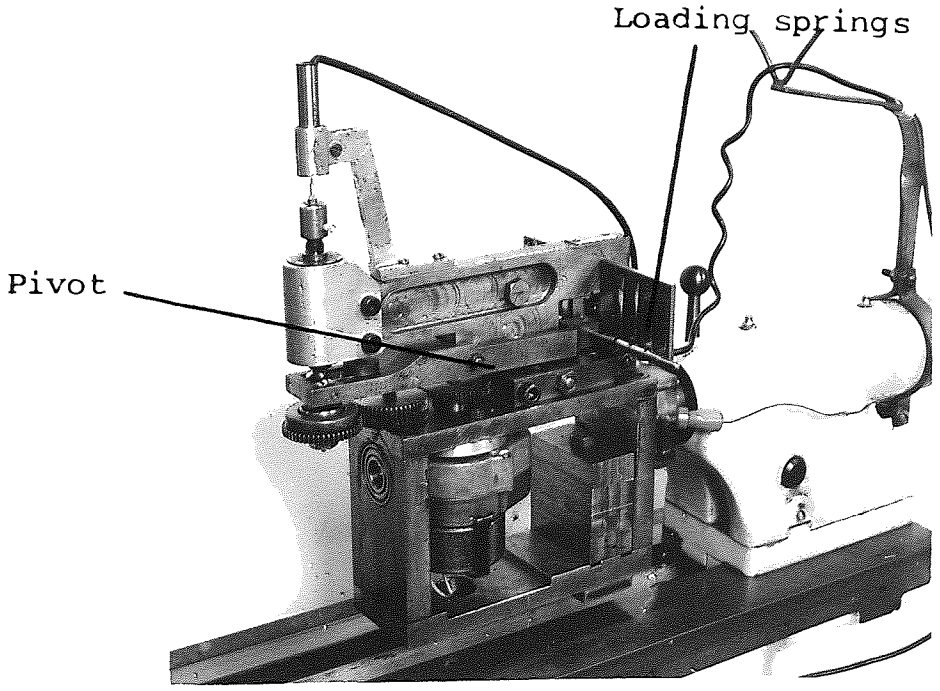

(b)

FIGURE 2.5a Measurement of Friction

FIGURE 2.5b Pin loading assembly

2.2.6 Load Application

The load was applied by a bank of "constant force" springs via a pivot and fork mechanism and remained constant irrespective of vertical pin movement due to wear (See Figure 2.5b). Each pair of springs provided 5 N load, therefore, it was possible to use loads of 5 N, 10 N, 15 N and 20 N. An additional lead weight of 1 N increased the load range available. These springs were easily added by passing a rod through the centre of the coiled part of the spring. Two small plain bearings were mounted horizontally at the end of the fork so that they pressed down on top of the thrust washer. This enabled the load to be transmitted to the pin holder whilst also allowing it to rotate.

2.2.7 Rotary Motion of Pin and Counterface

The supporting shaft of the pin holder was located in two combination bearings, so that the pin holder could move freely in the vertical plane whilst rotating. The pin holder was driven by a 5 r.p.m. synchronous motor through a 1 : 1 gear ratio with an idler gear in between.

Rotation of the pin caused wear to occur uniformly over the plane end of the pin and hence approximate line contact conditions were maintained irrespective of the extent of wear.

The counterface had a continuously variable range of speeds, from 1×10^{-3} ms^{-1} to 10 ms^{-1}. This was obtained by the use of a 0.25 kW, 1400 r.p.m., D.C. motor with thyristor speed

controller. An additional pulley and gearing system was also used to increase the range of speeds from the motor.

2.2.8 Lubricant Application

The lubricant was applied by allowing the bottom of the counterface to be immersed in a bath of the silicone fluid. This method of application was suitable over a wide range of speeds. However, at speeds greater than 1 ms^{-1} the fluid tended to fly off the counterface and lubrication was impossible to maintain.

2.2.9 Contact Band Width Measurements

These were accomplished by making a special counterface holder and replacing the normal steel counterface with one made of pyrex glass (See Figure 2.6a). When the glass counterface was in position the pin was loaded against it and the whole pin-loading assembly rotated through 90^{o} (See Figure 2.6b). This enabled a travelling microscope to be used for measuring the contact band width directly*. A camera was used to make a permanent record of the results. This process was repeated for each polymer at various loads.

* static bands

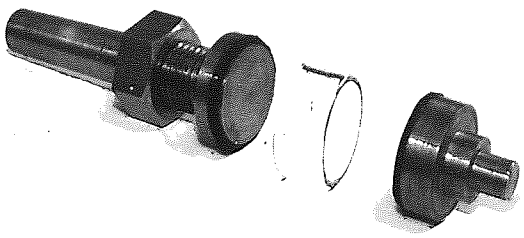

(a)

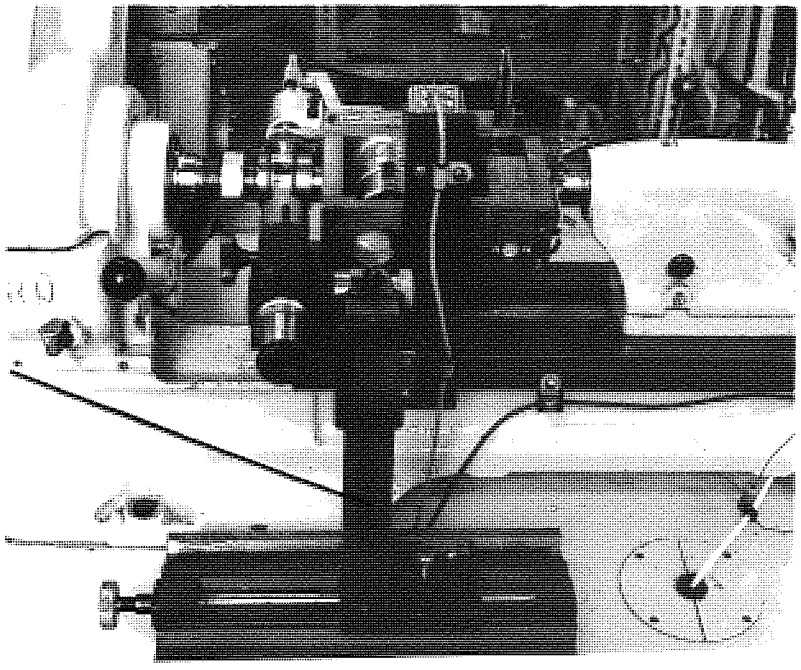

(b)

FIGURE 2.6a Glass disc and holder for the contact band width measurements

FIGURE 2.6b Measuring the contact band width on the Rotating Line Contact machine

2.3 UNI-DIRECTIONAL PIN ON DISC MACHINE

2.3.1 General Features

This equipment is based upon a single pin on disc design. The counterface consists of a large flat disc which is fixed to the face plate of a commercially available lathe. A cylindrical pin is loaded against the counterface and can be run dry or lubricated (See Figure 2.7a).

Friction and wear may be continuously monitored and recorded using a variable speed chart recorder.

2.3.2 Wear Counterface

The wear counterface consisted of a large hardened, and ground steel disc, made of E.N.31 (Containing ≈ 1% C, ≈ 1.5 % Cr).

Counterface preparation was exactly similar to the previous cases. However, the counterface was bolted to the face plate of the lathe with four cap-head screws.

2.3.3. Wear Pins and Holder

The wear pins were machined into a cylindrical form having a diameter of 2 mm and the plane end of the pin was worn against the counterface.

The pins were held in a specially designed collet which

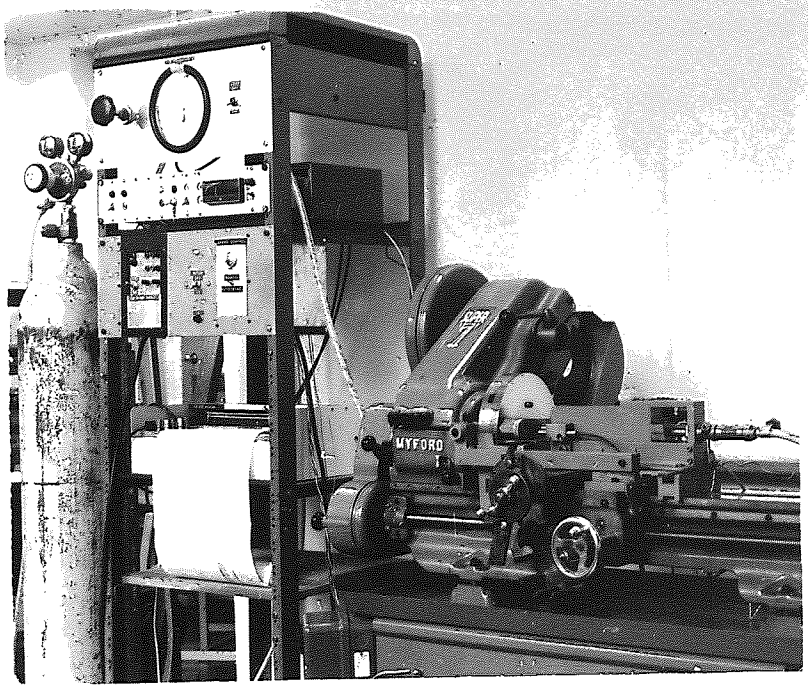

(a)

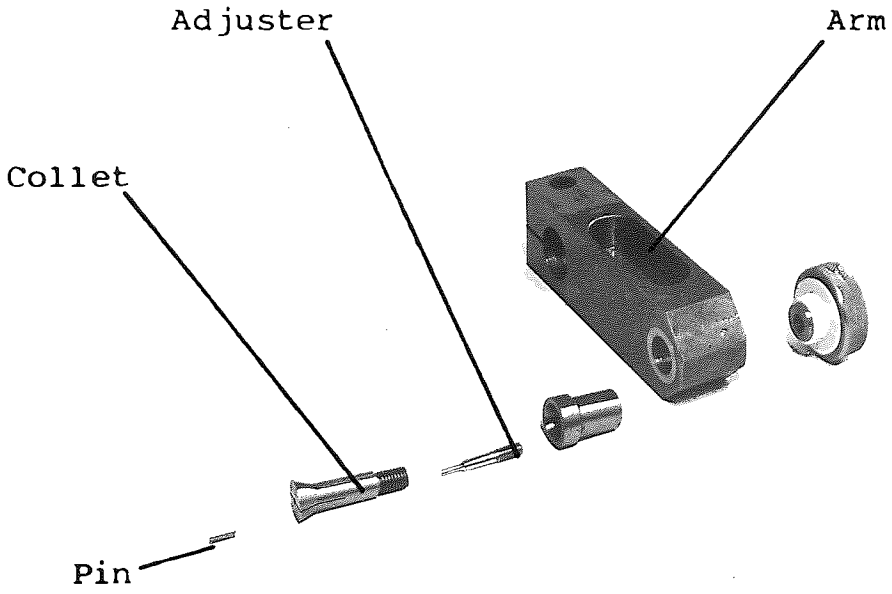

(b)

FIGURE 2.7a General view of the Uni-Directional pin on disc machine

FIGURE 2.7b Wear pin and holder

was mounted in a cranked arm fixed to the loading ram (See Figure 2.7b).

2.3.4 Measurement of Wear

The pin wear was continuously monitored by a linear voltage displacement transducer (See Figure 2.8). This detected any horizontal movement of the cranked arm which was in turn connected to the loading ram. The transducer response was linear over 1.5 mm of movement with a rated error of 0.3%.

The transducer was connected to an oscillator demodulator unit with adjustable span and zero controls. The output signal from this unit was fed into one input of a double channel chart recorder.

As the wear surface was circular the volume removed was calculated by multiplying this area by the transducer displacement.

As with the Rotating Line Contact machine the wear rate was calculated after a number of counterface revolutions ($\simeq$ 100) when steady state wear was occurring.

2.3.5 Measurement of Friction

The loading ram was located in a series of combination bearings which allowed horizontal movement when the pin was wearing, and rotational movement due to the frictional

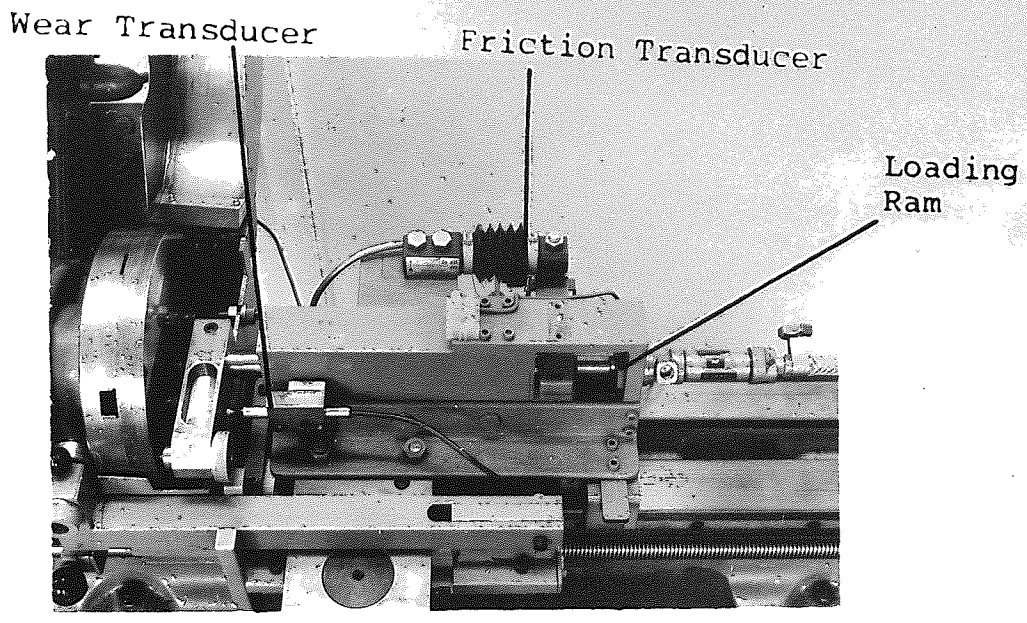

FIGURE 2.8 Loading unit and Transducers

force of the pin on disc. At each end of the loading ram was situated a cranked arm. The front arm was used to locate and hold the wear pin whilst the rear arm was used to transmit the frictional force to the beam load cell (See Figure 2.8). This beam load cell had a maximum capacity of 10 kg and was connected to an amplifier and then into the second channel of the chart recorder previously mentioned in 2.3.4.

The friction was monitored during a no load run and this was used as a zero for further experiments.

2.3.6 Load Application

The loading ram was operated by a compressed air system comprising:-

1) Air bottle with valve and gauges
2) Secondary valve and gauge
3) Air operated piston
4) On / Off switch.

The unit used could vary the load between 0 and 15 kg. However, 2.1 kg was used throughout the majority of the experiments.

2.3.7 Motion of Pin and Counterface

The pin was essentially stationary throughout the experiment when under load. The only pin movements were:-

i) Horizontal movement to allow for wear; and

ii) Rotational movement about the axis of the loading ram due to small fluctuations in the frictional force.

The counterface had a continuously variable range of speeds from $6x10^{-4}$ ms^{-1} - 8 ms^{-1}, when a 0.16 m diameter wear track was used. This speed range was achieved by the use of a 0.56 kW, 1500 r.p.m., D.C. motor, and thyristor speed controller. An additional pulley and gearing system was also used to increase the range of speeds from the motor.

2.3.8 Lubricant Application

Continuous lubrication was obtained by the use of a vane type electrical pump which transmitted the silicone fluid from the collector to the disc along butyl rubber tubes. A drip feed from a burette was also used successfully for short experiments.

A maximum speed of 1 ms^{-1} was used for lubricated experiments due to the difficulty in maintaining the fluid on the wear counterface.

2.4 RECIPROCATING LINE CONTACT MACHINE

2.4.1 General Features

This equipment has been comprehensively described by Lancaster (102, 103). The resulting geometry is similar to the Rotating Line Contact machine in that Hertzian line contact conditions are maintained throughout the experiment.

The equipment consists of three major units (See Figure 2.9a), these being:-

1) Drive motor complete with variable speed gearbox
2) Counterface holder and torque transducer
3) Specimen holder and loading unit.

Continuous lubrication was possible over a wide range of speeds.

Friction and wear were continuously monitored and recorded using a variable speed chart recorder.

2.4.2 Wear Counterface

The counterface used on this machine was the same as that used on the Rotating Line Contact machine, and the two were often interchanged. Counterface preparation was also the same with the bearing race being fitted to a notched holder which was identical to the one used on the Rotating Line Contact machine.

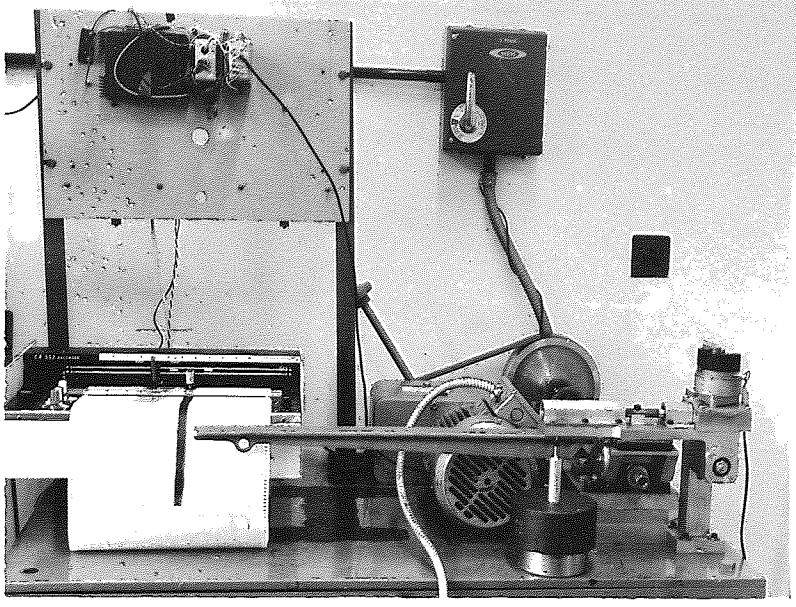

(a)

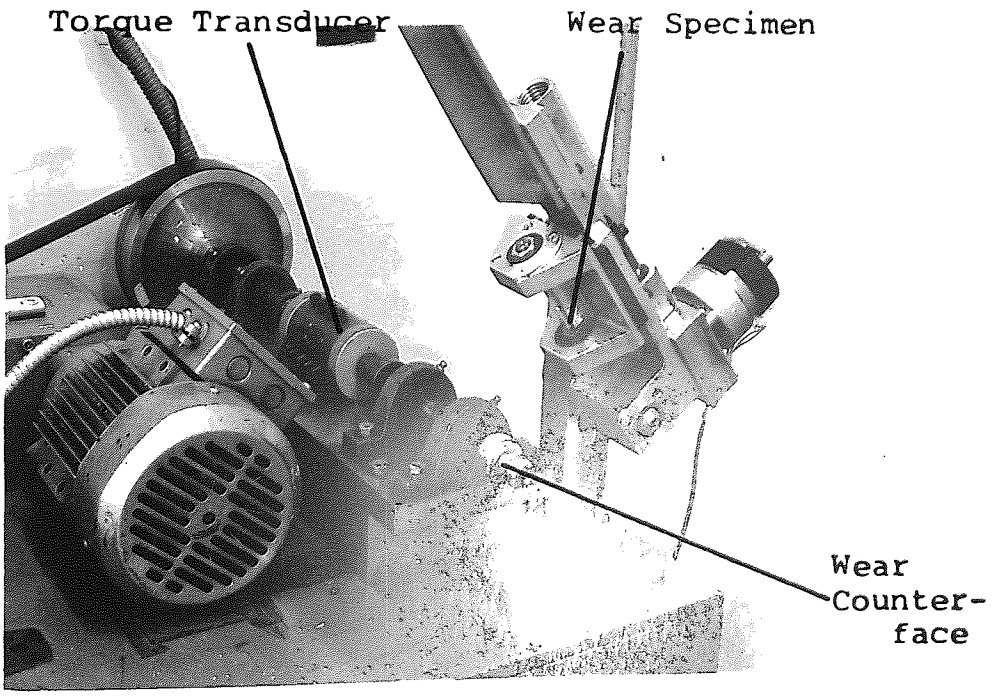

(b)

FIGURE 2.9a General view of the Reciprocating Line Contact Machine

FIGURE 2.9b Wear counterface holder and torque transducer

However, the counterface holder was mounted directly onto one of the shafts of the torque transducer and held in position by a nut and spacers (See Figure 2.9b).

2.4.3 Wear Specimen and Holder

The wear specimen was made from a strip measuring 3 mm thick, 6.35 mm wide and 50 mm long. These test strips were machined to the correct dimensions and a counter sunk hole added at each end to enable the strip to be mounted on the specimen holder (See Figure 2.10a).

The specimen holder was made of stainless steel and located accurately into the sliding carriageway which provided the reciprocating motion.

2.4.4 Measurement of Wear

The wear on the test strip was continuously monitored by a Linear voltage displacement transducer. This was positioned to detect any vertical movement of the loading arm which was directly attributable to wear. The transducer response was linear over 1.5 mm of movement with a rated error of 0.3%.

The transducer was connected to an oscillator demodulator unit with adjustable span and zero controls. The output signal from this unit was fed into one input of a double channel chart recorder.

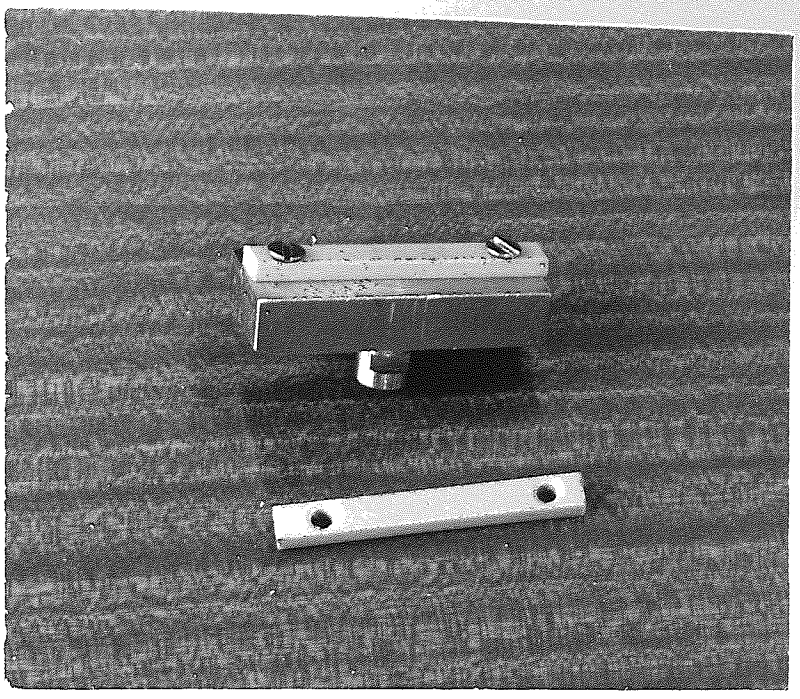

(a)

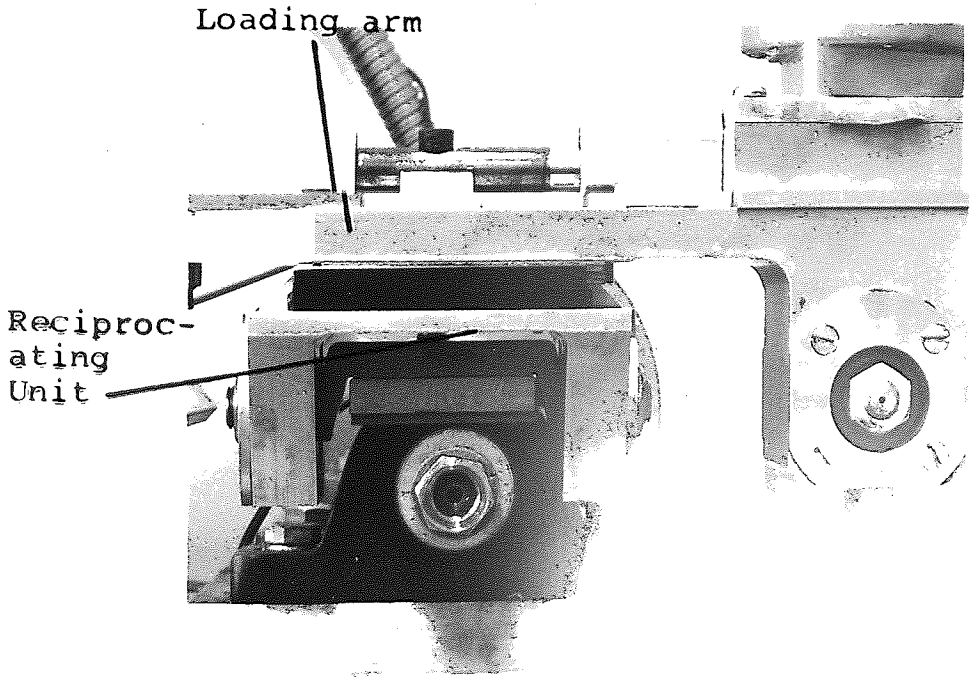

(b)

FIGURE 2.10a Wear specimen and holder

FIGURE 2.10b Reciprocating unit and Loading arm

As the wear surface consisted of a rectangle the volume removed was calculated by multiplying this area by the transducer displacement.

As with the Rotating Line Contact machine the wear rate was calculated after a number of counterface revolutions ($\simeq$ 1000) when steady state wear was occurring.

2.4.5 Measurement of Friction

The drive from the motor and gearbox was transmitted via a torque transducer to the counterface. This torque transducer continuously monitored the frictional force between the strip and counterface. The torque transducer was connected to an amplifier and then to the second input of the chart recorder previously mentioned in 2.4.4.

The friction was monitored during a no-load run and this was used as a zero for further experiments.

2.4.6 Load Application

The specimen holder was mounted underneath the sliding carriage which provided the reciprocating motion. This sliding carriage was pivoted about a fixed point so that movement in the vertical plane due to wear could be accommodated. The load on the specimen was 2.5 kg when the specimen holder and loading unit were resting on the counterface. This load could be increased to 9 kg by the addition of a 6:1 loading arm and thereafter to a maximum

of 45 kg by the addition of weights on the end of the arm.

Uniformity of loading along the contact line was ensured by allowing the specimen holder to pivot about an axis at right angles to that of the counterface cylinder. The specimen holder was cranked so that the pivot axis and sliding interface were co-planar (See Figure 2.10b).

2.4.7 Motion of Specimen and Counterface

The specimen holder was slowly reciprocated on rolling element slides (3 c.p.m.) over a stroke length of 12.5 mm by means of an electrically driven cam.

A 0.75 kW motor with a 11.3 Joules rating drove the variable speed gearbox to give a speed range of 0-400 r.p.m. This was then transmitted through a belt and pulley system with a 5:1 drive ratio, increasing the range to 0-2,000 r.p.m. The final useful speed range was therefore 3×10^{-3} ms^{-1} to 3 ms^{-1}.

2.4.8 Lubricant Application

The lubricant was applied by allowing the bottom of the counterface to be immersed in a bath of silicone fluid. This method of application was suitable over a wide range of speeds. However, like the Rotating Line Contact machine at speeds greater than 1 ms^{-1} the fluid tended to fly off the counterface.

2.4.9 Contact Band Width Measurements

A light source was set up to illuminate the area of contact between the counterface and specimen. This contact area was then viewed with a travelling microscope and the distance between the extremities of this area was measured by use of a vernier scale. This process was repeated for each polymer at various loads.

2.5 MATERIALS USED

2.5.1 Polymers

The three polymers used throughout the experiments were Poly (2,6-Dimethyl 1,4-Phenylene Oxide) (P.P.O.), Polyetheretherketone (P.E.E.K.), and Polytetrafluorethylene (P.T.F.E.). The chemical structures and formulas are shown in Figure 2.11.

P.P.O. has a rigid molecular structure and a Tg of 208^{o}C (13) and a Tm of 257^{o}C. Because of the small difference in Tg and Tm there is little time for crystallisation to occur on cooling from the melt, and processed polymer is usually amorphous. Crystalline P.P.O. however, has been prepared under certain closely confined conditions (104).

The solubility parameter is of the order 18.4-19 MPa$^{\frac{1}{2}}$; and the polymer is dissolved by halogenated and aromatic hydrocarbons of similar solubility parameter (13).

P.P.O. has exceptional dimensional stability amongst the engineering polymers, but the main disadvantage is in the difficulty of processing which is undertaken at 280-330^{o}C with heated moulds at 100-250^{o}C.

P.E.E.K. is a new high performance polymer developed by I.C.I. with a Tg of 143^{o}C and a high Tm of 334^{o}C. The maximum crystallinity of P.E.E.K. is 48% but the specimens used in the present wear experiments had a crystallinity

P.P.O.

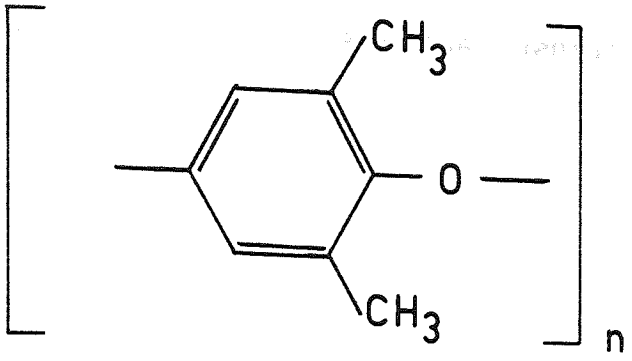

$[C_8H_8O]_n$

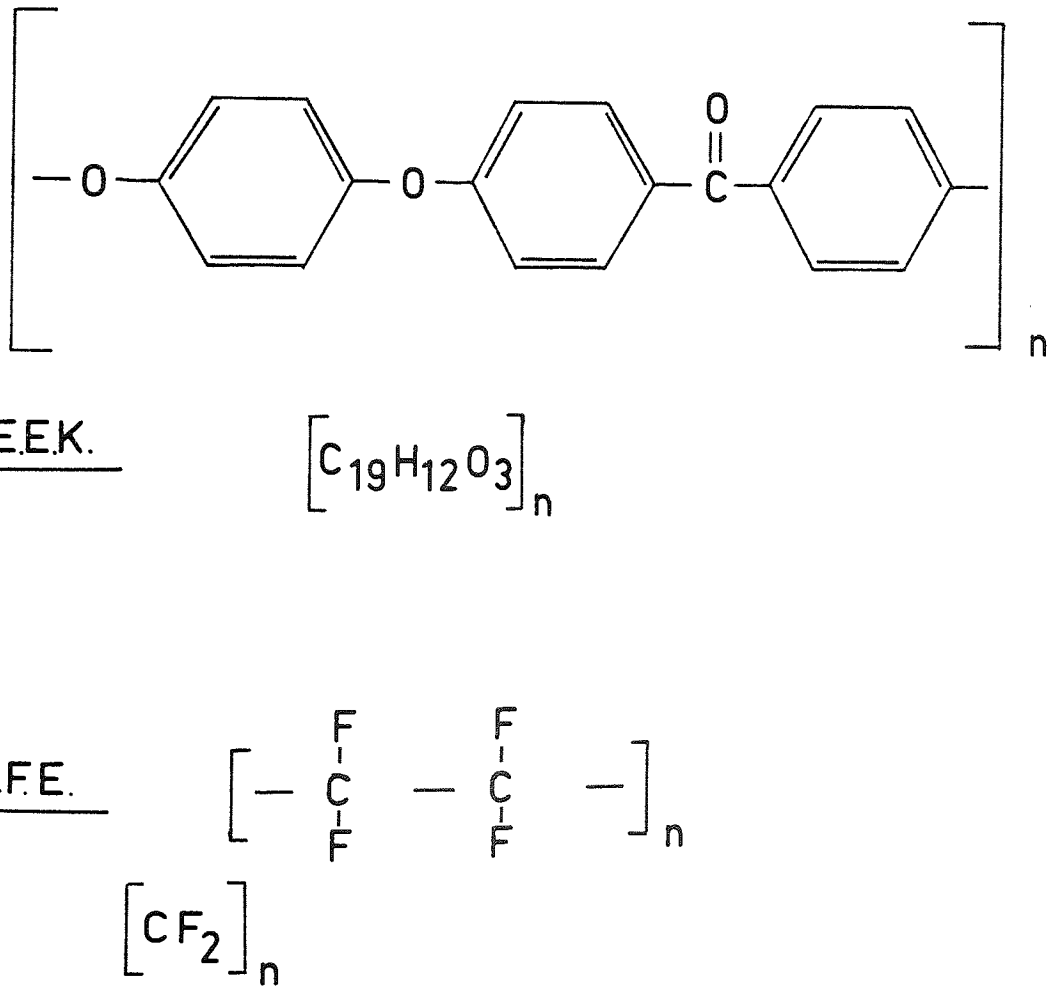

P.E.E.K. $[C_{19}H_{12}O_3]_n$

P.T.F.E.

$[CF_2]_n$

FIGURE 2.11 Chemical structures of P.P.O., P.E.E.K. and P.T.F.E.

of 21%. This was calculated using a simple standard formula (105) after determining the actual density of the specimen (See Appendix 1 for details).

Key properties of P.E.E.K. include its high service temperature (200^{o}C), low flammability and emission of smoke and toxic gases in fire situations, resistance to a very wide range of solvents and proprietary fluids. P.E.E.K. is processed at 370-400^{o}C by extrusion or injection moulding.

P.T.F.E. has a Tm of 327^{o}C, with a Tg at -113^{o}C (13, 106) and a secondary transition at 19^{o}C where it exhibits a 1% volume change and a maximum in its elongation to break (13). The Dynamic Storage Modulus also shows a fall from 9.2-8.8x10^{8} Nm^{-2} (Log E') at 19^{o}C (107), and the working temperature range is from -250^{o}C to +250^{o}C. At temperatures above 204^{o}C P.T.F.E. will start to decompose and gaseous products, if inhaled, may produce unpleasant symptoms (14).

The intermolecular attraction between P.T.F.E. molecules is very small, the computed solubility parameter being 12.6 MPa$^{\frac{1}{2}}$. The polymer in bulk does not therefore have a high rigidity or tensile strength usually found in high melting point polymers.

P.T.F.E. is a highly crystalline material and is usually about 90% crystalline as manufactured. The material used in the wear experiments was 86% crystalline. This was calculated using the same formula as before (105), (See Appendix 1 for details). P.T.F.E. can be made less crystalline

100% crystallinity. P.T.F.E. is not attacked by any chemical except for some alkali metals and complex fluorine compounds.

Although P.T.F.E. is a thermoplastic, it is not processed by conventional injection or compression moulding or standard extrusion, because of its high melt viscosity (13). Sintered materials such as rods, billets, plates etc. can be machined on conventional machine tools.

All P.P.O. wear specimens were made from the same batch of material as used by Skelcher (9,10), supplied by AKU/GE of Arnhem, Holland.

The P.E.E.K. wear specimens were machined from unfilled material which had been injection moulded and supplied directly by I.C.I.

All P.T.F.E. material was obtained commercially and conformed to British Standard Specification 4271, Grade B, Types 2.

Table 2.1 shows selected properties of the three polymers.

2.5.2 Lubricants

The lubricants used in all experiments were commercially available polydimethyl siloxanes (silicone fluid) supplied by Dow Corning. The fluid is available in a wide range of viscosities from 1 to 10^6 centistokes, each viscosity being chemically identical (See Figure 2.12). The difference between the viscosities is to be found in their different

POLYMER	YOUNG'S MODULUS ($N m^{-2}$)	POISSON'S RATIO	Tg(^{o}C)	Tm(^{o}C)
P.P.O.	2.3×10^{9} (12)	0.41 (12)	208 (13)	257 (13)
P.E.E.K.	2.82×10^{9} (107)	0.4	143 (21)	334 (21)
P.T.F.E.	3.48×10^{8} (108)	0.46 (12)	-113 (106)	327 (13)

Mild Steel	2.2×10^{11} (12)	0.28 (12)

TABLE 2.1 Selected properties of P.P.O., P.E.E.K. and P.T.F.E. compared to mild steel.
(for the purpose of comparison)
(Poisson's ratio for P.E.E.K. was estimated)

References in brackets

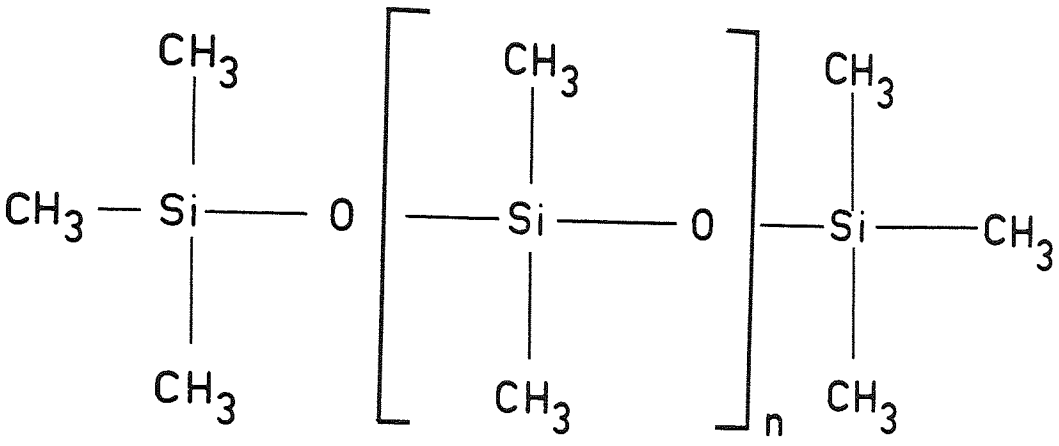

$[C_2H_6SiO]_n$

FIGURE 2.12 Chemical structure of Polydimethyl Siloxane

molecular weights (i.e. number of repeat units).

These fluids have a high thermal stability and their physical properties are consistent over a wide temperature range ($-40^{o}C$ to $200^{o}C$)(109). They have a low solubility parameter of 14.9 $MPa^{\frac{1}{2}}$ (13) and are insoluble in solvents of higher solubility parameter such as acetone, ethylene-glycol and water. However they are soluble in solvents such as Benzene, Cyclohexane, Gasoline, Toluene and Turpentine. Silicone fluids and greases are used as lubricants in conditions of high temperature operation for applications depending on rolling friction (110). They also have a wide range of industrial uses because they are colourless, odourless, non-toxic and have a low volatility (111,112).

2.6 STRIBECK CURVES

It was necessary to know which regime of lubrication the polymers were operating in on each machine for any given conditions. To determine this the classical Stribeck curves were produced for each polymer/machine combination. These were produced by recording the variation in the coefficient of friction with varying values of $\frac{nN'}{p}$ by altering the viscosity, sliding speed or the load.

The range of loads, speeds and fluid viscosities used in obtaining the Stribeck curves for each polymer on all three machines are shown in Table 2.2.

Wear Machine	Polymer	Load (N)	Speed (ms^{-1})	Viscosity (cs)
Rotating	P.P.O.	6,11	$6x10^{-4}$-1.0	$1,10,10^{3}$
Line-Contact	P.E.E.K.	6,11	$1.1x10^{-3}$-$8.2x10^{-1}$	$1,200,10^{3}$
Machine	P.T.F.E.	6,11,21	$1x10^{-3}$-$4x10^{-1}$	1,10,50
Uni-Directional	P.P.O.	21,70,103,135	$1x10^{-3}$-1.0	$1,10,10^{2}$
Pin on Disc	P.E.E.K.	21	$3x10^{-3}$-1.0	10
Machine	P.T.F.E.	21	$3x10^{-3}$-1.0	10
Reciprocating	P.P.O.	90,450	$3x10^{-3}$-1.0	$1.5,5,10,10^{2}$
Line-Contact	P.E.E.K.	90	$3x10^{-3}$-1.0	1.5,10,200
Machine	P.T.F.E.	90	$3x10^{-3}$-1.0	$1.5,5,10,10^{2}$

Table 2.2 Range of loads, speeds and viscosities used in constructing the Stribeck curves

2.7 DWELL TESTS

Wear tests were undertaken to observe any retention of the silicone fluid by the polymer. This retention was inferred by a prolonged period of low friction when excess fluid had been removed after the initial stage of the test. Therefore, the complete test was known as a dwell* test which was undertaken in two stages:-

i) The lubricated run - A wear specimen was worn against the wear counterface in the presence of silicone fluid with a preset load and sliding speed.

ii) The 'dry' run - All excess fluid was removed from the pin by wiping with a clean tissue. The wear counterface was replaced with a new clean one and the wear test re-started. The friction and wear rate were continuously recorded.

If the friction and wear rate remained at the lubricated values for a significant period then retention of the fluid by the polymer was assumed to have taken place.

The range of loads, speeds and number of lubricated revolutions used in the Dwell tests for each polymer on all three machines are shown in Table 2.3.

* term follows from work of Booser et al (94)

Wear Machine	Polymer	Load (N)	Speed (ms^{-1})	No.of Revs.with Lubricant x 1000
Rotating	P.P.O.	11,21	$3x10^{-3}$-$6x10^{-1}$	0.5 - 230
Line Contact	P.E.E.K.	21	$1.5x10^{-3}$-$5x10^{-3}$	3 - 38
Machine	P.T.F.E.	6,11,21	$1.5x10^{-3}$-$7x10^{-3}$	5 - 41
Uni-Directional	P.P.O.	21,135	$3x10^{-3}$	6 - 33.5
Pin on Disc	P.E.E.K.	21	$3x10^{-3}$	15
Machine	P.T.F.E.	21	$1.5x10^{-3}$-$3x10^{-3}$	10 - 36
Reciprocating	P.P.O.	25	$3x10^{-3}$	7 - 24
Line Contact	P.E.E.K.	88	$3x10^{-3}$	15 - 17
Machine	P.T.F.E.	25,88	$3x10^{-3}$	7 - 45

Table 2.3 Range of loads, speeds and number of revolutions with the lubricant used in the Dwell Tests

2.8 FRICTION AND WEAR EXPERIMENTS

It was necessary to know how friction and wear rates varied with speed, so that the values obtained during the dwell tests could be checked against standard data. This standard data was generated by allowing the polymer specimen to wear against the counterface at a set speed. When the wear rate and friction settled to a steady state a record of their values was made and the speed changed.

2.8.1 Rotating Line Contact Machine

This machine was run at speeds from 5×10^{-4} ms^{-1} to 4 ms^{-1} and at a load of 2.1 kg during the dry wear experiments. Under lubricated conditions using a 10 cs silicone fluid the maximum reliable speed attainable was no greater than 1 ms^{-1}. At speeds greater than this lubrication was impossible as the silicone fluid was flung from the disc. During the above range of speeds the pin rotated at a constant 5 r.p.m., although some experiments were conducted with the pin stationary and at 50 r.p.m. The wear rates were monitored with the debris being allowed to accumulate at the side of the wear track, and also with the debris being removed by a cold air blast from an electric fan, to observe any effect of debris accumulation.

2.8.2 Uni Directional Pin on Disc Machine

This machine was run at speeds from 6×10^{-4} ms^{-1} to 8 ms^{-1} and at a load of 2.1 kg during the wear experiments. As

with the Rotating Line Contact machine lubricated wear could not be undertaken at speeds greater than 1 ms^{-1} using a 10 cs silicone fluid. The wear rates were monitored with the debris being allowed to accumulate at the side of the wear track because the presence of an air blast made no difference to the results generated.

2.8.3 Reciprocating Line Contact Machine

This machine was run at speeds from $3x10^{-3}$ ms^{-1} to 3 ms^{-1} under a 2.5 kg load, which was the minimum load available. The maximum speed under lubricated conditions with the 10 cs silicone fluid was $5x10^{-1}$ ms^{-1}. The limit of $5x10^{-1}$ ms^{-1} was caused by the extremely small amount of wear that took place, hence making it virtually impossible to calculate an accurate value for the wear rate.

Specimens and wear debris were collected from each machine under dry and lubricated conditions at $3x10^{-3}$ ms^{-1} and occasionally at other speeds where necessary.

2.9 ANALYSES

2.9.1 Scanning Electron Microscopy (S.E.M.)

A Cambridge 150 scanning electron microscope was used to observe surface features of the wear specimens, and the debris generated during the experiments. It is difficult to obtain high resolution photographs of non-conductive materials (with low thermal conductivities) without damaging the specimens being observed. This is because electrostatic charging occurs in non-conductive materials which will lead to a temperature rise in the material. As polymers have low thermal conductivities this temperature rise builds up and leads to local melting of the surface, hence destroying any features in view. Charging also leads to image distortion and excessive contrast. This electrostatic charging can be overcome by coating the specimens with carbon or gold (300-400 Angstroms of carbon or 15-20 Angstroms of gold). The charges are then conducted across the surface of the specimen and into the specimen holder.

A Links System 860 was connected to the S.E.M. to perform x-ray microanalysis. This system employed an energy dispersive analyser which could detect many surface elements rapidly and simultaneously. Also incorporated in the system is a microprogrammed computer and specially developed software packages.

As well as producing quantitative analyses of the various elements in the surface, concentration profiles and x-ray

maps of the different elements could also be obtained.

The Links System 860 was used in connection with the search for silicon in the surface of the polymer specimens. To observe the depth of fluid retention in the polymer surface the specimens were mounted in conductive bakelite and sectioned. The resulting sectioned surface was polished with various grades of abrasive paper until it was possible to finish polish with 6μm and 1μm diamond paste. This surface was then given a conductive coating of carbon to dissipate electrostatic charging effects.

Silver conducting paint was applied to the pin surface before mounting, to enable the surface boundary of the pin to be clearly seen when sectioned.

CHAPTER 3

EXPERIMENTAL RESULTS

3. EXPERIMENTAL RESULTS

3.1 CONTACT BAND WIDTH MEASUREMENTS

The contact band widths on the Rotating Line Contact machine were recorded and examples are shown in Figure 3.1. The band width was measured for loads of 6 N, 11 N, 16 N, and 21 N, and the results are shown in Figure 3.2. Calculated values were also plotted (for comparison) on the same graph using the best available data, including estimates of poisson's ratio where necessary (this data is shown in Table 2.1). Although the calculated and measured values are similar, it was decided to use the measured values in all calculations of contact area, contact pressure etc.

The depth of disc penetration into the polymer and contact pressure was calculated from the measured values of the contact band width. The graphs of disc penetration and pressure versus load on the Rotating Line Contact machine (See Figures 3.3 and 3.4), show that for the same load P.E.E.K. operates at the highest pressure, and P.T.F.E. operates with the highest disc penetration. Therefore, if the fluid retention mechanism proposed by Skelcher (9,10) is due to mechanical working of the polymer surface, a more pronounced effect would be expected to occur with P.E.E.K. or P.T.F.E. If, however, the retention is due to an effect such as diffusion or plasticisation then it would be expected to be less with P.E.E.K. and P.T.F.E., because both of these polymers are very chemically stable

P.P.O.

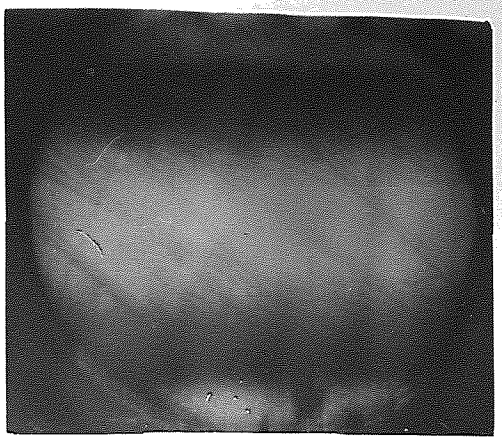

P.E.E.K.

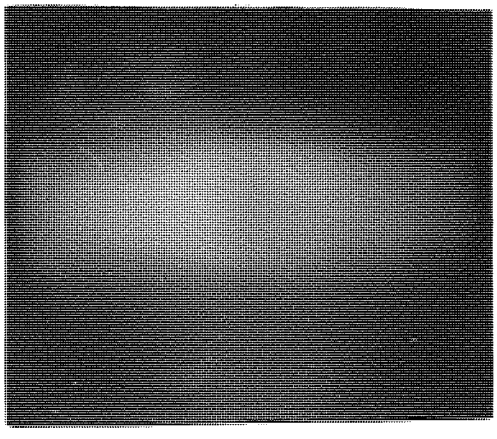

x 30

P.T.F.E.

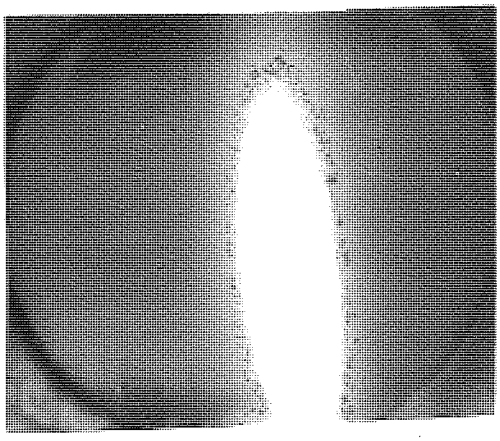

Figure 3.1 Contact band widths on the Rotating Line Contact machine for P.P.O., P.E.E.K. and P.T.F.E. under 2.1 kg load.

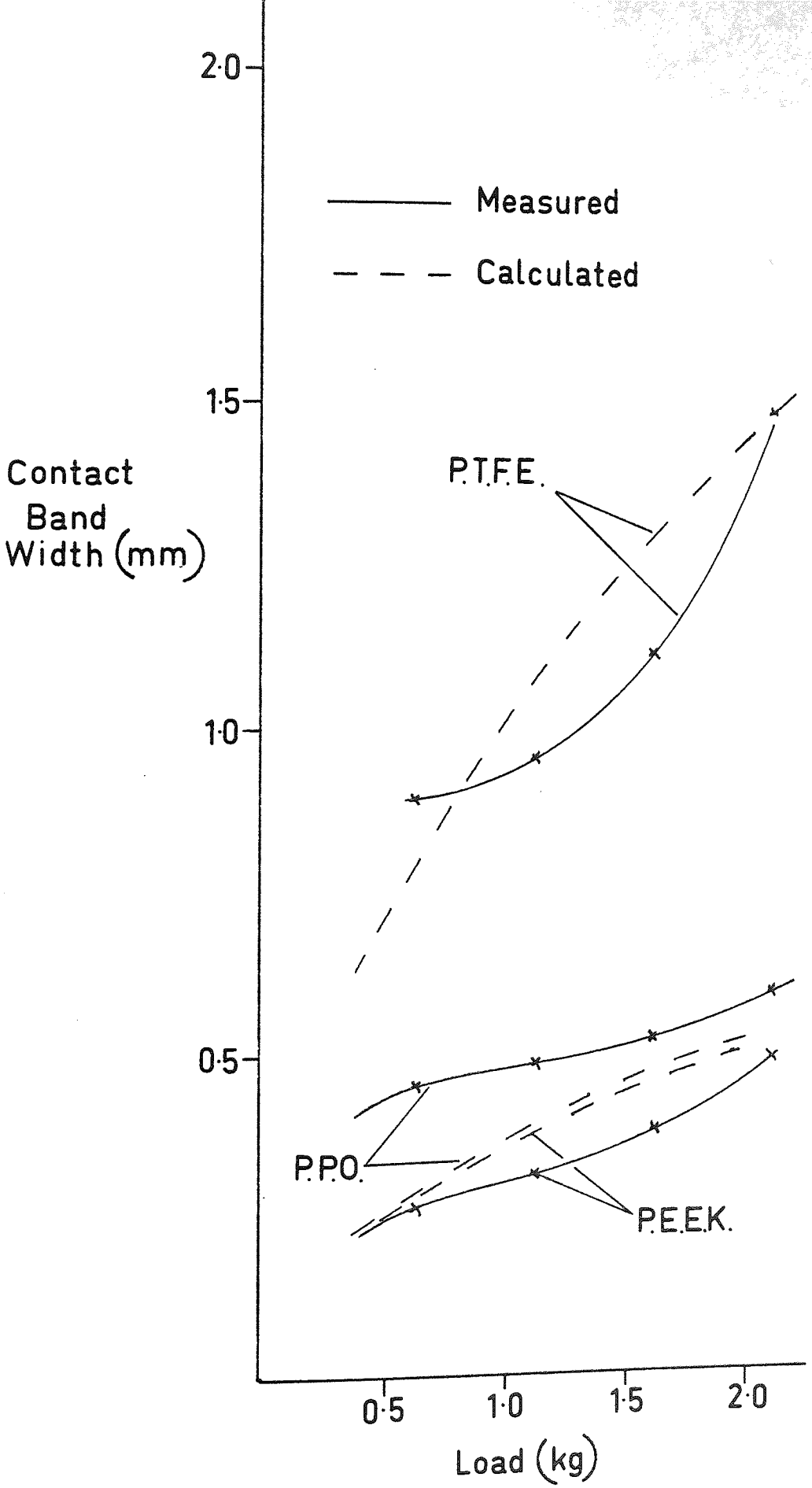

FIGURE 3.2 Graph of Contact Band Width versus Load on the Rotating Line Contact Machine

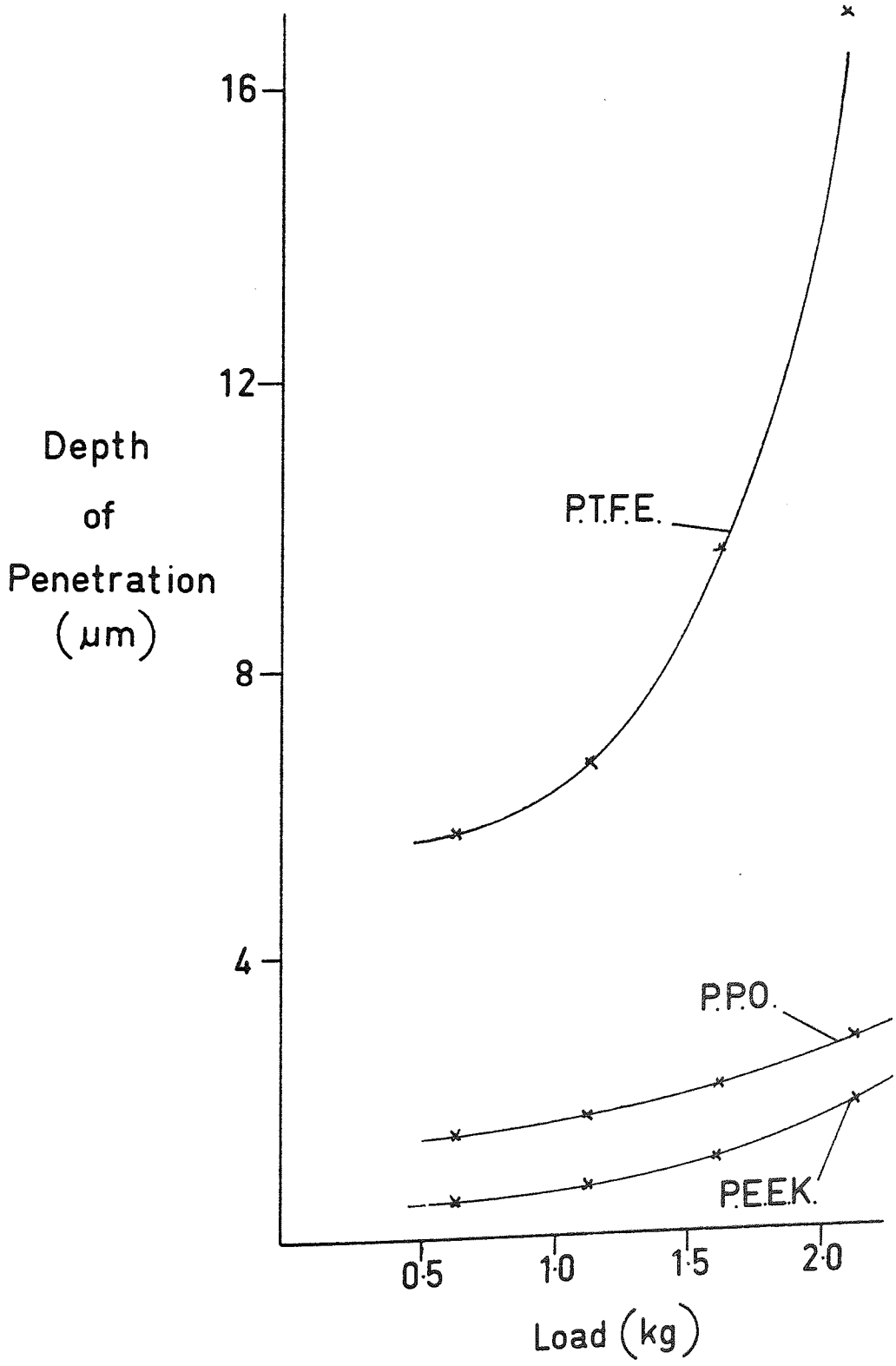

FIGURE 3.3 Graph of Disc penetration into pin versus load on the Rotating Line Contact Machine

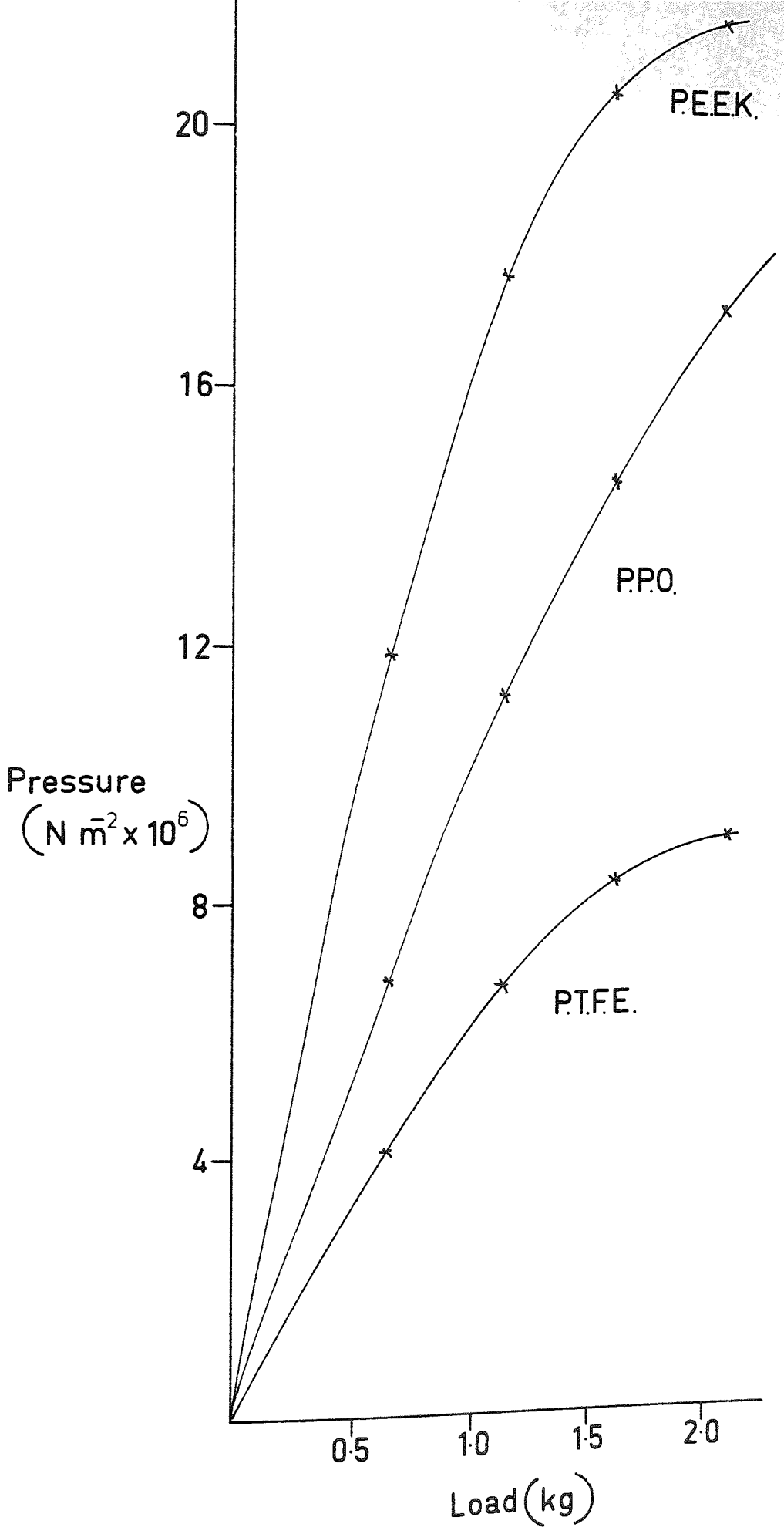

FIGURE 3.4 Graph of contact pressure versus load on the Rotating Line Contact Machine

and have few solvents.

The contact band widths were also measured on the Reciprocating Line Contact machine, and for a load of 88 N the values for P.P.O., P.E.E.K. and P.T.F.E. were 1.0, 1.0 and 1.7 mm respectively. This may be compared with calculated values of 0.53, 0.52 and 1.43 mm using the same data as for the calculated values on the Rotating Line Contact machine. Again the measured values were assumed to be more representative of the actual contact conditions.

3.2 STRIBECK CURVES

3.2.1 Rotating Line Contact Machine

The Stribeck curve for each polymer was plotted and are shown in Figure 3.5. The graphs follow the expected trend for the first half of a Stribeck curve (see Figure 1.14), and the region of graph where the friction is essentially constant with varying values of $\frac{nN'}{P}$ is quite wide. The shape of the curve for P.P.O. is exactly similar to that found by Skelcher (9,10). It was therefore possible to operate in 'boundary' lubrication* conditions with a wide variety of variables. This range of 'boundary' lubrication conditions lies within 10^{-13} to 10^{-10} for values of $\frac{nN'}{P}$.

3.2.2 Uni-Directional Pin on Disc Machine

The Stribeck curves for this machine are very similar to those found for the Rotating Line Contact machine. The curves are shown in Figure 3.6 and give a wide region of constant coefficient of friction at low values of $\frac{nN'}{P}$.

3.2.3 Reciprocating Line Contact Machine

Similar Stribeck curves were obtained for this machine to those obtained on the Rotating Line Contact machine and the Uni-Directional pin on disc machine. The curves shown in Figure 3.7 show boundary lubrication conditions over a wide range of values for $\frac{nN'}{P}$.

* see page 206 for definition of 'boundary' lubrication

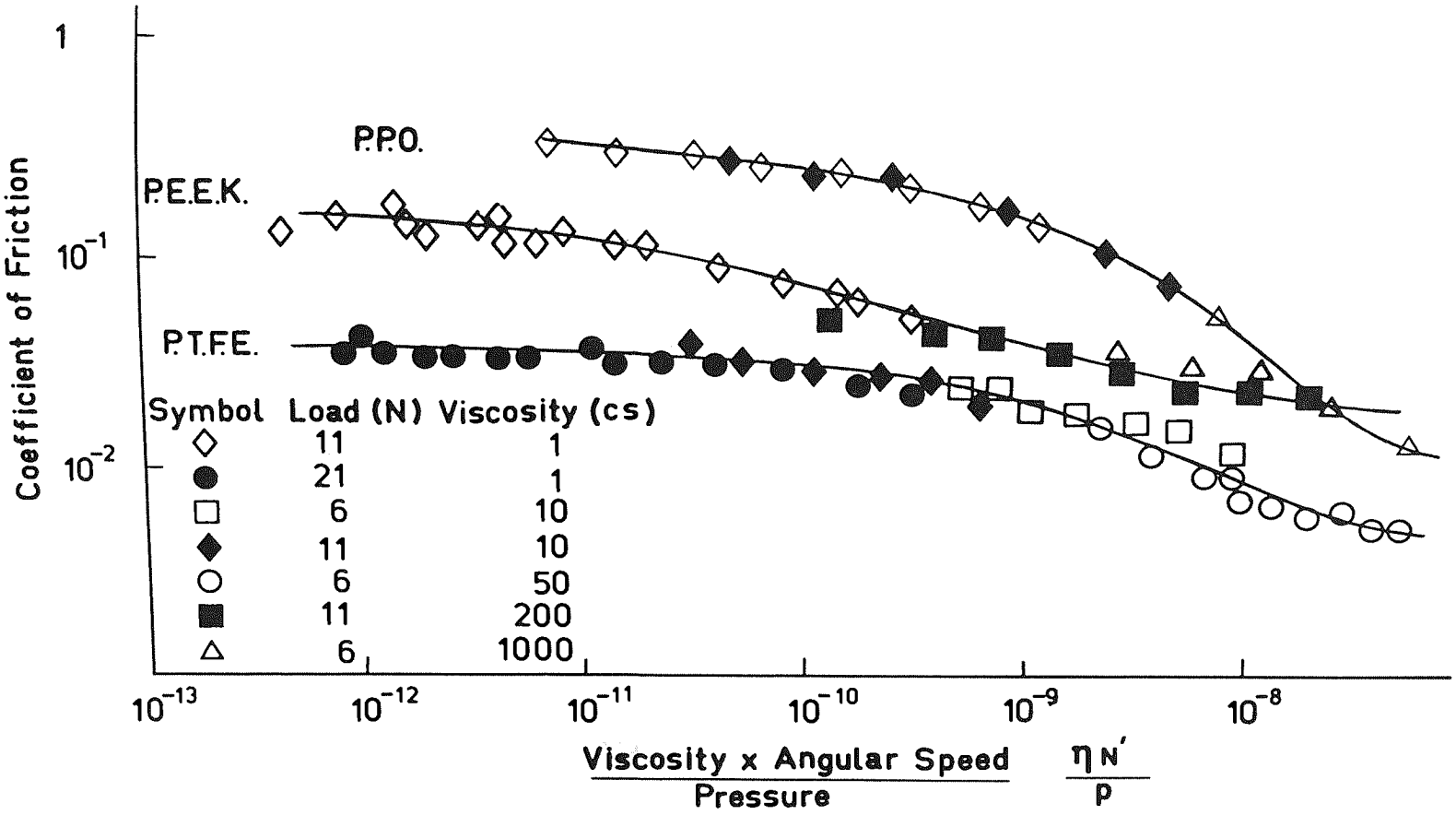

FIGURE 3.5 Stribeck Curves for the Rotating Line Contact Machine

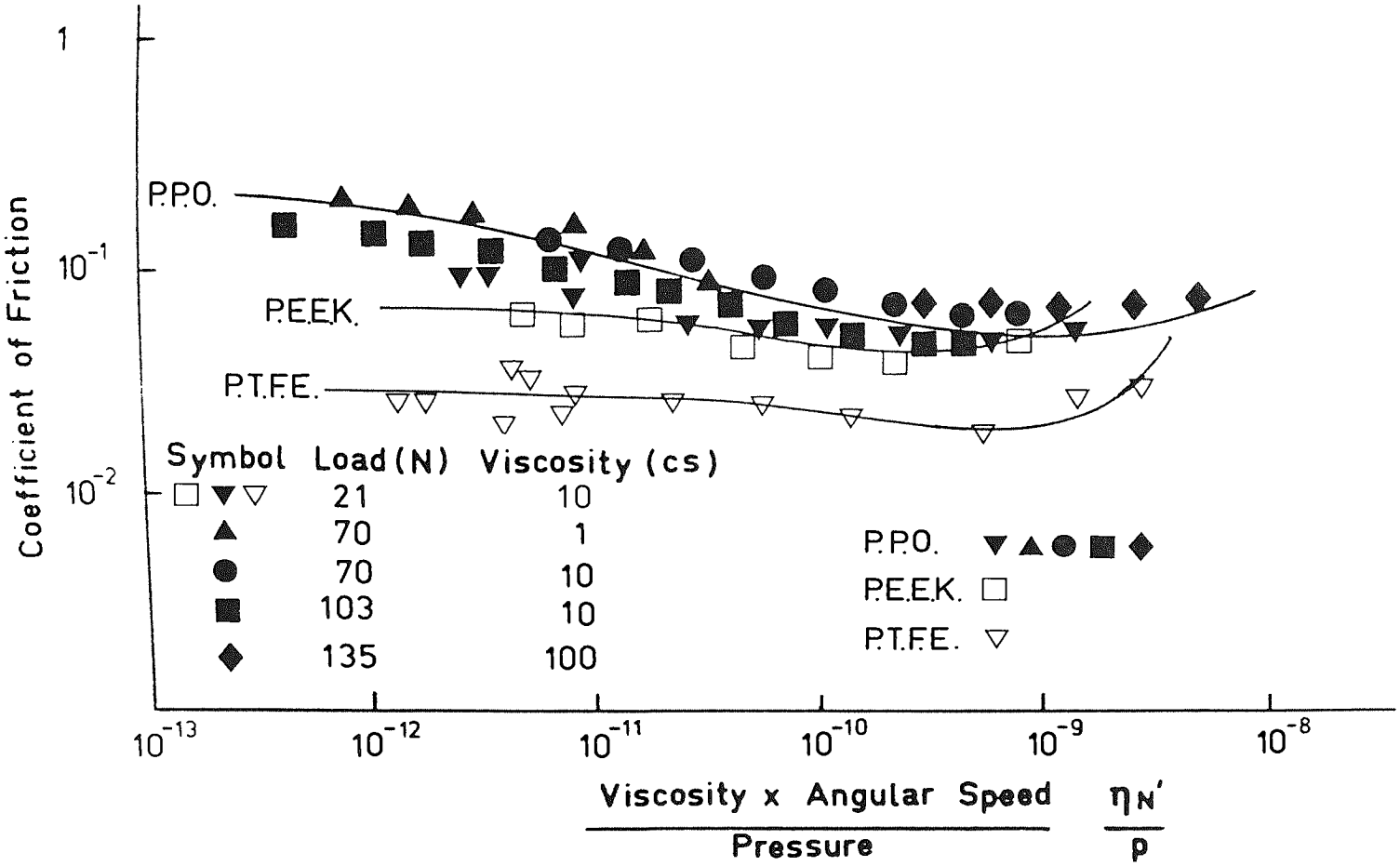

FIGURE 3.6 Stribeck Curves for the Uni-Directional Pin on Disc Machine

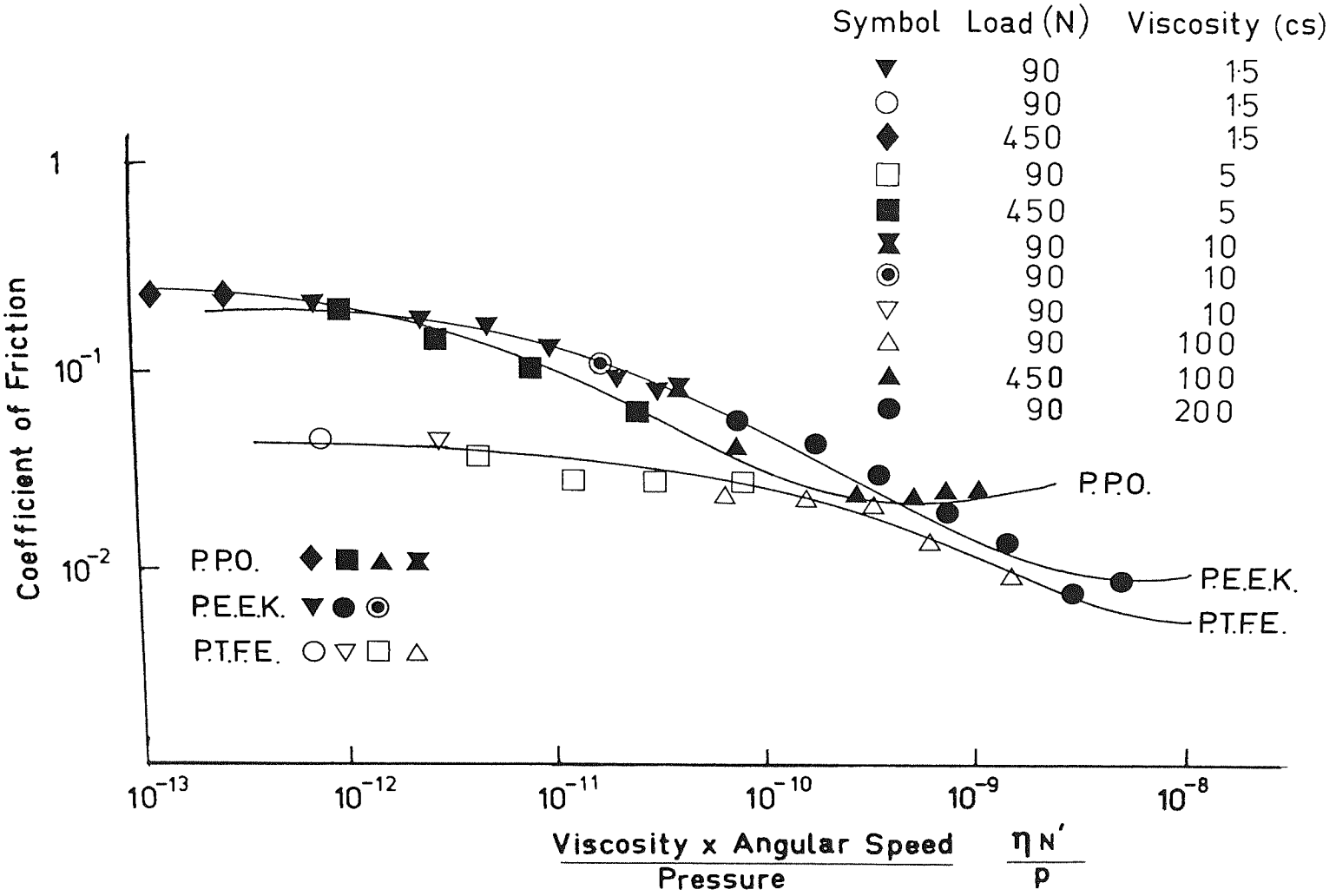

FIGURE 3.7 Stribeck Curves for the Reciprocating Line Contact Machine

3.3 DWELL TESTS

3.3.1 Rotating Line Contact Machine

Initial Dwell tests were undertaken using P.P.O. at a load of 11 N and a sliding speed of $5x10^{-3}$ ms^{-1}. The results of these tests are shown in Table 3.1, Tests 1 to 4, and seemed to confirm Skelchers (9,10) conclusion that silicone fluid was being retained in the surface of the pin. This was inferred from the fact that after all excess silicone fluid had been wiped away and a new clean disc used as the wear counterface, the coefficient of friction remained at the lubricated value. Operated under identical conditions of load and speed up to 30μ m of wear took place before the coefficient of friction returned to the dry value. An example of this can be seen in Figure 3.8 showing an abridged paper trace for test number 2.

Further tests were undertaken with P.P.O. but the pin surface was wiped more vigorously before the dry run (Tests 5 to 7). With the more vigorous* wiping none of the pins then showed signs of fluid retention at any speed, load or duration of lubricated sliding. In all cases the coefficient of friction returned to the normal dry value, within 100 disc revolutions after removal of the excess fluid. A typical abridged paper trace for this situation is shown in Figure 3.9 of test 5.

Further dwell tests with P.P.O. were undertaken to produce samples for surface analyses (these were from Tests 8 to

* i.e. more pressure

Test No.	Load (N)	Speed (ms^{-1})	Pin Speed (r.p.m.)	$\frac{nN'}{P}$	No.of Lub. Revs.	'Dry' Wear Before μ Increases (Depth μm)	Comments
1	11	$5x10^{-3}$	5	$4.1x10^{-11}$	500	10	All undertaken with gentle wiping of pin
2	"	"	"	"	1,000	25	
3	"	"	"	"	3,000	25	
4	"	"	"	"	4,000	30	
5	21	$3x10^{-3}$	5	$1.4x10^{-11}$	11,000	0	Vigorous wiping of the pin
6	"	"	"	"	20,000	0	
7	"	"	"	"	25,000	0	
8	21	$3x10^{-3}$	5	$1.4x10^{-11}$	3,000	-	Pins generated for analysis
9	"	"	"	"	"	-	
10	"	"	"	"	7,000	-	
11	"	"	"	"	"	-	
12	"	"	"	"	"	-	

(The duration of lubricated part of Dwell Test was between 1 and 400 hrs.)

Table 3.1 Cont.....

Test No.	Load (N)	Speed (ms^{-1})	Pin Speed (r.p.m.)	$\frac{nN'}{P}$	No.of Lub. Revs.	'Dry'Wear Before μ Increases	Comments
13	21	$3x10^{-3}$	5	$1.4x10^{-11}$	11,000	-	
14	"	"	"	"	"	-	
15	"	"	"	"	"	-	
16	"	"	"	"	"	-	
17	"	$2x10^{-2}$	"	$1.04x10^{-10}$	3,000	-	
18	"	"	"	"	7,000	-	Pins generated for analyses
19	"	"	"	"	11,000	-	
20	"	"	"	"	15,000	-	
21	"	$2.6x10^{-1}$	"	$1.25x10^{-9}$	11,000	-	
22	"	"	"	"	230,000	-	
23	"	$6.2x10^{-1}$	"	$3.00x10^{-9}$	200,000	-	

Table 3.1 Summary of Dwell Tests on the Rotating Line Contact machine with P.P.O.

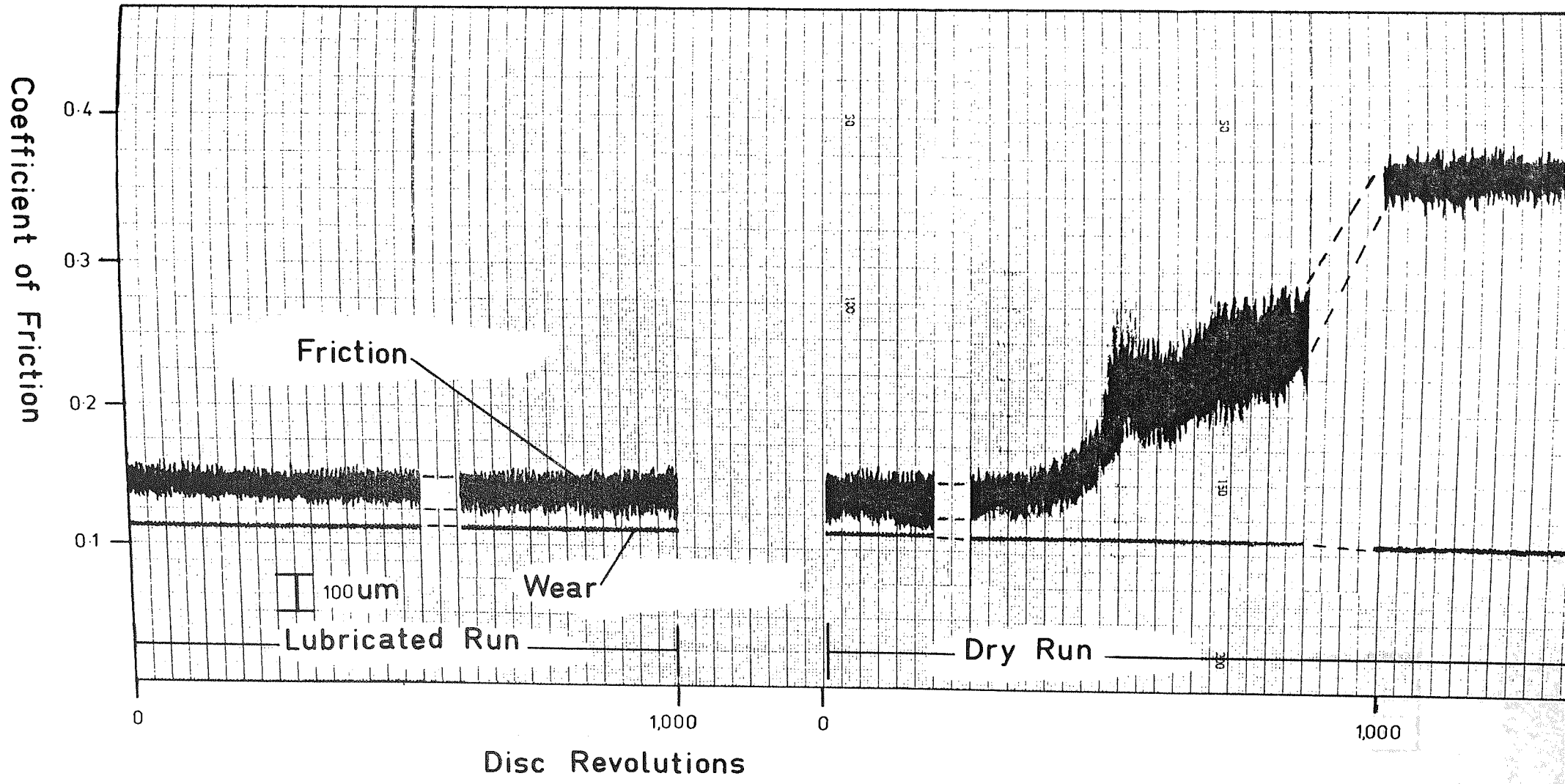

FIGURE 3.8 Abridged paper trace of Test No.2

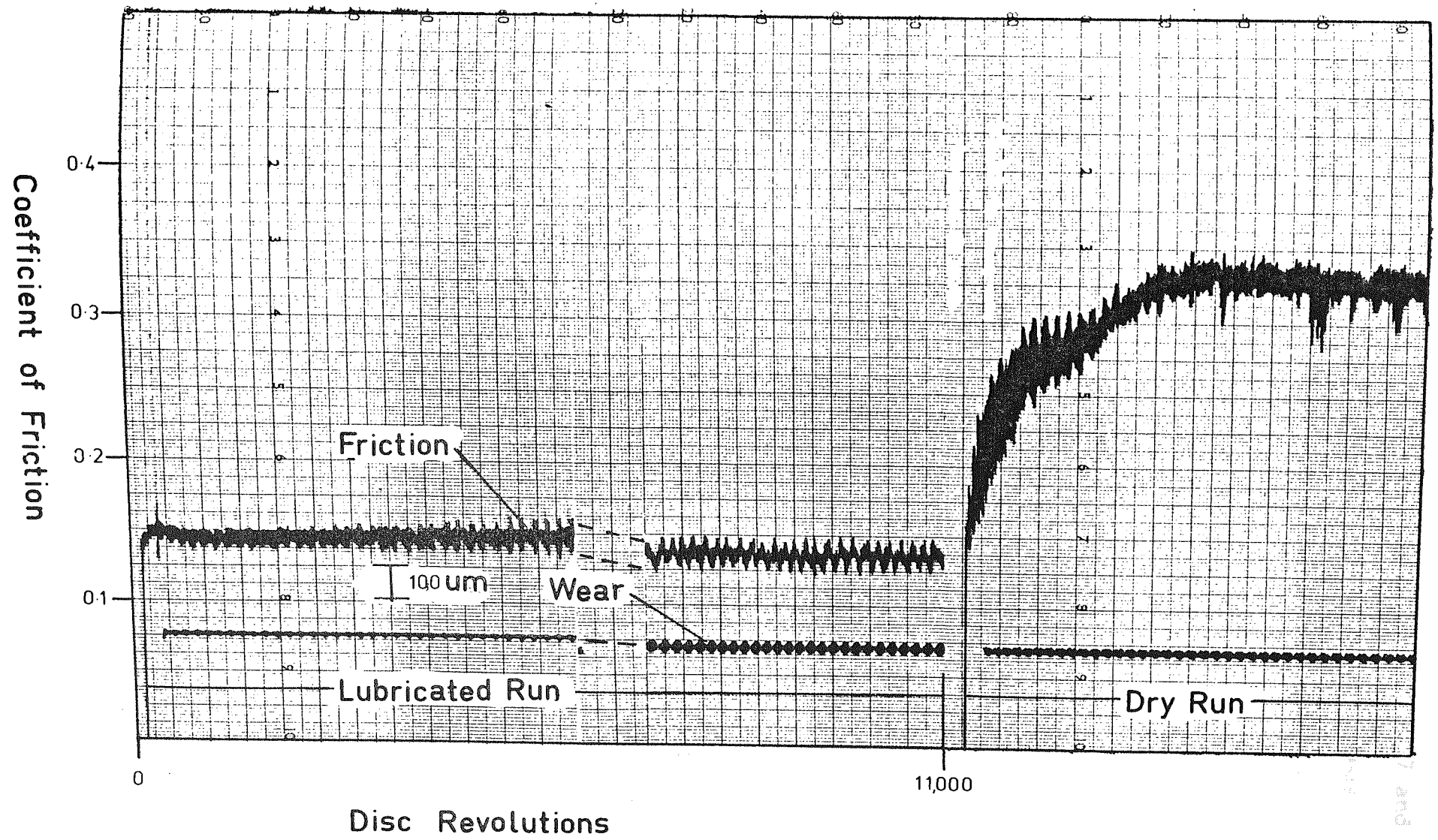

FIGURE 3.9 Abridged paper trace of Test No.5

23 in Table 3.1). These tests were run at four different speeds to observe any effect the difference in speed might have. At the lower speeds the pins were run for 3, 7 and 11 thousand disc revolutions, but at the higher speeds the pins were run for much longer. Samples from these tests were analysed and the results are reported in the Analyses section (3.5).

Dwell tests were also conducted on P.E.E.K. and P.T.F.E. but neither showed any indication of retaining silicone fluid. The coefficient of friction rose to the normal dry value at the beginning of the dry run (Tables 3.2 and 3.3). The paper traces for these tests were very similar to the one in Figure 3.9, except for different values of the dry and lubricated friction and wear rates (e.g. see Figure 3.10 for Test No.47). The P.E.E.K. and P.T.F.E. pins were also run at different speeds and loads and for varying lengths of time, but the coefficient of friction always returned to the dry value (within 100 disc revolutions) after surface cleaning of the pin and a change of wear counterface. Changing the rotational speed of the pin to 50 r.p.m. also had no effect on the fluid retention.

There were rare occasions when the coefficient of friction remained at the lubricated value during the 'dry' period of the experiment, but it was subsequently found that this was caused by impurities in the acetone used for washing the counterfaces. This problem was eliminated when Iso-propyl alcohol was used for cleaning.

Test No.	Load (N)	Speed (ms^{-1})	Pin Speed (r.p.m.)	$\frac{nN'}{P}$	No.of Lub. Revs.	'Dry' Wear Before μ Increases	Comments
24	21	$1.5x10^{-3}$	5	$6.2x10^{-12}$	3,500	0	
25	"	"	"	"	4,000	0	
26	"	"	"	"	5,000	0	
27	21	$3x10^{-3}$	5	$1.25x10^{-11}$	7,000	-	
28	"	"	"	"	"	-	Pins for analyses
29	"	"	"	"	20,000	0	
30	"	"	"	"	24,000	-	Pin for analyses
31	"	"	"	"	38,000	0	
32	21	$3x10^{-3}$	50	$1.25x10^{-11}$	16,000	0	
33	21	$5x10^{-3}$	5	$2.1x10^{-11}$	7,000	0	
34	"	"	"	"	11,000	0	
35	"	"	"	"	20,000	0	

Table 3.2 Summary of Dwell Tests on the Rotating Line Contact machine with P.E.E.K.

Test No.	Load (N)	Speed (ms^{-1})	Pin Speed (r.p.m.)	$\frac{nN'}{P}$	No.of Lub. Revs.	'Dry' Wear Before μ Increases	Comments
36	6	$5x10^{-3}$	5	$1.3x10^{-10}$	4,500	0	
37	"	"	"	"	5,000	0	
38	11	$1.5x10^{-3}$	5	$3.9x10^{-11}$	6,000	0	
39	11	$7x10^{-3}$	5	$1.8x10^{-10}$	18,000	0	
40	21	$1.8x10^{-3}$	5	$4.7x10^{-11}$	12,000	0	
41	21	$3x10^{-3}$	5	$7.8x10^{-11}$	7,000	-	Pin for analyses
42	"	"	"	"	10,000	0	
43	"	"	"	"	15,000	0	
44	"	"	"	"	15,000	0	
45	"	"	"	"	16,000	0	
46	"	"	"	"	36,000	0	
47	"	"	"	"	41,000	0	
48	21	$3x10^{-3}$	50	$7.8x10^{-11}$	18,000	0	

Table 3.3 Summary of Dwell Tests on the Rotating Line Contact machine with P.T.F.E.

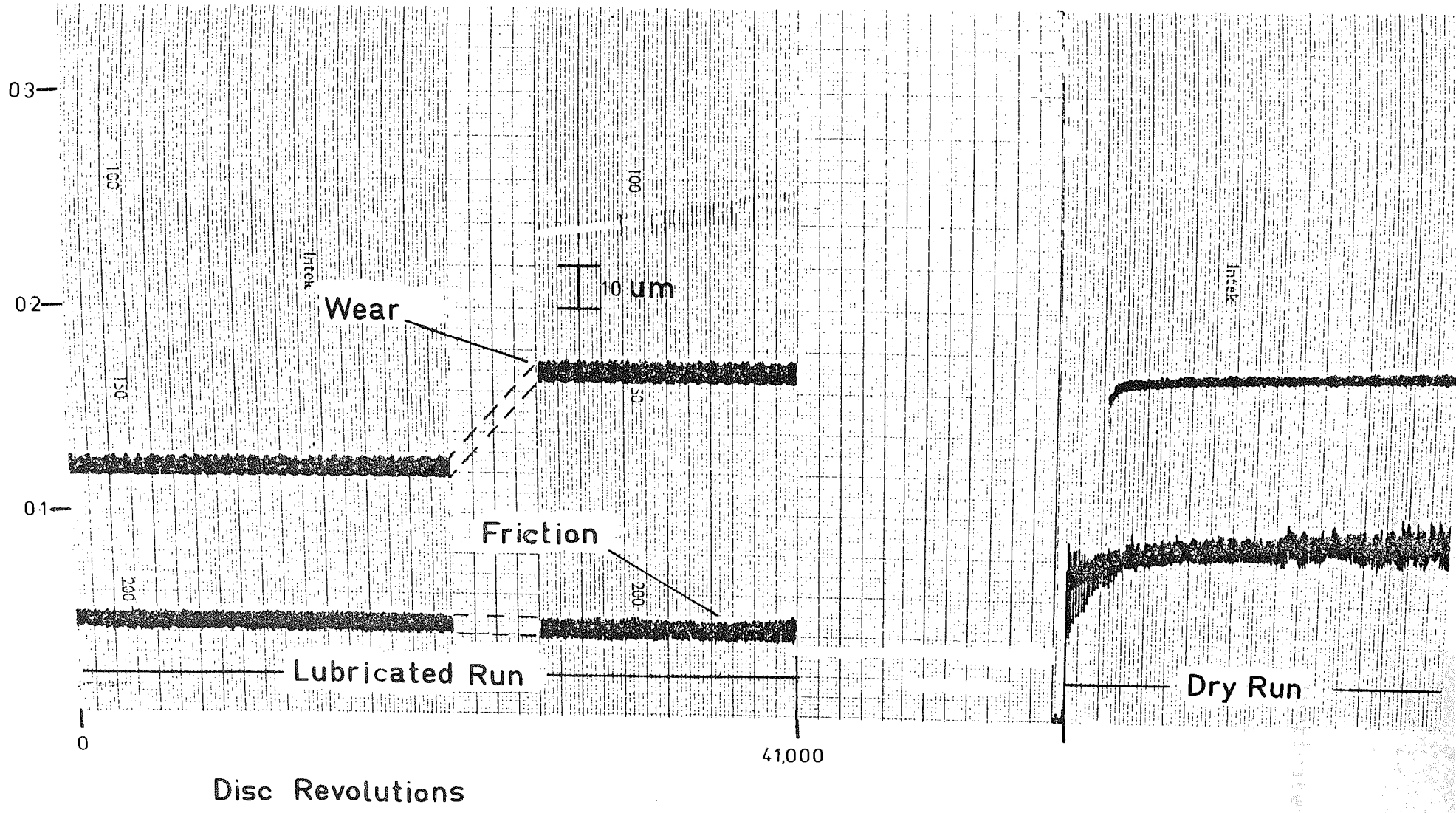

Figure 3.10 Abridged paper trace of Test No.47

3.3.2 Uni-Directional Pin on Disc Machine

When each of the polymers were worn dry after a lubricated run the coefficient of friction always returned rapidly to the normal dry value (See Table 3.4). This was the case irrespective of load, speed or duration of sliding. This return to the dry friction implied that no fluid retention was taking place and several pins were analysed to confirm this, the results of these analyses are reported in Section 3.5.

3.3.3 Reciprocating Line Contact Machine

As with the Uni-Directional Pin on Disc machine and Rotating Line Contact machine, each polymer was run lubricated under similar sliding conditions without giving any indication of fluid retention (See Table 3.5).

Test No.	Polymer	Load (N)	Speed (ms^{-1})	Pin Speed (r.p.m.)	$\frac{nN'}{P}$	No.of Lub. Revs. (Equivalent)	'Dry' Wear Before μ Increases	Comments
49	P.P.O.	21	$3x10^{-3}$	-	$8.5x10^{-12}$	15,000	-	Pin for analyses
50	"	"	"	-	"	33,500	0	
51	P.P.O.	135	$3x10^{-3}$	-	$1.1x10^{-12}$	6,000	0	
52	"	"	"	-	"	7,000	0	
53	"	"	"	-	"	9,000	0	
54	"	"	"	-	"	10,500	0	
55	P.E.E.K.	21	$3x10^{-3}$	-	$8.5x10^{-12}$	15,000	-	Pin for analyses
56	P.T.F.E.	21	$1.5x10^{-3}$	-	$4.2x10^{-12}$	10,000	0	
57	"	"	"	-	"	15,500	0	
58	P.T.F.E.	21	$3x10^{-3}$	-	$8.5x10^{-12}$	36,000	0	

Table 3.4 Summary of Dwell Tests on the Uni-Directional pin on disc machine

Test No.	Polymer	Load (N)	Speed (ms^{-1})	Pin Speed (r.p.m.)	$\frac{nN'}{P}$	No.of Lub. Revs.	'Dry' Wear Before μ Increases	Comments
59	P.P.O.	25	$3x10^{-3}$	-	-	7,000	-	Pins for analyses
60	"	"	"	-	-	24,000	-	
61	"	"	"	-	-	16,000	0	
62	P.E.E.K.	88	$3x10^{-3}$	-	$1.839x10^{11}$	15,000	-	Pin for analyses
63	"	"	"	-	"	17,000	0	
64	P.T.F.E.	25	$3x10^{-3}$	-	-	7,000	-	Pin for analyses
65	"	"	"	-	-	35,000	0	
66	"	"	"	-	-	45,000	0	
67	P.T.F.E	88	$3x10^{-3}$	-	$3.13x10^{11}$	32,000	0	

Table 3.5 Summary of Dwell Tests on the Reciprocating Line Contact machine

3.4 FRICTION AND WEAR MEASUREMENTS

3.4.1 Rotating Line Contact Machine

The results of the dwell tests implied that no fluid retention was occurring in any of the polymers under any conditions*. Therefore, it was necessary to investigate the friction and wear behaviour for the three polymers under both dry and lubricated conditions on all three machines.

In a wide range of experiments P.P.O. was run both dry and lubricated over the range of speeds 6×10^{-4} to $4\ ms^{-1}$. The friction and wear rates were plotted against speed and are shown in Figure 3.11. The dry friction is essentially constant at about 0.4 with various sliding speeds. The lubricated friction, however, falls with increasing speed. The dry wear rate decreases with increasing speed until a minimum value is reached at about $5 \times 10^{-2}\ ms^{-1}$. Above this speed the wear rate increases rapidly with increasing speed. The lubricated wear rate at very slow speeds is only slightly lower than the dry wear rate. However, as the sliding speed increases the lubricated wear rate continues to decrease with increasing sliding speed. These results for the friction and wear rates of P.P.O. are very similar to those found by Skelcher (9,10).

It was noticed that when the dry wear rate experiments were repeated in the range 1×10^{-1} to $1\ ms^{-1}$, in order to confirm initial results, large differences occurred in the

* except when gentle cleaning of the surfaces was employed

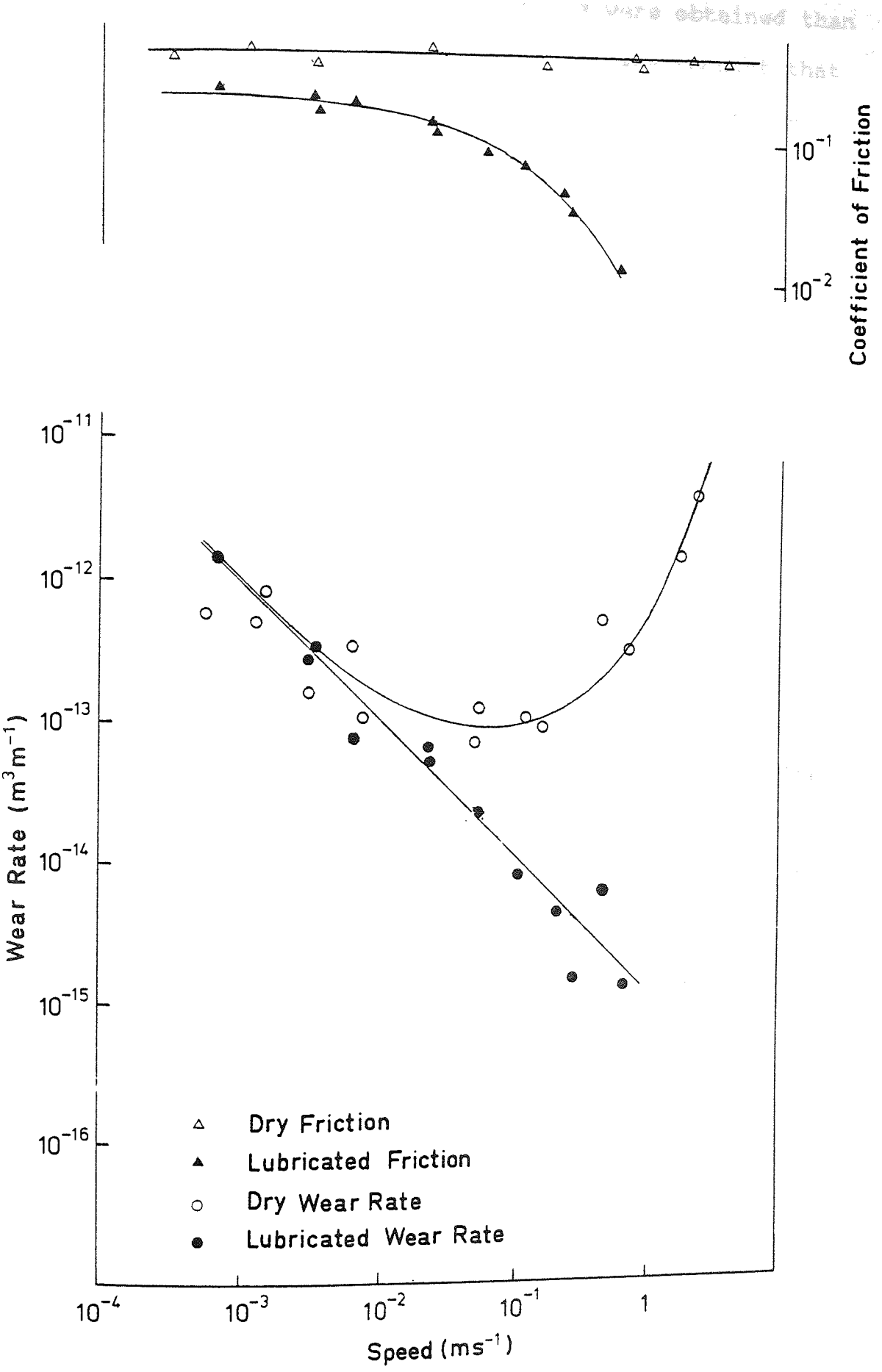

FIGURE 3.11 Friction and Wear rates for P.P.O. on the Rotating Line Contact machine (without continuous removal of wear debris under dry conditions) 2.1 kg load, 10 cs fluid

magnitude of the wear rate. When a new pin was run on a new clean disc, much higher wear rates were obtained than when the pin had worn for some time. It was thought that the accumulation of polymer debris on the counterface might have reduced the wear rate from the level found when no debris was present. It was therefore decided to determine the variation of wear rate with speed in conditions where the debris was removed continuously by a jet of air directed at the counterface. The results are shown in Figure 3.12 and it can be seen that the wear rate now remains independent of speed up to a critical value of approximately $2x10^{-1}\ ms^{-1}$ and then begins to increase rapidly.

P.E.E.K. was also run dry and lubricated over a similar range of speeds as P.P.O. The friction and wear rates are shown in Figure 3.13 and although the actual values for the friction and wear rates are different to those for P.P.O. the general trends are very similar. The dry friction for P.E.E.K ($\simeq 0.3$) is slightly lower than with P.P.O. ($\simeq 0.4$) and the lubricated friction also shows a similar decrease in magnitude with increasing speed. The minimum for the dry wear rate occurs at a slightly higher speed than with P.P.O. ($1x10^{-1}\ ms^{-1}$ instead of $5x10^{-2}\ ms^{-1}$). The lubricated wear rate at slow speeds is again only slightly lower than the dry wear rate. However, as the sliding speed increases the wear rate under lubricated conditions falls very sharply.

The variation in the dry wear rate for P.E.E.K. was also

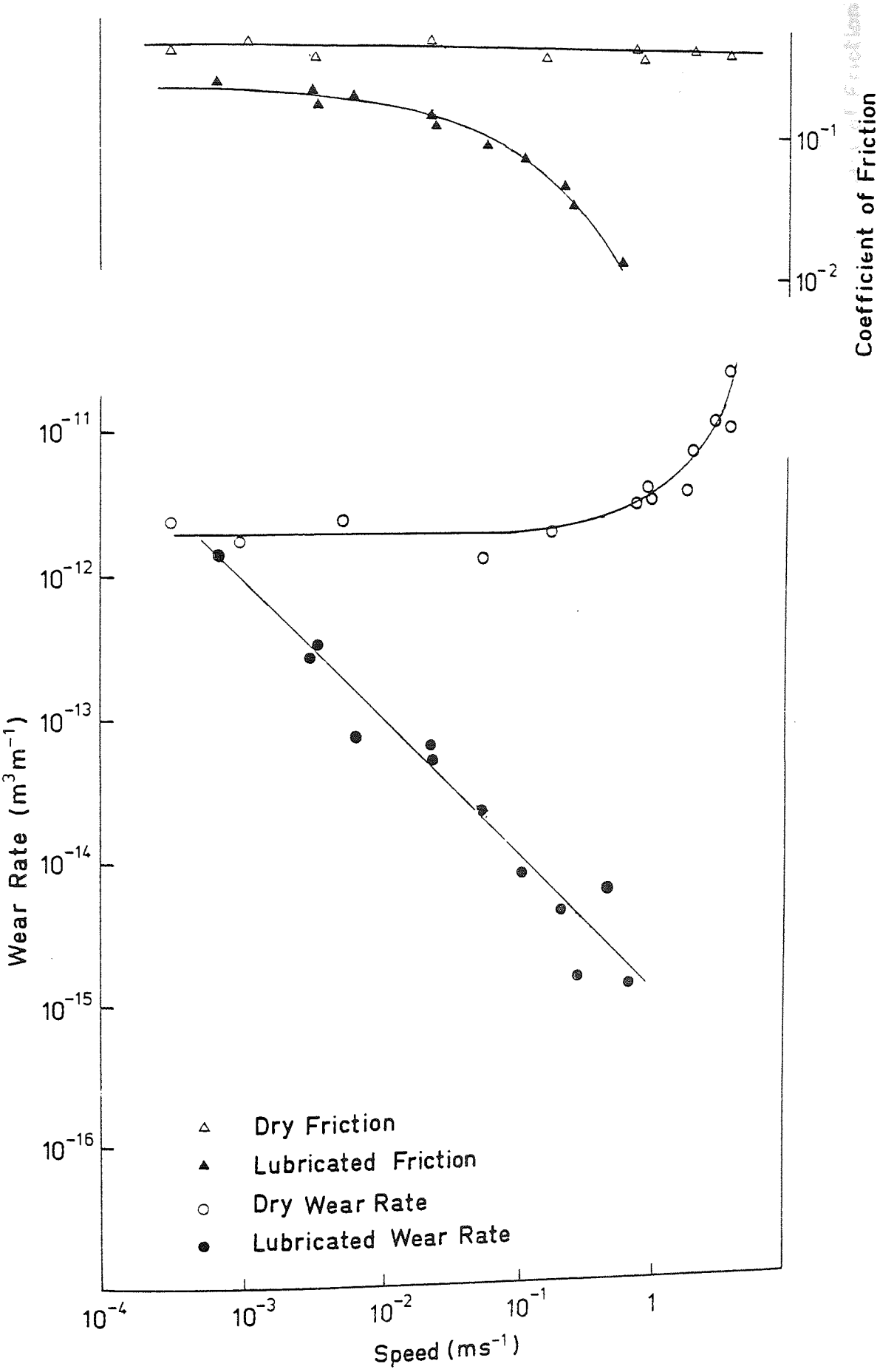

FIGURE 3.12 Friction and Wear rates for P.P.O. on the Rotating Line Contact machine (with continuous removal of wear debris under dry conditions) 2.1 kg load, 10 cs fluid

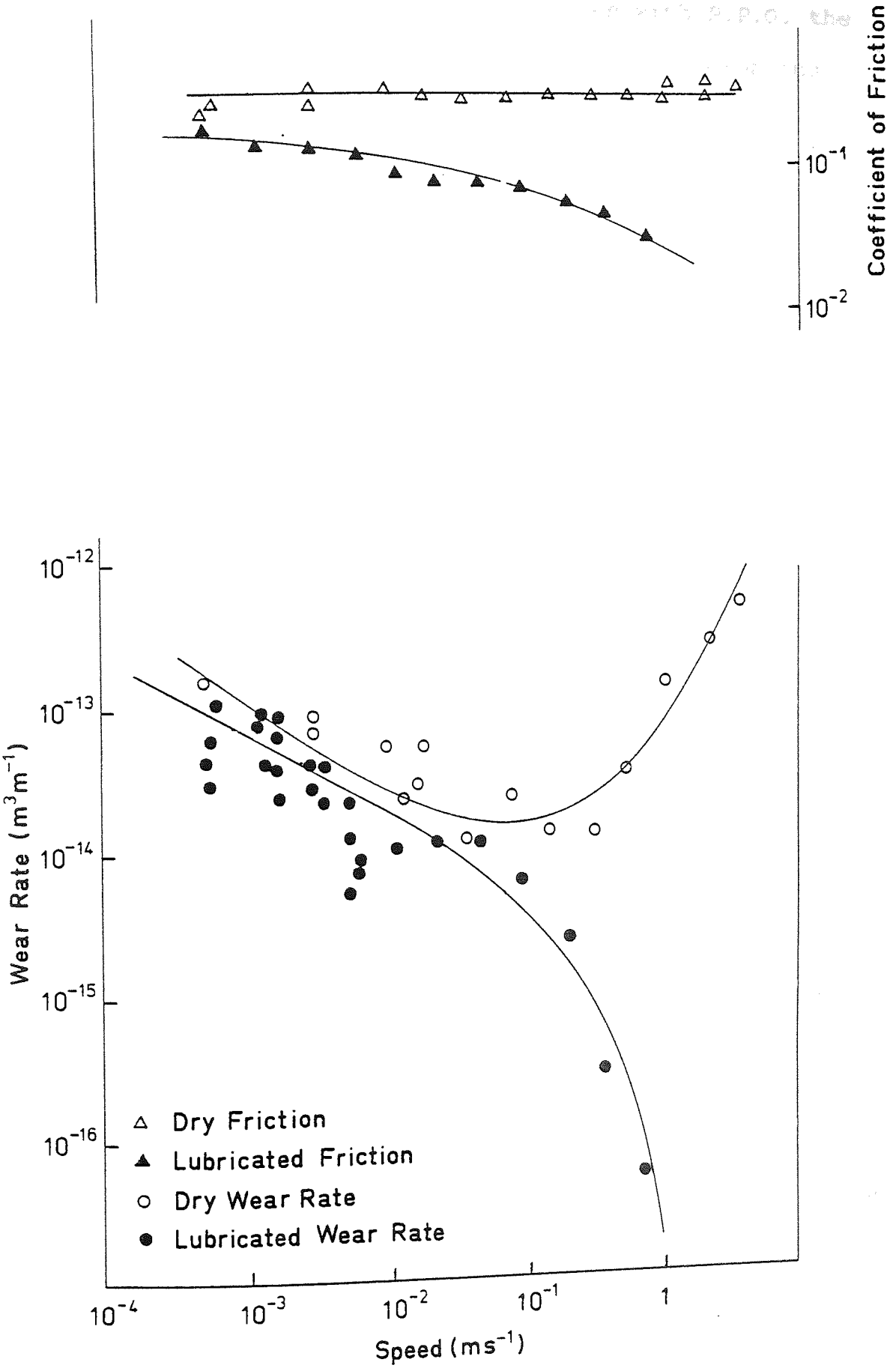

FIGURE 3.13 Friction and Wear rates for P.E.E.K. on the Rotating Line Contact machine (without continuous removal of wear debris under dry conditions) 2.1 kg load, 10 cs fluid

obtained with speed when the debris was continuously removed, and is shown in Figure 3.14. As with P.P.O. the wear rate remains essentially constant with increasing sliding speed.

The graphs of dry wear rate without the pin rotating and with debris removal are shown in Figure 3.15 to illustrate the effects of pin rotation and debris removal. This shows a lower wear rate when the pin is worn under the same sliding conditions but without pin rotation. However, as the sliding speed increases to $3x10^{-1}\ ms^{-1}$, the wear rate begins to increase with increasing speed until similar values are achieved at $3.5\ ms^{-1}$.

The friction and wear rate values for P.T.F.E.* were also checked over a wide range of speeds and are shown in Figure 3.16. The dry friction for P.T.F.E. steadily increases from 0.06 to 0.2 with increasing sliding speed, at approximately $2\ ms^{-1}$ the frictional values begin to level off. As with P.P.O. and P.E.E.K. the lubricated friction decreases with increasing speed. The curve for the dry wear rate follows a similar shape to the dry friction with increasing wear rate associated with increasing sliding speed. Again the lubricated wear rate is only slightly lower than the dry wear rate at slow sliding speeds and falls rapidly with increasing sliding speed.

3.4.2 Uni-Directional Pin on Disc Machine

In a further series of experiments P.P.O. was run dry and

* P.T.F.E. debris never collected under the contact area

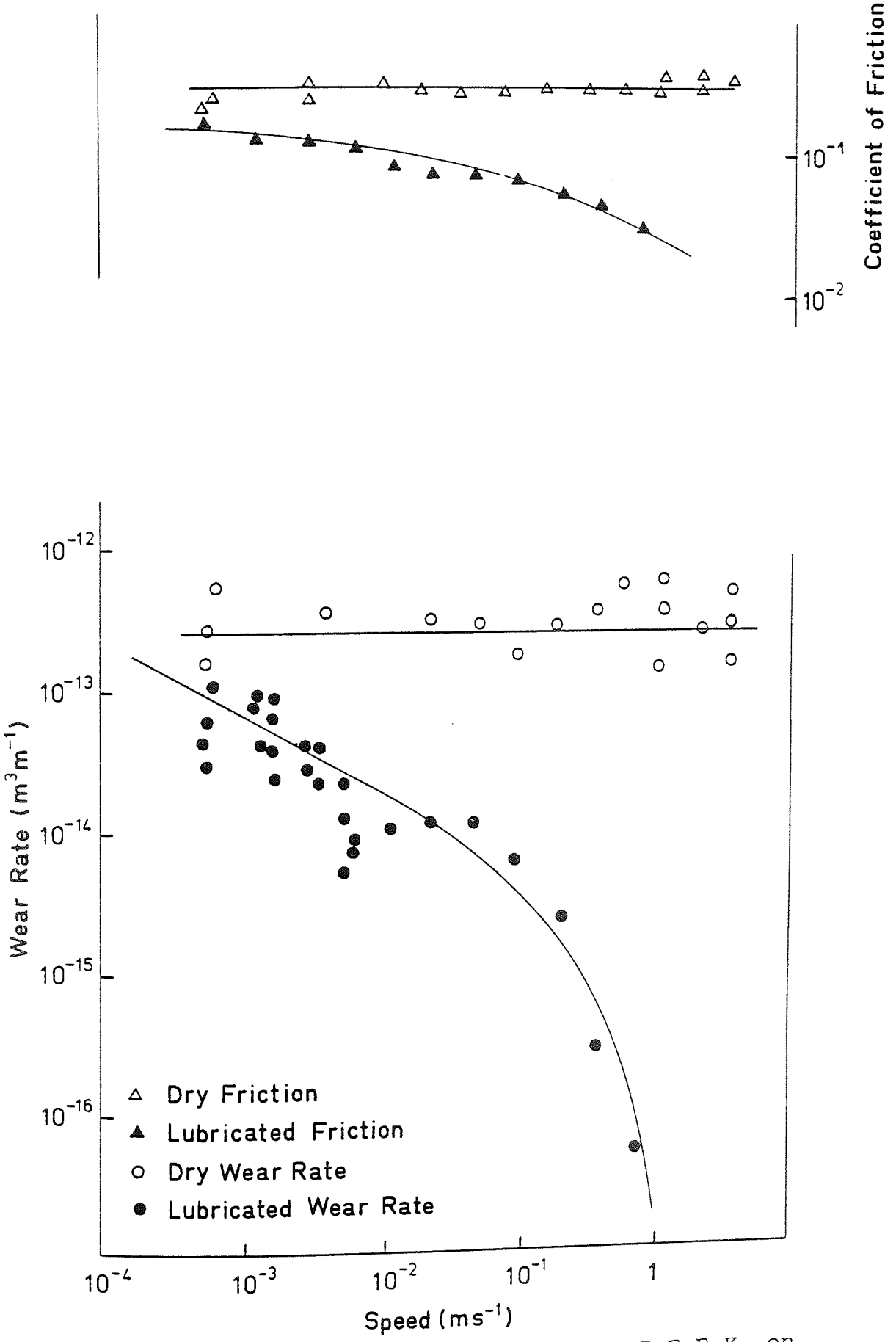

FIGURE 3.14 Friction and Wear rates for P.E.E.K. on the Rotating Line Contact machine (with continuous removal of wear debris under dry conditions), 2.1 kg load, 10 cs fluid

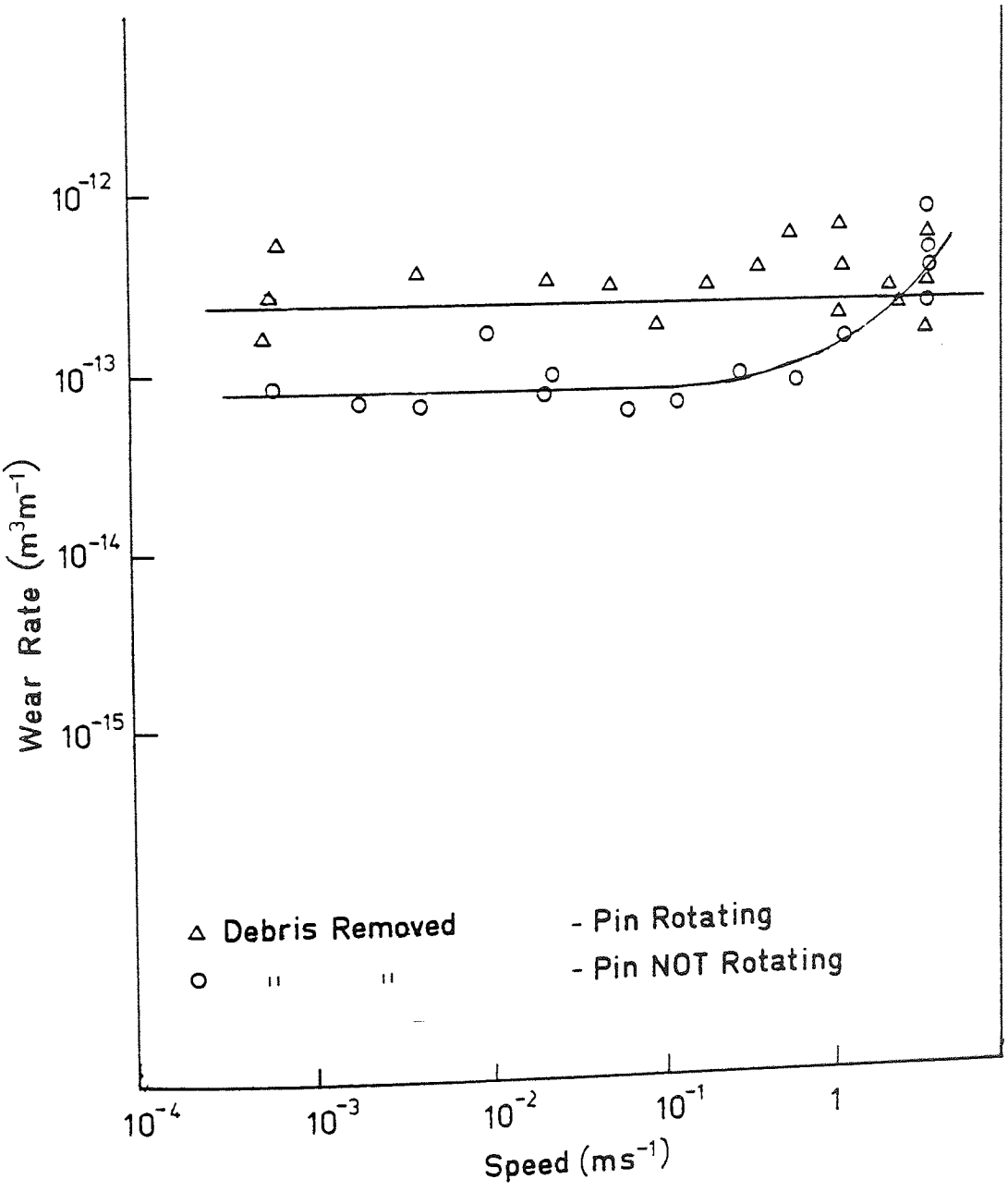

FIGURE 3.15 Dry Wear rates for P.E.E.K. on the Rotating Line Contact machine, 2.1 kg load

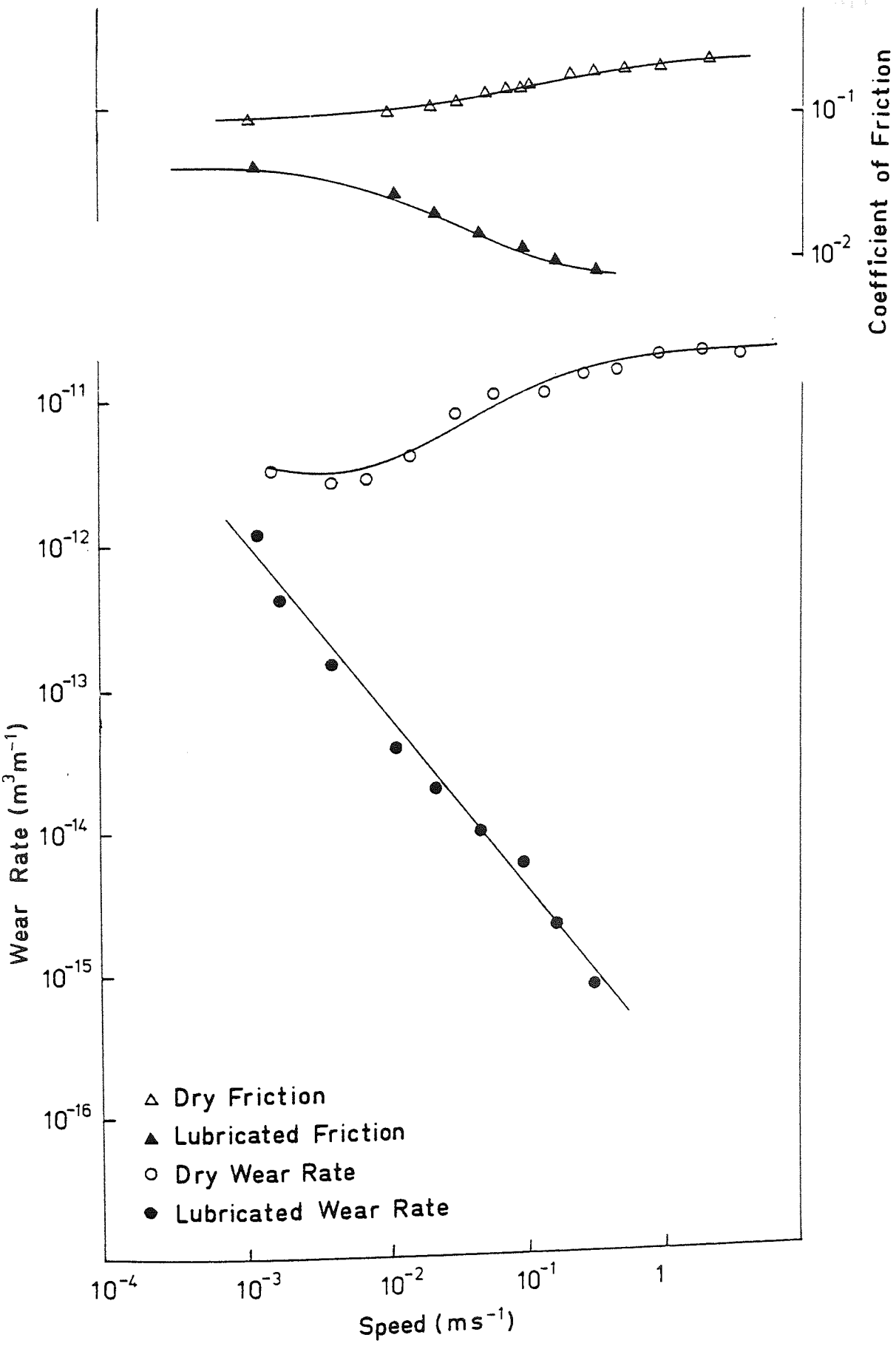

FIGURE 3.16 Friction and Wear rates for P.T.F.E. on the Rotating Line Contact machine, 2.1 kg load, 10 cs fluid

lubricated over the range of speeds $6x10^{-4}$ to $8\,ms^{-1}$. The friction and wear rates were plotted against speed and are shown in Figure 3.17. The dry friction on this machine is again essentially constant with varying speed, but at the higher values of 0.6, instead of 0.4 as recorded on the Rotating Line Contact machine. The lubricated friction at first falls with increasing speed then levels off at 0.06. The lubricated friction values, however, do not reach the very low values achieved on the Rotating Line Contact machine and this is probably due to the lack of a geometric wedge to cause hydrodynamic lubrication. The dry wear rates are identical to the values found on the Rotating Line Contact machine, however, the rise in dry wear rate at high speeds occurs at $5x10^{-1}\,ms^{-1}$ instead of $2x10^{-1}\,ms^{-1}$. The magnitude of the wear rates for dry and lubricated conditions are very similar to those found on the Rotating Line Contact machine.

The friction and wear rate results for P.E.E.K. give a similar graph to P.P.O. and are shown in Figure 3.18. The dry friction is again higher on this machine at 0.5 compared to 0.3 on the Rotating Line Contact machine, and the lubricated friction exhibits a smaller decrease in values over the whole speed range. The graphs of dry and lubricated wear rates are very similar to those on the Rotating Line Contact machine except that the dry wear rate does show an increase at very high speeds.

The graphs of friction and wear for P.T.F.E. are similar to those obtained for the Rotating Line Contact machine

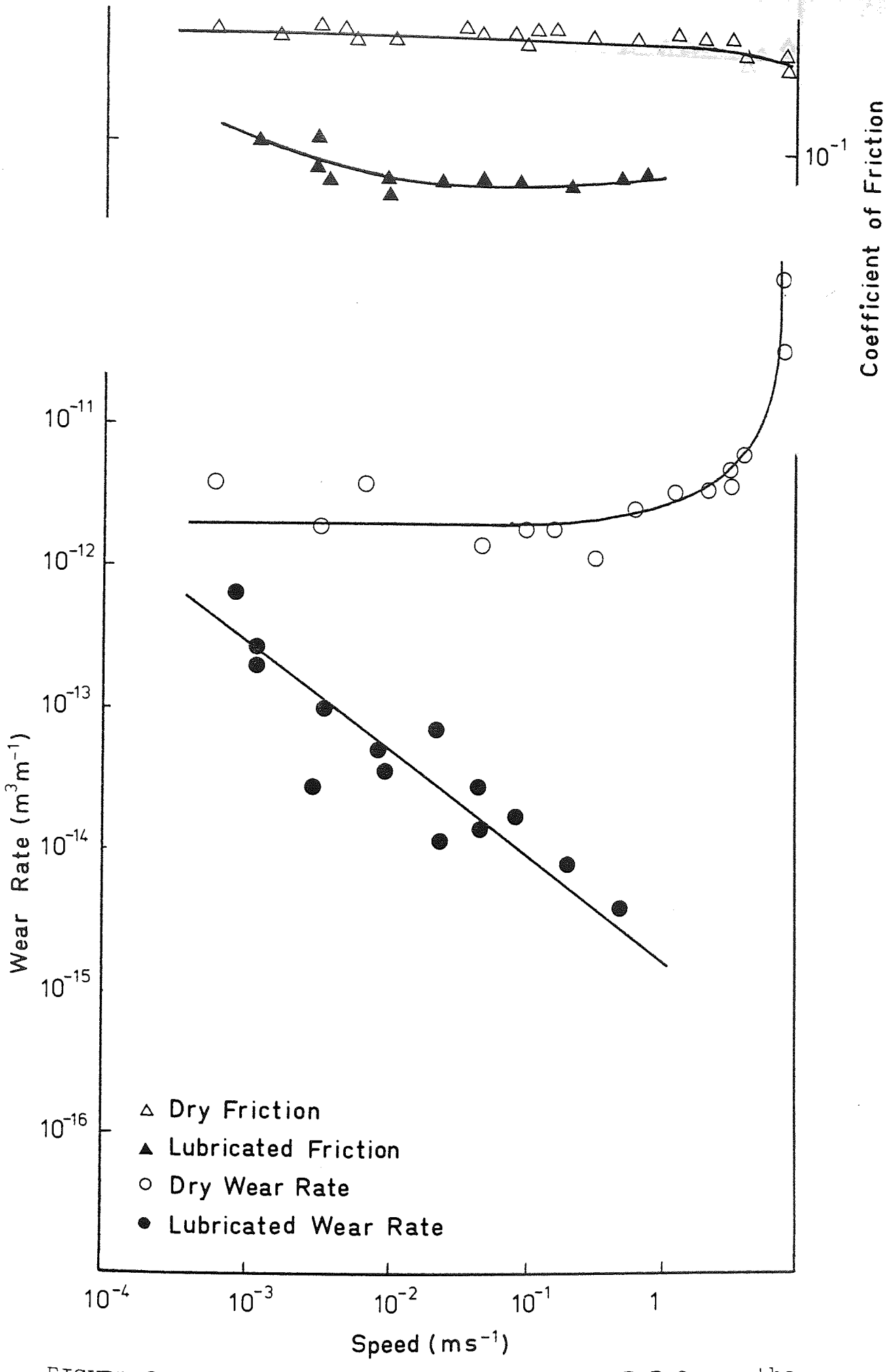

FIGURE 3.17 Friction and Wear rates for P.P.O. on the Uni-Directional Pin on Disc machine, 2.1 kg load, 10 cs fluid

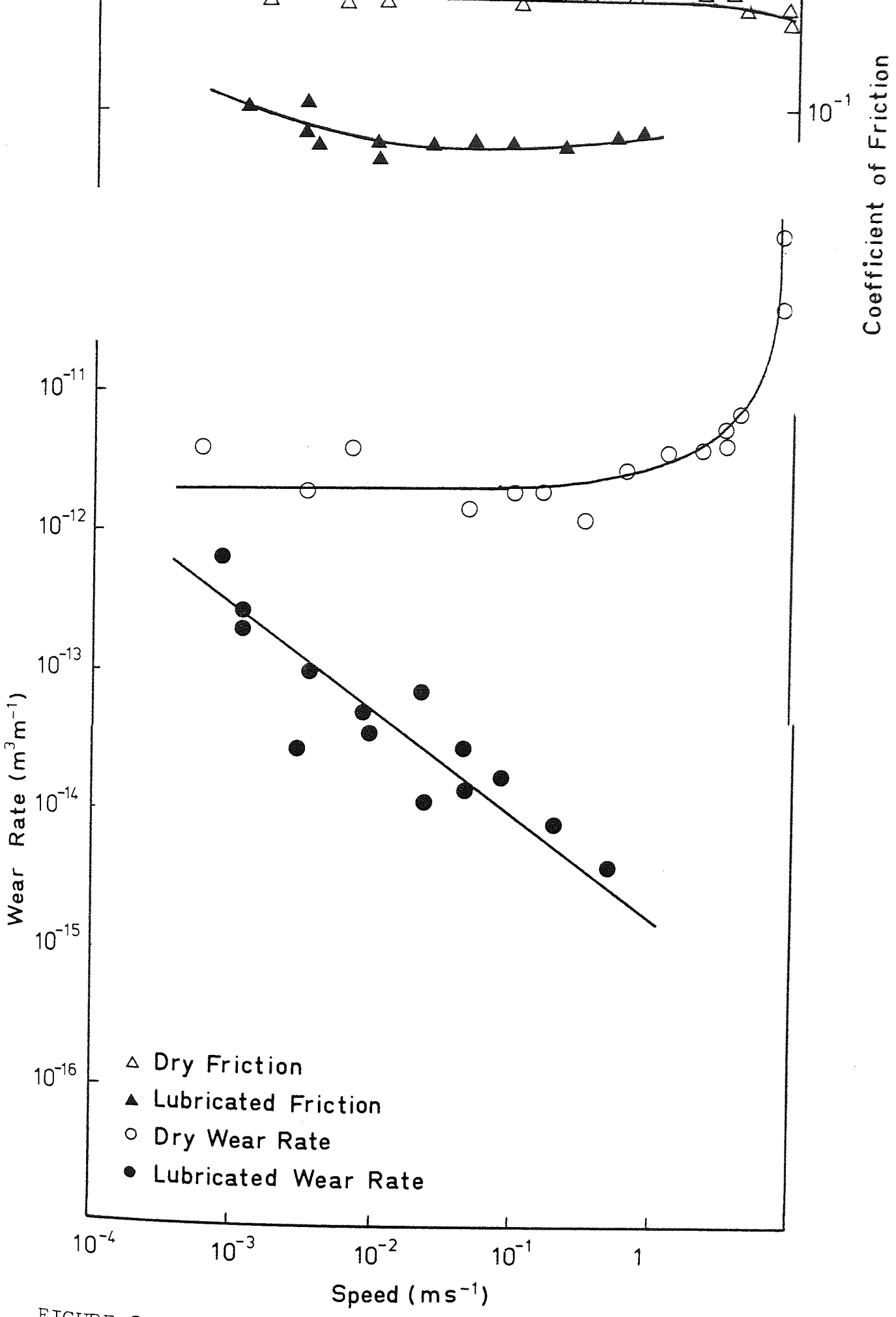

FIGURE 3.17 Friction and Wear rates for P.P.O. on the Uni-Directional Pin on Disc machine, 2.1 kg load, 10 cs fluid

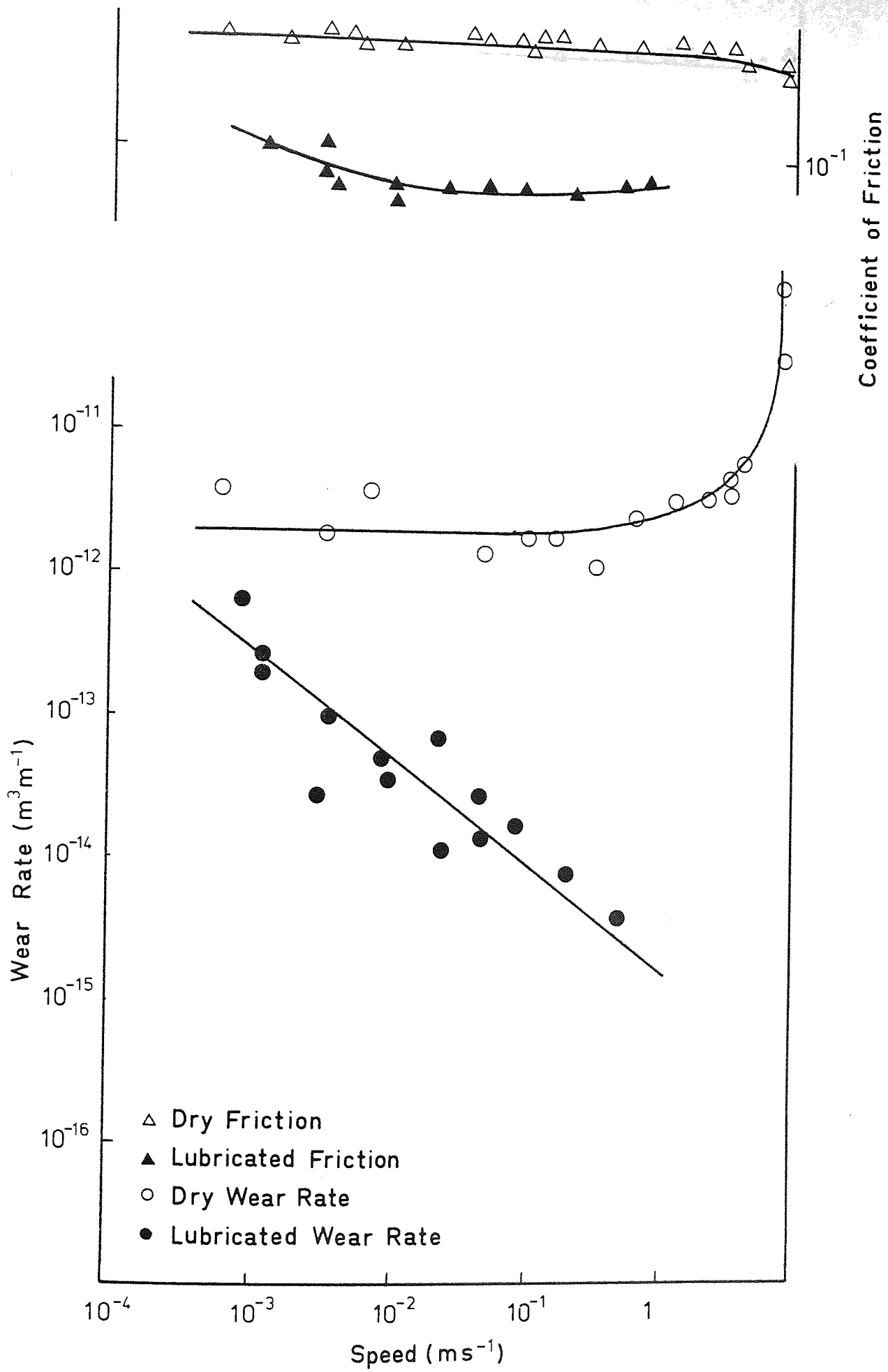

FIGURE 3.17 Friction and Wear rates for P.P.O. on the Uni-Directional Pin on Disc machine, 2.1 kg load, 10 cs fluid

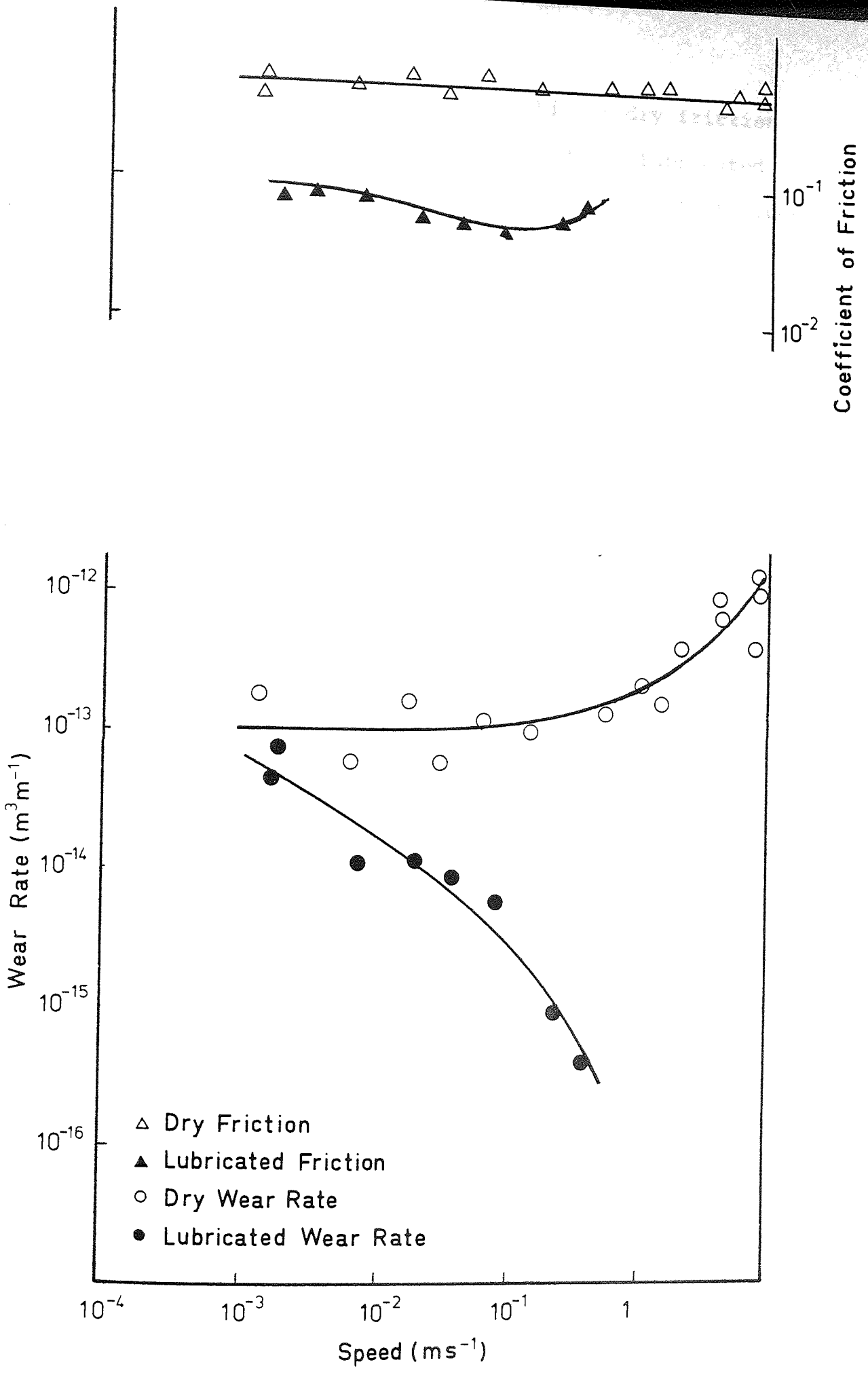

FIGURE 3.18 Friction and Wear rates for P.E.E.K. on the Uni-Directional Pin on Disc machine, 2.1 kg load, 10 cs fluid

and are shown in Figure 3.19. Again higher dry friction values are obtained on this machine and the lubricated friction gives a smaller decrease over the available speed range. The major difference between the two sets of results is with the dry wear rate. Whereas on the Rotating Line Contact machine a minimum occurred at $5x10^{-3}$ ms^{-1}, on this machine the dry wear rate continues to decrease with decreasing speed.

By extrapolation of the trends in wear rates with speed for P.P.O. and P.E.E.K., it seems reasonable to conclude that at very low speeds the lubricated wear rates will become approximately the same as the dry wear rates. With P.T.F.E. however, extrapolation suggests that the lubricated wear rates at very low speeds, are likely to become much greater than the dry wear rates. This very low wear rate for dry conditions at very slow sliding speeds is probably due to the formation of a transfer film (See Section 1.7) and two conditions are thought to occur:-

1) The transfer films are only likely to form under dry conditions as fluids impede their formation (58).

2) The transfer film effect on the wear rate under dry conditions is likely to be much greater at very low speeds, where the films are thin, highly orientated and strongly attached to the counterface (43). Whereas, at high speeds they become thicker, more lumpy, less orientated and not so strongly attached. This leads to a high level of film removal and replacement and therefore a higher wear rate.

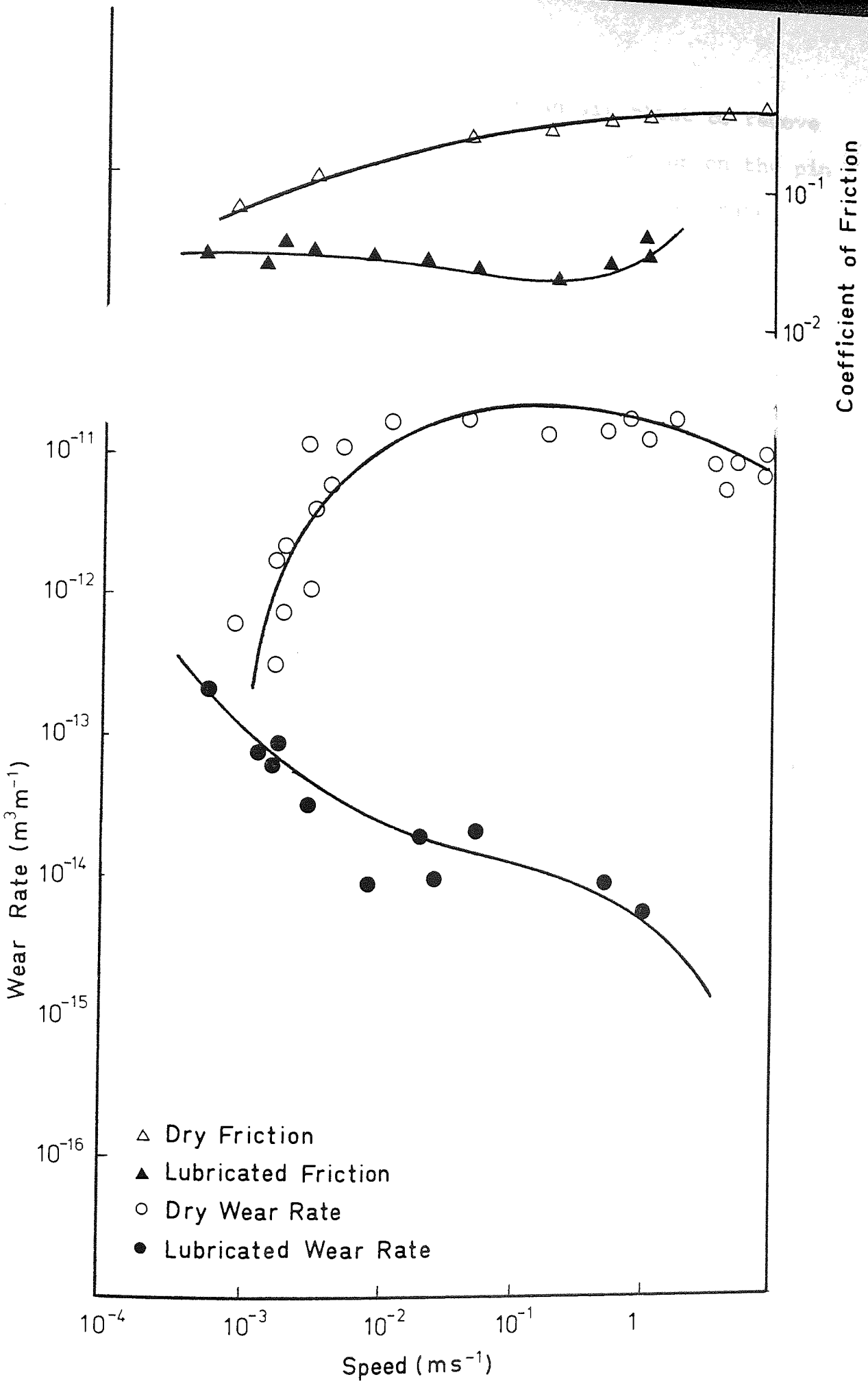

FIGURE 3.19 Friction and Wear rates for P.T.F.E. on the Uni-Directional Pin on Disc machine, 2.1 kg load, 10 cs fluid

No experiments were undertaken with an air blast to remove debris on this machine because debris collection on the pin surface was not seen to be a problem and the wear rates showed only a minimal scatter.

3.4.3 Reciprocating Line Contact Machine

Due to the lack of time available and the more restricted speed range on this machine experiments were conducted mainly with P.T.F.E., although P.P.O. and P.E.E.K. specimens were also used to study the debris and surface features generated. However, the values obtained were very similar to those found on the other wear machines and the general trends were almost the same. This is shown in Figure 3.20 where the dry friction increases with sliding speed, whereas, the lubricated friction is essentially constant. The dry wear rate is very similar to those found before with the lubricated wear rate decreasing rapidly with increasing sliding speed.

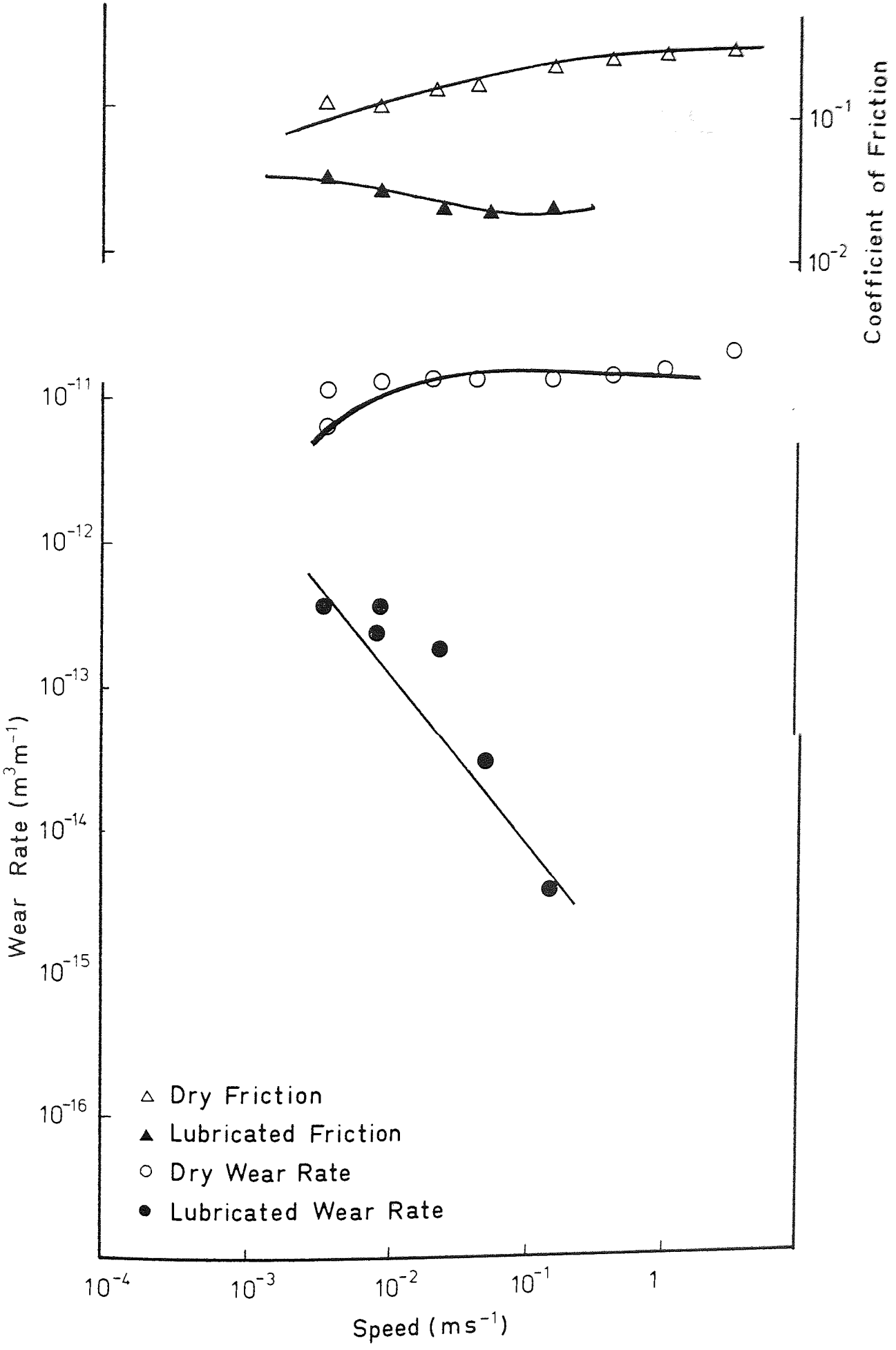

FIGURE 3.20 Friction and Wear rates for P.T.F.E. on the Reciprocating Line Contact machine, 2.5 kg load, 10 cs fluid

3.5 ANALYSES

3.5.1 Surface Features of Specimens and Debris

The P.P.O. specimens worn dry on the Rotating Line Contact machine showed a generally smooth surface, but with an agglomeration of debris in the centre of the pin. It is probable that this agglomeration had been formed by debris collecting in the gap between the pin and disc, and then being forced together to form one large particle of debris. This agglomeration will in future be referred to as the 'debris layer'.

The debris layer was made up of P.P.O. debris which was angular in shape and varied in size between 0.5 and 5μm thick. This debris layer is shown in Figure 3.21a and it appears that when the layer became too thick, excess material was extruded from the centre, in the form of a thin sheet approximately 5μm thick (See Figure 3.21b). The surface of the debris layer is shown in Figure 3.22a at a much higher magnification and the deformed debris particles can be clearly observed. At the same magnification, the pin surface outside the area of layer formation shows pitting of the P.P.O. in the direction of sliding, with the deeper end of the pit being first in contact with the disc. These pits are shown in Figure 3.22b and are approximately 0.5 to 5μm across. The debris left on the wear counterface tended to consist of large plates up to 200 μm across and 20μm thick. One such plate is shown in Figure 3.23a and it can be seen that it is made up of

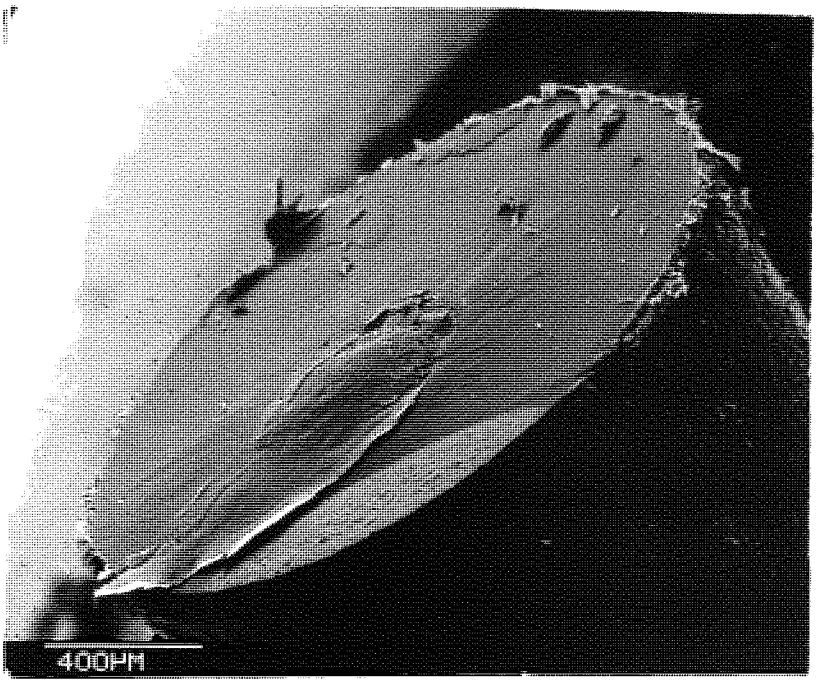

(a)

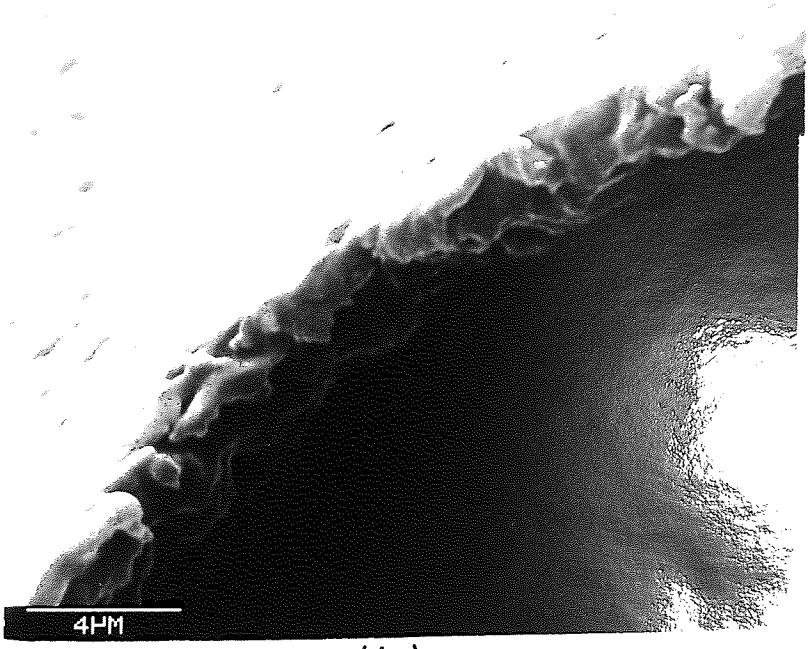

(b)

Figure 3.21a P.P.O. pin from the Rotating Line Contact machine run dry at $3x10^{-3}$ ms^{-1}, 2.1 kg load showing the debris layer

Figure 3.21b Edge of the debris layer shown in Figure 3.21a

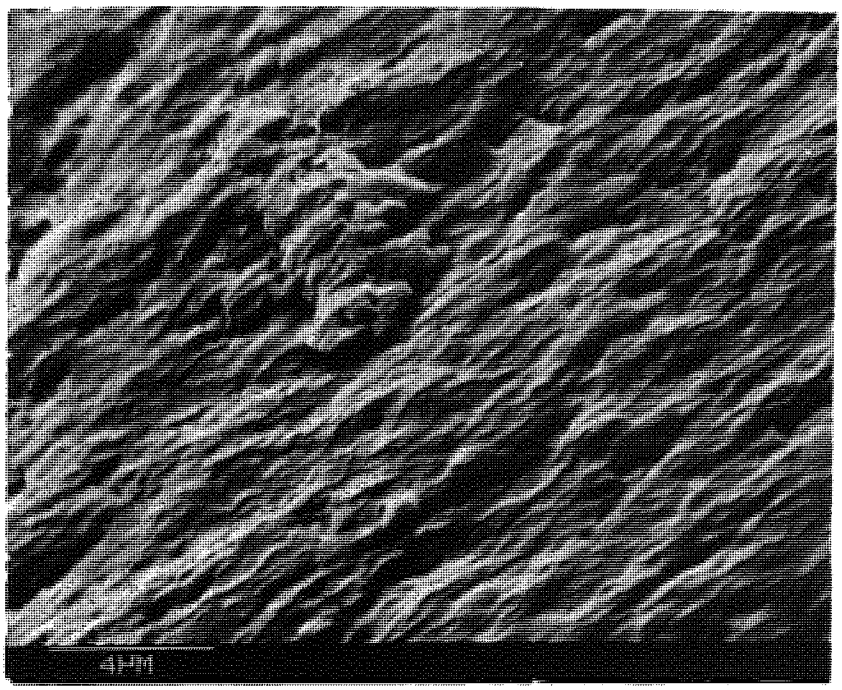

(a)

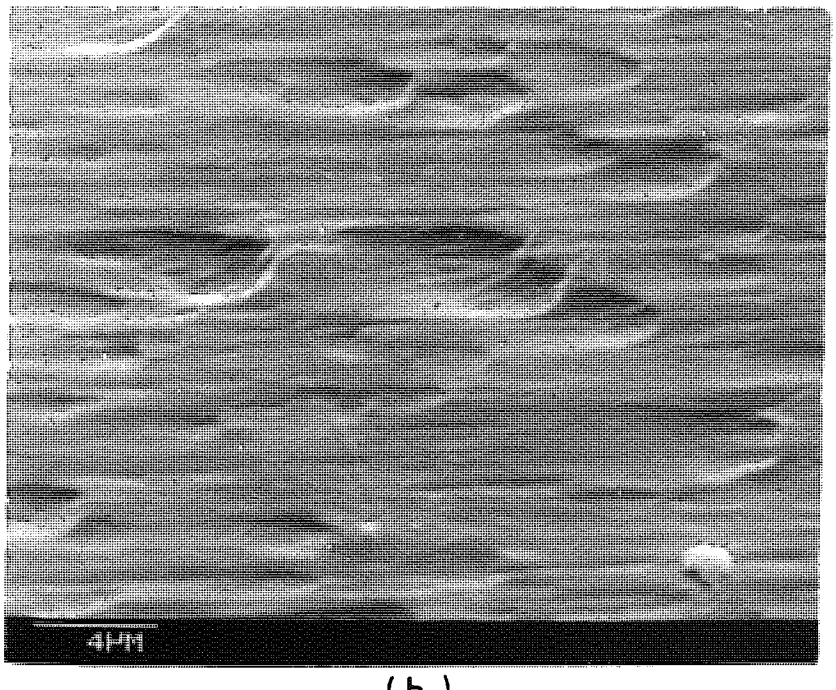

(b)

Figure 3.22a Surface of the debris layer shown in Figure 3.21a

Figure 3.22b Pits on the pin surface outside the area of the debris layer shown in Figure 3.21a

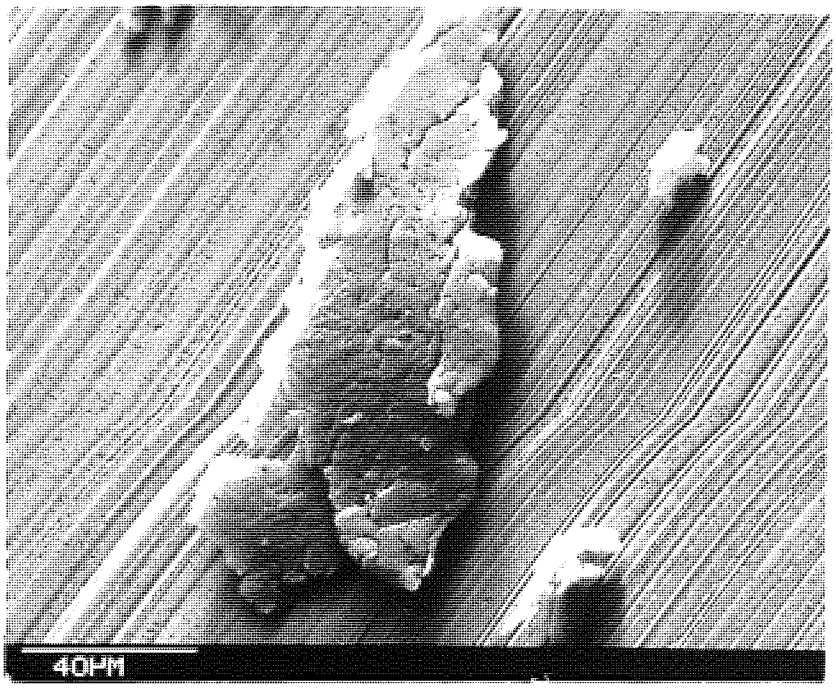

(a)

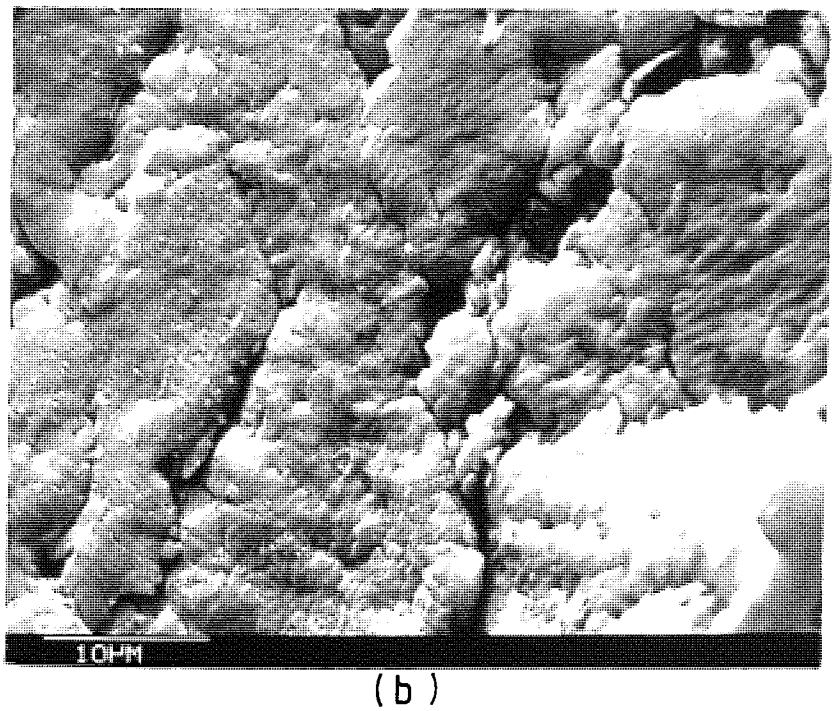

(b)

Figure 3.23a P.P.O. debris after wearing pin dry as shown in Figure 3.21a

Figure 3.23b Debris in Figure 3.23a at higher magnification

an agglomeration of numerous smaller particles (See Figure 3.23b). P.P.O. surfaces generated under lubricated conditions exhibited essentially the same features, with a layer of debris made up of deformed particles. However, pitting did not occur under lubricated conditions but ridges were formed in the polymer surface, transverse to the direction of sliding (See Figure 3.24a). The debris tended to be small particles up to 5μm across which were joined together into large flakes. Figure 3.24b shows that the debris remains at the side of the wear track, and higher magnification in Figure 3.25 shows that the debris formed under lubricated conditions is more rounded in appearance than the debris formed under dry conditions.

As with P.P.O. on the Rotating Line Contact machine, the P.E.E.K. specimens also exhibit a layer of debris in the centre of the pin when worn under dry conditions (See Figure 3.26a). This layer is also made up of deformed debris and looks exactly similar to the layer formed with P.P.O. Again the debris tends to be in the form of large plates as shown in Figure 3.26b, (consisting of deformed particles). The debris formed at high speeds (See Figure 3.27) tended to form smaller flakes. No pitting or ridges could be seen on the pin surface outside the area of layer formation, whether the pin was run under dry or lubricated conditions. The pins run under lubricated conditions did not have a debris layer, and debris was very angular with little evidence of the plate like formations seen after dry wear (See Figure 3.28a and b). The actual wear surface was generally very smooth except for isolated wear grooves.

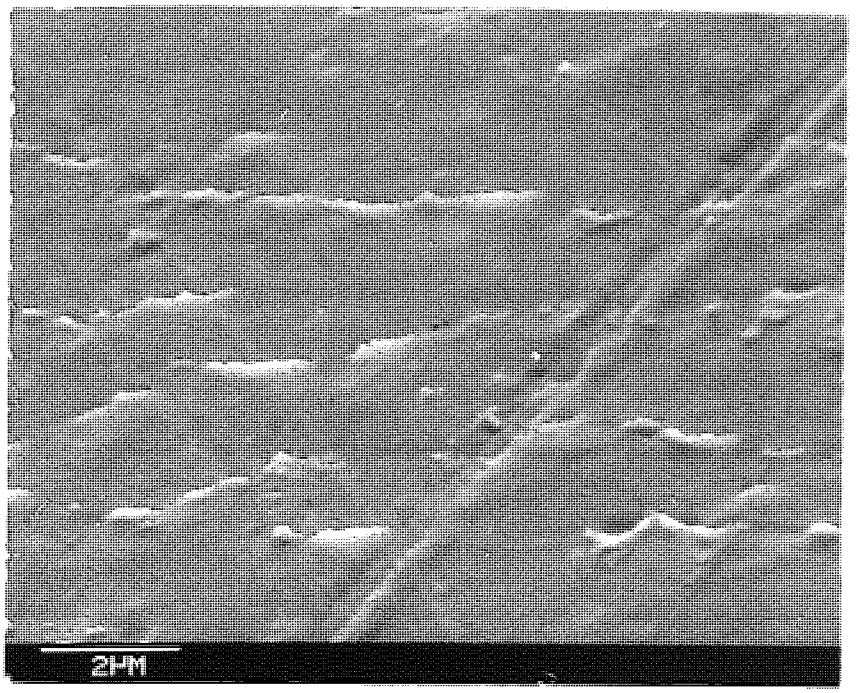

(a)

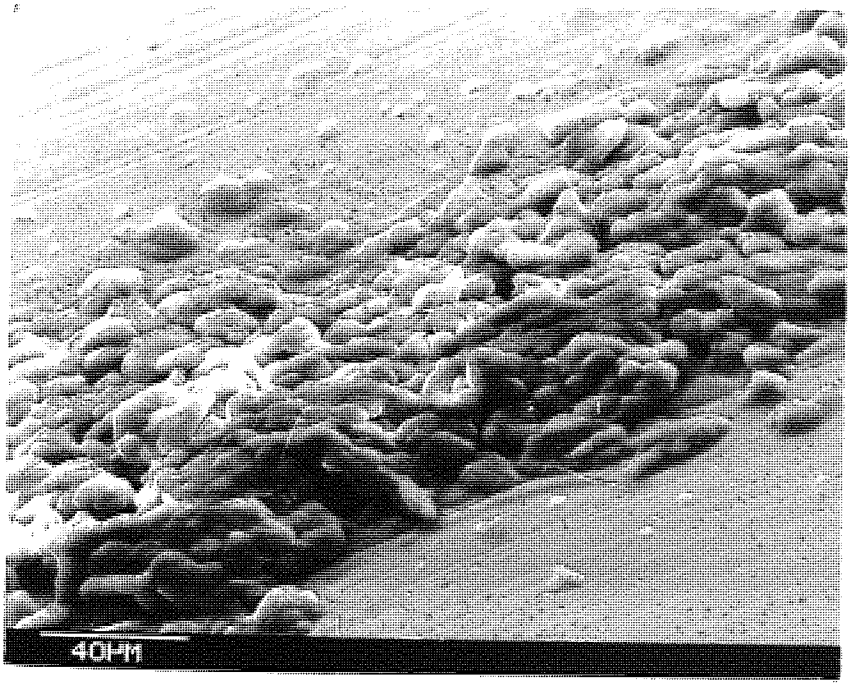

(b)

Figure 3.24a Surface of P.P.O. pin worn on the Rotating Line Contact machine under lubricated conditions; $3x10^{-3}$ ms^{-1}, 2.1 kg load, 10 cs fluid

Figure 3.24b Wear debris from pin in Figure 3.24a

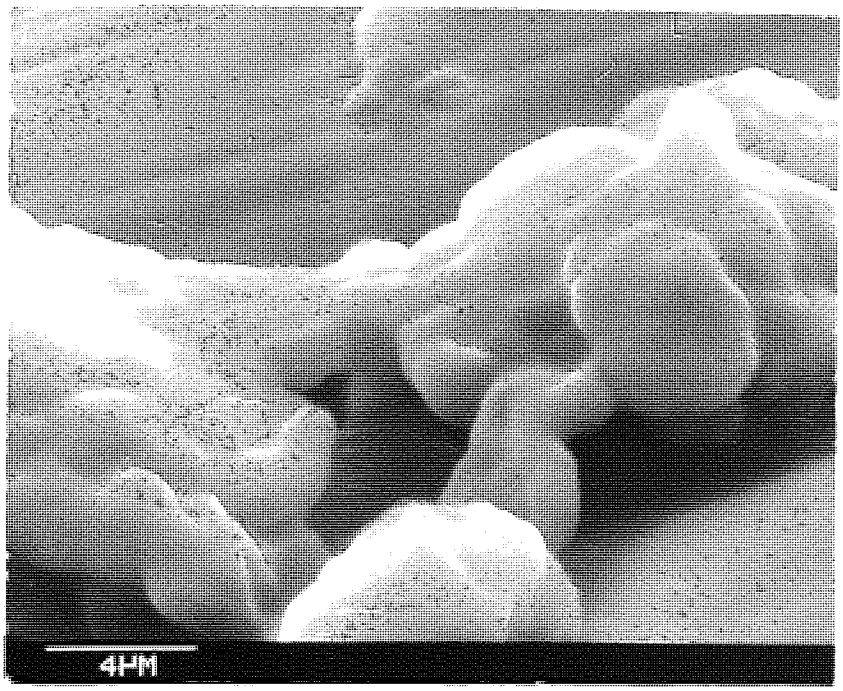

Figure 3.25 Wear debris from pin in Figure 3.24a at higher magnification

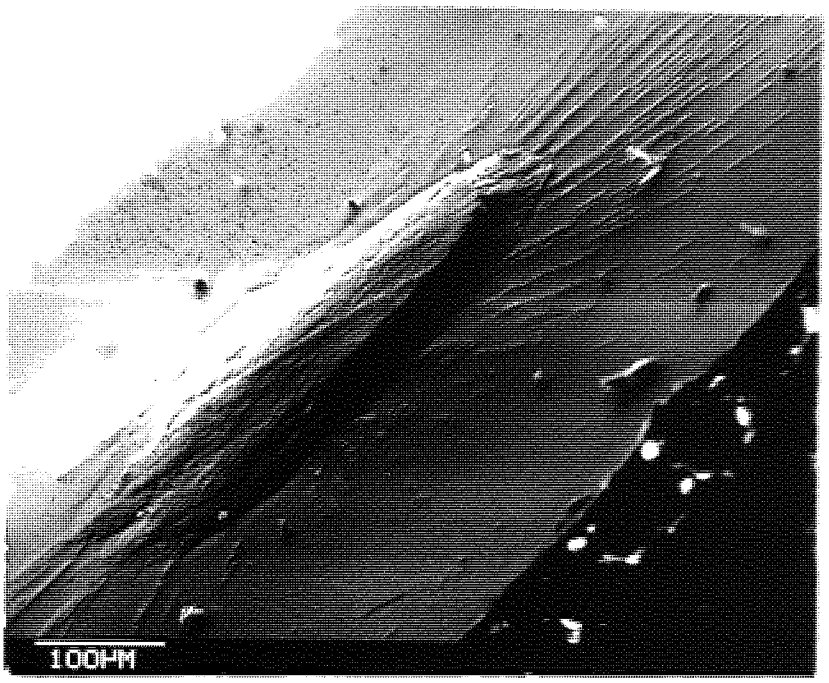

(a)

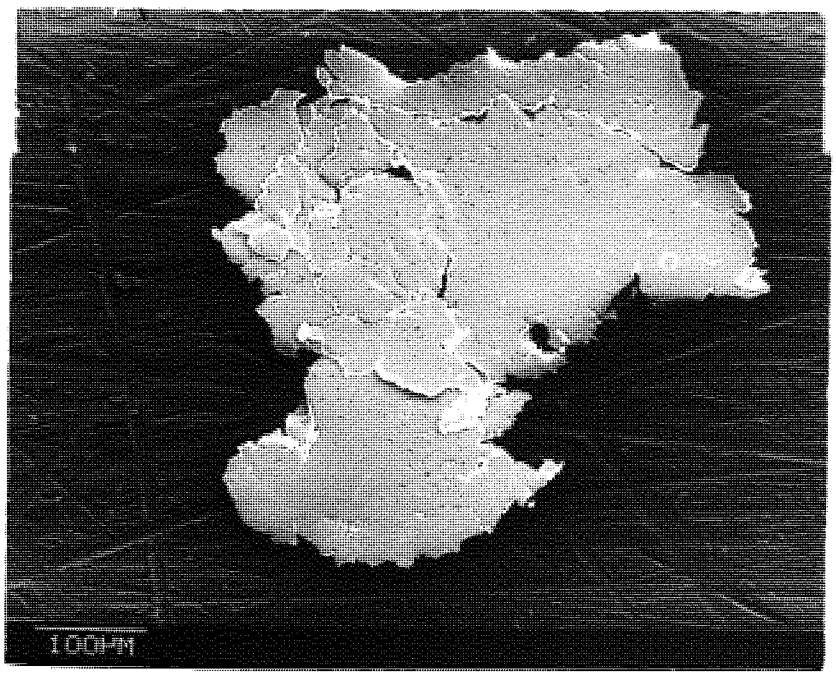

(b)

Figure 3.26a P.E.E.K. pin from the Rotating Line Contact machine run dry at $3x10^{-3}$ ms^{-1}, 2.1 kg load, showing the debris layer

Figure 3.26b P.E.E.K. debris from the pin in Figure 3.26a

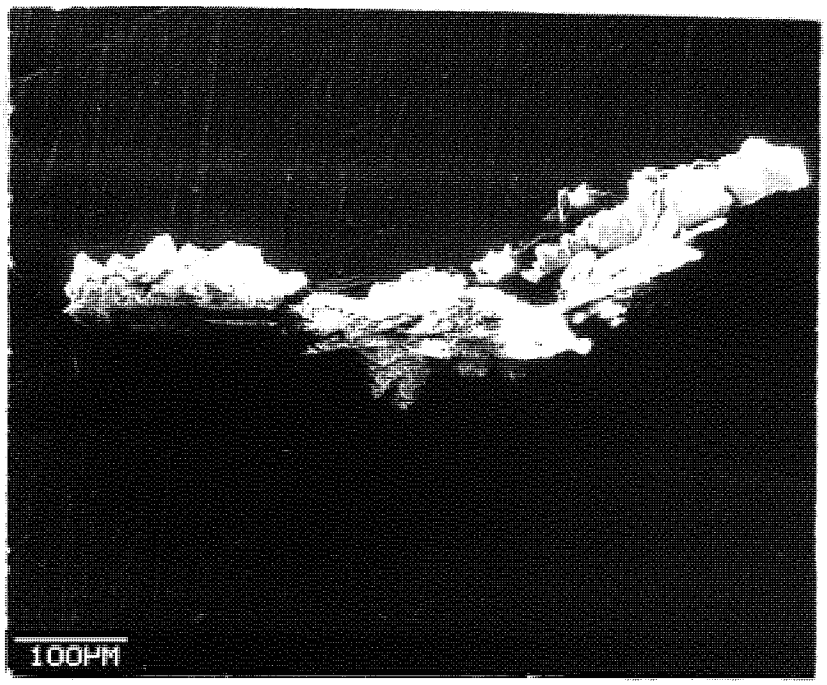

Figure 3.27 P.E.E.K. debris from dry run on the Rotating Line Contact machine at $2\,ms^{-1}$, 2.1 kg load

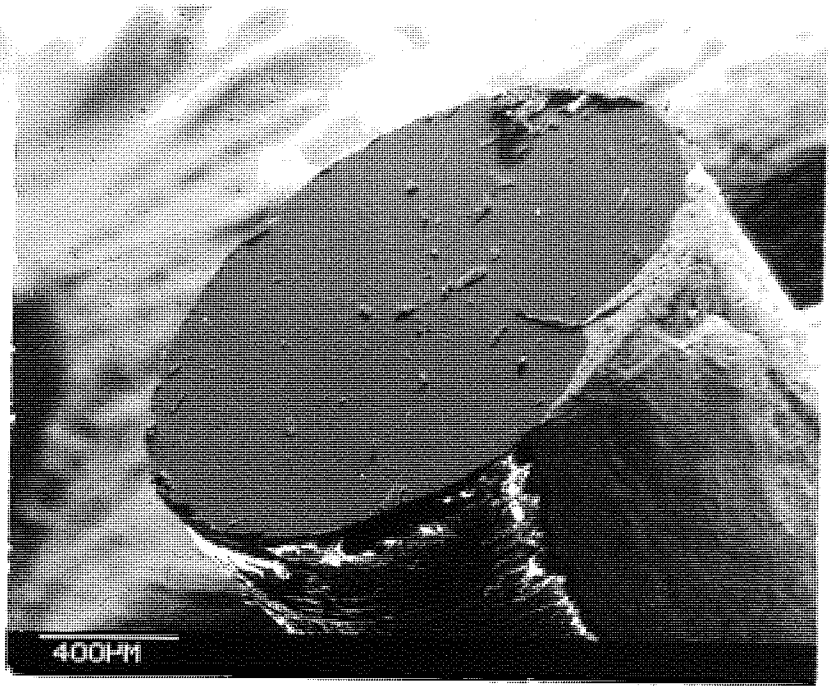

(a)

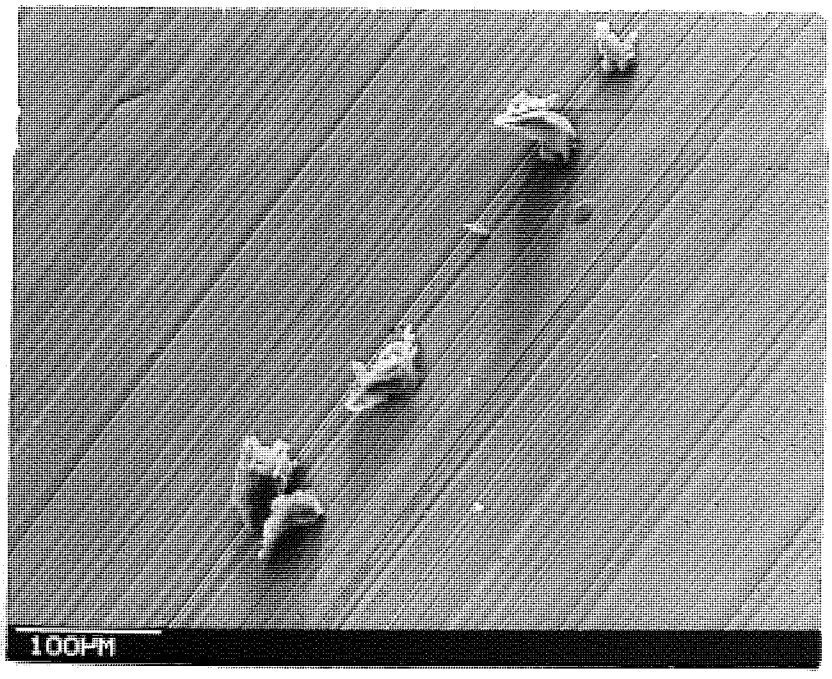

(b)

Figure 3.28a P.E.E.K. pin run under lubricated conditions on the Rotating Line Contact machine at $3x10^{-3}$ ms^{-1}, 2.1 kg load, 10 cs fluid

Figure 3.28b Debris from pin in Figure 3.28a

P.T.F.E. specimens worn on the Rotating Line Contact machine under dry conditions, only showed a layer of the debris on rare occasions, an example of which can be seen in Figure 3.29a. It was more usual, however, for a small protuberance to be formed in the centre of the pin, with polymer then being extruded out towards the edge of the pin, (See Figure 3.29b), in the form of flakes. Ripples on the surface of the pin radiated in a spiral fashion from the centre to the edge, and Figure 3.30a shows that these ripples are approximately 5μm apart and 0.5μm deep. (The ripples resemble shallow waves in a liquid surface). Figure 3.30b shows that the debris flakes could be quite large but they were usually 100-150μm across. The surface of these flakes under high magnification shows stretching of the polymer with voids opening up in the surface (See Figure 3.31). Heavy transfer of the P.T.F.E. debris occurred onto the counterface at slow speeds. Figures 3.32a and 3.32b show how the transferred debris is made up of drawn out material several microns thick.

Under lubricated conditions the surface features of the P.T.F.E. pin appeared very different. No debris layer occurred on the pin, nor were there any ripples or extruded debris at the edge of the pin. The surface was very flat without the protuberance seen with dry wear (See Figure 3.33). No transfer occurred at any time during lubricated wear and the volume of debris was too small to be recovered from the fluid.

On the Uni-Directional pin on disc machine the P.P.O.

(a)

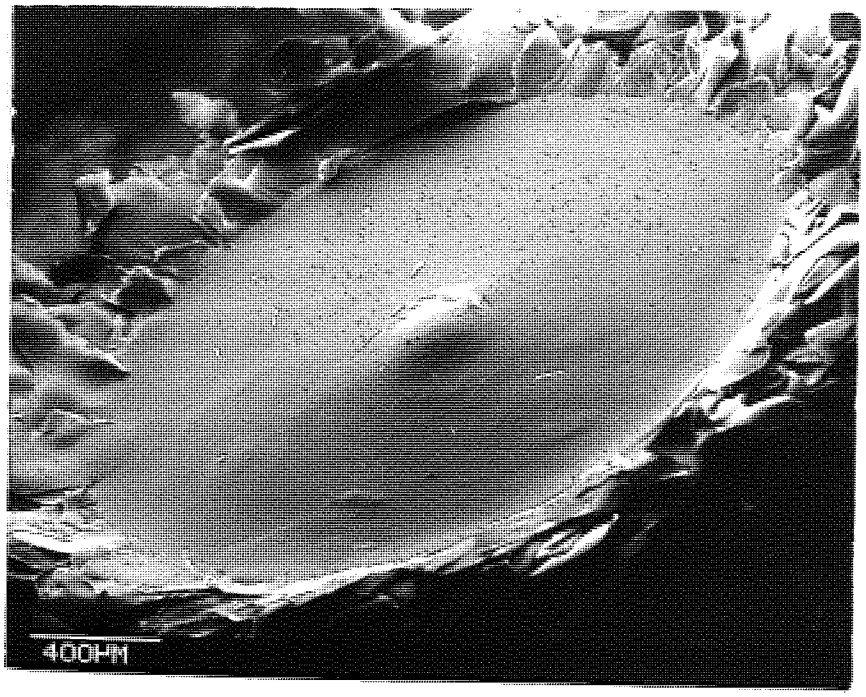

(b)

Figure 3.29a Surface of P.T.F.E. pin run under dry conditions on the Rotating Line Contact machine, $3x10^{-3}$ ms^{-1}, 2.1 kg load

Figure 3.29b As for Figure 3.29a

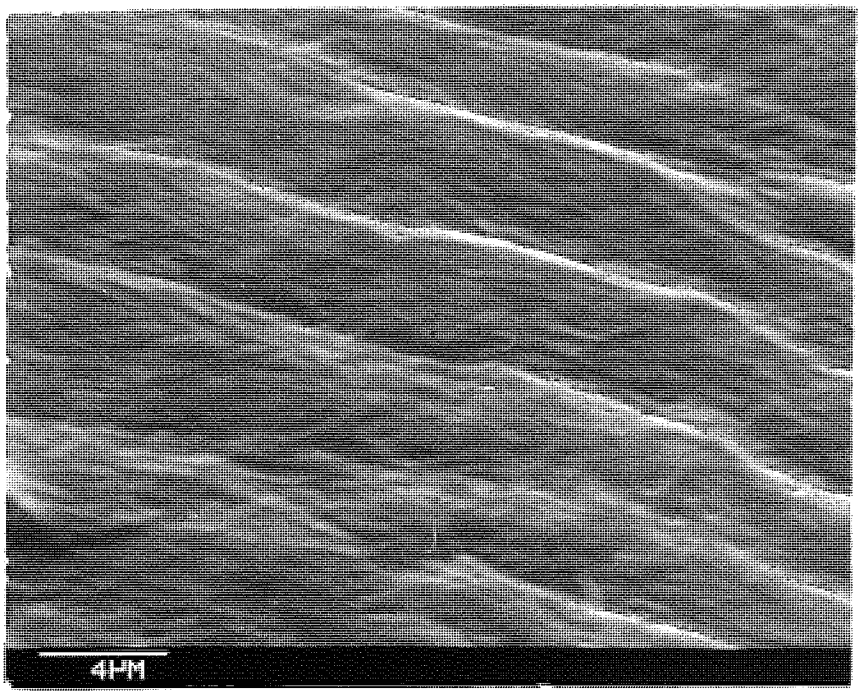

(a)

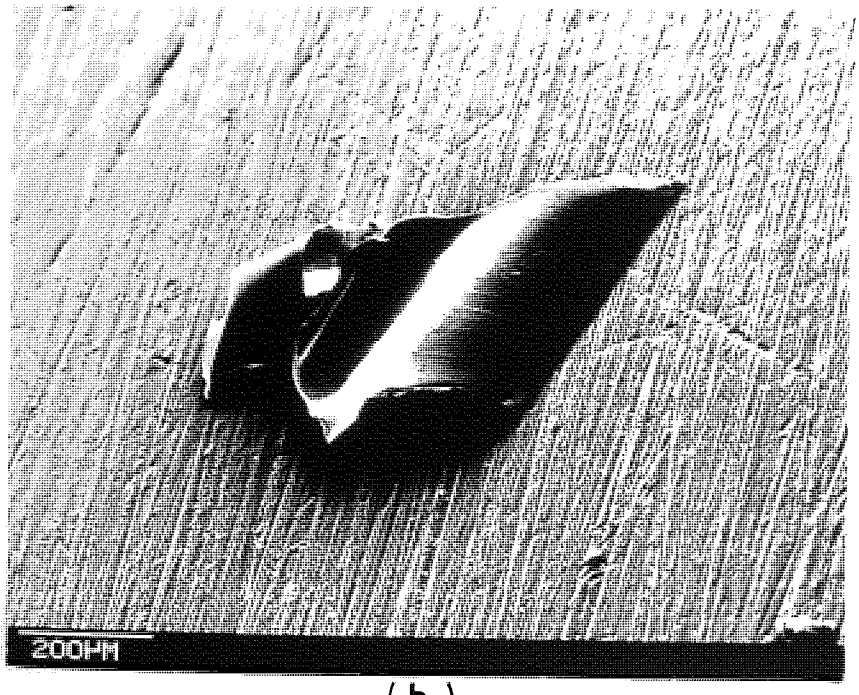

(b)

Figure 3.30a Surface of pin in Figure 3.29a at higher magnification

Figure 3.30b P.T.F.E. debris from pin shown in Figure 3.29a

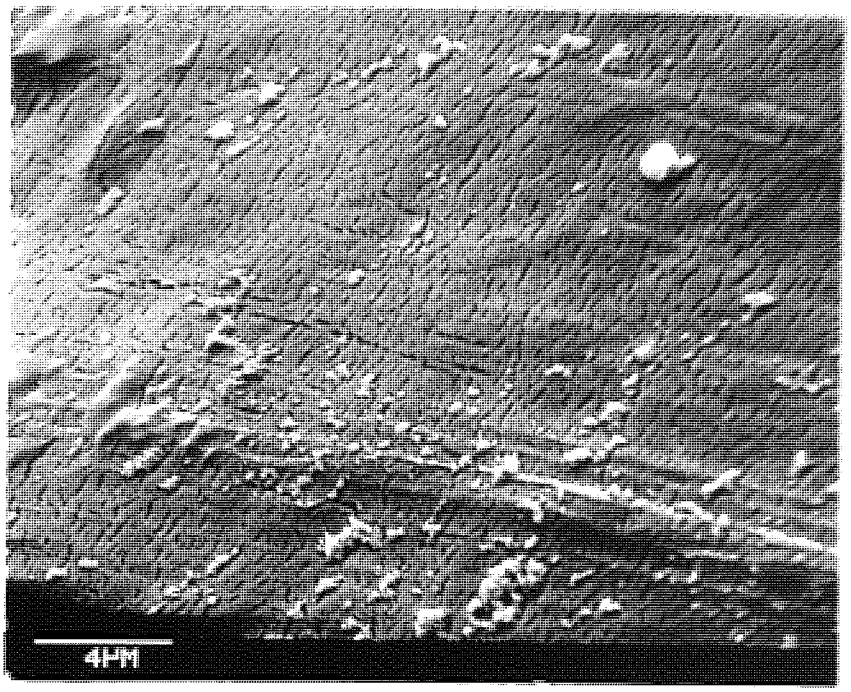

Figure 3.31 P.T.F.E. debris from pin shown in Figure 3.29a at high magnification

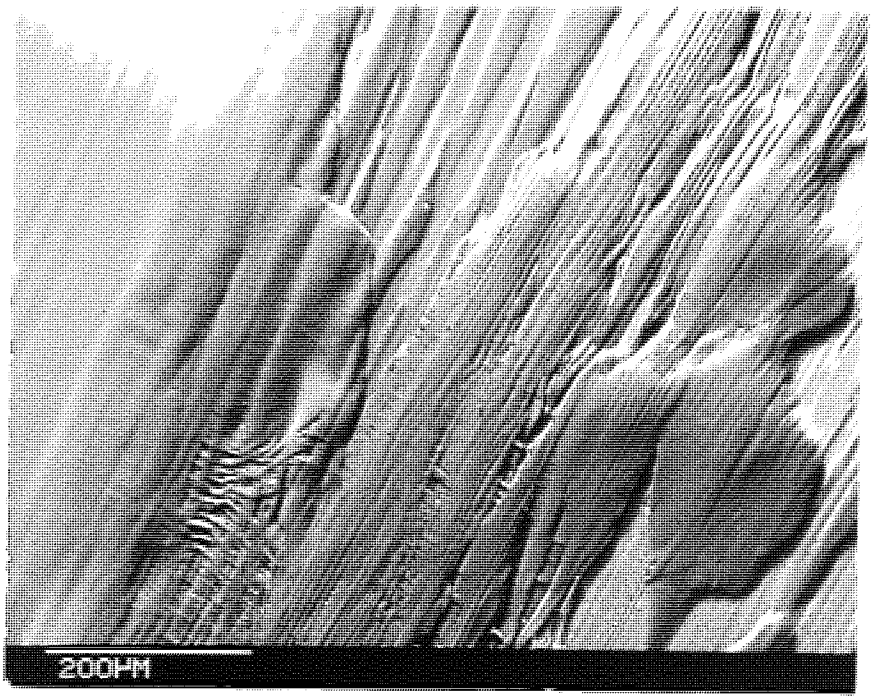

(a)

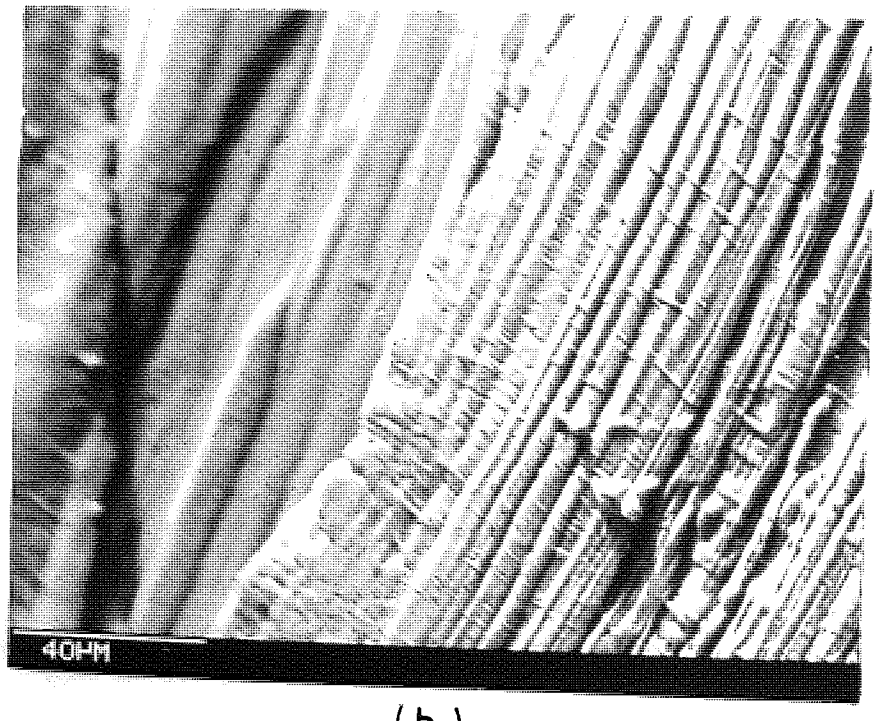

(b)

Figure 3.32a Transferred P.T.F.E. material onto the wear counterface from pin shown in Figure 3.29a

Figure 3.32b As for Figure 3.32a but at higher magnification

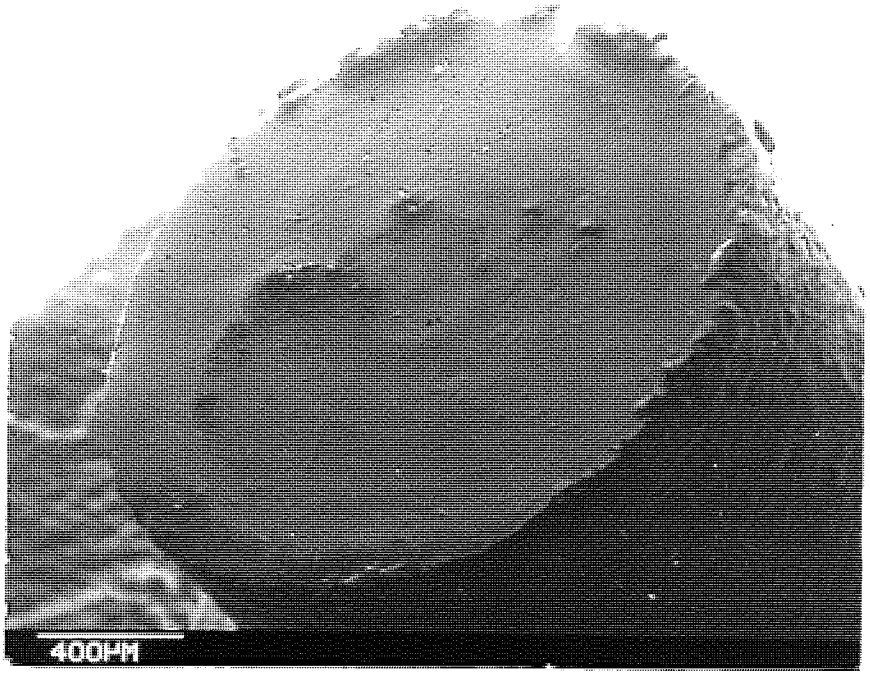

Figure 3.33 P.T.F.E. pin run under lubricated conditions on the Rotating Line Contact machine at 3×10^{-3} ms^{-1}, 2.1 kg load and 10 cs fluid

specimens worn dry showed only minor amounts of a debris layer on the pin (See Figure 3.34a). The pin surface was generally smooth (See Figure 3.34b) although some wear grooves and pitting can be seen (See Figure 3.35a). The pits were very similar to those seen on the Rotating Line Contact machine and approximately of the same size. The debris tended to be small and angular at slow speeds as shown in Figure 3.35b, whereas, at high speeds strips of debris were present and were probably produced by polymer melting and extrusion (See Figures 3.36a and b) leaving the pin with a flower like appearance. Figure 3.37a shows that under lubricated conditions the pin was left with a smooth surface having no debris layer or pitting, but showed the distinctive ridges seen with P.P.O. specimens on the Rotating Line Contact machine under lubricated conditions (the large pits in the pin surface seen in Figure 3.37a are the remains of machining marks left when producing the pin). The ridges seen in Figure 3.37b were usually separated by approximately 2-3μm and could be up to 50μm wide.

When P.E.E.K. was worn on the Uni-Directional pin on disc machine under dry and lubricated conditions, the pin surface generated was again smooth except for a few isolated wear grooves (See Figure 3.38a). No debris layer pitting, ridges or ripples were noticed and the debris produced under dry conditions was usually angular, as shown in Figure 3.38b. No debris could be collected for examination during the lubricated experiments as the amount was too small.

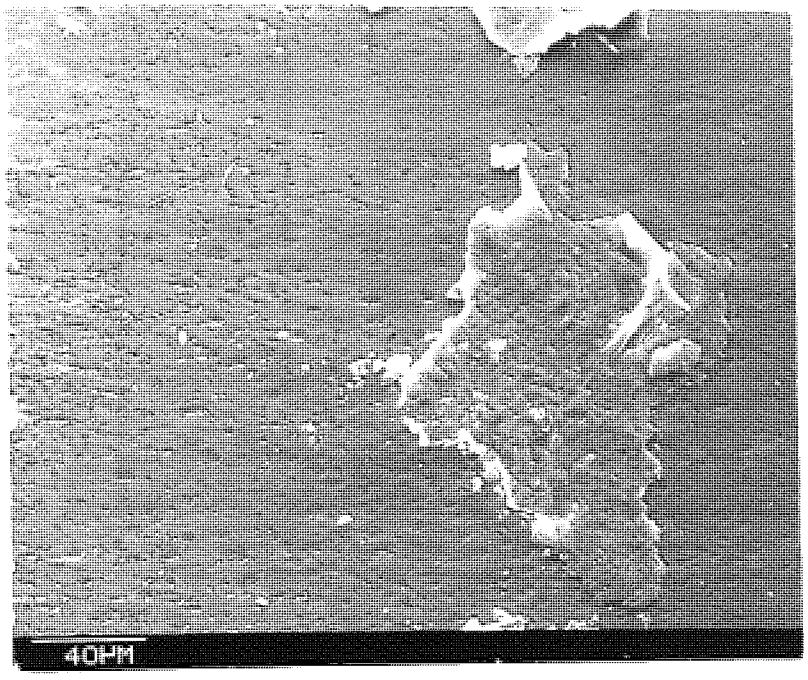

(a)

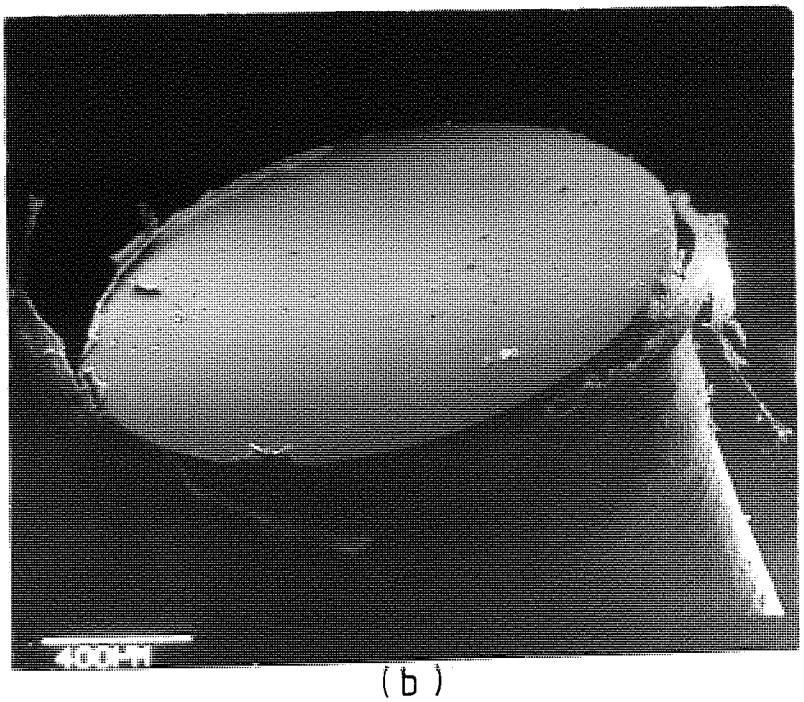

(b)

Figure 3.34a Surface of P.P.O. pin run dry on the Uni-Directional Pin on Disc machine at 3×10^{-3} ms^{-1} and 2.1 kg load

Figure 3.34b As for Figure 3.34a showing the whole of the pin

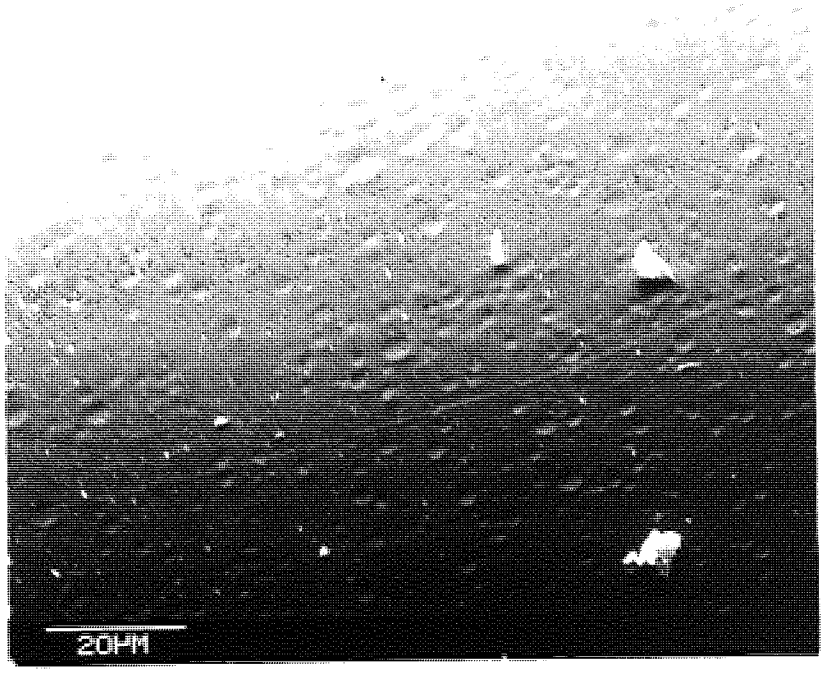

(a)

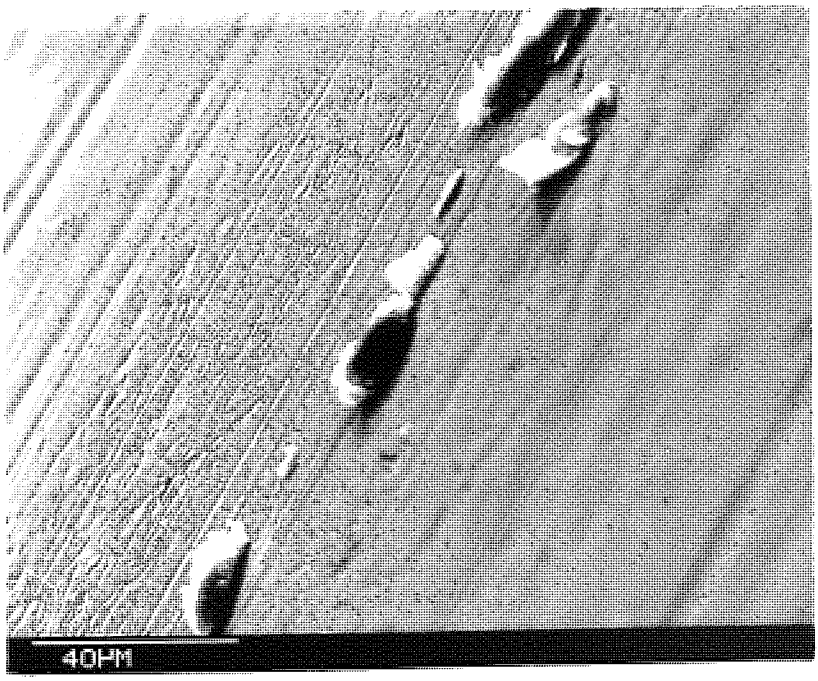

(b)

Figure 3.35a Surface of P.P.O. pin as shown in Figure 3.34a at higher magnification

Figure 3.35b Debris from pin shown in Figure 3.34a

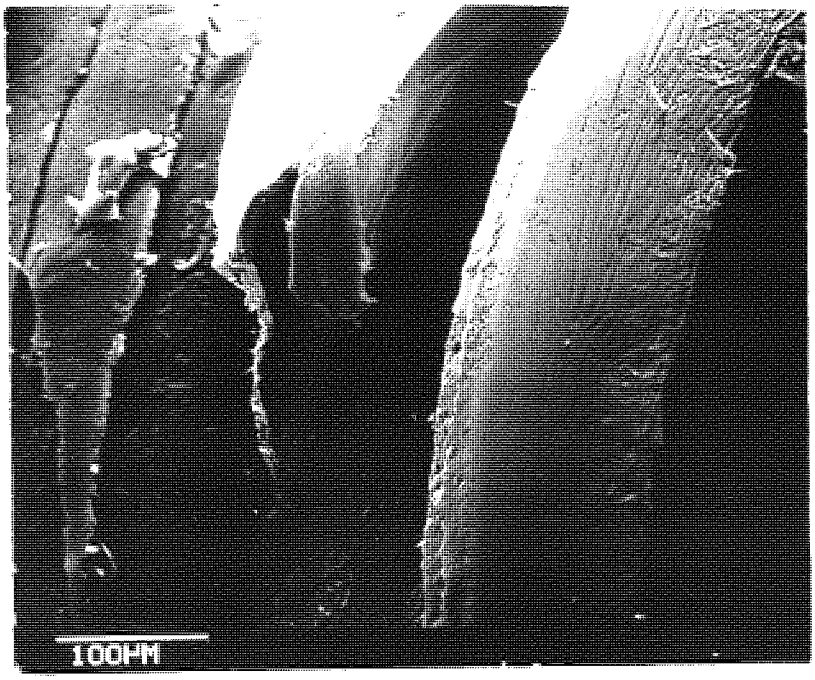

(a)

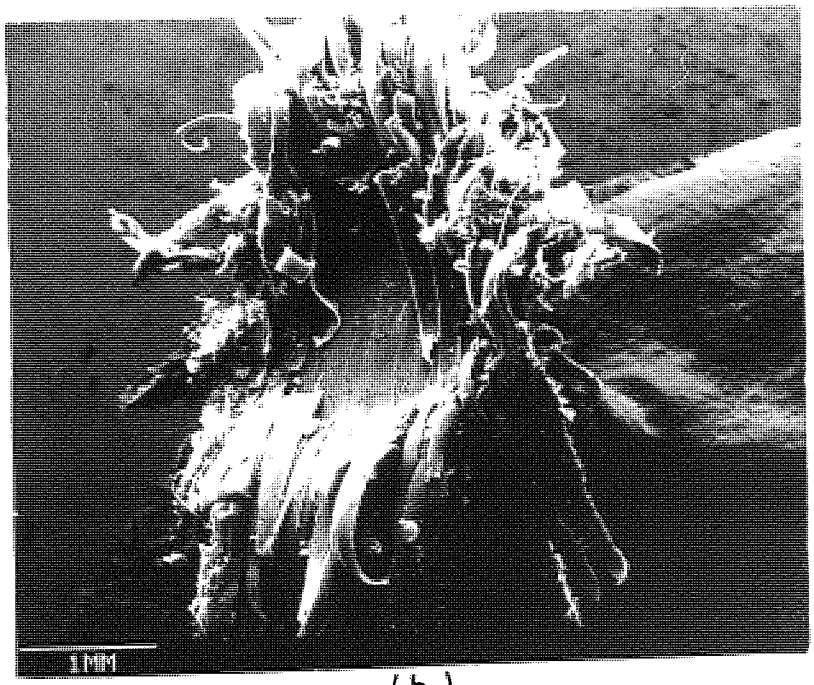

(b)

Figure 3.36a P.P.O. debris produced at high speed ($4.2\,ms^{-1}$) on the Uni-Directional Pin on Disc machine under dry conditions

Figure 3.36b Pin associated with debris in Figure 3.36a

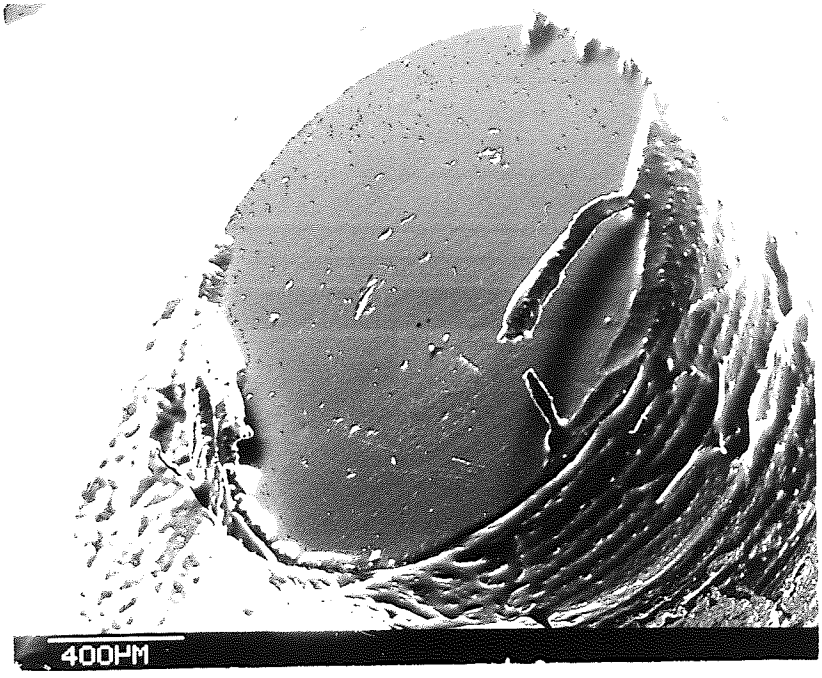

(a)

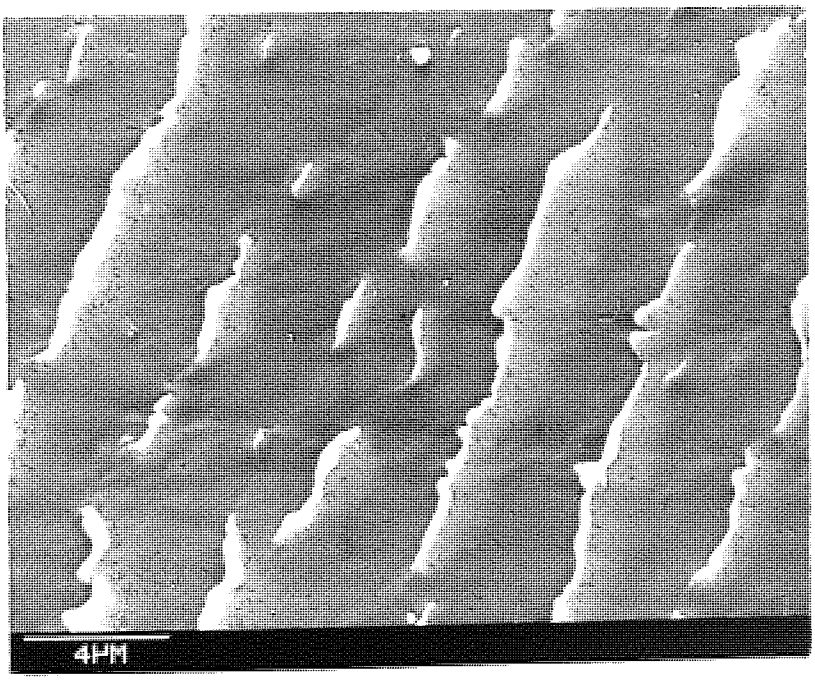

(b)

Figure 3.37a P.P.O. pin run under lubricated conditions on the Uni-Directional Pin on Disc machine at $3x10^{-3}$ ms^{-1}, 2.1 kg load and 10 cs fluid

Figure 3.37b Surface of pin in Figure 3.37a

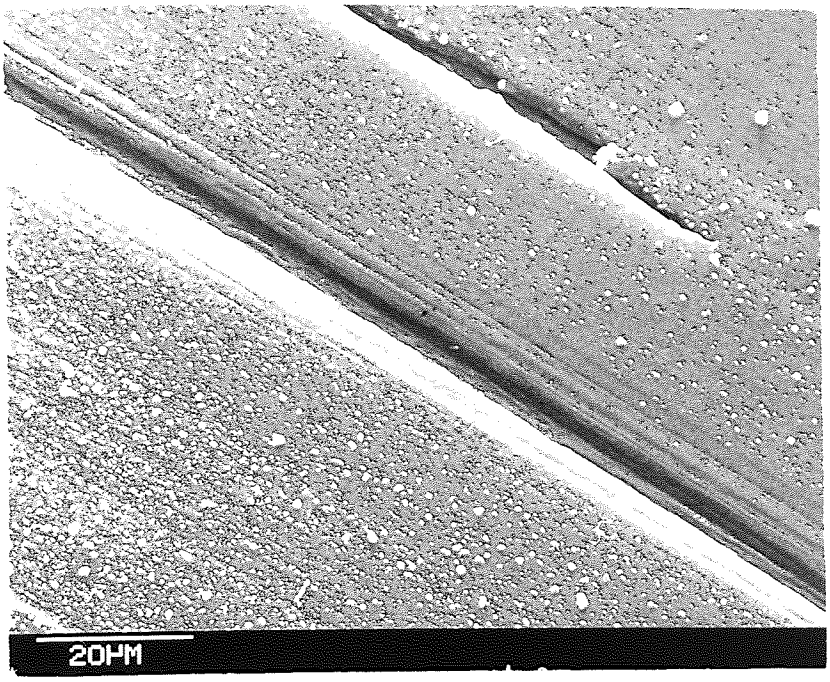

(a)

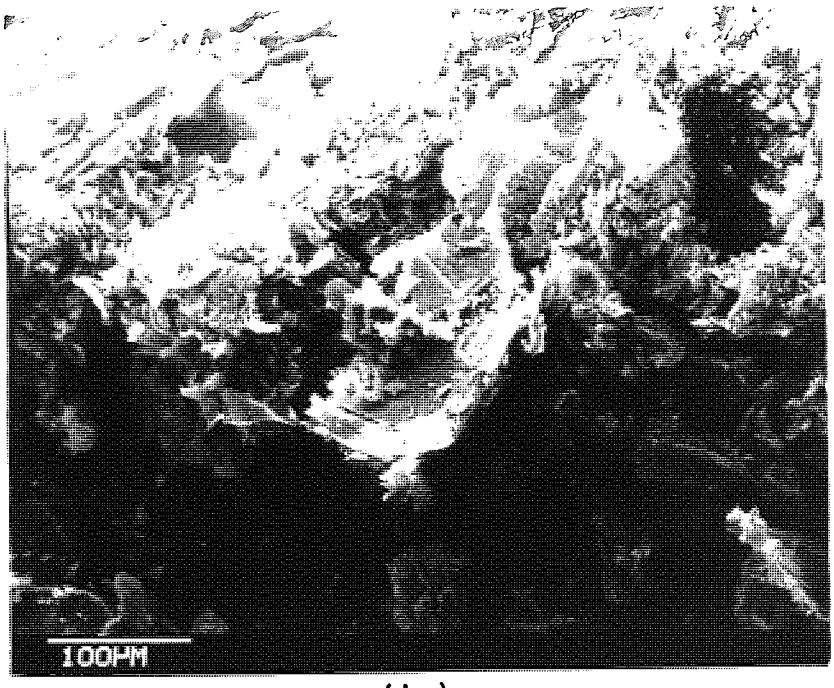

(b)

Figure 3.38a Surface of P.E.E.K. pin run under dry conditions on the Uni-Directional Pin on Disc machine at $3x10^{-3}$ ms^{-1}, 2.1 kg load

Figure 3.38b Debris from pin in Figure 3.38a

With P.T.F.E. on the Uni-Directional pin on disc machine under dry conditions material tended to be extruded from the rear of the pin (See Figure 3.39a), leaving the surface with the distinctive ripples seen before on the Rotating Line Contact machine (See Figure 3.39b). No debris layer was observed and very loosely attached debris was left on the disc in strips and showed considerable stretching (See Figures 3.40a and b, 3.41a). A side view of the strip seen in Figure 3.41b shows them to be approximately 5μm thick. Under lubricated conditions the surface of the P.T.F.E. pin was smooth with no debris layer or ripples and with no transfer to the disc (See Figure 3.42). Again it was not possible to collect debris for examination from the lubricated experiments.

For experiments conducted on the Reciprocating Line Contact machine for P.P.O. under dry conditions, pitting was again obvious as shown in Figure 3.43a. Debris layers were not formed except at high speeds when there were indications that some melting of the polymer surface had taken place (See Figure 3.43b). The debris produced under dry conditions tended to be made up of small particles joined together into flakes (See Figures 3.44a and b). When the P.P.O. was worn under lubricated conditions the surface showed no debris layer, pitting or ripples but ridges could be seen which were transverse to the sliding direction (See Figure 3.45a). The debris from lubricated sliding experiments was similar to that from the Rotating Line Contact machine for P.P.O. worn under lubricated conditions (See Figure 3.45b).

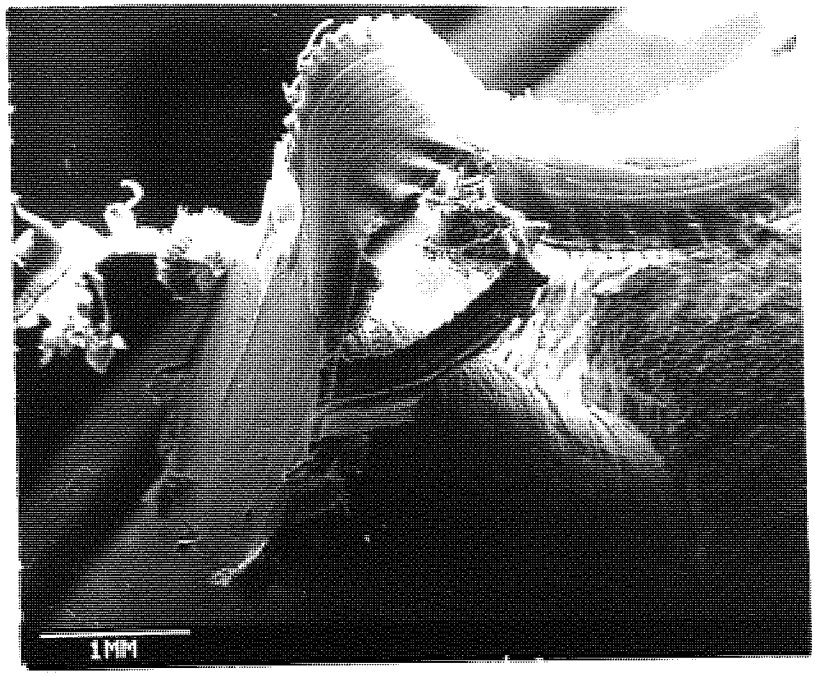

(a)

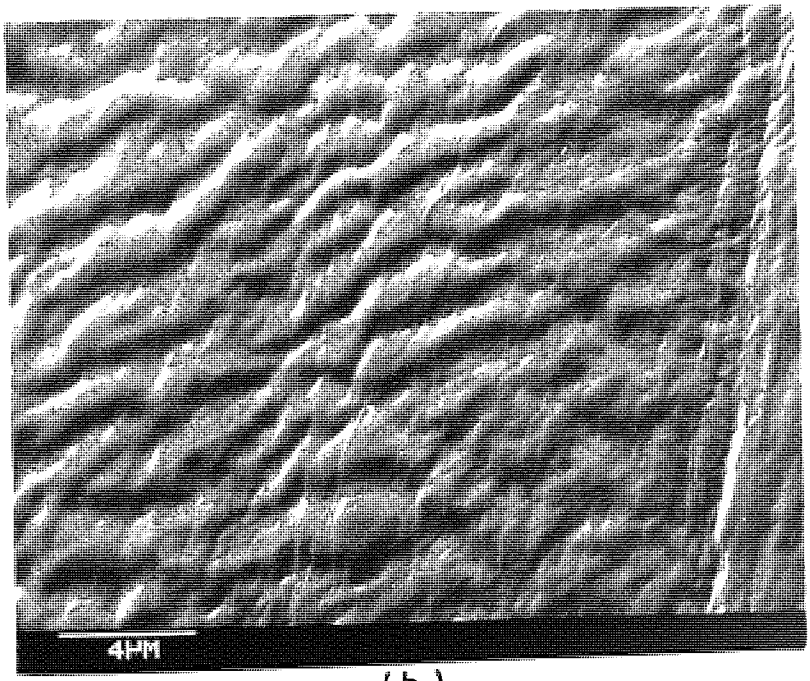

(b)

Figure 3.39a P.T.F.E. pin run under dry conditions on the Uni-Directional Pin on Disc machine at $3x10^{-3}ms^{-1}$ and 2.1 kg load

Figure 3.39b Surface of pin in Figure 3.39a

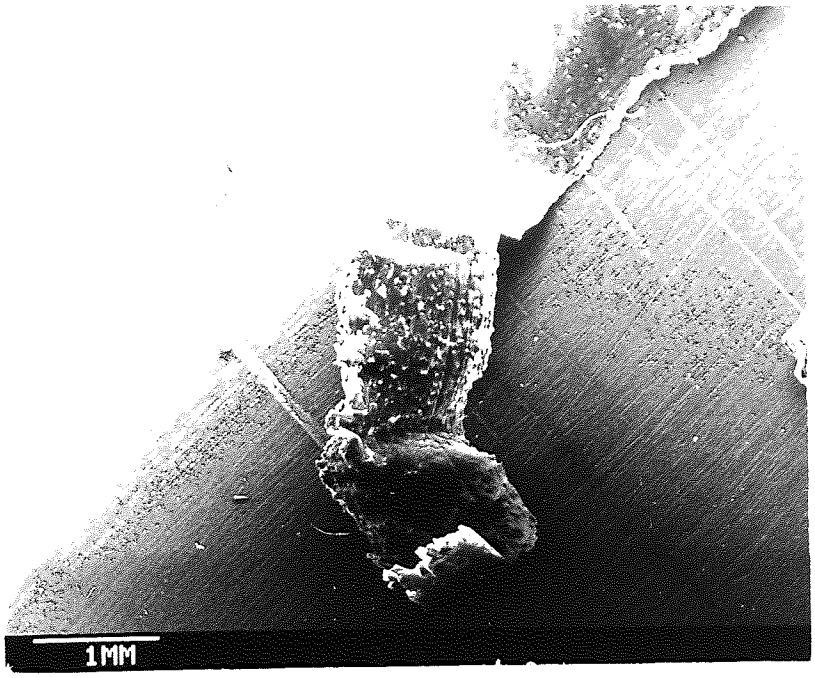

(a)

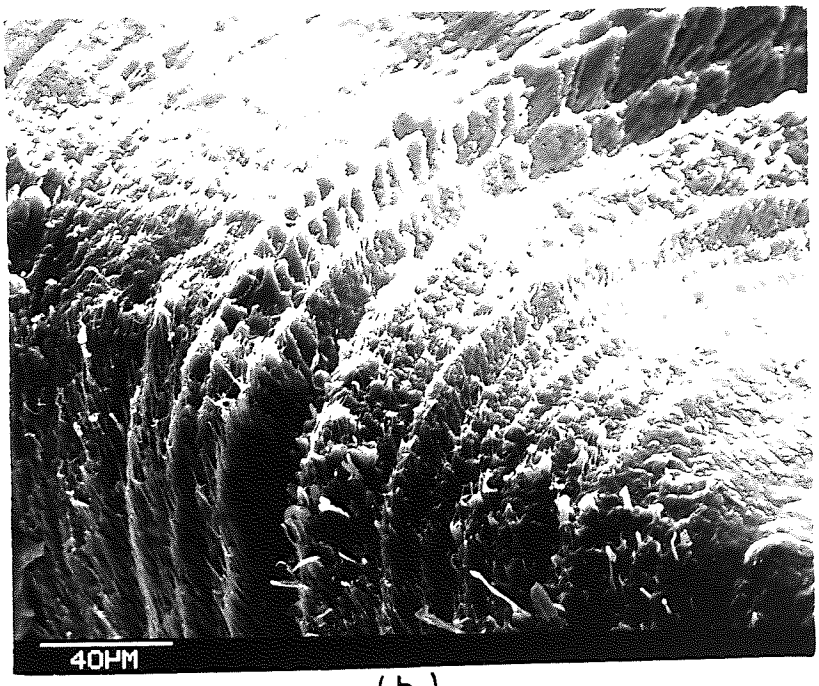

(b)

Figure 3.40a Debris from pin shown in Figure 3.39a

Figure 3.40b As for Figure 3.40a but at higher magnification

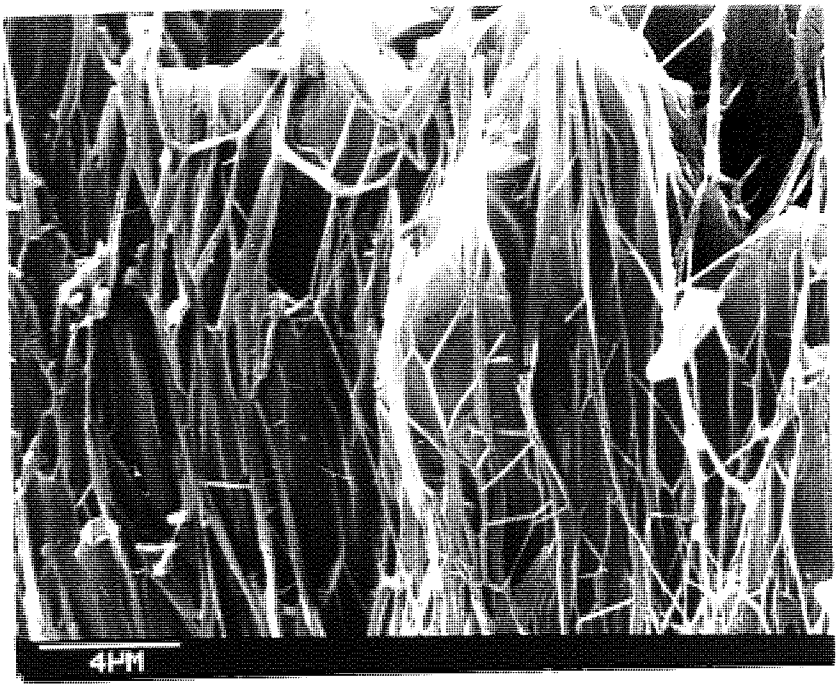

(a)

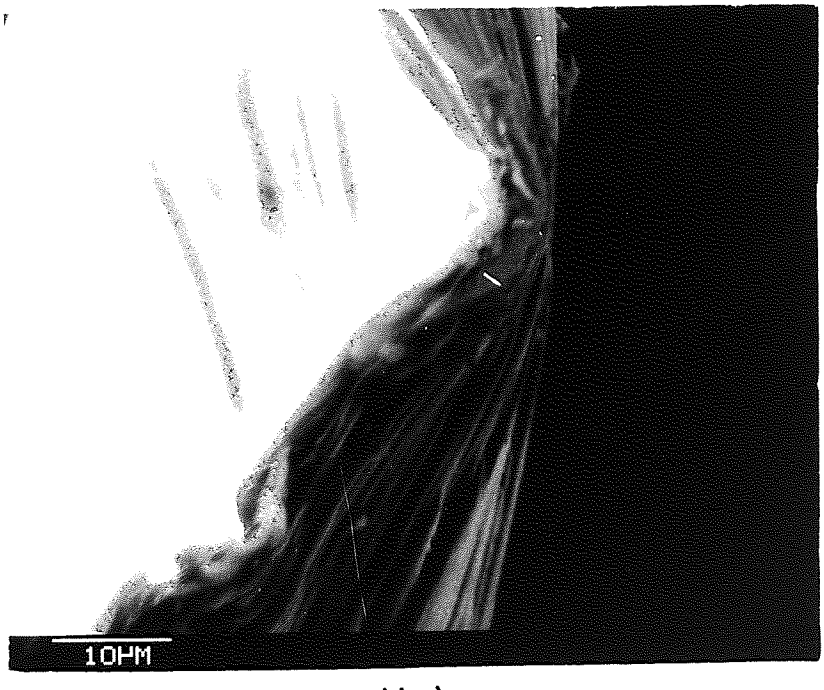

(b)

Figure 3.41a Debris from pin shown in Figure 3.39a

Figure 3.41b Edge of debris shown in Figure 3.39a

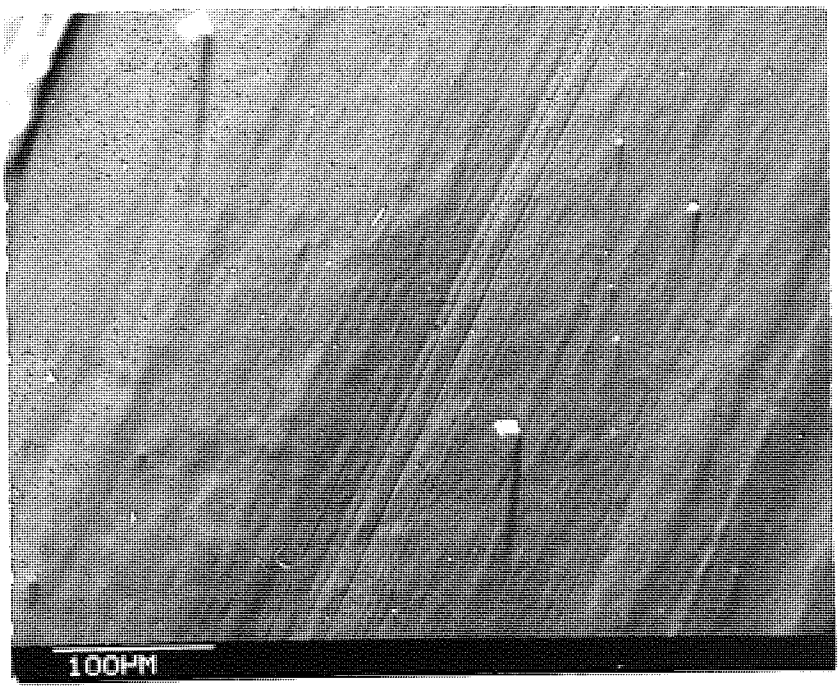

Figure 3.42 Surface of P.T.F.E. pin run under lubricated conditions on the Uni-Directional Pin on Disc machine at $3x10^{-3}$ ms^{-1}, 2.1 kg load and 10 cs fluid

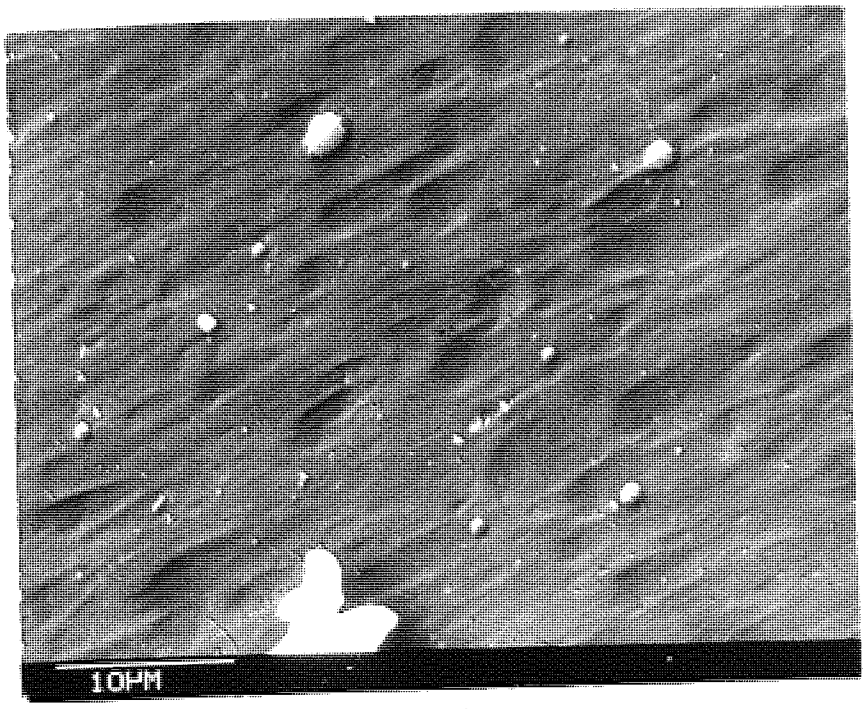

(a)

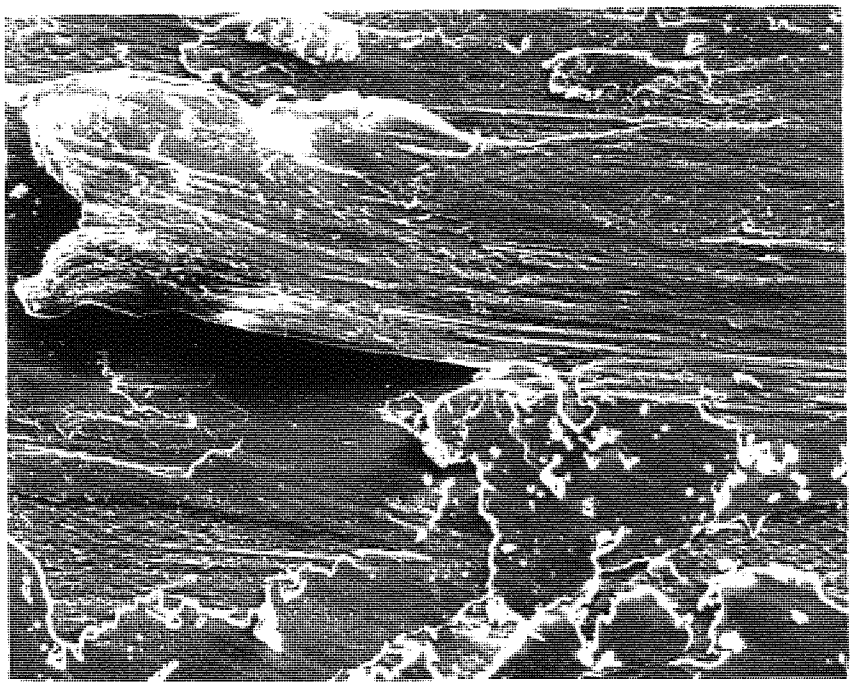

(b)

Figure 3.43a Surface of P.P.O. specimen run dry on the Reciprocating Line Contact machine at 3×10^{-3} ms^{-1}, 2.5 kg load

Figure 3.43b As for Figure 3.43a but at the higher speed of 1.8 ms^{-1}

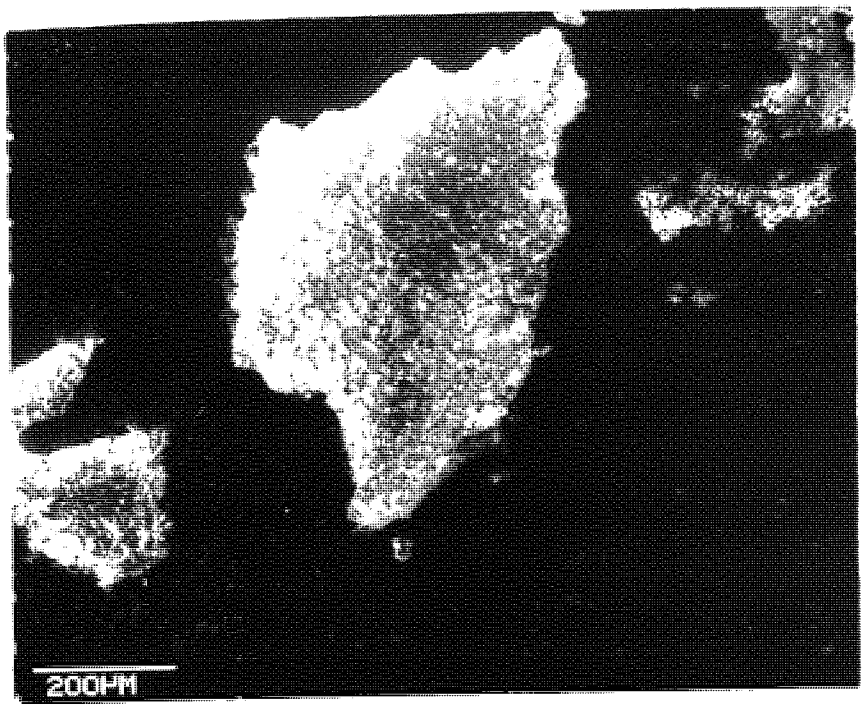

(a)

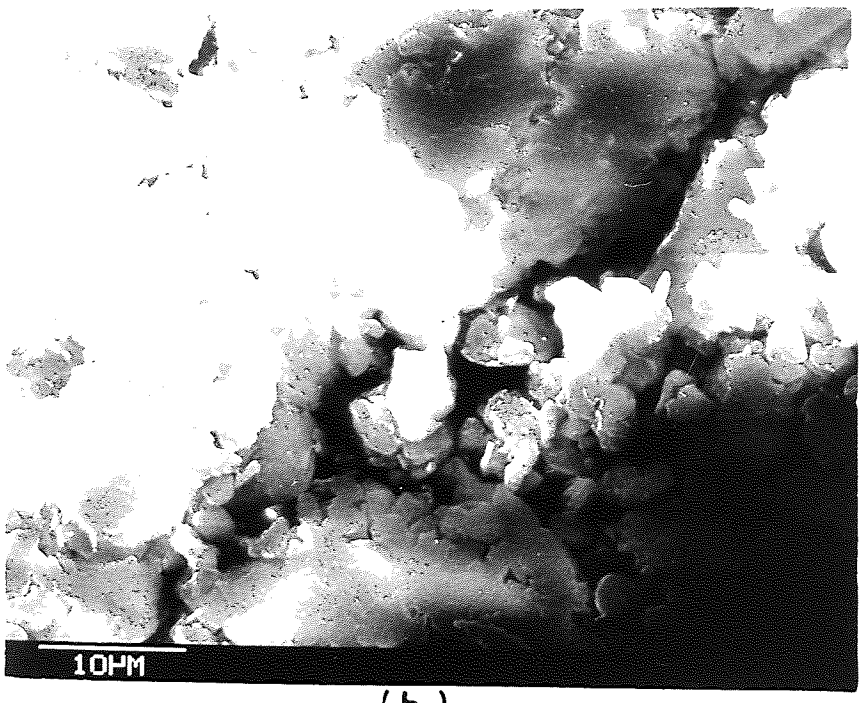

(b)

Figure 3.44a Debris from specimen shown in Figure 3.43a

Figure 3.44b As for Figure 3.44a but at higher magnification

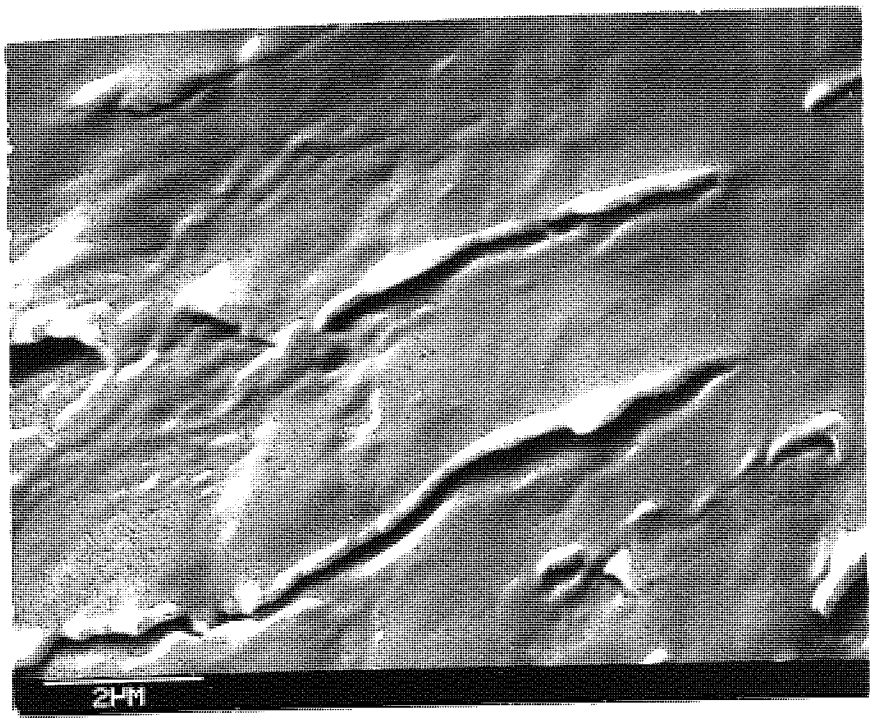

(a)

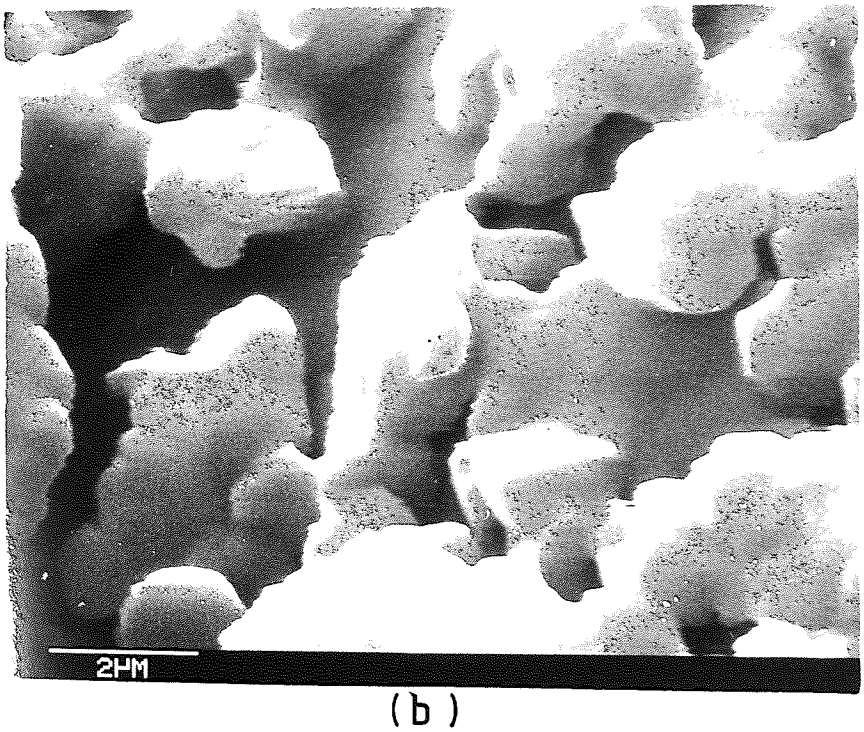

(b)

Figure 3.45a Surface of P.P.O. specimen run under lubricated conditions on the Reciprocating Line Contact machine at 3×10^{-3} ms^{-1}, 2.5 kg load and 10 cs fluid

Figure 3.45b Debris from specimen in Figure 3.45a

P.E.E.K. specimens worn on the Reciprocating Line Contact machine showed no debris layer, pitting, ridges or ripples when run under dry or lubricated conditions. In both cases the surface was smooth except for occasional wear grooves. A wear groove being formed by P.E.E.K. debris is shown in Figure 3.46a. The debris was made up of small particles joined together to form flakes and is shown in Figure 3.46b. Under lubricated conditions the debris tended to remain as single particles (See Figure 3.47).

When P.T.F.E. was run on the Reciprocating Line Contact machine debris layers were only observed on rare occasions, and an example of this is shown in Figure 3.48a. These flakes were from debris extruded from between the disc and specimen. They were loosely attached to the surface and showed signs of stretching (See Figure 3.48b). As with worn surfaces from the other two machines surface ripples were again seen transverse to the sliding direction. Transfer of the debris to the disc was observed, the debris being made up of the extruded material which took the form of flakes (See Figure 3.49). Under lubricated conditions the surface generated was very smooth with no debris layer, ridges or ripples, the only features being the wear grooves. As in previous experiments it was not possible to collect debris from the lubricated tests for examination.

3.5.2 X-Ray Mapping and Quantitative Analyses

Control specimens from all three machines were prepared

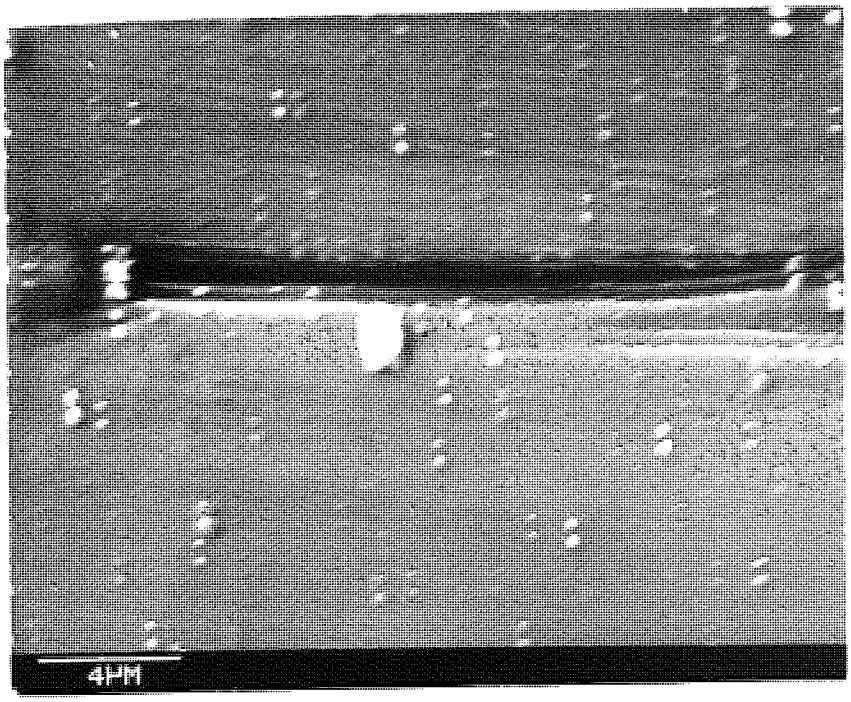

(a)

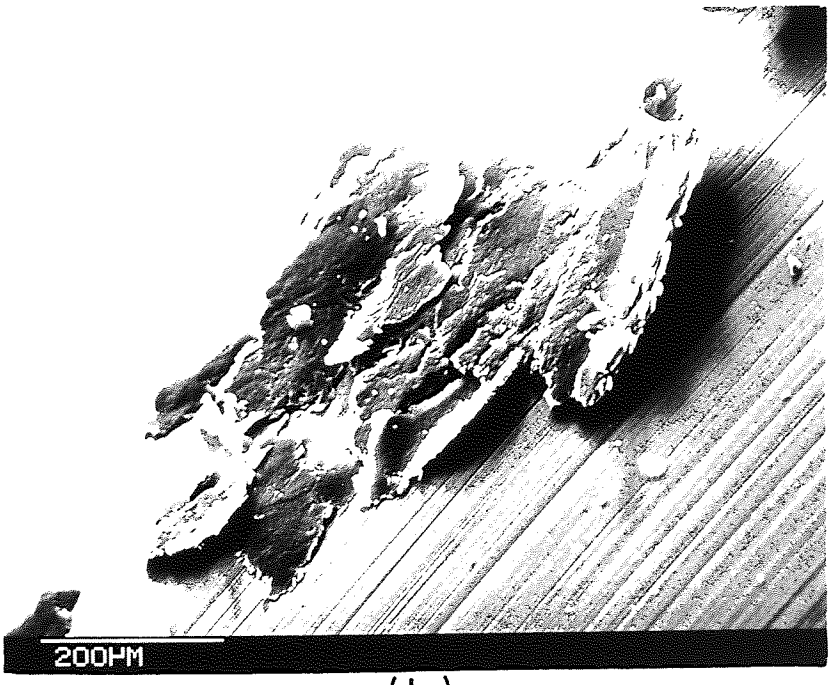

(b)

Figure 3.46a Surface of P.E.E.K. specimen run under dry conditions on the Reciprocating Line Contact machine at 3×10^{-3} ms^{-1}, 2.5 kg load

Figure 3.46b Debris from specimen in Figure 3.46a

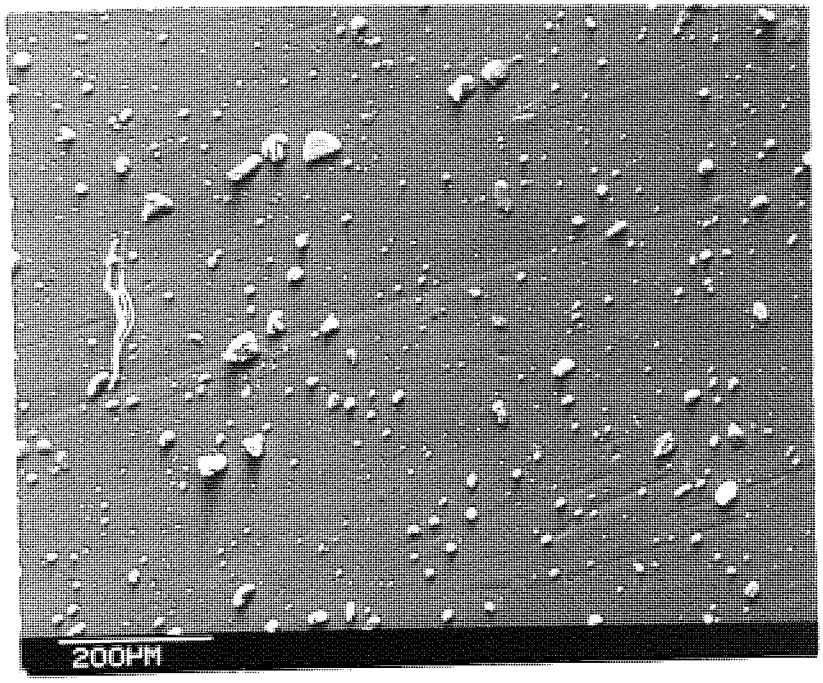

Figure 3.47 Debris from P.E.E.K. specimen run under lubricated conditions on the Reciprocating Line Contact machine at $3x10^{-3}$ ms^{-1}, 2.5 kg load and 10 cs fluid

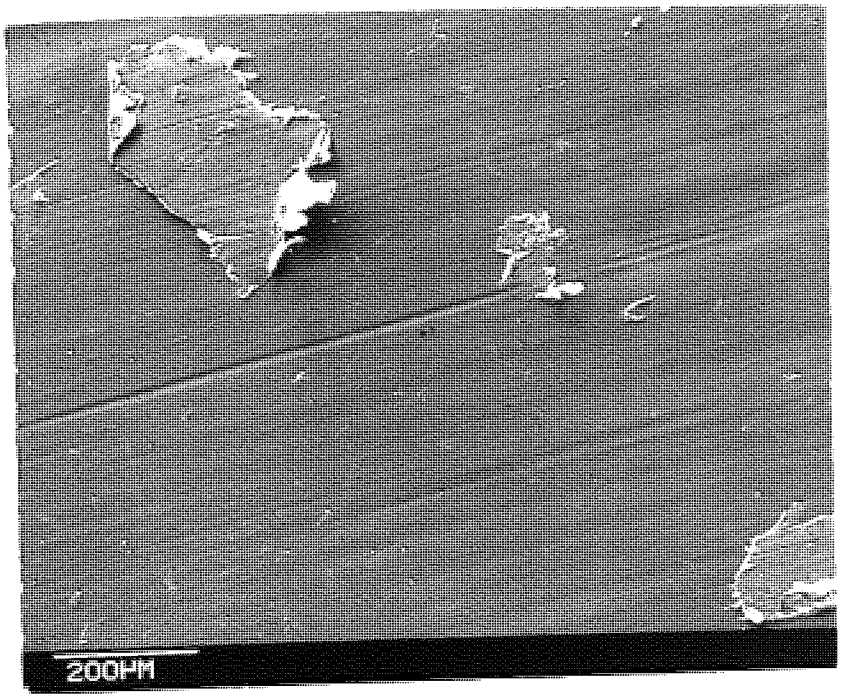

(a)

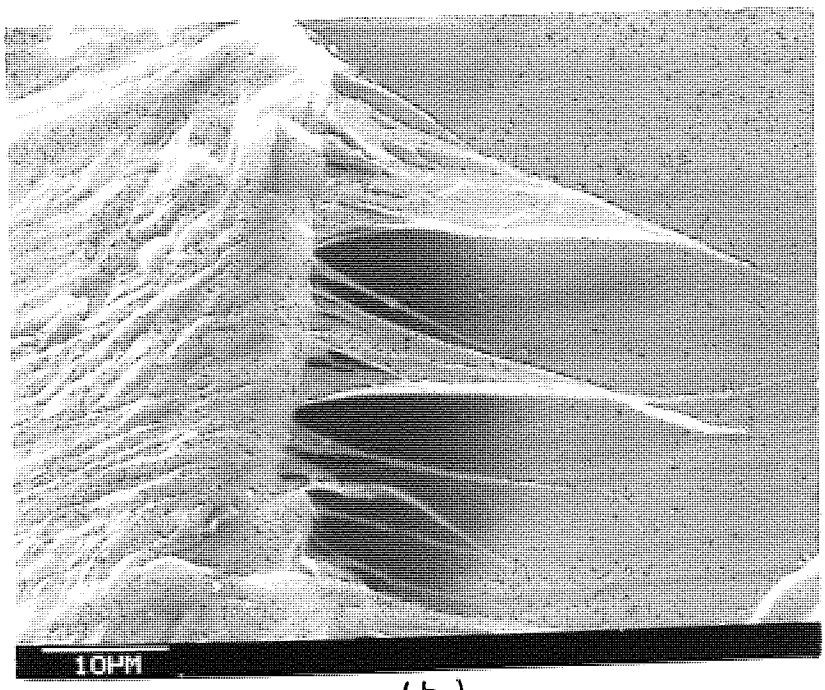

(b)

Figure 3.48a P.T.F.E. specimen run under dry conditions on the Reciprocating Line Contact machine at 3×10^{-3} ms^{-1}, 2.5 kg load

Figure 3.48b Debris from specimen in Figure 3.48a

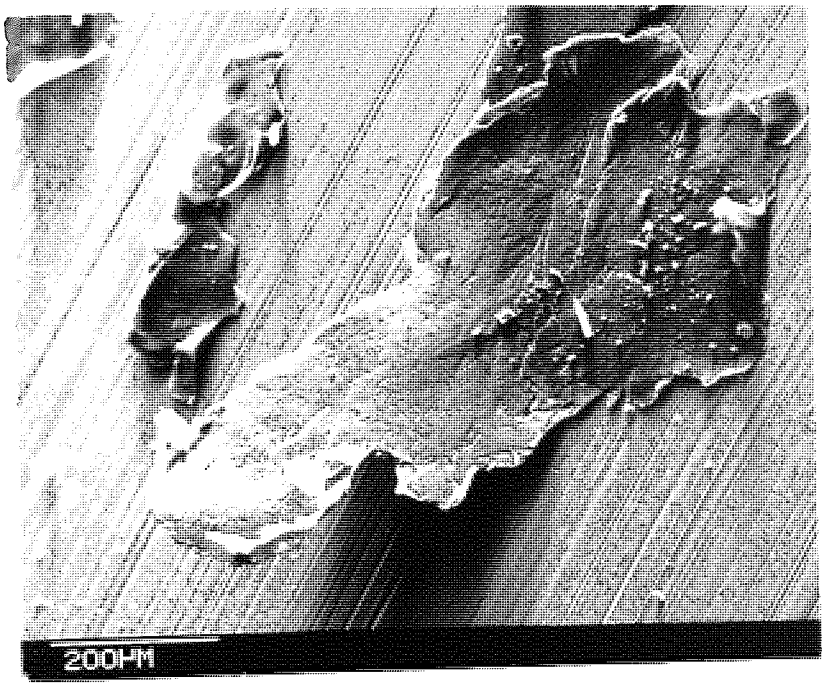

Figure 3.49 Debris from specimen shown in Figure 3.48a

in order to detect any silicon* in the sectioned wear surface. The control specimens consisted of:-

i) Clean and unworn specimens

ii) Unworn specimens dipped in 10 cs silicone fluid then wiped clean

iii) Specimens worn dry.

An example of a sectioned specimen worn dry on the Rotating Line Contact machine at 2.1 kg and $3x10^{-3}$ ms^{-1} is shown in Figure 3.50. The polymer is on the left hand side of the image (as is the case in all photos of sections), whilst silver paint can be seen on the right. The silver paint was used simply to show the edge of the pin. However, when the conductive bakelite cooled in the mould it contracted, and pulled away from the wear pin surface making the silver paint partially redundant. The silver map clearly shows significant amounts of silver present only in the silver paint, whilst the silicon map shows a small amount of silicon in the silver paint but shows a background level only in the polymer. These results were confirmed by the concentration profiles (See Figure 3.51), and by the energy dispersive analyser (Z.A.F. Analyses) in the Links System 860 which performed quantitative elemental analyses. This analyses indicated less than 0.1% silicon in the polymer but the resolution of the analyser was approximately $\pm$1.0%, therefore the level detected was below the expected background level.

Silicon was not found in any of the control specimens from any of the machines, which indicated that specimen

* due to silicone fluid diffusion

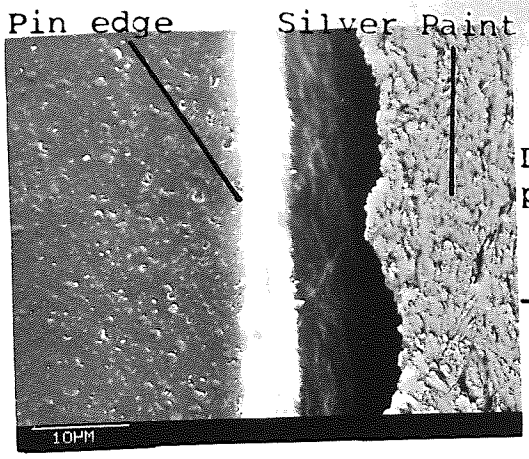

Electron Image

Depth into polymer μm	Silicon concentration %
1	0.072
5	0.006
10	0.016

Quantitative analyses of silicon concentration

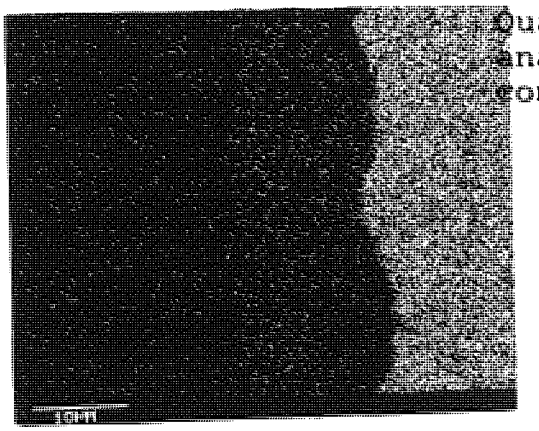

Silver Map

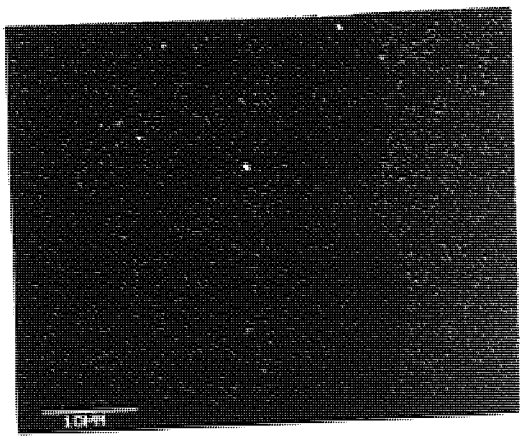

Silicon Map

FIGURE 3.50 Sectioned P.P.O. pin run under dry conditions on the Rotating Line Contact machine at $3x10^{-3}\,ms^{-1}$, 2.1 kg load. With quantitative analyses of silicon concentration in the pin

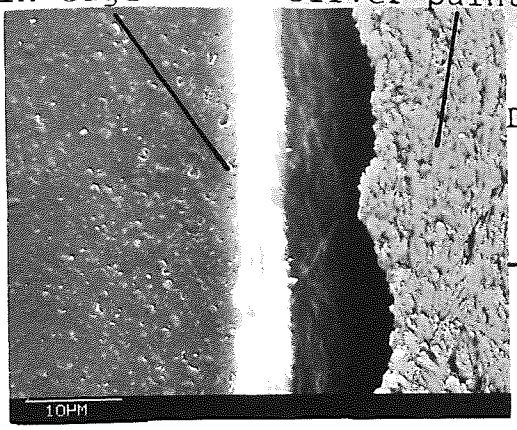

Electron Image

Depth into polymer μm	Silicon concentration %
1	0.072
5	0.006
10	0.016

Quantitative analyses of silicon concentration

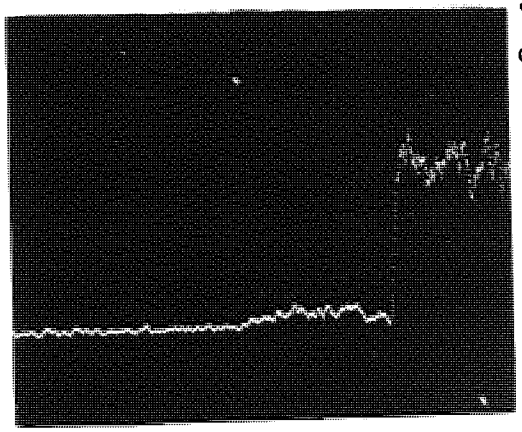

Silver Profile

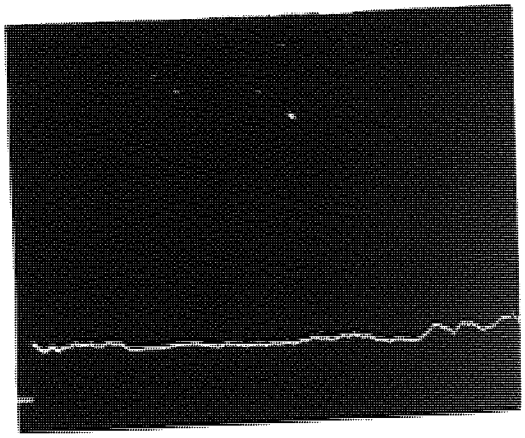

Silicon Profile

FIGURE 3.51 As for Figure 3.50 but showing element profiles

mounting and preparation had not contaminated the surface.

P.P.O. specimens were run on the Rotating Line Contact machine under 'boundary-lubrication' conditions, and then the wear surface was wiped to remove excess fluid. When the wiping was reasonably vigorous the debris layer from the centre of the pin was removed. In that case no silicon was found in the sectioned surface as shown in Figures 3.52 and 3.53.

However, if gentle wiping was employed and the debris layer was not removed then silicon was detected in the surface (See Figures 3.54 and 3.55) and varied in concentration from 2-15%.

Occasionally small pockets of silicon were found in the debris layer at concentrations up to 80% (See Figures 3.56 and 3.57).

When the wear specimens were observed without mounting and sectioning, the debris layer in the centre of the pin was seen without difficulty (See Figure 3.58). The silicon x-ray maps showed that this debris layer contained the majority of silicon and this was supported by the concentration profiles and quantitative analyses shown in Figures 3.59 and 3.60.

For P.E.E.K. and P.T.F.E., debris layers did not occur under boundary lubrication conditions on any of the three machines. A sectioned P.T.F.E. specimen from the Rotating

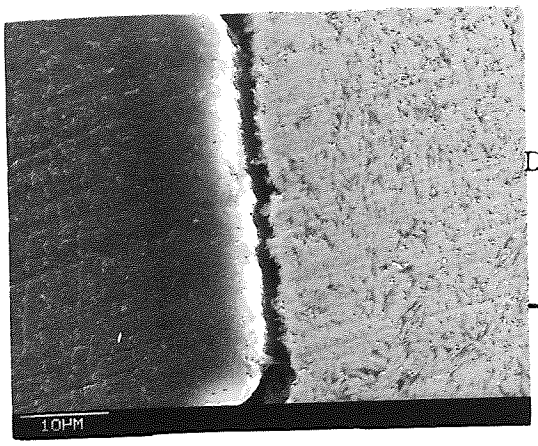

Electron Image

Depth into polymer μm	Silicon concentration %
1	0.142
5	0.149
10	0.114

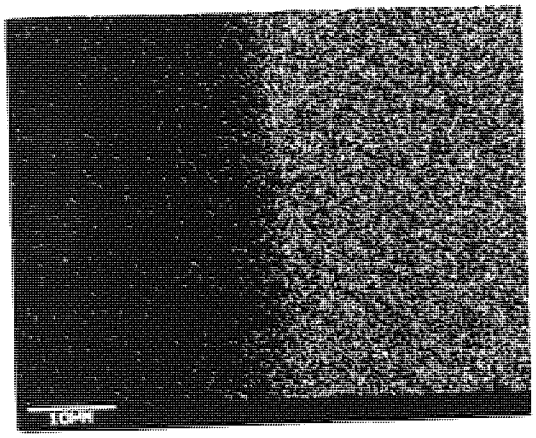

Silver Map

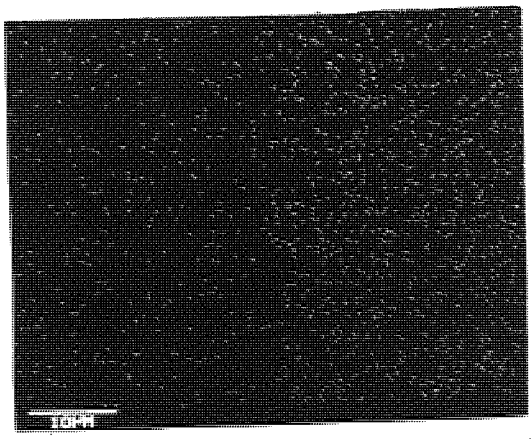

Silicon Map

FIGURE 3.52 Sectioned P.P.O. pin run under lubricated conditions on the Rotating Line Contact machine at 3×10^{-3} ms^{-1}, 2.1 kg load and 10 cs fluid, then vigorously cleaned

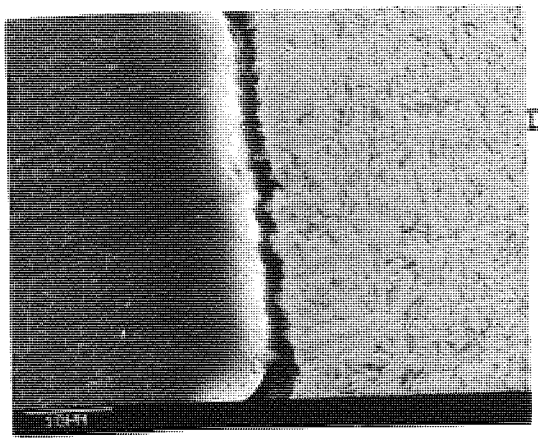

Electron Image

Depth into polymer µm	Silicon concentration %
1	0,142
5	0.149
10	0.114

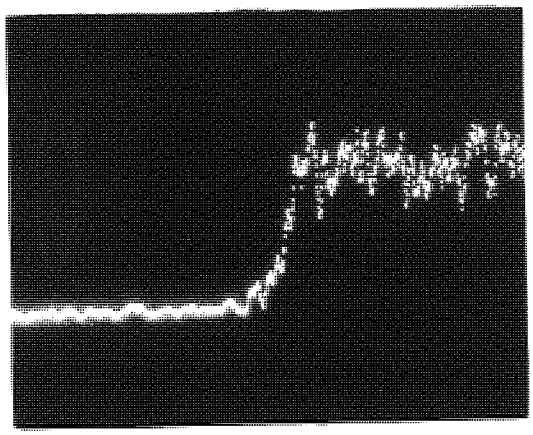

Silver Profile

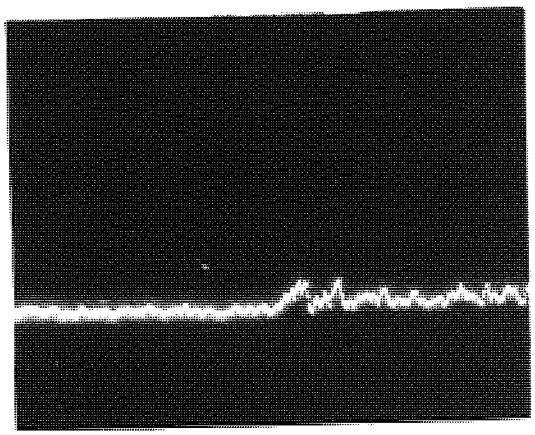

Silicon Profile

FIGURE 3.53 As for Figure 3.52 but showing element profiles

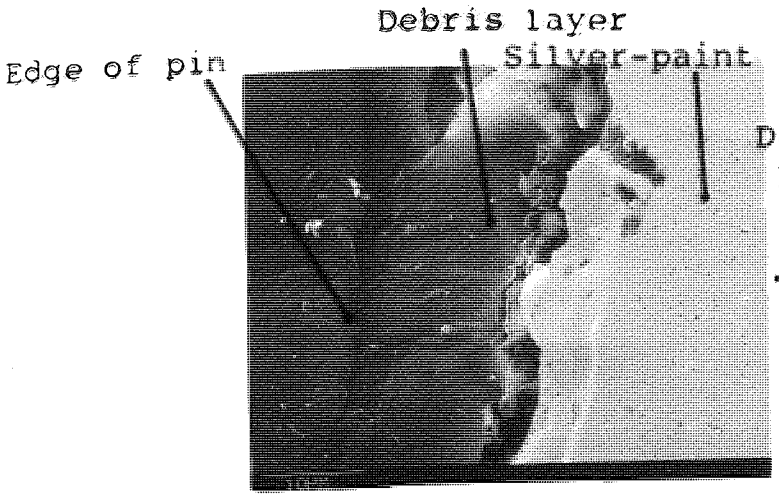

Electron Image

Depth into polymer µm	Silicon concentration %
1	7.616
3	7.511
5	8.236
8	3.902
10	2.214

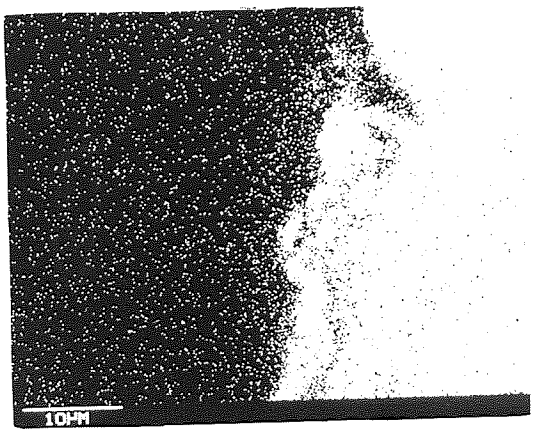

Silver Map

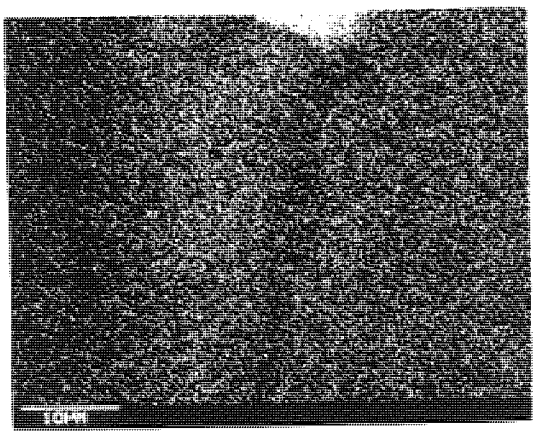

Silicon Map

FIGURE 3.54 Sectioned P.P.O. pin run under lubricated conditions on the Rotating Line Contact machine at 3×10^{-3} ms^{-1}, 2.1 kg load and 10 cs fluid, with gentle cleaning of the pin surface

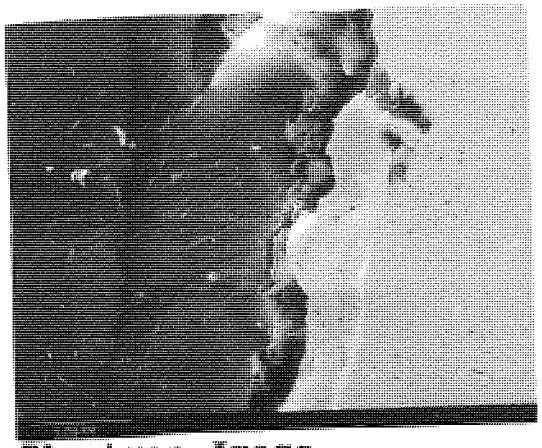

Electron Image

Depth into polymer µm	Silicon Concentration %
1	7.616
3	7.511
5	8.236
8	3.902
10	2.214

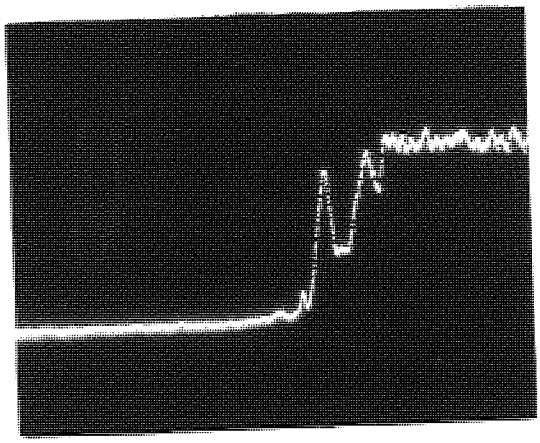

Silver Profile

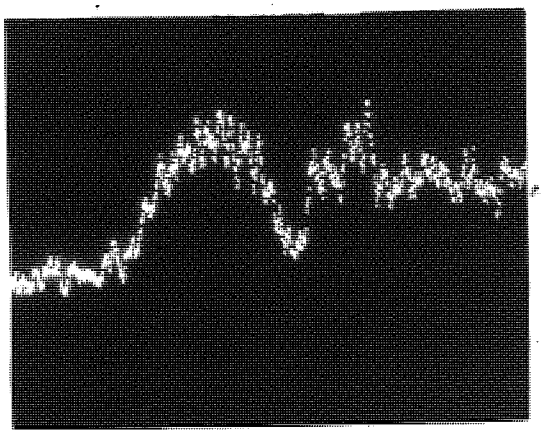

Silicon Profile

FIGURE 3.55 As for Figure 3.54 but showing element profiles

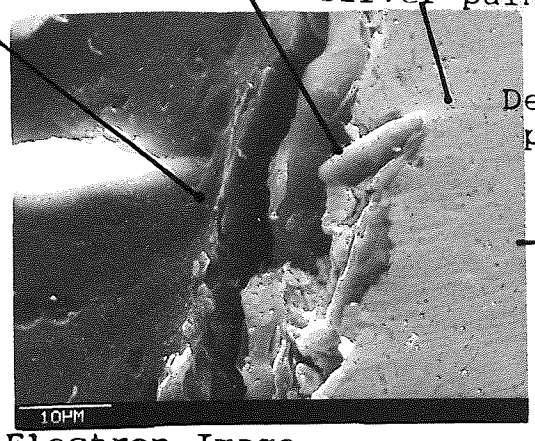

Electron Image

Depth into polymer µm	Silicon Concentration %
Upper pocket	79.009
Lower pocket	75.632
1	2.598
3	2.619
5	2.838

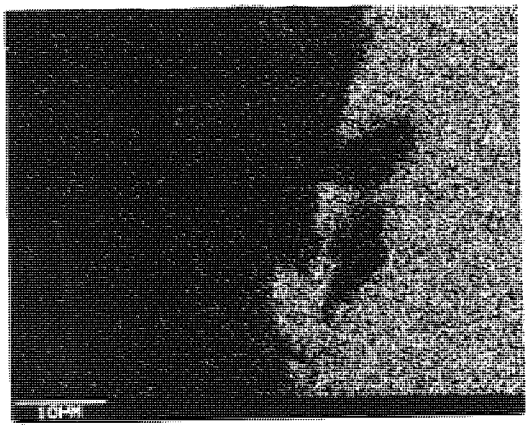

Silver Map

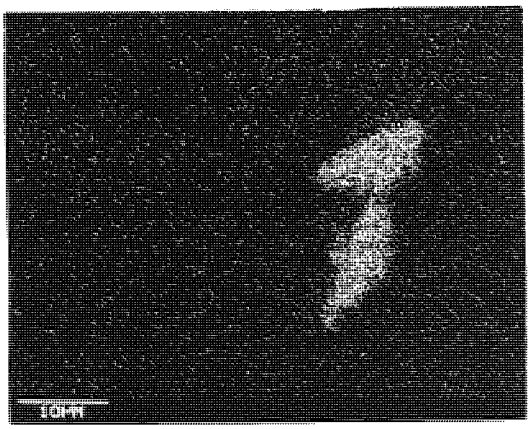

Silicon Map

FIGURE 3.56 As for Figure 3.54 but showing small pockets of high concentrations of silicon

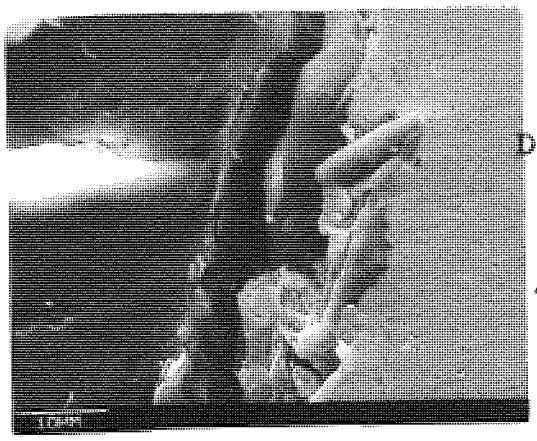

Electron Image

Depth into polymer µm	Silicon Concentration %
Upper pocket	79.009
Lower pocket	75.632
1	2.598
3	2.619
5	2.838

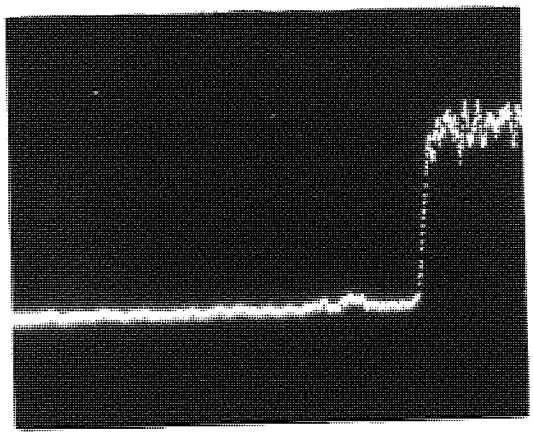

Silver Profile

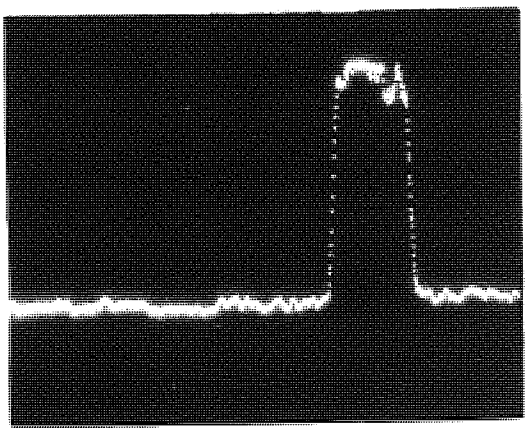

Silicon Profile

FIGURE 3.57 As for Figure 3.56 but showing element profiles

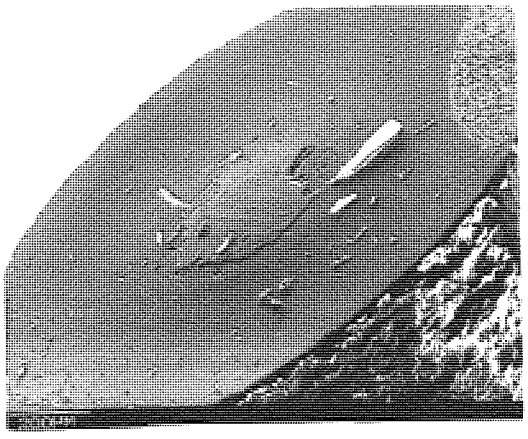

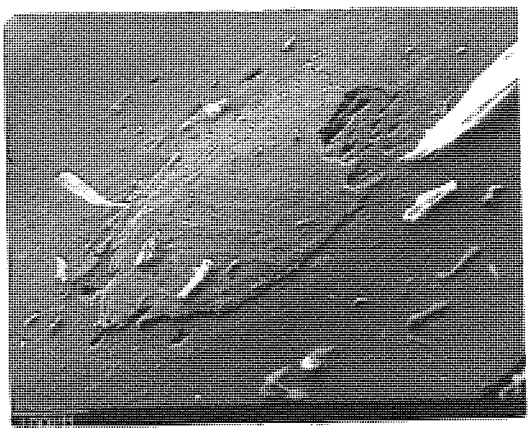

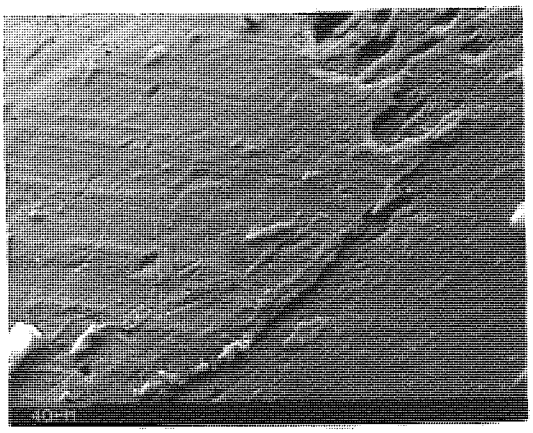

FIGURE 3.58 Surface of P.P.O. pin run under lubricated conditions on the Rotating Line Contact machine at $3x10^{-3}$ ms^{-1}, 2.1 kg load and 10 cs fluid. Showing the debris layer at three magnifications

Debris layer

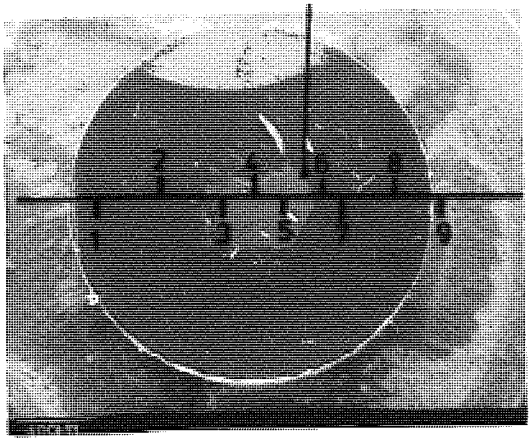

Electron Image

Position	Silicon Concentration %
1	0.155
2	0.148
3	0.197
4	16.753
5	15.870
6	15.834
7	0.410
8	0.215
9	0.318

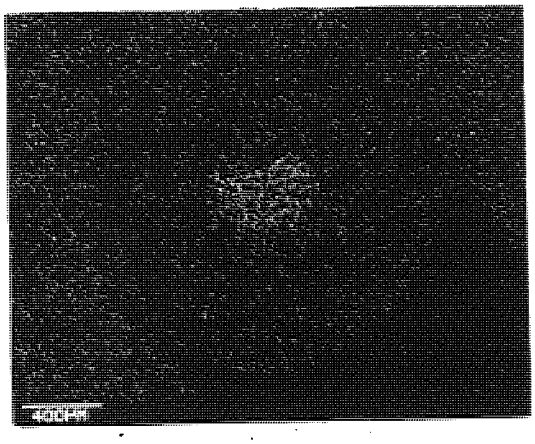

Silicon Map

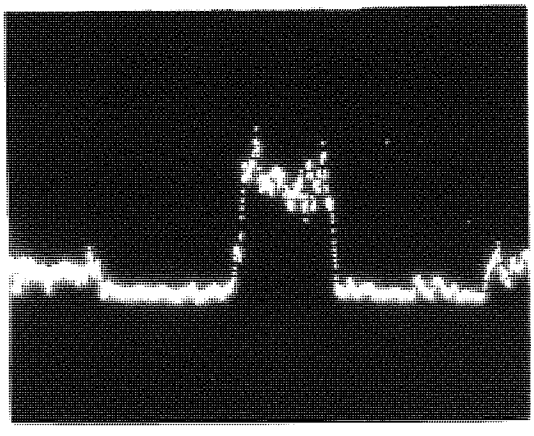

Silicon Profile

FIGURE 3.59 As for Figure 3.58 showing silicon map and profile

Debris layer

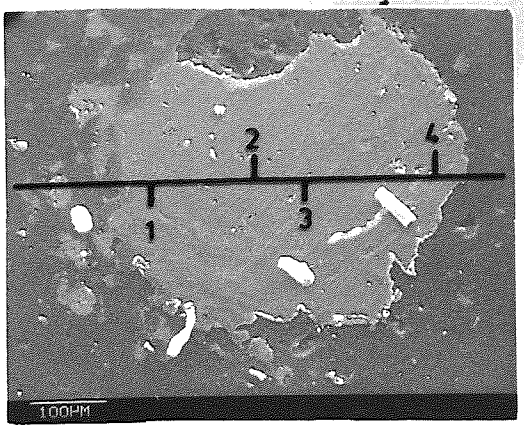

Electron Image

Position	Silicon Concentration %
1	15.885
2	14.415
3	13.950
4	15.234

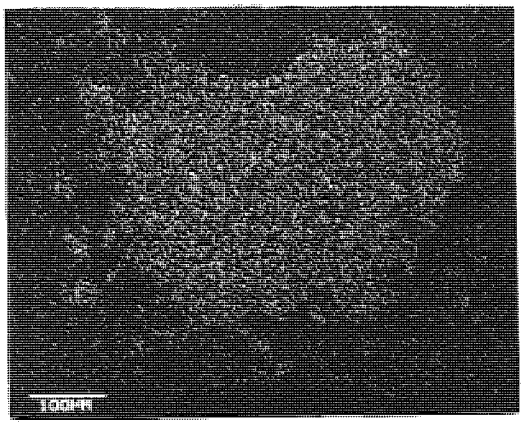

Silicon Map

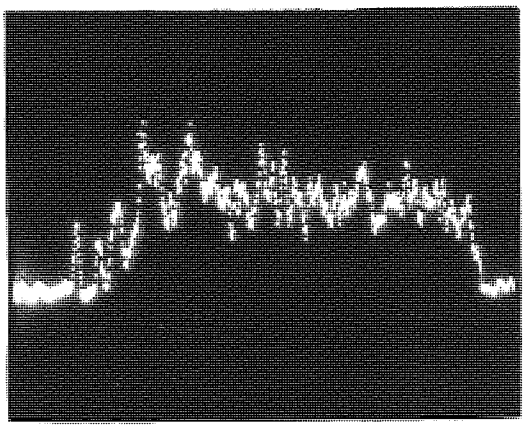

Silicon Profile

FIGURE 3.60 As for Figure 3.59 but at higher magnification

e Contact machine is shown in Figures 3.61 and 3.62.
arly there are no significant amounts of silicon in
wear surface.

specimens from the Uni-Directional pin on disc machine
wed that no silicon fluid was being retained in the
r surface (See Figures 3.63, 3.64, 3.65 and 3.66).

hough a debris layer of P.P.O. was observed on one
asion on the Reciprocating Line Contact machine, in
eral, fluid retention did not occur with any of the
ymers as shown in Figures 3.67, 3.68, 3.69 and 3.70
P.P.O. and P.T.F.E.

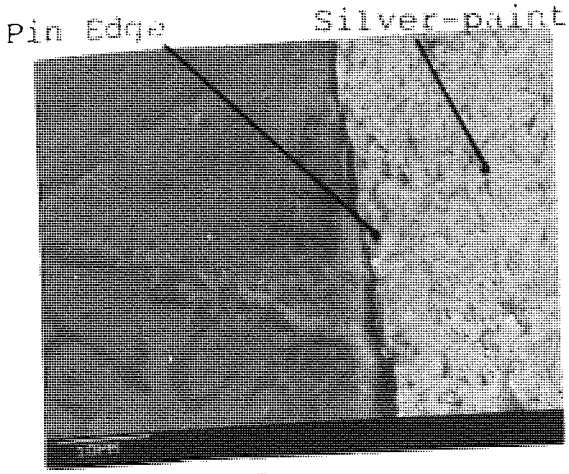

Electron Image

Depth into polymer µm	Silicon Concentration %
1	0.000
5	0.170
10	0.076

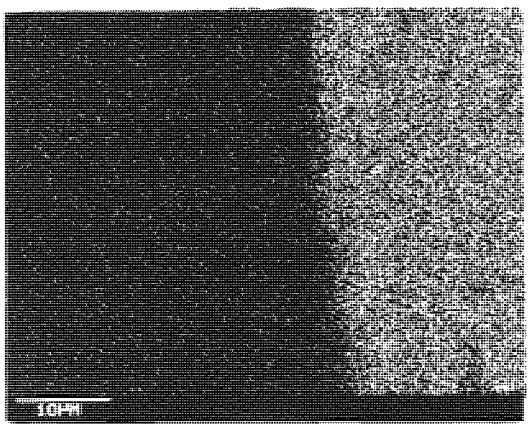

Silver Map

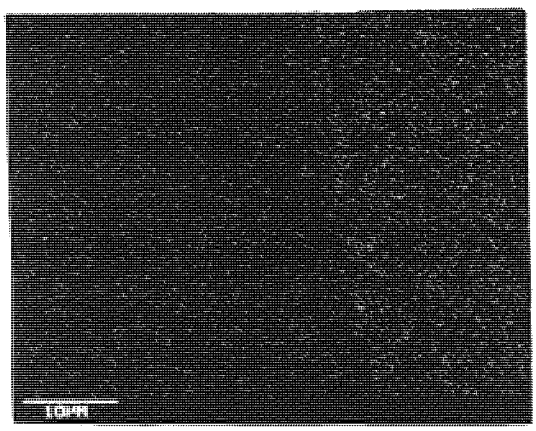

Silicon Map

FIGURE 3.61 Sectioned P.T.F.E. pin run under lubricated conditions on the Rotating Line Contact machine at $3x10^{-3}$ ms^{-1}, 2.1 kg load and 10 cs fluid, with gentle cleaning of pin surface

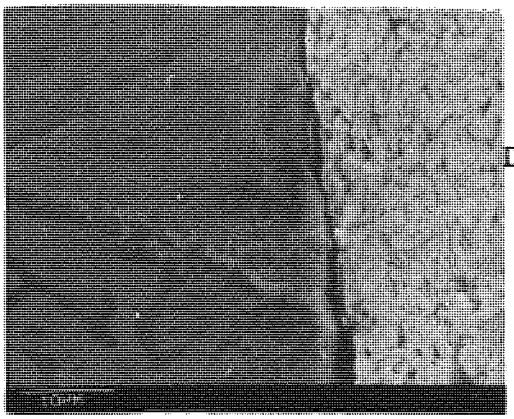

Electron Image

Depth into polymer µm	Silicon Concentration %
1	0.000
5	0.170
10	0.076

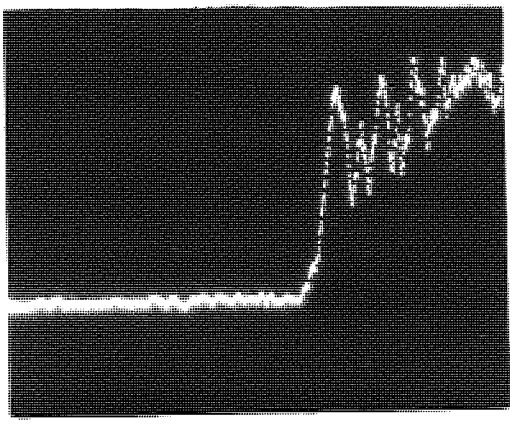

Silver Profile

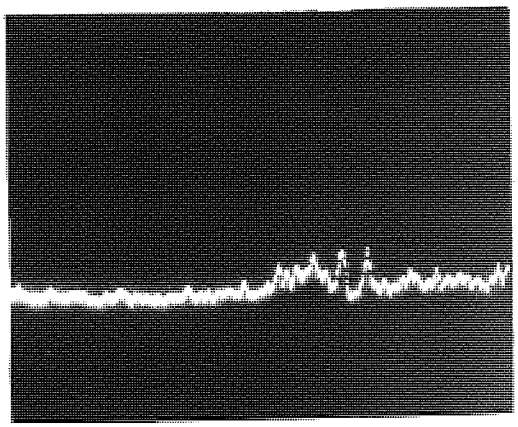

Silicon Profile

FIGURE 3.62 As for Figure 3.61 but showing element profiles

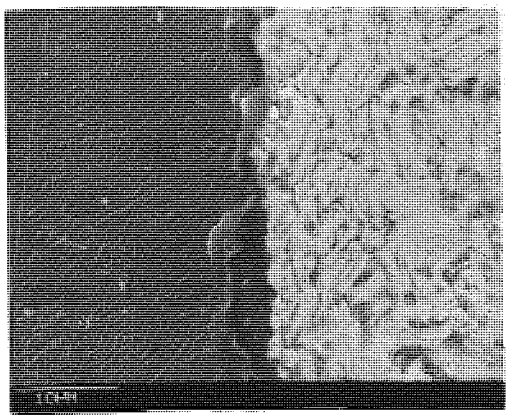

Electron Image

Depth into polymer µm	Silicon Concentration %
1	0.891
1.5	0.861
3	0.501
5	0.269
10	0.044

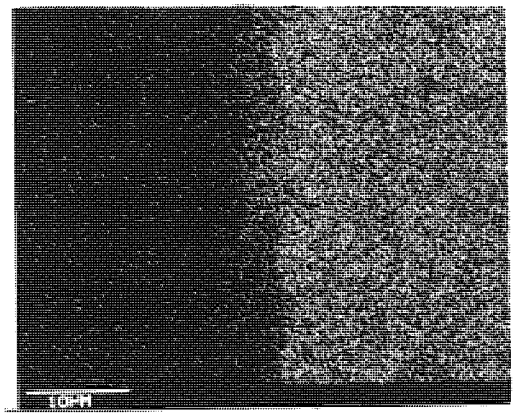

Silver Map

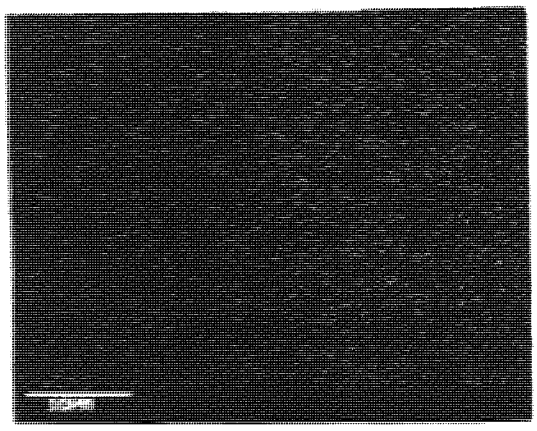

Silicon Map

FIGURE 3.63 Sectioned P.P.O. pin run under lubricated conditions on the Uni-Directional Pin on Disc machine at 3×10^{-3} ms^{-1}, 2.1 kg load and 10 cs fluid, with gentle cleaning of pin surface

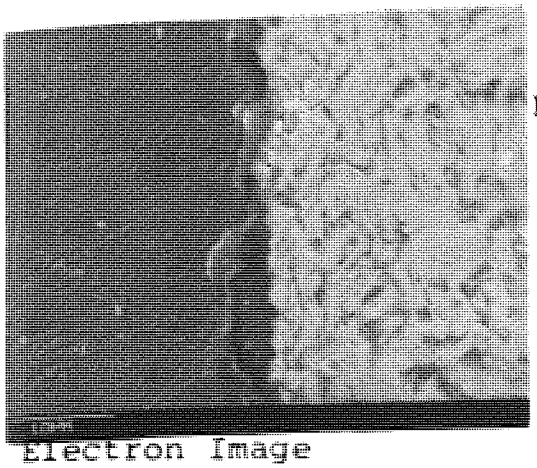

Electron Image

Depth into polymer µm	Silicon Concentration %
1	0.891
1.5	0.861
3	0.501
5	0.269
10	0.044

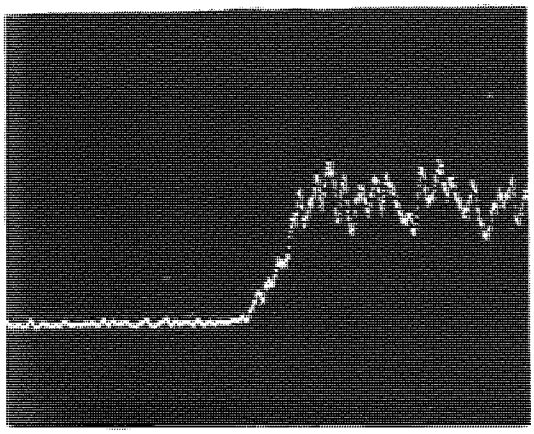

Silver Profile

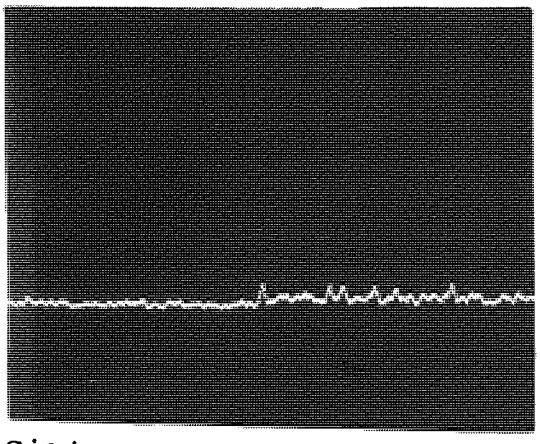

Silicon Profile

FIGURE 3.64 As for Figure 3.63 but showing element profiles

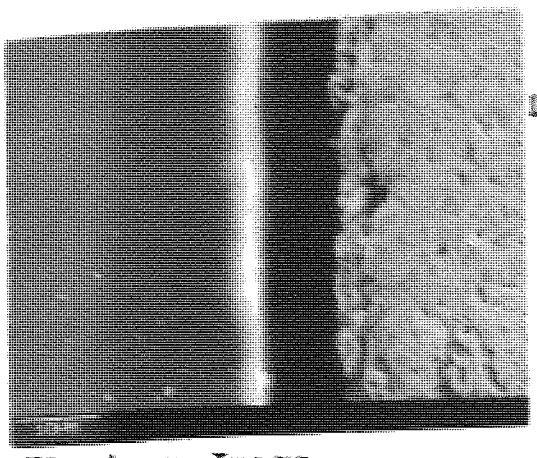

Depth into polymer µm

1

5

10

Electron Image

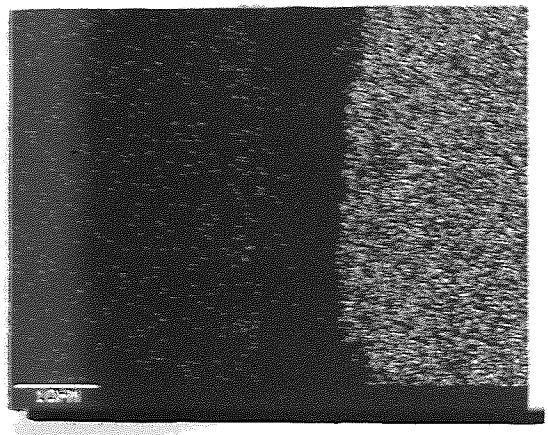

Silver Map

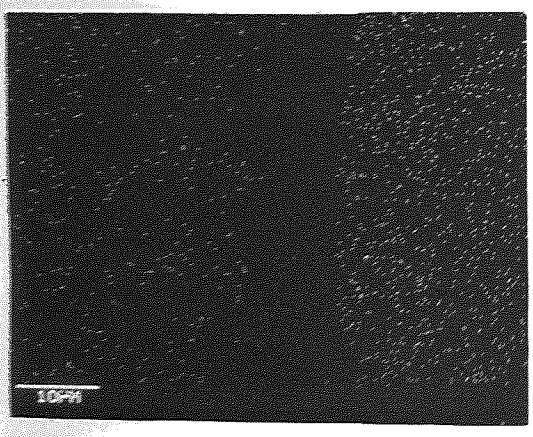

Silicon Map

FIGURE 3.65 Sectioned P.T.F.E. pin run under lubricated conditions on the Uni Directional Pin on Disc machine $3x10^{-3}$ ms^{-1}, 2.1 kg load and 10 cs with gentle cleaning of the pin

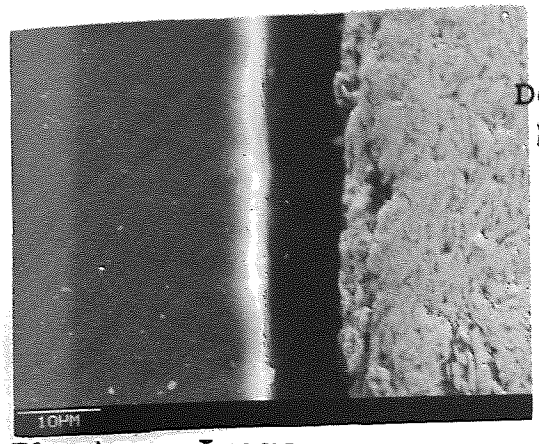

Electron Image

Depth into polymer μm

1

5

10

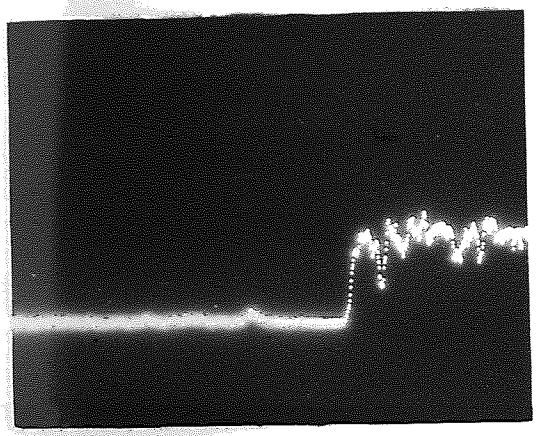

Silver Profile

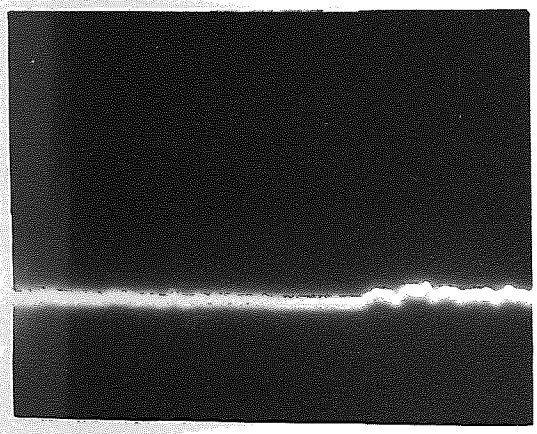

Silicon Profile

FIGURE 3.66 As for Figure 3.65 but showing element profiles

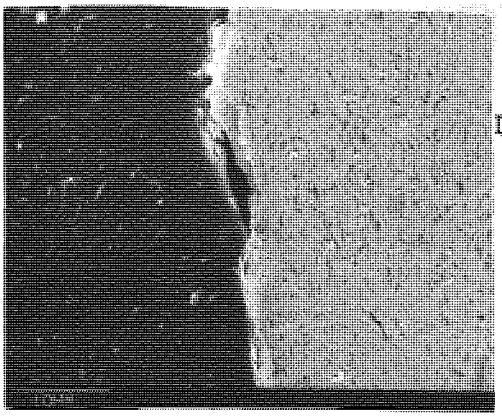

Electron Image

Depth into polymer µm	Silicon Concentration %
1	0.216
3	0.142
5	0.064
10	0.121

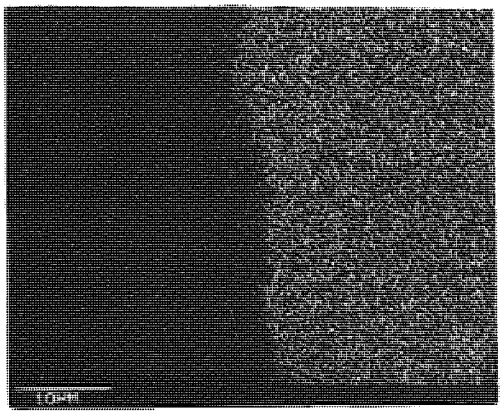

Silver Map

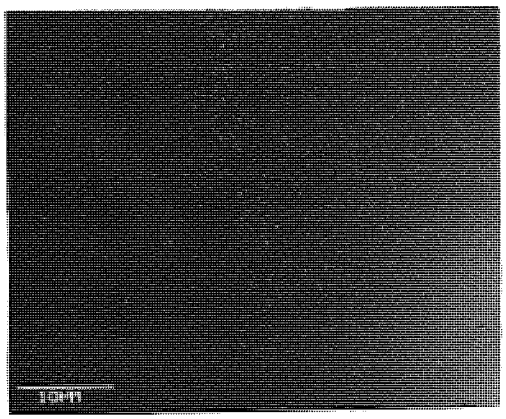

Silicon Map

IGURE 3.67 Sectioned P.P.O. specimen run under lubricated conditions on the Reciprocating Line Contact machine at 3×10^{-3} ms^{-1}, 2.1 kg load and 10 cs fluid, with gentle cleaning of the pin surface

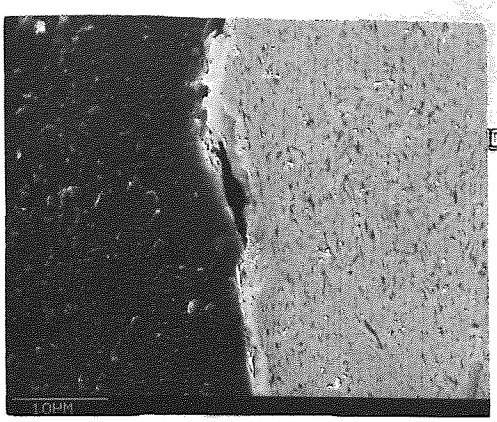

Electron Image

Depth into polymer μm	Silicon Concentration %
1	0.216
3	0.142
5	0.064
10	0.121

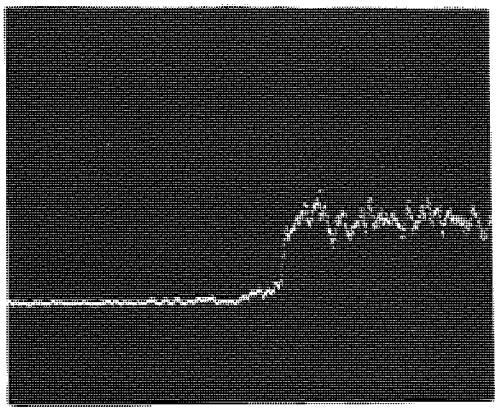

Silver Profile

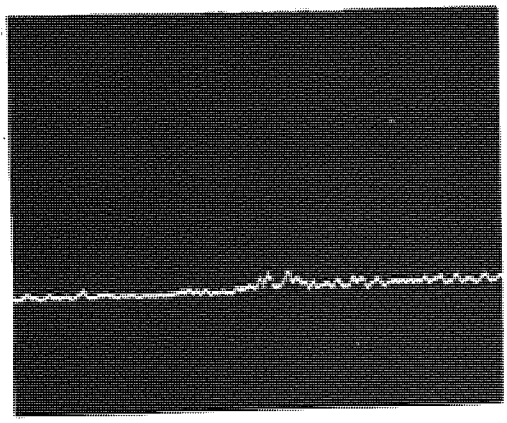

Silicon Profile

FIGURE 3.68 As for Figure 3.67 but showing element profiles

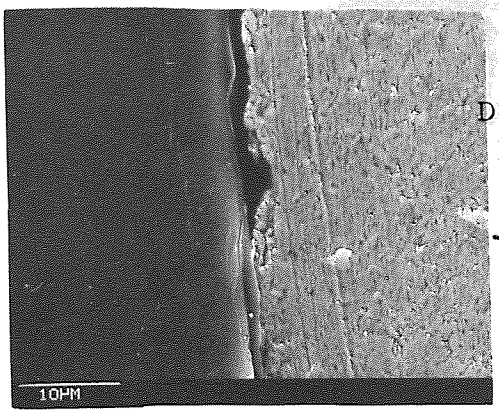

Electron Image

Depth into polymer μm	Silicon Concentration %
1	0.140
3	0.094
5	0.051

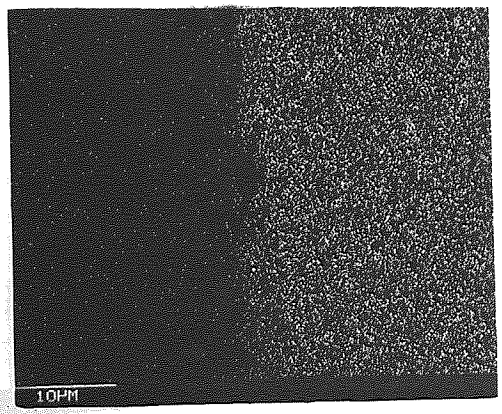

Silver Map

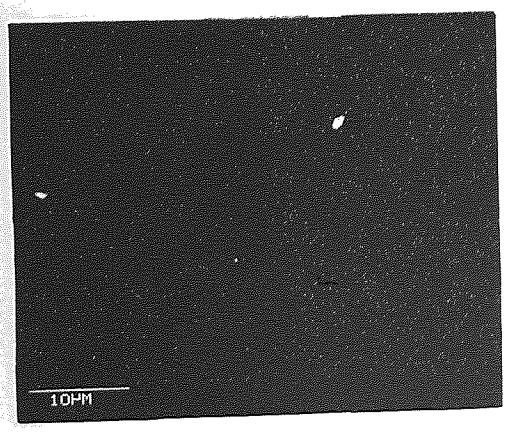

Silicon Map

FIGURE 3.69 Sectioned P.T.F.E. specimen run under lubricated conditions on the Reciprocating Line Contact machine at 3×10^{-3} ms^{-1}, 2.1 kg load and 10 cs fluid, with gentle cleaning of the pin surface

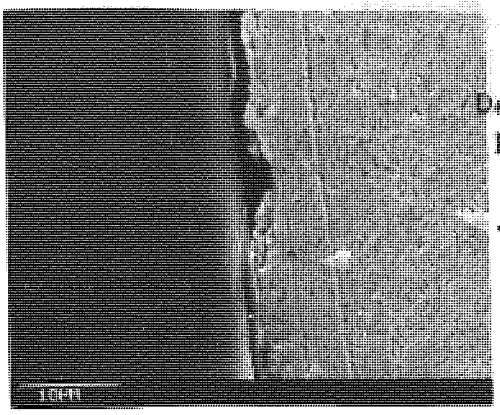

Electron Image

Depth into polymer µm	Silicon Concentration %
1	0.140
3	0.094
5	0.051

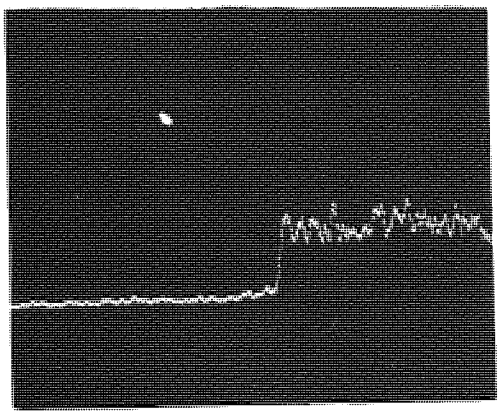

Silver Profile

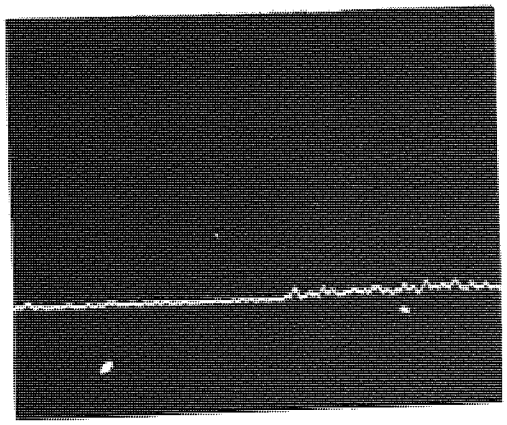

Silicon Profile

FIGURE 3.70 As for Figure 3.69 but showing element profiles

CHAPTER 4

DISCUSSION

4. DISCUSSION

The calculated and measured values for the contact band widths on the Rotating Line Contact machine (See Figure 3.2) are reasonably similar, although the two sets of results for the Reciprocating Line Contact machine (See Section 3.1) exhibit a greater difference. This may be due to the use of greater loads on the Reciprocating Line Contact machine (88 N instead of 5-21 N). The disadvantages of using the calculated values have been discussed previously (See Section 1.9), and this was the main reason for using the measured values throughout all further work.

Although it is realised that true boundary lubrication conditions (i.e. where the load is supported by an adsorbed monolayer on the surface asperities) did not occur with the use of silicone fluid, throughout this work the term 'boundary lubrication' conditions applies to the conditions when the value of the coefficient of friction remains independent of varying values of $\frac{nN'}{P}$ (i.e. at very low values of $\frac{nN'}{P}$).

The Stribeck curves for all three wear machines (See Figures 3.5, 3.6 and 3.7) show that boundary lubrication conditions only occur at low speeds, with low viscosity fluids and high loads. At very low values of $\frac{nN'}{P}$ (e.g. 10^{-13} to 10^{-12}) P.P.O. exhibits the highest lubricated friction value on all three machines, and P.T.F.E. the lowest. The values for lubricated friction, however, for P.P.O. and P.E.E.K. are relatively close (e.g. 0.3 and 0.15

respectively on the Rotating Line Contact machine) and at higher values of $\frac{nN'}{P}$ P.E.E.K. usually exhibits a higher friction value than P.P.O. This change in ranking may be due to the Young's Modulus values for P.P.O. and P.E.E.K. It has been shown earlier (See Section 1.8.4) that softer materials are more likely to operate under Elastohydrodynamic conditions than boundary conditions. As P.P.O. tends to move out of boundary conditions more rapidly than P.E.E.K. on all three wear machines this may be an example of the above observation. This hypothesis, however, seems to be contradicted by the lubricated friction behaviour of P.T.F.E. All three Stribeck curves for P.T.F.E. show that this material remains in boundary lubrication conditions over the widest range of values for $\frac{nN'}{P}$. This, however, may be due to the lack of a geometric wedge on the Uni-Directional pin on disc machine (at any load) and Rotating Line Contact machine at high loads. This absence of a geometric wedge would reduce the possibility of any fluid film support. The radial clearance (Rc) between the pin circumference and the counterface disc on the Rotating Line Contact machine is illustrated in Figure 4.1. The value of Rc can be calculated by simple trigonometry, provided the disc penetration is known. Therefore:

$$Rc = \sqrt{(R-Pp)^2 + (\frac{Dp}{2})^2} - R$$

where R = radius of counterface cylinder (17.5 mm)

Pp = pin penetration (2.57×10^{-3} mm)

Dp = pin diameter (2 mm)

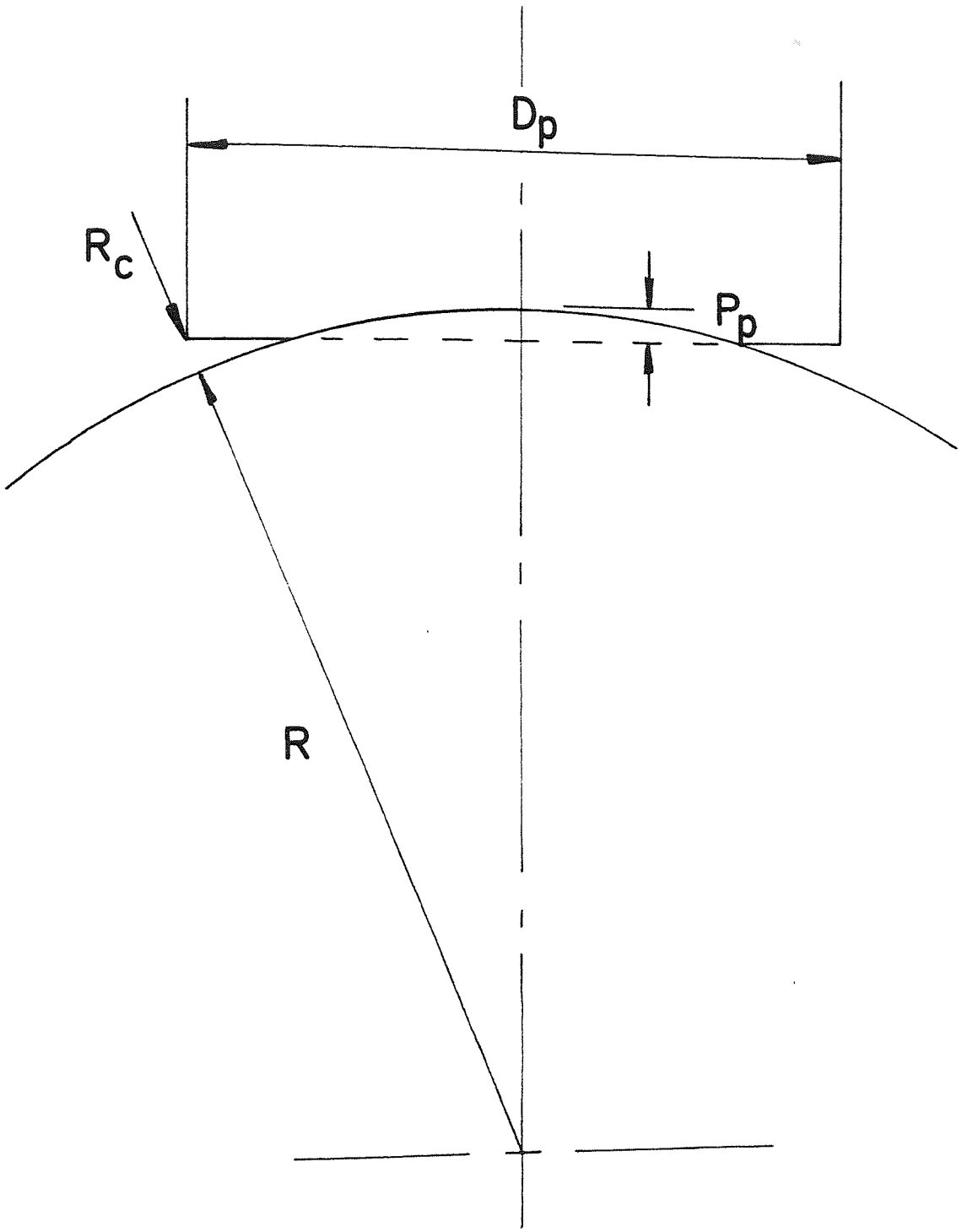

FIGURE 4.1 Radial clearance between pin and disc on the Rotating Line Contact machine

The Rc values for P.P.O., P.E.E.K. and P.T.F.E. are 0.026, 0.027 and 0.0125 mm respectively, for a 2.1 kg load. This shows that Rc for both P.P.O. and P.E.E.K. are very similar, but that Rc for P.T.F.E. is much less at 12.5 μm . Therefore, although P.T.F.E. has a much lower Young's Modulas than P.P.O. or P.E.E.K., the size of geometric wedge for P.T.F.E. is likely to be the main factor in determining its regime of lubrication. This lack of geometric wedge will not, however, occur on the Reciprocating Line Contact machine, and the Stribeck curve for P.T.F.E. on this machine does exhibit a more rapid move out of boundary conditions than on the other wear machines.

There are two major differences between the Stribeck curves for the three wear machines (Figures 3.5, 3.6 and 3.7) and the typical Stribeck curve in Figure 1.14:-

1) None of the Stribeck curves for the wear machines significantly move into hydrodynamic lubrication. This is because the machines are generally designed for boundary lubricated operation and do not have the necessary speed range to operate at the very high speeds required for complete hydrodynamic lubrication.

2) The Stribeck curves for the wear machines do not show the dramatic reduction in friction between the boundary and elastohydrodynamic lubrication regimes shown in Figure 1.14. This is because the Stribeck curve in Figure 1.14 is representative of a metal-metal sliding combination. In the hydrodynamic regime the friction value is entirely dependent on the fluid properties, whereas in the boundary

regime the friction is heavily dependent upon the bearing materials. Therefore, with a metal-metal combination the friction will rise substantially from the elastohydrodynamic regime to the boundary regime. Polymers, however, usually have much lower friction values than metals* and so the rise in friction will be much less.

Observation of the dry and lubricated friction values revealed some interesting results. On the Rotating Line Contact and Uni-Directional pin on disc machines the dry friction values for P.P.O. are essentially constant with sliding speed (See Figures 3.11 and 3.17). The friction values on the Uni-Directional pin on disc machine, however, are always higher than on the Rotating Line Contact machine (0.6 and 0.4 respectively). Under lubricated conditions the reverse occurs, with higher friction values on the Rotating Line Contact machine (0.1 and 0.2 at $1x10^{-3}$ ms^{-1}). These values were checked many times and it is considered that the different friction values are due to the different sliding geometries. Therefore, a discussion will follow on how a variation in the sliding geometry may affect the friction level.

It is interesting to note that the use of the silicone fluid with P.P.O. reduces the coefficient of friction by 50% on the Rotating Line Contact machine and by 83% on the Uni-Directional pin on disc machine. Bartenev and Lavrentev (46) suggested that the use of a lubricant would completely remove any adhesive component of friction. If this is the situation on the Rotating Line Contact and

* however, rubber like polymers can show a large variation

Uni-Directional pin on disc machines, then the adhesive and deformation components for P.P.O. can be calculated to give:

1) Rotating Line Contact machine

Dry Fa = 4.12 N

Fd = 4.12 N when $\mu = 0.4$, $W' = 20.6$ N

Lubricated Fd = 4.12 N when $\mu = 0.2$, $W' = 20.6$ N

2) Uni-Directional pin on disc machine

Dry Fa = 10.26 N

Fd = 2.1 N when $\mu = 0.6$, $W' = 20.6$ N

Lubricated Fd = 2.1 N when $\mu = 0.6$, $W' = 20.6$ N

There is therefore, a greater deformation component on the Rotating Line Contact machine and a greater adhesive component on the Uni-Directional pin on disc machine. In retrospect, it is obvious that the geometry of the Rotating Line Contact machine will lead to a high deformation component, because the disc penetration into the polymer has to be overcome (See Figure 4.1). Whereas, on the Uni-Directional pin on disc machine the majority of the deformation will occur at the surface asperities. This then, explains why the lubricated friction for P.P.O. is higher on the Rotating Line Contact machine, but not why there is a large difference in the adhesive components of friction for the two machines.

Bowden and Tabor's (4) theory $Fa = Ar\,s'$ shows that the

adhesive component of the frictional force is proportional to the real area of contact. With hard materials the real area of contact may be very much smaller than the apparent area of contact. When one material is relatively soft (as in polymers) then the softer material will deform to a greater extent and the real area of contact may be virtually the same as the apparent area. Therefore, if the apparent contact area (and hence the real contact area) is increased there may be a proportional increase in the coefficient of friction. On the Rotating Line Contact machine there is a relatively narrow band of contact between the pin and disc, which gives a contact area of 1.17 mm^2 for P.P.O. If it is assumed that the apparent contact area is the same as the real contact area on the Uni-Directional pin on disc machine, then this gives a contact area of 3.14 mm^2. There is, therefore, a close similarity between the increase in contact area and Fa, from the Rotating Line Contact to the Uni-Directional pin on disc machine - 268% and 249% respectively for P.P.O.

The lubricated friction values for P.P.O. on the Rotating Line Contact and Uni-Directional pin on disc machines (See Figures 3.11 and 3.17) follow part of the classical Stribeck curve and this has been discussed previously.

The dry friction values for P.E.E.K. on the Rotating Line Contact and Uni-Directional pin on disc machines are essentially constant with sliding speed (See Figures 3.14 and 3.18). As with P.P.O. the dry friction is higher on the Uni-Directional pin on disc machine at 0.5 instead of

and the lubricated friction is lower at 0.08 instead 13 at $1x10^{-3}$ ms^{-1}. The use of the silicone fluid gives ar reductions in friction to those with P.P.O., that % and 84% for P.E.E.K. on the Rotating Line Contact ne and Uni-Directional pin on disc machine respect-, compared to 50% and 83% for P.P.O. When the ases in the contact area and Fa, from the Rotating Contact to the Uni-Directional pin on disc machine, alculated then values of 277% and 334% respectively ound. This seems to support the arguments put forward ously concerning the roles of adhesion and deformation ese two machines.

ubricated friction values for P.E.E.K. follow a ar pattern to those found with P.P.O., and the ns for the shape of the curves have already been ssed with respect to the Stribeck curves. It should served, however, that the Rotating Line Contact ne remains in the boundary regime for a wider range lues of $\frac{nN'}{P}$ than on the Uni-Directional pin on disc ne. This is due to the higher Hertzian stresses ved on the Rotating Line Contact machine.

aphs of dry friction for P.T.F.E. on all three wear ies are very different to those for P.P.O. and P.E.E.K. igures 3.16, 3.19 and 3.20). The P.T.F.E. values ise with increasing speed and this has also been ved by others, such as McLaren and Tabor (53) and ima and Tanaka (115). McLaren and Tabor suggested that crease in friction and subsequent decrease with

creasing speed (decrease was associated with speeds gher than those available on the three wear machines), s due to dynamic losses in the polymer and not due to ictional heating. This proposal is supported by the aphs of dry friction and the calculated flash temperat- es using Lancaster's theory (27). Figure 3.20 shows that e dry friction increases from 0.06 at $1x10^{-3}$ ms^{-1} to 0.22 $1x10^{-1}$ ms^{-1}. However, the calculated flash temperature .y increases by $3^{o}C$ over this range, a temperature rise ich is unlikely to have such a marked effect on the .ction values.

e dry friction values for P.T.F.E. are slightly higher the Uni-Directional pin on disc machine (as with P.P.O. l P.E.E.K.) with a value of 0.1 at $3x10^{-3}$ ms^{-1} as against)85 on the Rotating Line Contact machine. The calculated .ues of Fa and contact area exhibit an increase of 146% l 137% respectively, illustrating the close relationship :ween these variables and further reinforces previous ruments. The lubricated friction values follow the aracteristic Stribeck shape on all three machines and es similar graphs as those with P.P.O. and P.E.E.K.

graphs of wear rate for each polymer on the three hines have also provided some interesting details. For mple, the graphs of dry wear rate versus speed for P.P.O. e Figures 3.11, 3.12 and 3.17) show two very different hanisms of wear depending upon the wear machine in stion, and whether debris is continuously removed from counterface, these are:-

) Wear when polymer debris is allowed to collect on the wear counterface (See Figure 3.11).

i) The second wear mechanism can be described as 'Normal' wear and occurs when the debris is not allowed to come between the wear specimen and the wear counterface.

ı all three wear machines P.P.O. forms similar basic ebris, this being small irregular particles. These may ccur because of abrasive wear by the counterface, but ıis is unlikely due to its smooth surface. It is more robable that the small particles are formed by a micro- sperity fatigue process discussed in Section 1.5.3. This ay account for the formation of pits in the P.P.O. urface under dry conditions (See Figures 3.22b, 3.35a ıd 3.43a). These pits, however, have not been observed .th P.E.E.K. which is thought to have a similar wear echanism and this will be discussed later.

e may speculate that a

ssible cause could be incomplete moulding of the polymer wder, although no firm evidence exists for this. Under y conditions on the line contact machines the small P.O. particles are compressed into an agglomeration to rm large debris flakes (See Figures 3.23a and 3.44a). ese are formed when the small debris particles enter the p between the wear pin and counterface on the Rotating ne Contact machine (See Figure 4.2); or between the ar strip and counterface on the Reciprocating Line ntact machine (See Figure 4.3). This flake formation is likely to occur to any great extent on the Uni-Directional

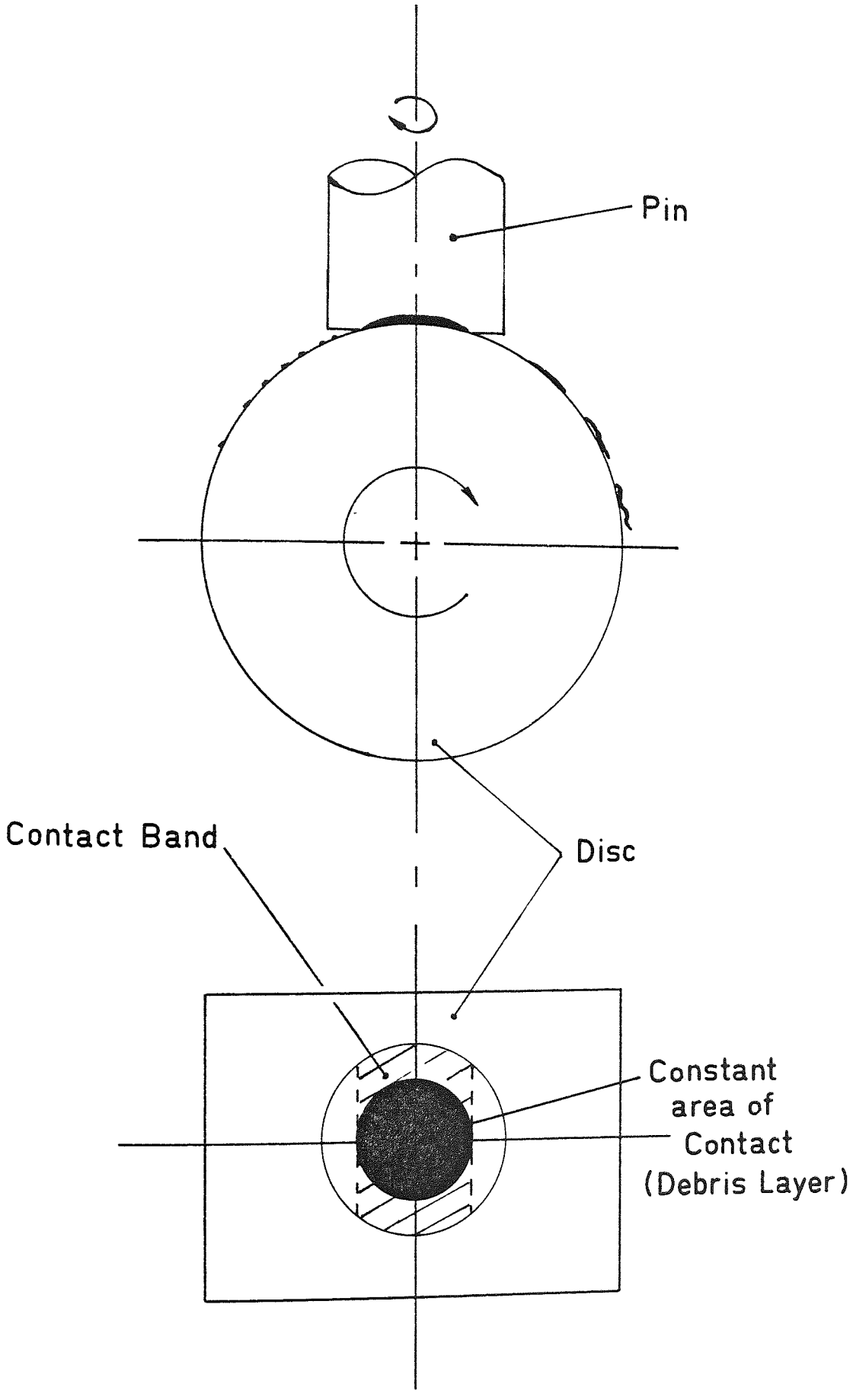

'IGURE 4.2 Debris formation on the Rotating Line Contact machine

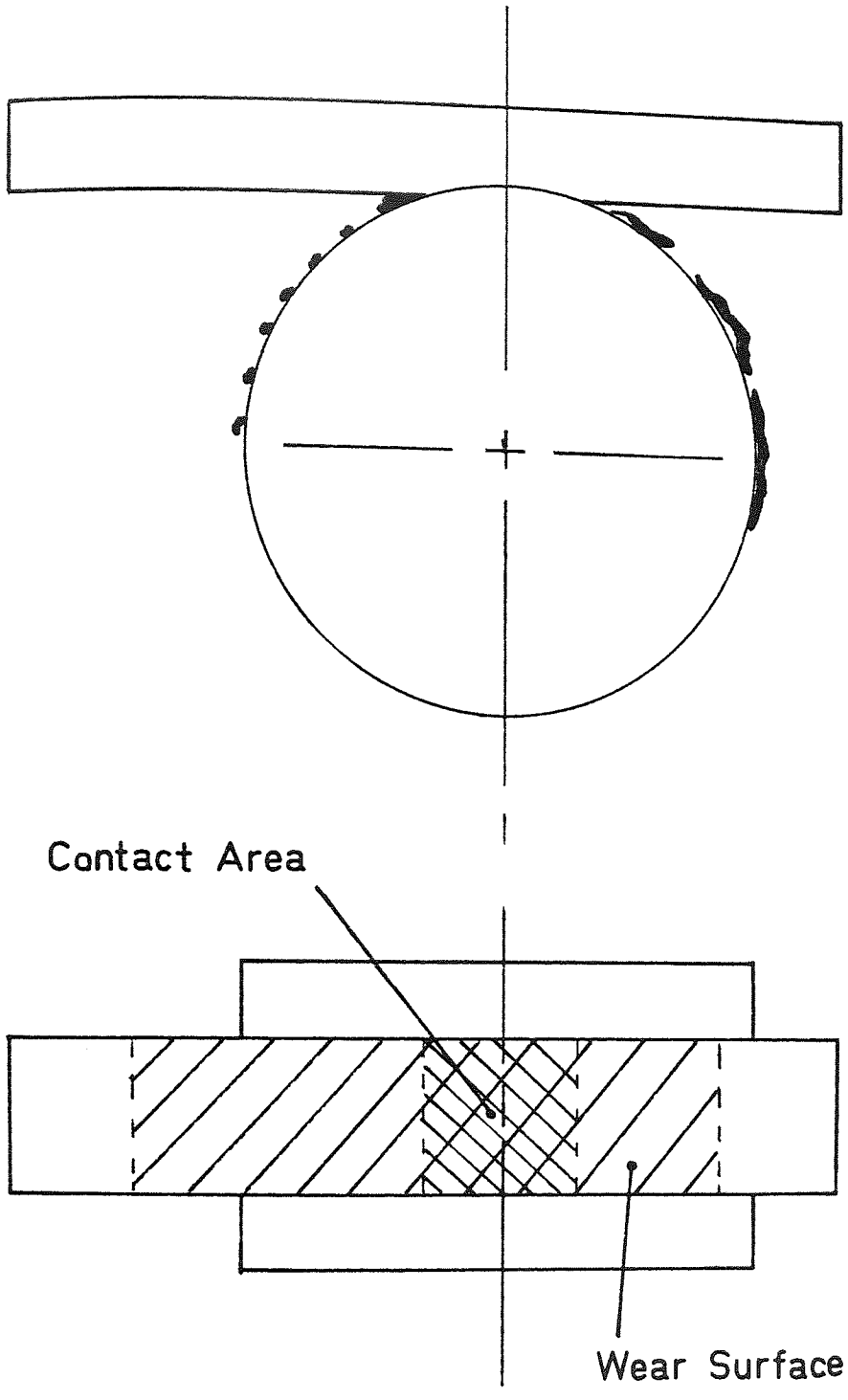

FIGURE 4.3 Debris formation on the Reciprocating Line Contact machine

pin on disc machine, because there is no large gap between the pin and counterface. On this machine the debris is simply pushed to the side of the wear track where it collects (See Figure 3.35b).

On the Rotating Line Contact machine some of the P.P.O. wear debris is held between the pin and counterface for long periods. This is possible because the debris is retained above the area of constant contact (See Figure 4.2). This area functions as a 'dead-trap' for any debris, which is only removed when the volume of trapped debris becomes too large and unstable. This leads to extrusion of the debris which then takes up position on the pin surface outside the area of constant contact. Any debris on the surface outside the area of constant contact is in intermittent contact with the wear counterface, and this tends to break up the extruded debris layer. There is also a possibility of a debris layer becoming established on the Reciprocating Line Contact machine. This is due to the existance of a similar type of gap between the wear strip and counterface into which debris can enter and be compressed against the specimen. There is, however, no area of constant contact on this machine, and the inter-mittent contact breaks up the debris layer. The possibility of any debris layer being formed on the Uni-Directional pin on disc machine is minimal because of the lack of gap for debris to enter

) Wear with a debris layer

The presence of this debris layer reduces the dry wear

rate considerably at low speeds, so that the values found are very similar to those obtained with the silicone fluid. This is because the pin is supported on the wear counter-face by the debris layer and wear occurs mainly on this debris layer. As debris particles are removed from the layer they are carried around the circumference of the counterface and eventually re-enter the gap to be once more compressed onto the debris layer. The process is therefore, partially regenerative and thus reduces the wear rate.

At very slow sliding speeds, the debris is more likely to be pushed to the side of the wear track, due to the relatively high rotary motion of the pin. Therefore, any reduction in the wear rate at very slow sliding speeds is likely to be less and this has been observed in the wear experiments.

There are two other actions which oppose the reduction in the wear rate caused by the debris layer. These are due to thermal softening of the polymer at high speeds (which will be discussed later) and the removal of debris from the counterface by centrifugal force. Therefore, at very slow sliding speeds (e.g. $5 \times 10^{-4}\ ms^{-1}$) the debris is swept to the side of the wear track by the relatively high rotary speed of the pin, and the debris layer is likely to wear more rapidly because the removed debris is not quickly replaced. However, as the sliding speed increases the rotary motion of the pin becomes insignificant and the debris is able to enter the gap between the pin and disc

more easily. This reduces the wear rate and is supported by Figure 3.11. The minimum in the wear rate occurs at a sliding speed of $5x10^{-2}$ ms^{-1}. Upon further increases in speed the thermal effects and debris removal due to centrifugal forces cause the wear rate to rise rapidly. Also, as the sliding speed increases the contact band width approaches the pin diameter due to thermal softening, and the entrapment gap between the pin and wear counterface becomes smaller, thereby reducing the access of debris to the pin. This reduction in access inhibits the formation of a debris layer and this is illustrated by the difference in debris at high and low speeds. At high speeds the debris is small and angular (e.g. See Figure 3.27), whereas, at low speeds the debris is in the form of large flakes which have been removed from the debris layer.

ii) 'Normal' wear

In this situation the wear rate remains constant at all the various speeds. At a sliding speed of $2x10^{-1}$ ms^{-1}, however, the wear rate for P.P.O. increases rapidly on the Rotating Line Contact machine. This is due to thermal softening of the polymer caused by frictional heating. The flash temperature of the contacting asperities can be calculated using Lancaster's theory for high speed sliding (27), where the flash temperature

$$Tf = 5.7x10^{-5} \mu p_m^{\frac{3}{4}} (W')^{\frac{1}{4}} V^{\frac{1}{2}}$$

For P.P.O. μ is essentially constant at 0.4 and the flow pressure is $72x10^{6}$ Nm^{-2} with a load of 21 N, therefore:-

$$Tf = 38.15 \times V^{\frac{1}{2}}$$

For a sliding speed of $2 \times 10^{-1}\ ms^{-1}$ this gives a calculated flash temperature of $17^{o}C$ and at $4\ ms^{-1}$ a temperature of $76.3^{o}C$. The surface temperature of the disc, however, was measured with a thermocouple, after wearing P.P.O. at $4\ ms^{-1}$ under a load of 2.1 kg for several thousand disc revolutions. The thermocouple indicated a surface temperature (Ta) up to $95^{o}C$, giving a total asperity temperature of $171.3^{o}C$. This is well above the value of Tg of $147^{o}C$ found by Skelcher (9,10) using a thermomechanical analyser, and accounts for the thermal softening of the P.P.O. asperities at high sliding speeds and its associated increase in wear rate.

The dry wear rate for P.P.O. on the Uni-Directional pin on disc machine starts to rise at higher sliding speeds than on the Rotating Line Contact machine ($5 \times 10^{-1}\ ms^{-1}$ instead of $2 \times 10^{-1}\ ms^{-1}$). The coefficient of friction is higher on the Uni-Directional pin on disc machine (0.6) and so

$$Tf = 57.225 \times V^{\frac{1}{2}}$$

Therefore, for a sliding speed of $5 \times 10^{-1}\ ms^{-1}$ Tf is $40.5^{o}C$ which is significantly higher than the flash temperature at which the wear rate begins to rise on the Rotating Line Contact machine. This high flash temperature is likely to be offset by the much greater mass of the wear counterface on the Uni-Directional pin on disc machine, which allows more heat to flow from the wear track. Therefore, although the flash temperature is higher on

the Uni-Directional pin on disc machine, the mean temperature of the counterface (Ta) is likely to be much less. The effects of thermal softening on the wear specimens can be clearly seen in Figures 3.36 and 3.43b.

The P.E.E.K. specimens on three wear machines produce small debris particles which are very similar to those from the P.P.O. specimens. A similar wear mechanism (micro-asperity fatigue:-See Section 1.5.3) is thought to be responsible, and the formation of debris flakes on the line contact machines is again probably due to debris entering the gap between the wear specimens and the disc, and then being compressed into an agglomeration. As with P.P.O., flake formation is not possible on the Uni-Directional pin on disc machine.

With P.E.E.K. also on the Rotating Line Contact machine there are two wear mechanisms under dry conditions:-

i) Wear when polymer debris is allowed to collect on the wear counterface and form a debris layer (See Figure 3.26a) which reduces the wear rate (See Figure 3.13). The same mechanisms, which give a minimum in the wear rate, are thought to be involved as with P.P.O.

ii) The second wear mechanism is again described as 'normal' wear, when debris is unable to collect on the counterface and form a debris layer on the pin.

The only difference between the two dry wear curves for P.P.O. and P.E.E.K., on the Rotating Line Contact machine,

when the debris layer is able to form, is that the minimum for P.P.O. occurs at $5x10^{-2}$ ms^{-1}, whereas, the minimum for P.E.E.K. occurs at $1x10^{-1}$ ms^{-1} (See Figures 3.11 and 3.13). This may be due to the slightly higher thermal resistance with P.E.E.K. because the flash temperatures at the same speed tend to be slightly higher with P.P.O.

Figures 3.15 and 3.18 show that the dry 'normal' wear rate for P.E.E.K. on the Rotating Line Contact machine without pin rotation is virtually the same as the dry wear rate on the Uni-Directional pin on disc machine*. This is as expected, because the wear geometry for these two conditions is then very similar. Figure 3.15 shows that rotation of the pin is responsible for a large proportion of wear at low sliding speeds, but at high speeds all wear rates are the same because thermal softening and polymer extrusion overrides any other wear mechanism.

The wear mechanism for P.T.F.E. on the wear machines under dry conditions appears to be very different to the mechanism for P.P.O. and P.E.E.K. All of the S.E.M. photographs (See Figures 3.29b, 3.39a and 3.48b) indicate that the polymer is being drawn out of the bulk in a very slow extrusion type process. This is probably due to the low value for Young's modulus and low creep resistance of P.T.F.E. The interfacial shear strength (s') of P.T.F.E. is very similar to its bulk shear strength (Ss) so that bulk shear is likely to occur when the friction is relatively high (e.g. 0.1). The debris is already in the form of sheets and flakes when it is initially removed,

* it would also be interesting to study the initial transient stages

and is likely to enter the gap between the wear strip and counterface on the Reciprocating Line Contact machine to be further deformed and may occasionally adhere to the wear strip as shown in Figure 3.48a. There is much less likelihood that the debris will enter the gap between the pin and counterface on the Rotating Line Contact machine, because the gap is much smaller with P.T.F.E., as previously discussed. Therefore, the possibility of P.T.F.E. forming a debris layer on the Rotating Line Contact machine is much less than with P.P.O. or P.E.E.K. The P.T.F.E. pin material on the Rotating Line Contact machine is likely to be drawn out in a spiral fashion due to the rotation of the pin, and this process is indicated by the surface features shown in Figure 3.29a. The material under the area of constant contact will take a greater time to be extruded than the material at the circumference of the pin. This is thought to be the mechanism which leads to the formation of a protuberance in the centre of the pin with P.T.F.E. on the Rotating Line Contact machine. On all three machines, with P.T.F.E. only, ripples can be observed on the surface of the wear specimens (See Figures 3.30a and 3.39b) when worn under dry conditions. These ripples show some similarity to the abrasion patterns which are formed on rubber, but on a much smaller scale (113). Reznikovskii and Brodskii (113) called this particular pattern, roll-formation, and suggested that it could only occur in highly elastic materials. Aharoni (114), however, has shown this phenomena to occur in a number of more rigid polymers including P.T.F.E. A schematic description of the mechanism of wear by roll-formation is given in

Figure 4.4. The formation of a roll starts with a smooth counterface being loaded against a soft and ductile material. When the two materials move relative to each other at a velocity V they will be in contact at certain points. If the coefficient of friction is high enough these points will remain in contact during the relative motion and the softer material will be deformed. The deformed material will only form into a roll if the interfacial shear strength (s') is higher than the bulk shear strength (Ss) of the softer material. There appears to be some confusion as to what conditions are likely to give complete roll formation with a particular polymer (46, 113, 114), but examination of all P.T.F.E. specimens from the three wear machines showed that stage 2 in Figure 4.4 was never passed. This may be due to the high pressures used on the three wear machines (114). The ripples in the surface of the P.T.F.E. specimens do bear some resemblance to the ridges formed on P.P.O. specimens under lubricated conditions and this will be discussed later.

The P.T.F.E. debris from the three wear machines under dry conditions shows considerable signs of stretching (See Figure 3.31) and drawing-out of the material along with orientation of the P.T.F.E. 'fibres' (See Figures 3.41a and 3.48b). This coincides with orientation of the transferred material on the wear counterface (See Figures 3.32a and 3.32b), which has been observed previously by Steijn (77).

The dry wear graphs for P.T.F.E. follow a similar curve to the dry friction, with the dry wear rate increasing with

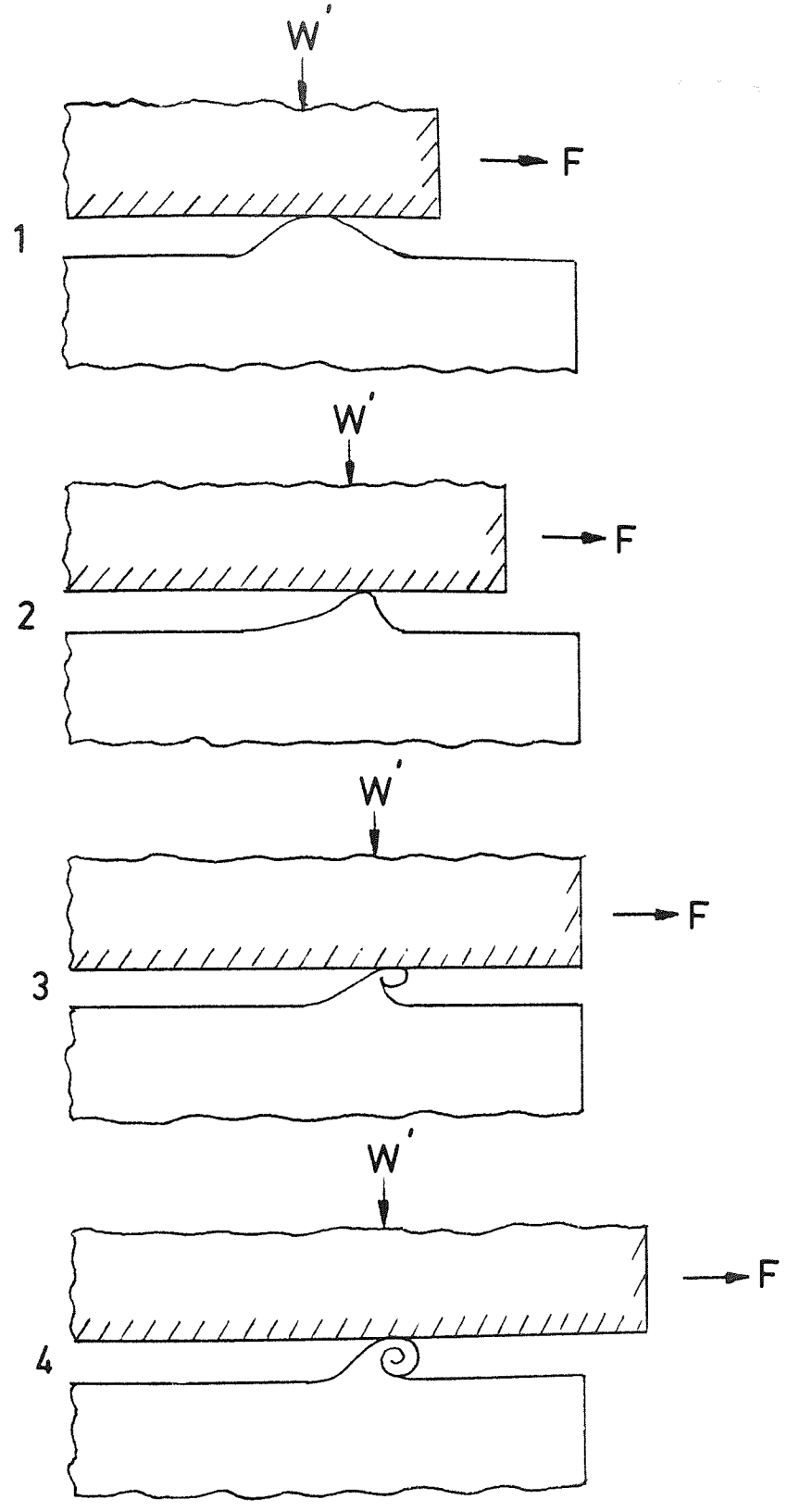

FIGURE 4.4 Roll formation of polymers.
(illustrating the four stages
involved)

increasing sliding speed until it levels off at $1x10^{-3}$ ms^{-1}. This has also been observed by Uchiyama and Tanaka (115) and is again probably due to dynamic losses in the polymer.

The dry wear rate for P.T.F.E. at slow speeds is very different on the Rotating Line Contact machine (See Figure 3.16) compared to the Uni-Directional pin on disc machine (See Figure 3.19). The higher wear rate at slow speeds on the Rotating Line Contact machine is believed to be due to the rotation of the pin. It was shown earlier that the pin rotation was a major factor in the wear of P.E.E.K. at slow sliding speeds, and this is thought to be a similar action.

Under lubricated conditions the P.P.O. debris is again made up of small particles but has a slightly different appearance in that the particles appear to be more rounded and easily compressed (See Figures 3.25 and 3.45b). This observation suggests that the particles are softened by some process, and plasticisation which has been observed by others (7, 8, 93) is an obvious possibility. This is reinforced by observation of the P.P.O. wear specimens from all three wear machines under lubricated conditions (See Figures 3.24a, 3.37b and 3.45a). All P.P.O. specimens have ridges on their surface after being worn in the presence of silicone fluid. These ridges are very similar to the surface features observed by Evans and Lancaster (8), when sliding P.P.O. against stainless steel in n-hexane. The ridges could be formed either by the surface of the polymer cracking (58, 91, 92), or by material being drawn

out of a plasticised layer. No freshly formed cracks without the raised ridge were ever observed and close observation of the ridges in the Figures indicate that plasticisation is the more likely cause. These ridges may have been produced by a similar mechanism to roll-formation which is believed to have produced the ripples in P.T.F.E. under dry conditions. However, no complete rolls were ever observed and a simple extrusion type of process seems to be the more likely cause.

Under lubricated conditions pitting does not occur on any machine with P.P.O., this may be due to the reduced adhesive component of friction and will be discussed later.

The debris particles are again formed into large flakes under lubricated conditions and the same mechanism as in dry conditions (i.e. micro-asperity fatigue) is thought to be responsible, resulting in the debris layer observed before. If plasticisation was occuring then this may have helped the formation of flakes and a debris layer by allowing the debris particles to be more easily compressed and by increasing the contact area between each particle due to its softened nature.

The lubricated wear rates for P.P.O. on the Rotating Line Contact and Uni-Directional pin on disc machine (See Figures 3.12 and 3.17) show a marked reduction as the sliding speed increases. The corresponding lubricated friction graphs show that as the sliding speed is increased

the conditions are moving towards the hydrodynamic regime. The two friction graphs clearly show how two different sliding geometries operate in different regimes for the same sliding conditions. For example on the Rotating Line Contact machine (where high Hertzian stresses are involved) at $1x10^{-3}$ ms^{-1}, the system is operating in the boundary regime. Whereas, on the Uni-Directional pin on disc machine at $1x10^{-3}$ ms^{-1}, the system is operating in the mixed regime with greater fluid film support and greater separation of the pin from the disc. This is the main reason why the dry and lubricated wear rates at slow speeds are much closer on the Rotating Line Contact machine than on the Uni-Directional pin on disc machine. However, the lubricated wear rate on the Rotating Line Contact machine exhibits a much greater reduction with increasing speed, due to the effect of the geometrical wedge on this machine. The fact that the dry and lubricated wear rates for P.P.O. in the boundary regime are very similar indicates that adhesion has little effect on the wear and that deformation which causes fatigue is the main reason for wear (the proposal that adhesion plays a minor role is supported by the absence of pitting under lubricated conditions). As the sliding speed is increased and greater fluid film support occurs, then deformation of the surface is likely to be much less prevalent and this is supported by the very low wear rates at high speeds.

The basic difference between the wear of P.E.E.K. and P.P.O. under lubricated conditions is that the presence of the silicone fluid prevents the formation of debris flakes and

a debris layer on the surface of the P.E.E.K. pins on the Rotating Line Contact machine. The importance of this difference will be seen later in the discussion on fluid retention. On all three wear machines under lubricated conditions the P.E.E.K. debris remains angular and separate (See Figures 3.28b and 3.47). There are also no ridges on the P.E.E.K. surface which resemble those found with P.P.O. This infers that the P.E.E.K. specimens are not being affected by the silicone fluid, and, whereas possible plasticisation of the P.P.O. may help the formation of debris flakes and a debris layer on the pin, this is definitely not the case with P.E.E.K. Therefore, the important points to note are:-

1) Silicone fluid does not appear to plasticise P.E.E.K.*

2) Whereas a debris layer was allowed to form on the P.E.E.K. pins (on the Rotating Line Contact machine) under dry conditions, the presence of the silicone fluid prevented this. This is because the silicone fluid prevented the individual wear particles from being compressed into a large agglomeration.

The graphs of lubricated wear for P.E.E.K. (See Figures 3.13 and 3.18) are very similar to those found with P.P.O. and similar wear mechanisms are thought to be occurring to reduce the wear rate at high speeds and to give similar dry and lubricated wear rates at low speeds.

For P.T.F.E. also under lubricated conditions debris layers do not occur on the wear specimens, and this is

* relative solubility parameters do not seem to have any effect

thought to be due to a combination of geometrical factors which prevent debris layer formation under dry conditions, and because P.T.F.E. is very resistant to most chemicals (including silicone fluid) and therefore very unlikely to be plasticised (13). It is also probable that the presence of a fluid is the reason for the absence of any transferred P.T.F.E. on all the wear counterfaces. The presence of the silicone fluid considerably reduces the friction level and therefore prevents the extrusion of material and the formation of rolls, and a protuberance on the Rotating Line Contact machine. On all three machines the wear mechanism for P.T.F.E. under lubricated conditions is probably due to micro-asperity fatigue, discussed in Section 1.5.3., because the counterface is too smooth to cause any significant amount of abrasion, and no extrusion/drawing-out of the material is observed. Some debris could be seen in the fluid but this was very small and very difficult to separate out. Therefore, debris examination by scanning electron microscopy was not successfully achieved.

The lubricated wear rates for P.T.F.E. on all three machines exhibit the characteristic decrease with increasing sliding speed, this is again thought to be due to increased fluid film support and has previously been explained. The dry and lubricated wear rates for P.T.F.E. are very close at low speeds and similar mechanisms are thought to be occurring as with P.P.O. and P.E.E.K.

The initial experiments, with P.P.O. on the Rotating Line Contact machine, to observe fluid retention, have been

undertaken in exactly the same manner as described by Skelcher (9,10). This has entailed cleaning the wear pins with a soft tissue to remove any excess fluid after the lubricated part of the experiment. This method of cleaning the pins gives prolonged periods of low friction during the 'dry' run (dwell period) and infers that some fluid retention has occurred (See Table 3.1, Test 1-4). When the wear pins are studied with an optical microscope before the dwell period it can be seen that the debris layer, discussed previously, is still in place. When the wear pins are subjected to more vigorous cleaning, before the dwell period, then microscopic examination shows that the debris layer is removed and no prolonged periods of low friction occur with these wear pins. This initial work indicates that fluid retention is caused by the presence of the debris layer formed under lubricated conditions, and is exclusive to P.P.O. on the Rotating Line Contact machine. Fluid retention could not be inferred from any of the dwell tests with P.E.E.K. and P.T.F.E. on the Rotating Line Contact machine at any time, and neither have the dwell tests with any of the three polymers on the Reciprocating Line Contact or Uni-Directional pin on disc machines. This is also matched by the total absence of a debris layer under lubricated conditions with these combinations.

S.E.M. analyses of the P.P.O. wear pins from the Rotating Line Contact machine show that if the debris layer formed under lubricated conditions, is removed with vigorous wiping of the tissue then no silicon can be detected in

the sectioned pins (See Figures 3.52 and 3.53). If, however, the debris layer is not removed (when gentle wiping is employed) then observation by S.E.M. of the sectioned pin clearly shows the thickness of this layer and its interface with the main body of the pin (See Figures 3.54 and 3.55). The thickness of the layer varies between 5 and 15 μm but is usually about 10 μm (this is similar to Skelcher's (9,10) observation of the depth of fluid retention). The x-ray maps and concentration profiles clearly show retained silicon only in the debris layer, and quantitative analysis gives silicon concentration values up to 15% with occasional small pockets of high concentrations up to 80% (See Figures 3.56 and 3.57). These values are also similar to Skelcher's (9,10) (obtained by Rutherford Backscattering) who suggested that retention occurred in the bulk of the polymer. The results of the analysis also show the detected silicon returning to a background level in the main body of the pin, indicating that no fluid penetration into the bulk of the polymer occurs.

Any remaining doubts about silicone fluid being retained only in the debris-layer, are removed by the analysis at a direction which is normal to the whole pin wear surface. This clearly shows the debris layer, and that silicon is only detected in this layer and not in the bulk of the pin (See Figures 3.58, 3.59 and 3.60).

It is clear that fluid retention is dependent upon the combination of P.P.O. and silicone fluid and the geometrical design of the Rotating Line Contact machine. The results

of the autoclave experiments (See Appendix 2) indicate that no significant quantity of silicone fluid is diffusing into the polymers. It seems therefore, that P.P.O. is only affected by silicone fluid to any great extent, when it is being mechanically worked (this situation is prevalent in bearing systems). It is therefore proposed that the mechanism of fluid retention with P.P.O. on the Rotating Line Contact machine is as follows:-

1) Micro-asperity fatigue wears the pin surface (under dry and lubricated conditions) and small debris particles are removed.

2) The debris particles are softened by the silicone fluid due to plasticisation

3) A mixture of debris particles and silicone fluid forms a debris layer (the debris layer also occurs under dry conditions) under the area of constant contact with the fluid induced plasticisation aiding or at least not inhibiting particle adhesion.

4) Although some fluid may be absorbed into the surface of the debris particles, most fluid remains between the particles and on rare occasions this can lead to small pockets of fluid, up to 80%.

Fluid retention does not occur with P.E.E.K. because of two reasons:-

1) The P.E.E.K. debris particles are not softened by the silicone fluid and do not appear to be plasticised.

2) It is obvious that fluid retention is dependent upon the presence of a debris layer on the pin surface. However, whereas under dry conditions a P.E.E.K. debris layer will form, under lubricated conditions the silicone fluid prevents the formation of a debris layer (See Figures 3.28a and 3.47).

Fluid retention also does not occur with P.T.F.E. because the debris layer is unable to form for two reasons:-

1) Debris cannot enter the gap between the pin and disc very easily because it is too small.

2) As with P.E.E.K., P.T.F.E. is chemically resistant to silicone fluid and the presence of a fluid impedes the joining together of debris particles as it also impedes the formation of a transferred layer on the counterface (See Figures 3.61, 3.62, 3.65, 3.66, 3.69 and 3.70).

Fluid retention can also not occur on the Uni-Directional pin on disc or Reciprocating Line Contact machines because debris layers are unable to form on these machines. This is illustrated by Figures 3.63, 3.64, 3.67 and 3.68 which clearly illustrate the absence of a debris layer or any significant quantity of silicon.

CHAPTER 5

CONCLUSIONS AND FURTHER WORK

5. CONCLUSIONS AND FURTHER WORK

The work described in this dissertation has highlighted a number of important points on the friction and wear of P.P.O., P.E.E.K. and P.T.F.E. The initial work in constructing the Stribeck curves for each wear machine has shown that the shape of the Stribeck curve is not only dependent upon the dimensionless parameter of $\frac{n N}{P}$, but that the bearing materials and contact geometry also play an important role. Observation of the Stribeck curves has shown that their shape can vary from one wear machine to another when operating under identical conditions.

The value of the coefficient of friction for polymers has also been shown to be dependent upon the contact geometry which directly affects the values of the adhesive and deformation components of friction.

The most fundamental observation to this work is that two different wear mechanisms occur on the line contact machines with unfilled P.P.O. and P.E.E.K. these are:-

1) Wear when debris is allowed to collect between the wear specimen and counterface.

2) Wear when debris is continuously removed and not allowed access between the wear specimen and counterface.

When the former occurs with the presence of a 'dead-trap' for any debris then very low dry wear rates are observed

and are similar in magnitude to the lubricated wear rates over the lower half of the speed range. However, all dry wear rates for both P.P.O. and P.E.E.K. are the same at high speeds due to thermal softening of the polymer asperities and hence polymer extrusion. The work with the three wear configurations has also shown that the sliding speed at which thermal softening occurs is not only dependent upon the variables of μ, V and W', but also on the mass of the wear counterface - that is those with a large mass are more able to conduct heat from the wear track to atmosphere and enable the critical speed for softening to increase.

The wear mechanism for P.T.F.E. under dry conditions appears to be very different to the mechanisms for P.P.O. and P.E.E.K. P.T.F.E. appears to be drawn out from the bulk in a slow extrusion type process and does not suffer from thermal softening at high speeds. This is due to its low coefficient of friction which gives lower energy dissipation at the asperities and hence low asperity flash temperatures.

On the Uni-Directional pin on disc machine the dry and lubricated wear rates for P.P.O. and P.E.E.K. are very close at slow sliding speeds. However, the dry wear rate for P.T.F.E. may be lower than the lubricated wear rate. This is due to the presence of a transferred film under dry conditions which leads to very low wear rates.

The important difference between the three polymers

(P.P.O., P.E.E.K. and P.T.F.E.) is that during wear there is evidence to suggest that P.P.O. is plasticised by the silicone fluid whereas P.E.E.K. and P.T.F.E. are not. Due to this plasticisation the fluid does not prevent the formation of a debris layer on the P.P.O. pins from the Rotating Line Contact machine, and indeed may actually help its formation. The silicone fluid does prevent debris layers occurring with P.E.E.K. due to the fact that the fluid separates the debris particles and will not allow adhesion, whereas P.T.F.E. has never shown any substantial layer formation. The analyses of the P.P.O. pins has shown that the retained silicone fluid is held between or on the surface of the debris particles which make up the debris layer, and that no diffusion of the fluid occurs into the bulk of the polymer pins.

Therefore, this work has conclusively shown that the retention of silicone fluid by the P.P.O. pins is a combination of plasticisation of the P.P.O. debris and the unique geometry of the Rotating Line Contact machine.

These conclusions indicate a number of important points to consider in the future. The first is that it is necessary to construct a complete Stribeck curve for each material on each wear machine when conducting a series of lubricated wear experiments, otherwise the regime of lubrication cannot be defined.

The relationship between the contact geometry and the magnitude of the friction force could have some important

implications for the use of polymers in bearings. It would be interesting to study the affects of different configurations on the coefficient of friction in rolling element bearings and sliding bearings for both dry and lubricated conditions.

Previous work (119) has shown that when using filled polymers the trapped debris between the wear specimen and counterface can increase the wear rate due to the abrasiveness of the filler. This work has shown the opposite effect with unfilled P.P.O. and P.E.E.K. If debris layers could be formed with less abrasive fillers then a reduction in the wear rate should occur. A wear test program is therefore required to try and find a polymer/filler combination which gives a debris layer and low wear rate.

In practical situations the thermal softening of polymer bearings may be reduced by increasing the mass of the wear track, this however, will be restricted by the design limits in force.

Further work is required to test the suggestion that the wear rate for P.T.F.E. at very slow sliding speeds could be lower under dry conditions than lubricated conditions. If this suggestion is correct then lubricants could be detrimental to the wear rate of unfilled and filled polymers at very slow sliding speeds. This will require a very slow motor on the wear machine so that sliding speeds of $1 \times 10^{-4}\ ms^{-1}$ can be obtained.

The work on the retention of silicone fluid has shown that to use this principal in a practical situation a number of factors are required:-

1) The bearing design must promote the formation of a debris layer.

2) The debris layer must strongly adhere to the bulk of the polymer.

3) A polymer-fluid combination is required in which the fluid does not inhibit the formation of the debris layer.

These points indicate a number of areas for further research:-

a) Identification of practical bearing configurations which promote the formation of a debris layer.

b) Determine whether fluid retention occurs with filled polymers.

c) Determine whether fluid retention occurs with common lubricants such as water, engine oils, fuels etc.

d) Study the effects of sliding speed and ambient temperature on fluid retention.

APPENDICES

APPENDIX 1

The actual densities of the P.E.E.K. and P.T.F.E. specimens (P.P.O. is amorphous) were calculated using a simple formula quoted by Brandrup and Immergut (105) where:

$$\text{Crystallinity} = \frac{dc}{d}\left(\frac{d - da}{dc - da}\right) \times 100 \quad (\%)$$

where d = measured density (grams cm^{-3})

da = amorphous density (grams cm^{-3})

dc = crystalline density (grams cm^{-3})

The measured density of the P.E.E.K. material was 1.276 grams cm^{-3}, whereas, da and dc were 1.265 and 1.320 grams cm^{-3} respectively (21).

$\therefore$ P.E.E.K. Crystallinity = 20.7%

The measured density of the P.T.F.E. material was 2.253 grams cm^{-3}, whereas, da and dc were 2.00 and 2.302 grams cm^{-3} respectively (105).

$\therefore$ P.T.F.E. Crystallinity = 85.6%

APPENDIX 2

As plasticisation had been previously proposed (9,10) as a possible mechanism of fluid retention in P.P.O., it was thought necessary to determine whether silicone fluid would diffuse into P.P.O., P.E.E.K. or P.T.F.E. under high pressures.

A 200 cc Hastalloy "C" autoclave was used for these experiments. The autoclave consisted of a large, thick-walled cylinder for containing the specimens and fluid. A lid screwed onto the top of the cylinder and made a seal to prevent any escape of gas or fluid. A safety valve was connected to the top of the lid in series with a pressure gauge. The gas used was Nitrogen which was supplied from a high pressure bottle nearby.

The specimens were placed under pressure for 20 hours at 120 Atmospheres, they were then removed and any weight change was recorded. The polymers were then placed in the autoclave for a further 280 hours at 120 Atmospheres and again any weight change was recorded at the end of the experiment.

The final period in the Autoclave was for 24 hours at 140-150 Atmospheres and at a temperature of $100^{o}C$.

The results of the autoclave experiments are shown in Table A2.1. P.E.E.K. and P.T.F.E. exhibited no weight gain under any of the set conditions. P.P.O. exhibited a very

small weight gain, but as the experimental procedure was only accurate to $\pm$0.3% this result is not really statistically significant.

Polymer	Initial Wt. (grms)	% Wt. gain (1^{st} Rec.)	% Wt. gain (2^{nd} Rec.)	% Wt. gain (Final Rec.)
P.P.O.	0.660	0	0.15	0.15
P.E.E.K.	0.634	0	0	0
P.T.F.E.	0.909	0	0	0

Table A2.1 Results of Autoclave Experiments

APPENDIX 3

Each polymer has a molecular weight distribution, the shape of which will depend upon its composition, the degree of mechanical or thermal processing to which it has been subjected and the inclusion of any additives, such as plasticisers and colouring agents. It was thought essential to know the molecular weight distribution for each fluid viscosity being used in the lubricated experiments. Without this information it would have been difficult to compare the various results obtained from the different viscosities. One method of obtaining the molecular weight distribution of polymers is by Gel Permeation Chromotography. This technique involves the separation by molecular size of molecules in solution, and hence, the polymer to be analysed must be dissolved in an appropriate solvent.

A polymer molecule in solution has an "effective size" that is closely related to its molecular weight. This "effective size" is also known as the chain length of the molecule with the chain being made up of the basic repeat units in the molecule. Therefore, if the molecular weight of a repeat unit is known the distribution of chain lengths can be found directly from the molecular weight distribution.

A G.P.C. spearation is accomplished by injecting a polymer solution into a continually flowing stream of solvent (See Figure A3.1). This flowing stream of solvent passes through a bed of highly porous, rigid particles closely packed together in a column. The pore sizes between these

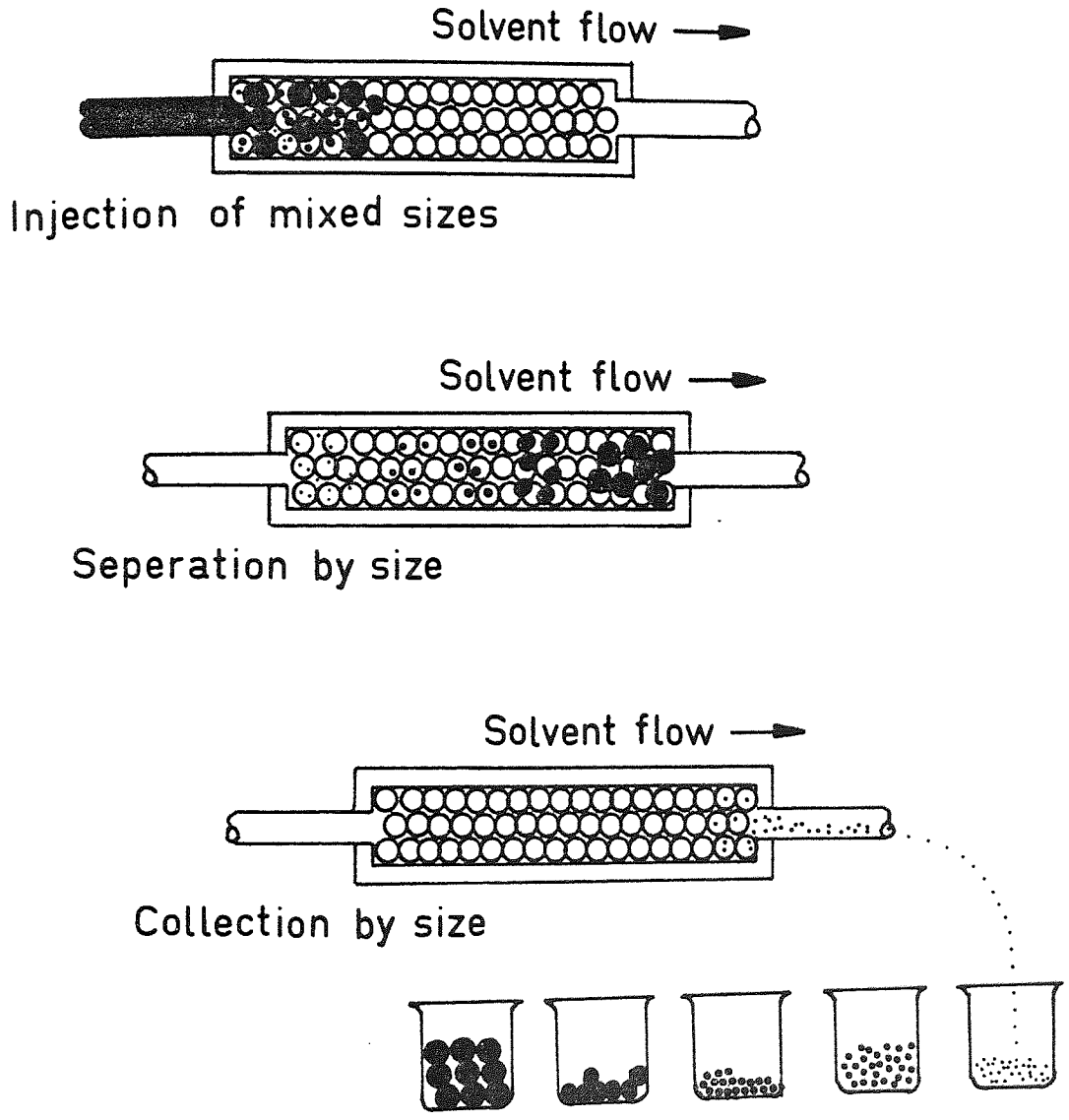

FIGURE A3.1 Gel-Permeation Chromotography: Molecular Separation

particles may vary from very small to very large.

As the solution flows through the packing bed, molecules with small effective sizes (low molecular weights) will penetrate more pores than molecules with larger effective sizes. The lower molecular weight molecules will take longer to emerge from the column than the larger molecules, because the larger molecules do not enter as many pores as deeply. The result will be a size separation with the larger molecules exiting the packed columns first.

If the pore sizes of the packings are so large that all the molecules can enter all the pores, or if the pore sizes are so small that none of the molecules can enter any of the pores, no separation occurs. The pore size range must match the molecular size distribution for effective separation.

The refractive index of a molecule varies with any change in molecular weight, therefore, the large molecules will have a different refractive index to the smaller ones. This difference is usually detected by a differential refractometer which in turn is connected to a paper trace recorder (See Figure A3.2). The G.P.C. user therefore obtains a record of the molecular weight distribution of his polymer, and this can be compared to the molecular weight distribution of known standards.

Solutions of each of the viscosities of silicone fluid (containing 1% Silicone fluid) were made up in Toluene

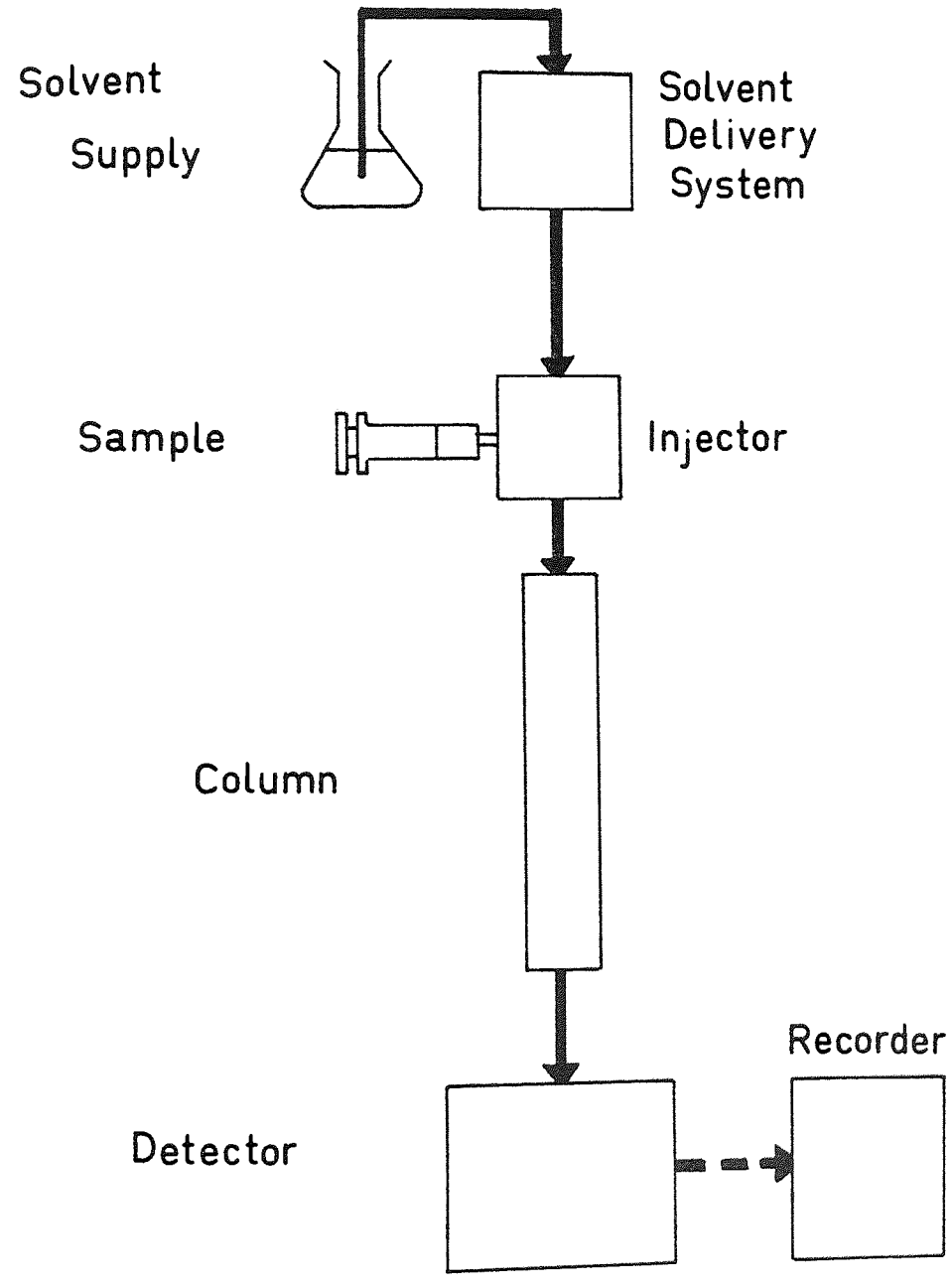

FIGURE A3.2 Schematic diagram of Gel-Permeation Chromotography Equipment

and then injected into a Waters Gel Permeation Chromatograph. A graph was automatically plotted on a chart recorder showing the distribution of molecular weights in the silicone fluid. The equipment was calibrated with Polystyrene standards of known molecular weight.

The molecular weight distribution was obtained for each viscosity of silicone fluid available. These were 0.65, 1.0, 5.0, 10, 50, 100, 500, 1000, 12,500, 30,000, 60,000 and 100,000 cs. The number of repeat units or chain length distribution, was found for each viscosity from the molecular weight distribution. These are shown in Figure A3.3.

Generally, the higher the viscosity of fluid, the wider was the distribution of repeat units. For example in a 0.65 cs fluid the distribution of repeat units was between 1 and 3. However, for a fluid with a viscosity of 100,000 cs the distribution was between 10 and 25,000 repeat units. The range of chain lengths and their peak positions are shown in Table A3.1 for each viscosity.

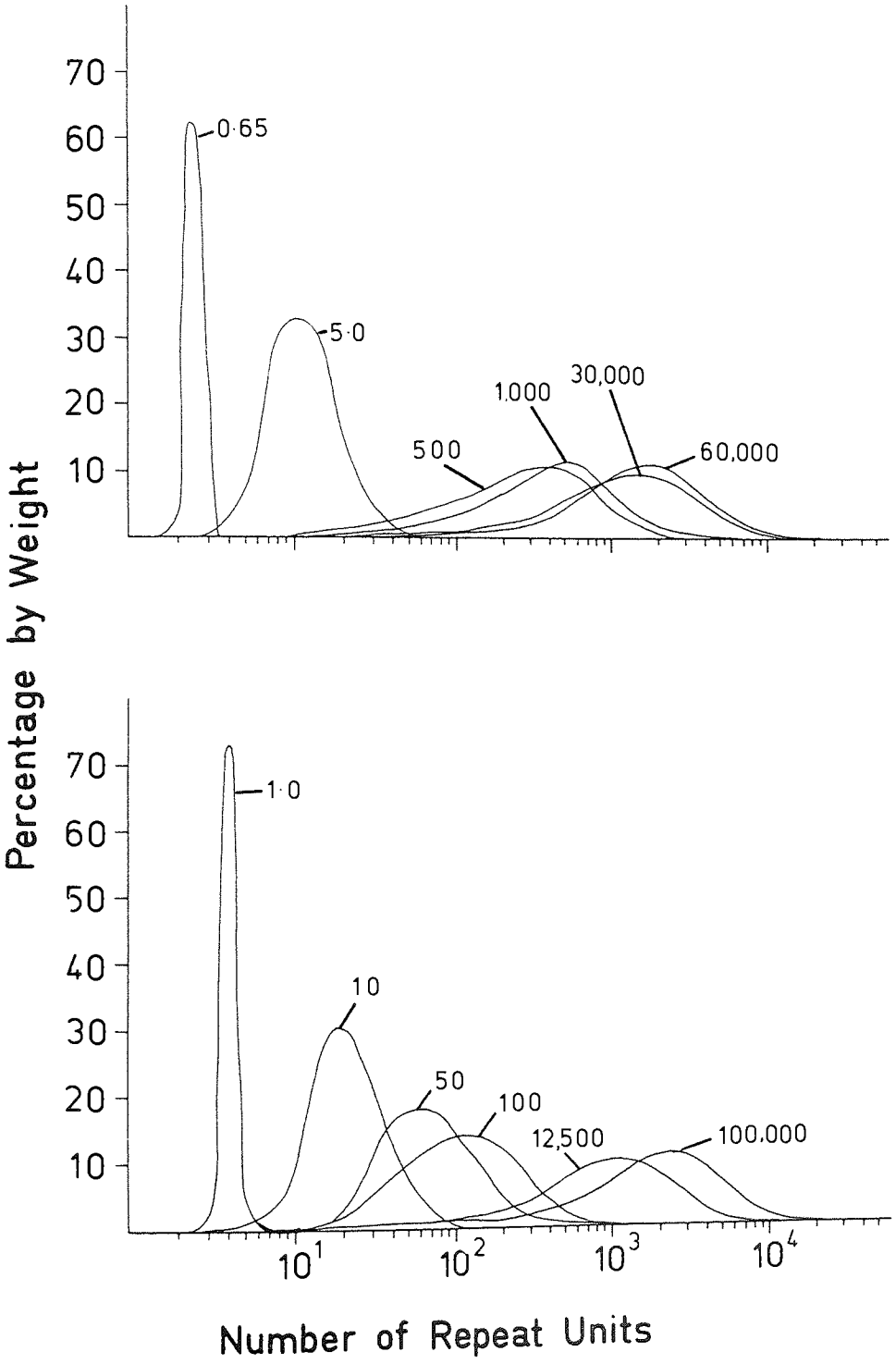

FIGURE A3.3 Distribution of Chain lengths for each viscosity (c s) of Polydimethylsiloxane

Viscosity (cs)	Range of Repeat Unit Length	Peak Position (Repeat Units)
0.65	1 - 3	2.5 - 3
1.0	2 - 7	4 4
5.0	3 - 80	10
10	3 - 300	20
50	4 - 2,000	60
100	7 - 1,200	100
500	7 - 3,300	350
1,000	7 - 6,000	500
12,500	8 - 17,000	1,300
30,000	8 - 19,000	1,500
60,000	8 - 20,000	2,000
100,000	10 - 25,000	2,500

Table A3.1 Range of chain length and peak positions for each viscosity (cs) of Polydimethylsiloxane.

APPENDIX 4

It was found that when 1 cs silicone fluid was used as a lubricant, if the fluid bath was not continually topped-up, the fluid would evaporate because the low viscosity silicone fluids are much more volatile than the high viscosity fluids. When the fluid evaporated the coefficient of friction fell from its normal lubricated value to a new lower value. The friction would then stay at this lower value for a considerable period of time before slowly rising to the normal dry value (See Figure A4.1). This phenomena occurred on all three machines and with each of the polymers.

The new lower friction reached after the fluid had evaporated was similar in magnitude to that observed with a 100 cs fluid.

If more 1 cs fluid was added then the friction returned to its normal lubricated value. However, if after the 1 cs fluid had evaporated the friction fell and the wear counterface was replaced by a new clean one, the friction returned to the normal dry value very rapidly.

The Dwell tests conducted with 1 cs silicone fluid were interesting, in that it was unusual to observe a reduction in the coefficient of friction with the evaporation of the fluid. The key to understanding this phenomena, however, lay in the results of the Gel-Permeation Chromotography (G.P.C.). These results showed the 1 cs fluid to have a

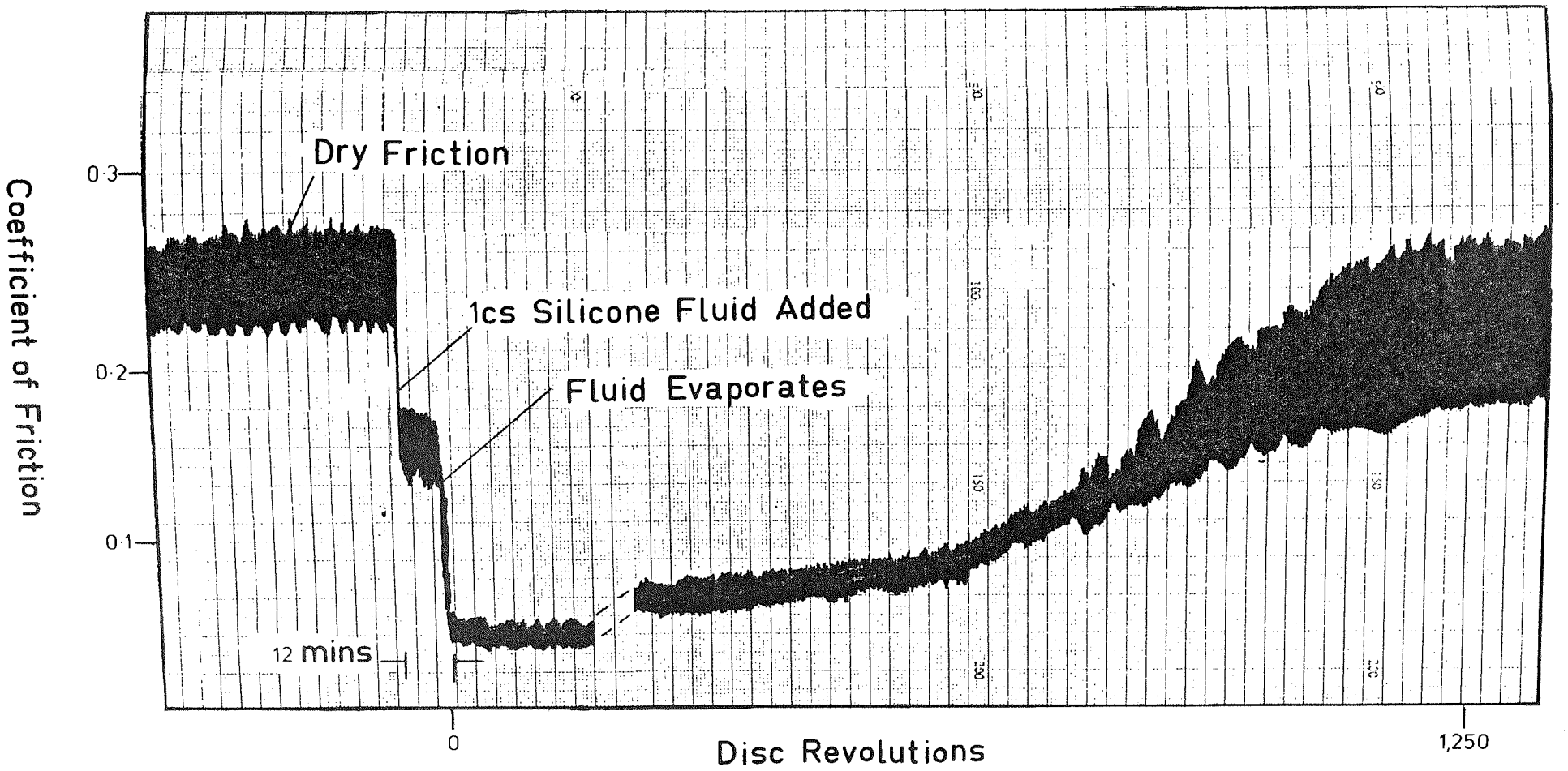

FIGURE A4.1 Typical friction trace for P.E.E.K. on the Rotating Line Contact machine when using 1 cs silicone fluid as a lubricant

very narrow distribution of chain lengths, whereas the higher viscosity fluids had a very wide distribution. Indeed, a 1,000 cs silicone fluid had a distribution between 7 and 6,000 repeat units, whereas the 1 cs fluid was between 2 to 7 repeat units. Therefore, the silicone fluids having a viscosity between 1 and 1,000 cs shared some common chain lengths.

The decrease in the coefficient of friction was thought to be an indirect result of the evaporation of the fluid. When the fluid evaporated the smaller chains evaporated first leaving behind the longer chains. This changed the distribution of chain lengths and hence increased the viscosity of the fluid. With the increased viscosity the friction fell and the process continued until all the smaller chains had evaporated leaving a higher viscosity fluid than was originally used. The fall in the observed friction was more rapid than expected but this may have been due to polymerisation of the fluid, which would have accelerated the process. It is interesting to note that Tabor and Willis (116), Willis and Shaw (117), and Willis (118) have detected very thin dimethysilicone polymer films at temperatures as low as 100^{o}C. Eventually the fluid that remained was either broken into smaller chains and then evaporated, or was pushed to the side of the wear track leading to a rise in the friction to the normal dry value.

REFERENCES

1. AUSTIN,T.C and HELLMAN,K.H. "Passenger Car Fuel Economy-Trends and Influencing Factors" S.A.E. paper 730790 presented at National Combined Farm, Construction and Industrial Machinery and Fuels and Lubricants Meetings, Milwaukee, Wis.,Sept.10-13 1973. pp 17-20

2. HILL,P and VIELVOYE,R. "Energy in Crisis", Robert Yeatman Ltd., 1974, p 220

3. DONGHAM,M.A.(Ed) "Technological Advances in Vehicle Design", Ford Energy Report, Proc. of the Int. Ass. of Vehicle Design, 1982, p 127

4. BOWDEN,F.P. and TABOR,D. "The Friction and Lubrication of Solids" Vol.I, Oxford Univ. Press, London, (1950)

5. FLOM,D.G. and PORILE,N.T. "Friction of Teflon Sliding on Teflon" J. Appl. Phys. Vol.26, No.9, (Sept.1955) pp 1088-1092

6. ATHWAL,S.S. "Wear of Low Alloy Steels at Elevated Temperatures" Ph.D. Thesis, (1983), University of Aston in Birmingham.

7. RUBENSTEIN,C. "Lubrication of Polymers", J. Appl. Phys. Vol.32, No.8 (1961) pp1445-1450

8. EVANS,D.C. and LANCASTER,J.K. "Polymer-Fluid Interaction in Relation to Wear", Royal Aircraft Establishment, Farnborough, Technical Report 76099, July 1976

9. SKELCHER,W.L. "The Wear of Polymers during Sliding under Fluid-Contaminated Conditions", Ph.D. Thesis (1982), University of Aston in Birmingham

10. SKELCHER,W.L., QUINN,T.F.J. and LANCASTER,J.K. "The Influence of Polydimethyl Siloxane on the Friction and Wear of Polyphenylene Oxide Under Boundary Lubrication Conditions", presented at ASLE/ASME Lub. Conf., New Orleans, Louisiana, Oct.5-7, 1981

11. HALL,C. "Polymer Materials", Macmillan (1981)

12. KREVELEN,D.W.V. "Properties of Polymers", Elsevier Sci. Pub. (1976)

13. BRYDSON,J.A. "Plastics Materials", Butterworths, London, (1975)

14. DRIVER,W.E. "Plastics Chemistry and Technology", Van Nostrand Reinhold Pub. Co., N.Y. (1979)

15. BUECHE,F. "Physical Properties of Polymers", Interscience Publishers, N.Y. (1962)

16. BUNN,C.W., COBBOLD,A.J. and PALMER,R.P. "The Fine Structure of P.T.F.E.", J. Polymer Sci., Vol.28 (1958) pp 365-376

17. SPEERSCHNEIDER,C.J. and LI,C.H. "Some Observations on the Structure of P.T.F.E.", J. Appl. Phys., Vol.33, No.5 (1962) pp 1871-1875

18. OGORKIEWICZ,R.M.(Ed), "Thermoplastics: Properties and Design", John Wiley & Sons, London (1974)

19. RITCHIE,P.D.(Ed.) "Physics of Plastics", D.Van Nostrand Pub. Co., (1965).

20. HARPER,C.A.(Ed) "Handbook of Plastics and Elastomers", McGraw Hill (1975)

21. I.C.I. Data Sheet on Polyetheretherketone (P.E.E.K.)

22. ROSS,R.B., "Metallic Materials Specification Handbook", E. & F.N.Spon Ltd.,(Pub.) 1980

23. E.S.D.U. 76029 "A Guide on the Design and Selection of Dry Rubbing Bearings", Nov.1976

24. DOWSON,D. "History of Tribology", Longman (1979)

25. National Centre of Tribology, "Polymer Materials for Bearing Surfaces:- Selection and Performance Guide", 1983

26, LANCASTER,J.K. "Wear Mechanisms of Metals and Polymers", Trans. Inst. Metal Finishing, 1978, Vol.56, pp 145-153

27. Lancaster,J.K. "Estimation of the Limiting PV Relationships for Thermoplastic Bearing Materials", Tribology, May 1971, pp 82-86

28. LANCASTER,J.K. "Dry Bearings: a survey of materials and factors affecting their performance", Tribology, Dec.1973, pp 219-251

29. BHUSHAN,B and WILCOCK,D.F. "Frictional behaviour of polymeric compositions in dry sliding", Proc. of the 7th Leeds-Lyon Symposium on Tribology, Leeds, Sept.1980, Paper IV(IV) pp 103-113

30. BELY,V.A. et al "Friction and Wear in Polymer-Based Materials", Permagon Press, 1982

31. EVANS,D.C. "Polymer-fluid interactions in relation to wear", Proc. of the 3rd. Leeds-Lyon Symposium on Tribology, Leeds, 1976, paper III(i), pp 47-55

32. CAMPBELL,G.R. "The lubricated wear of plastic lined bearings", Proc. of the 3rd Leeds-Lyon Symposium on Tribology, Leeds, 1976, paper X(ii), pp 252-256

33. MUSTAFAEV,T.K. et al "The lubricated wear of high density polyethylene with mineral oil and stearic acid", Proc. of the 3rd Leeds-Lyon Symposium on Tribology, Leeds, 1976, paper III(IV), pp 65-71

34. ARKLES,B. and THEBERGE,J. "Migratory Internal Lubrication of Thermoplastic Resins", A.S.L.E./A.S.M.E. Lub. Conf.,Atlanta, Georgia, Oct.16-18, 1973, Vol.29, No.12, pp 552-555

35. DUNCAN,A. and SMITH,R. "Silicon-lubricated thermoplastic", Modern Plastics, Nov.1972, pp 114-116

36. FEARON,F.W.G. and SMITH,R.F. "Wear Characteristics of Silicone Modified Polystyrene", Advances in Polymer-Friction and Wear, Vol.5B, Lee,L.H.(Ed.), Plenum Press, N.Y., 1974, pp 481-490

37. ABOUELWAFA,M.N. et al "The wear and mechanical properties of silicone impregnated polyethylene", Proc. of the 3rd Leeds-Lyon Symposium on Tribology, Leeds, 1976, paper III(ii), pp 56-59.

38. OWENS,D.K. "Friction of Polymer Films", J. Appl. Polymer Sci. (1970) Vol.14, pp 185-192

39. ARCHARD,J.F. "Contact and Rubbing of Flat Surfaces", J. Appl. Phys., Vol.24, No.8, Aug.1953, pp 981-988

40. DEMKIN,N.B. and KOROTKOV,M.A. "Influence of Oxide Films on Real Area of Contact and the Friction of Metal Surfaces", Proc. of 1st European Tribology Congress, 1973, I.M.E., pp 127-135

41. KRAGELSKY,I.V. et al "Peculiarities of Real Contact Area Formation of Polymers during Friction Interactions", Advances in Polymer Friction and Wear, Vol.5B, Lee,L.H.(Ed.), Plenum Press, N.Y.,1974, pp 729-741

42. TABOR,D. "Friction, Adhesion and Boundary Lubrication of Polymers", Advances in Polymer Friction and Wear, Vol.5A, Lee,L.H.(Ed.), Plenum Press, N.Y., 1974, pp 5-30

43. POOLEY,C.M. and TABOR,D. "Friction and molecular structures: the behaviour of some thermoplastics", Proc. Roy. Soc., Lond. A.329, 22 Aug.1972, pp 251-274

44. LEE,L.H. "Effect of Surface Energetics on Polymer Friction and Wear" Advances in Polymer-Friction and Wear, Vol.5A, Lee,L.H.(Ed.), Plenum Press, N.Y., 1974 pp 31-68

45. BRAINARD,W.A. and BUCKLEY,D.H. "Adhesion and Friction of P.T.F.E. in contact with metals as studied by Auger Spectroscopy, Field Ion and Scanning Electron Microscopy", Wear, 26 (1973), pp 75-93

46. BARTENEV,G.M. and LAVRENTEV,V.V. "Friction and Wear of Polymers" (Ed. Lee,L.H. and Ludema,K.C.), Elsevier Scientific Publishing, N.Y., 1981, pp 71-72, 248-252

47. BIKERMAN,J.J. "The Nature of Polymer Friction", Advances in Polymer-Friction and Wear, Vol.5A, Lee,L.H.(Ed), Plenum Press, N.Y., 1974, pp 149-163

48. WEST,G.H. and SENIOR,J.M. "Frictional Properties of Polyethylene", Wear, 19 (1972) pp 37-52

49. BOWDEN,F.P. and TABOR,D. "The Friction and Lubrication of Solids", Vol.II, Oxford Univ. Press, London (1964)

50. BAHADUR,S. "Dependence of Polymer sliding friction on normal load and contact pressure", Wear, 29 (1974) pp 323-336

51. BRISCOE,B.J. "The friction of polymers: a short review", Proc of the 7th Leeds-Lyon Symposium on Tribology, Leeds, Sept.1980, Paper IV(i), pp 81-92.

52. Private correspondance from Stanton Redcroft (Thermal Analysis Equipment). Copper Mill Lane, London

53. McLAREN,K.G. and TABOR,D. "Friction of Polymers at Engineering Speeds: Influence of Speed, Temperature and Lubricants", Inst. Mech. Engrs. Lub. and Wear Conv. (1963) pp 210-215

54. BRISCOE,B.J. "Polymer Friction and Wear: Fundamental aspects", Paper presented at Selection and Performance of Dry Bearings Conf., 25th May 1983, National Centre of Tribology, Risley, England

55. RABINOWICZ,E. "Friction and Wear of Materials", J.Wiley, N.Y., 1965

56. HALLIDAY,J.S. "Surface Examination by Reflection Electron Microscopy", Proc. Inst. Mech. Engrs. Lond., Vol.169 (1955), pp 777-788

57. LANCASTER,J.K. "Abrasive Wear of Polymers", Wear, 14(1969), pp 223-239

58. EVANS,D.C. and LANCASTER,J.K. "The Wear of Polymers", Treatise on Materials Science and Technology, Vol.13, Academic Press (1979), pp 85-139

59. GREENWOOD,J.A. and WILLIAMSON,J.B.P. "Contact of nominally flat surfaces", Proc. Roy. Soc. Lond. A, Vol.295 (1966), pp 300-319

60. HOLLANDER,A.E. and LANCASTER,J.K. "An application of Topographical analysis to the wear of polymers", Wear, 25(1973), pp 155-170

61. DOWSON,D. et al "The influence of counterface roughness on the wear rate of polyethylene", Proc. of the 3rd Leeds-Lyon Symposium on Tribology, Leeds, 1976, paper IV(iv), pp 99-102

62. RATNER,S.B. et al, "Connection between Wear-Resistance of plastics and other mechanical properties" Abrasion of Rubber, James,D.I.(Ed.), McLaren Ltd., (1967) pp 145-154

63. JAIN,V.K. and BAHADUR,S. "Development of a Wear Equation for Polymer-Metal sliding in terms of the fatigue and topography of the sliding surfaces", Wear, 60 (1980), pp 237-248

64. KRAGELSKI,I.V. and NEPOMNYASHCHII,E.F. "Fatigue Mechanisms of the Wear of tyre treads", Abrasion of Rubber, James,D.I.(Ed.) McLaren Ltd., (1967) pp 3-13

65. SUH,N.P. "An overview of the Delamination Theory of Wear", Wear, 44 (1977), pp 1-16

66. CLERICO,M. "Sliding Wear Mechanisms of Polymers", Fundamentals of Tribology, (Ed.Suh,N.P. and Saka,N.) M.I.T. Press, Cambridge, Mass. (1980) pp 769-785

67. CLERICO,M and PATIERNO,V. "Sliding Wear of Polymeric Composites", Wear, 53(1979), pp 279-301

68. TABOR,D. "The wear of non-metallic materials: a brief review", Proc. of the 3rd Leeds-Lyon Symposium on Tribology, Leeds, 1976, paper I(i), pp 3-8

69. SPURR,R.T., "Temperatures reached during sliding", Wear, 55 (1979), pp 289-293

70. JAEGER,J.C. "Moving sources of heat and the temperature at sliding contacts, Proc. Roy. Soc., N.S.W., Vol.76 (1942) pp 203-224

71. ARCHARD,J.F. "The Temperature of Rubbing Surfaces", Wear, 2 (1958/59), pp 438-455

72. RHEE,S.H. and LUDEMA,K.C. "Transfer films and severe wear of polymers", Proc. of the 3rd Leeds-Lyon Syposium on Tribology, Leeds, 1976, paper II(i) pp 11-17

73. WHEELER,D.R. "P.T.F.E. Transfer film studied with X.P.S.", NASA, T.P.-1728, Nov.1980

74. PEPPER,S.V. "Auger analysis of films formed on metals in sliding contact with halogenated polymers", J. Appl. Phys., Vol.45 (July 1974), No.7, pp 2947-2956

75. BRISCOE,B.J. "Friction and Wear of organic solids and the adhesion model of friction", Phil. Mag. A, 1981, Vol.43, No.3, pp 511-527

76. MAKINSON,K.R. and TABOR,D. "The friction and transfer of P.T.F.E." Proc. Roy. Soc. A, Vol.281, pp 49-61

77. STEIJN,R.P. "The sliding surface of P.T.F.E.: an investigation with the electron microscope", Wear, 12 (1968), pp 193-212

78. TANAKA,K. et al. "The Mechanism of Wear for P.T.F.E.", Wear, 23 (1973), pp 153-172

79. KAR,M.K. and BAHADUR,S. "Micromechanism of Wear at Polymer-Metal sliding interface", Wear, 46 (1978), pp 189-202

80. KRAGELSKII,I.V. "Friction and Wear", Butterworths, 1965.

81. DOWSON,D. "Transition to Boundary Lubrication from Elastohydrodynamic Lubrication", Boundary Lubrication: An appraisal of World Literature, (Ed.Ling,F.F.; Klaus,E.E and Fein,R.S.), A.S.M.E. (1969), Ch.11, pp 229-240

82. CAMPBELL,W.E. "Boundary Lubrication", Boundary Lubrication: An appraisal of World Literature, (Ed. Ling,F.F., Klaus,E.E. and Fein,R.S.), A.S.M.E., (1969) Ch.6, pp 87-117

83. STRIBECK,R. "Die wesentlichen Eigenschaften der Gleit-und Rollenlager", Zeitschrift des Vereines Deutscher Ingenieure, Vol.46, No.36 (6th Sept. 1902), pp 1341-48, 1432-38, 1463-70 (In German)

84. BENNETT,A. and HIGGINSON,G.R. "Hydrodynamic lubrication of soft solids", J. Mech. Eng.Sci., Vol.12, No.3 (1970), pp 218-222

85. CURDWORTH,C.J. and HIGGINSON,G.R. "Friction of Lubricated Soft Surface Layers" Wear, 37 (1976), pp 299-312

86. HOOKE,C.J. and O'DONOHUGUE,J.P. "Elastohydrodynamic Lubrication of Soft, Highly Deformed Contacts", J. Mech. Eng. Sci., Vol.14 (1972), pp 34-48

87. KOUTKOV,A.A. "A brief summary of recent work on the friction and wear of metals and polymers under boundary conditions", Wear, 15 (1970), pp 294-296

88. FORT,T. "Adsorption and Boundary Friction on Polymer Surfaces", J. Phys. Chem. Vol.66 (1962), pp 1136-1143

89. MATVEEVSKY,R.M. "The effect of the Polarity of Oil on the Friction of some Plastics", Wear, 4 (1961), pp 300-310

90. VINOGRADOV,G.V. and BEZBORODKO,M.D. "Friction, Wear and Lubrication of Plastics", Wear, 5(1962), pp 467-477

91. BETHUNE,B. "The surface cracking of glassy polymers under a sliding spherical indenter", J. Mat. Sci., Vol.11 (1976), pp 199-205

92. MAI,Y.W. and ATKINS,A.G. "Effects of rate, temperature, and absorption of organic solvents on the fracture of plain and glass filled polystyrene", J. Mat. Sci., Vol.11 (1976), pp 677-688

93. SHCHERBAKOV,S.V. and KAPLAN,M.B., "The effects of lubricants on the strength of polymers", Russian Engineering Journal, Vol.54 (1974), No.11, pp 37-39

94. BOOSER,E.R., SCOTT,E.H. and WILCOCK,D., "Compatability Testing of Bearing Materials", Proc. Inst. Mech. Eng. Lubr. and Wear Conf., London, pp 366-370 (1957)

95. LEWIS,R.B. "Lubrication of Teflon", S.A.E., National Combined Fuels and Lubricants and Transportation Meetings, Houston, Texas, Nov.4-7, 1969, No.690777, pp 1.12

96. BRISCOE,B.J. and STOLARSKI,T.A. "Combined rotating and linear motion effects on the wear of polymers", Nature, Vol.281 (1979), pp 206-208

97. BRISCOE,B.J. and STOLARSKII,T.A. "The effect of the Complex Motion in the Pin-on-disc machine on the friction and Wear mechanism of organic polymers", Proc. of Eurotrib. 81, 3rd Int. Tribology Congress, 1981, Vol.4, paper 9, pp 80-99

98. TIMOSHENKO,S.P. and GOODIER,J.N. "Theory of Elasticity", McGraw-Hill, New York (1951)

99. SCHWARTZ,S.S. and GOODMAN,S.H. "Plastics Materials and Processes", Van Nostrand Reinhold, New York (1982).

100. LAWN,B. and WILSHAW,R. "Review of Indentation fracture principles and applications", J. Mat. Sci. 10 (1975), pp 1049-1081

101. GILROY,D.R. and HIRST,W. "Brittle fracture of glass under normal and sliding loads", Brit. J. Appl. Phys. (1969), Ser.2. Vol.2. pp 1784-1787

102. LANCASTER,J.K. "Accelerated wear testing of P.T.F.E. composite bearing materials" Tribology Int. April 1979, pp 65-75

103. LANCASTER,J.K. "Assessment of the Wear of Composite Coatings in Reciprocating Line Contact Conditions", Selection and Use of Wear Tests for Coatings, A.S.T.M. STP 769, R.G.Bayer (Ed.), American Society for Testing and Materials, 1982, pp 92-117

104. HORIKIRI,S. "Single Crystals of Poly(2,6-dimethyl-phenylene Oxide)", J. Polymer Sci., PT A-2, Vol.10 (1972) pp 1167-1170

105. BRANDRUP,J. and IMMERGUT,E.H. "Polymer Handbook", Wiley-Interscience (1975)

106. BUSH,S. "Polymer Types and their General Properties", Selection and Performance of Dry Bearings Conf., National Centre of Tribology, May 1983

107. Results of Differential Thermal Mechanical Analyses by Stanton Redcroft, Copper Mill Lane, London

108. HOLMES-WALKER,W.A. "Polymer Conversion", Appl.Sci. Publishers, London (1975)

109. DOW CORNING "Information about Silicone Fluids", Bulletin:22-069E-01

110. DOW CORNING, "M S Silicone Fluids", Technical Data Sheet G1, pp 1-18

111. FREEMAN,G.G. "Silicones: an introduction to their chemistry and applications", Iliffe Book Ltd., London (1962)

112. NOLL,W. "Chemistry and Technology of Silicones", Academic Press, New York, (1968)

113. REZNIKOVSKII,M.M. and BRODSKII,G.I. "Features of the mechanism of Abrasion of Highly Elastic Materials", Abrasion of Rubber, James,D.I.(Ed.), MacLaren, London, (1967) pp 14-22

114. AHARONI,S.M. "Wear of Polymers by Roll-Formation", Wear, 25 (1973), pp 309-327

115. UCHIYAMA,Y and TANAKA,K. "Wear Laws for P.T.F.E.", Wear, 58 (1980), pp 223-235

116. TABOR,D. and WILLIS,R.F. "The formation of silicone polymer films on metal surfaces at high temperatures and their boundary lubricating properties", Wear,13 (1969), pp 413-442

117. WILLIS,R.F. and SHAW,R.F. "The Thermal Oxidative Decomposition of Polyorganosiloxane Fluids at Metal Surfaces", J. Coll. and Int. Sci., Vol.31, No.3, November 1969, pp 397-408

118. WILLIS,R.F. "Thermal Decomposition of Silicone Fluids at Metal Surfaces", Nature, Vol.221, March 22, 1969, pp 1134-1135

119. ANDERSON,J.C. "Review of N.C.T. Test Work on Commercially Available Dry Bearing Materials", Paper presented at Selection and Performance of Dry Bearings Conf. 25 May 1983, National Centre of Tribology, Risley

120. DERJAGUIN,B.V. and TOPOROV,Yu.P. "Influence of Adhesion on the Sliding and Rolling Friction", Microscopic aspects of Adhesion and Lubrication : Proc. 34th Int. Mtg. of Societe de Chime Physique : Paris, Sept. 14-18, 1981.

121. TABOR,D and WINTERTON,R.H.S., "The direct measurement of normal and retarded van der Walls forces", Proc. Roy. Soc. A312, (1969), pp435-450.

122. JOHNSON,K.L.; KENDALL,K. and ROBERTS ,A.D. "Surface energy and the contact of elastic solids", Proc. Roy. Soc. A324 (1971), pp301-313.

123. CHERRY,B. "Polymer Surfaces", Cambridge University Press, Cambridge, (1981).

124. AIRD,P.J. and CHERRY,B.W. "Frictional Properties of Branched Polyethylene", Wear, Vol. 51, No. 1, Nov. 1978, pp147-155.

125. GREENWOOD,J.A; MINSHALL,H. and TABOR,D., "Hysteresis losses in rolling and sliding friction", Proc. Roy. Soc. Lond. A(1960), Vol. 259, pp480-507.

126. SABEY,B.E. "Pressure Distributions beneath spherical and conical shapes pressed into a Rubber plane, and their Bearing on the coefficients under wet conditions Proc. Roy. Soc. 71(1958), pp979-988.